Proceedings of The Third International Conference on Luminescence Dosimetry, held at the Danish AEC Research Establishment Riso 11-14 October 1971

Part 2

Forskningscenter Risø, Roskilde

Publication date:
1971

Document Version
Publisher's PDF, also known as Version of record

Risø Report No. 24
Part II (pp.444 - 879)

Risø Report No. 249
Part II (pp. 444 - 879)

Danish Atomic Energy Commission

Research Establishment Risø

Proceedings of The Third International Conference on Luminescence Dosimetry, held at the Danish AEC Research Establishment Risø 11-14 October 1971

Sponsored by The Danish Atomic Energy Commission and
The International Atomic Energy Agency

December 1971

Sales distributors: Jul. Gjellerup, 87, Sølvgade, DK-1307 Copenhagen K. Denmark
Available on exchange from: Library, Danish Atomic Energy Commission, Risø, DK-4000 Roskilde, Denmark

U. D. C.
535.37:539.12.08

December 1971

Risø Report No. 24[illegible]
Part II (pp. 444-879)

Proceedings of the Third International Conference on Luminescence Dosimetry

Held at

The Danish Atomic Energy Commission
Research Establishment Risø

October 11-14 1971

Sponsored by

The Danish Atomic Energy Commission

and

International Atomic Energy Agency

Editor

V. Mejdahl

ISBN 87 550 01 20 3
ISBN 87 550 01 23 8

CONTENTS

PART I

Page

Page

MISCELLANEOUS PROPERTIES, EFFECTS AND APPLICATIONS

Chairman: H. Francois, C.E.A., Paris, France

Dose Relationship, Energy Response and Rate Dependence of LiF-100, LiF-7 and $CaSO_4$-Mn from 8 KeV to 30 MeV.

by

G. Eggermont+, R. Jacobs, A. Janssens+, O. Segaert, G. Thielens.
Dept. of Radiological Protection and Control and Natuurkundig Laboratorium(+)
Ghent State University, Proeftuinstraat, 86, 9000 Gent, Belgium

Abstract

The energy response, the dose relationship and the dose rate dependence of commercially available Harshaw LiF-100 ribbons, Con-Rad LiF-7 teflon rods and Con-Rad $CaSO_4$-Mn teflon rods are investigated within the energy region from 8 keV to 30 MeV. The energy response calculations for different grain sizes are based on the general cavity theory for gamma ray energies from 10 keV to 3 MeV and for electron energies between 10 MeV and 30 MeV. The experimental results obtained with $CaSO_4$-Mn confirm the Burlin theory and the grain size dependence of the T.L. dosemeter response. The decreased sensitivity of LiF-100 at high electron energies can only partially be explained by the cavity theory.

Dose response curves are given for doses ranging from 10 rads to 10^6 rads for LiF-7 for 8.3 keV eff X rays and cobalt-60 and for LiF-100 for cobalt-60 gamma rays and 15.3 MeV electrons . Dose estimation is made by evaluation of the integrated area and the peak value of the glow curve. Variation of supralinearity and saturation is established for the different radiation qualities.

The modification of the Con-Rad 5100 reader extending its sensitivity and its possibilities is discussed briefly.

Introduction

In order to obtain a consistent view on the dose relationship, energy response and rate dependence of thermoluminescent materials a systematic theoretical and experimental study is made on Con-Rad $CaSO_4$-Mn teflon rods, LiF-7 teflon rods and Harshaw LiF-100 ribbons.

The experimental work by Zanelli[1] indicates a grain size dependence of the thermoluminescence dosemeter response. A theoretical approach based on the cavity theory was published by Chan and Burlin[2]. The present investigation was undertaken in order to predict the theoretical dose response for a number of thermoluminescent materials of different grain sizes, to make a comparison with the experimental results and to test the validity of the cavity theory. Attention is also given to the energy dependence of supralinearity of LiF-100 and LiF-7 phosphors.

Theoretical treatment of the energy dependence of thermoluminescent response.

If the energy dependence of thermoluminescent dosemeters varies with the grain size of the thermoluminescent material together with the nature of the surrounding substance and if the grain forms a cavity in the irradiated medium (e.g. a teflon matrix or a perspex phantom etc.) then the cavity theory relates the dose in the TL grain D_c to the dose in the medium D_m through the relationship $D_c = f^c_m D_m$, where f^c_m is the energy and grain size dependent stopping power ratio, cavity to medium. The f-value can be calculated exactly for every material and size by means of the general cavity theory. Since the TL response is proportional to D_c, the stopping power ratio f^c_m is proportional to (TL response / D_m).

In order to evaluate the energy dependence of a given TL material to its cobalt-60 response, stopping power ratios must be calculated for all energies including the cobalt-60 photon energy and for the specific size and nature of phosphor and medium.

From the equation derived by Burlin[3,4]

$$f^o_m(T_o,\Delta) = \frac{(Z/A)c}{(Z/A)m}\left\{1 + \frac{d}{T_o}\left[\int_{\Delta}^{T_o} R_m(T_o,T)\left(\frac{B_c(T)}{B_m(T)} - 1\right) dT + \Delta . R_m(T_o,\Delta).\left(\frac{B_c(\Delta)}{B_m(\Delta)} - 1\right)\right] + (1-d)\left[\frac{(\mu_{en}/\rho)c}{(\mu_{en}/\rho)m} \cdot \frac{(Z/A)m}{(Z/A)c} - 1\right]\right\}$$

stopping power ratios are calculated for Conrad $CaSO_4$-Mn in teflon rods, Con-Rad LiF-7 teflon rods and Harshaw LiF-100 ribbons in perspex.

In the case of electron beams the ratio of the mass energy absorption coefficients is replaced by the ratio of the electron densities, hence the last term in the equation vanishes . For initial electron energies $T_o \leq$ the energy Δ at which electrons will on the average just cross the cavity, the integral from Δ to T_o is replaced by zero. The ratio of the total to the primary electron flux $R_m(T_o, T)$ is calculated for teflon and perspex using the expression derived by Spencer and Attix[2], μ_{en}/ρ is the mass energy absorption coefficient derived from the tables of Storm and Israel[5]

$$R_m(T_o,T) = 1 + \tau^{-1}\int_{2\tau}^{1} d\tau'\left[1-\tau(\tau'-\tau)^{-1}\right]\frac{R_m(T_o,T')}{B_m(T')}$$

With $\tau = T/T_o$ and $\tau' = \frac{T'}{T_o}$, assuming charged particle equilibrium,

secondary electron energies less than $T_o/2$ and neglecting bremsstrahlung-corrections. This Volterra integral equation is solved as indicated by Spencer and Fano[1].

The numerical calculations are executed on a PDP computer with an accuracy better than 1 %.

Stopping power ratios are evaluated for 1°) Conrad $CaSO_4$-Mn (4 % by weight) in a teflon matrix with an unknown grain size distribution (maximum diameter of 75 micron with a mean value of 5 micron) for grain diameters of 1.25 micron, 5 micron and 49 micron. The teflon medium has a density of 2.09 g/cm^3.

2°) Conrad LiF-7 (4 % by weight) teflon rods with an unknown grain size distribution (maximum diameter of 75 micron with a mean value of 12 micron) for grain diameters of 12 micron, 56 micron and 1,4 micron.

3°) LiF-100 ribbons of (3.175 mm x 3.175 mm x . 89 mm).

The stopping numbers B(T) are directly deduced from the continuous slowing down approximation collision stopping power data tabulated by Pages[8]. The Values for the cavity sizes are derived from the values for air tabulated by Spencer and Attix[9,10], simply by multiplication with the ratio of the continuous slowing down approximation ranges in the medium to the corresponding values in air. The range-energy relations used in the derivation of the weighting factor d are taken from Katz and Penfold[11] for electron energies from 10 keV to 2.5 MeV and from Marcus[12] in the region from 2.5 MeV to 30 MeV.
The stopping power ratio must be averaged over the energy spectrum of the electrons generated by the incident monoenergetic gamma rays. The contributions to the mass stopping power ratio of the photoelectric, Compton and pair production processes are weighted by their respective mass energy absorption coefficients.
The photoelectric electron energy is the gamma ray energy minus the binding energy , for the Compton process the average Compton recoil energy and for pair production the middle of the symmetric energy distribution is chosen. From the calculations of stopping power ratios for Compton spectra and for monoenergetic electrons made by Spencer and Attix[10] can be concluded, that for the low Z materials under consideration, this approximation rather than taking into account the whole spectrum does not introduce errors greater than 1 %.

Instrumentation and experimental techniques

a) Irradiation facilities

In order to cover the wide range of X, gamma and electron energies different sources and machines were used. 1) X-ray I (contact therapy machine) $E_{Max.}$ = 50 kVp, $E_{eff.}$ = 8.3 keV, I = 2 mA, no added filter. 2) X-ray II (dental X-ray machine) $E_{max.}$ = 60 kVp, $E_{eff.}$ = 15 -45 keVeff. by adding filters. 3) X-ray II (diagnostic X-ray machine) $E_{max.}$ = 93 kVp, $E_{eff.}$ = 22 and 38 keV eff. by adding filters. 4) X-ray IV (therapy machine) $E_{max.}$ = 200 kVcp, added filter 2 mm Al + 0.5 mm Cu : 84 keV eff., $E_{max.}$ = 100 kVcp, added filter 2 mm Al : 40 keV eff. 5) Cobalt source (gamma cell 220) cylindrical shape 3400 Ci dose rate 50 rads/s . 6) Radium source, 300 mCi point source. 7) Linear accelerator E = 10 - 30 MeV energy resolution 1 % , I (max.) = 1 μA, pulsewidth 0,25 μ sec, 50 Hz, collimated beam; used with perspex phantom following A.A.P.M. recommendations[13] .

b) The TLD read-out system

For the read out of the dosemeters a Con-Rad 5100 reader is used. The integrator and the cathode follower circuit are modified into an active integrator using an operational amplifier. This allowed to obtain an increase of its sensitivity by a factor of 33, the extension of its range up to 9 decades and the possibility of automatic range switching within 5 decades [15]

c) Calibration

Victoreen Radocon ionisation chambers for low, medium and high energy were used together with a Victoreen Condenser Ratemeter and a Farmer secondary standard. In addition to this, ferrous sulfate Fricke solution in perspex cells were used at the cobalt-60 irradiation facility and at the linear accelerator. In order to express the dose in rad in the medium cavity theory was taken into account.

Correction factors are calculated accounting for the attenuation (both in the wall and in the cavity) and the divergence of the beam. The choice of the effective attenuation coefficients is justified on account of the following statements.
Fricke solutions in cylindrical perspex cells of different sizes and wall thicknesses received a constant dose within the cylindrical cobalt-60 unit. For the cells used the stopping power ratios (Fricke solution to perspex) are nearly independant of the cavity size, consequently the systematic difference between the dosemeter responses are due to variations of attenuation and absorption for different sample geometries. Correction factors were evaluated using respectively attenuation coefficients or absorption coefficients for wall and cavity. The deviation is minimised and brought back within the experimental error, by using the attenuation coefficient excluding coherent scatting for the perspex wall and using the energy absorption coefficient for the cavity.
For the cylindrical shape of the cobalt-60 source a computer programm was worked out to evaluate these correction factors.

Theoretical and experimental results

1) Energy dependence

From equation (1) it can be shown that theory and experiment are related by the equation

$$\frac{\left(\frac{TL}{rad_m}\right)_E}{\left(\frac{TL}{rad_m}\right)_{Co}} = \frac{f_E}{f_{Co}} \qquad (2)$$

The ratio f_E/f_{Co} is the stopping power ratio normalised to the stopping power ratio of cobalt-60 deduced from the calculations based upon the general cavity theory. In order to intercompare the experimental and theoretical results , the f_{Co}-value is derived from the total spectrum within the irradiation facility, allowing for lower energy scattered radiation[14].

At 1.25 MeV this results in a f_{Co} value difference of 0.01 % down to 1.3 %, according to size and wall thickness.

The theoretical curves of f_E/f_{Co} for different grain sizes for each of the three thermoluminescent materials are shown in figures 1, 2 and 3, together with the μ_{en}/ρ - ratio,

$$\left[\left(\frac{\mu_{en}}{\rho}\right)_c \Big/ \left(\frac{\mu_{en}}{\rho}\right)_m\right]_E : \left[\left(\frac{\mu_{en}}{\rho}\right)_c \Big/ \left(\frac{\mu_{en}}{\rho}\right)_m\right]_{Co},$$ which is usualy taken as the

theoretical expression for the energy dependence of the dosemeter response.

The theoretical evaluation of the energy dependence of LiF-100 ribbons was made using the average pathlength across the cavity and using a pathlength equal to the thickness of the cavity in the direction of the incident beam. For electromagnetic radiation this makes no difference (cfr. figure 1). In figure 2 the representation of (μ_{en}/ρ)- ratio curve for $CaSO_4$-Mn, coincides practically with curve 3. In figure 1 the (μ_{en}/ρ)- ratio curve for LiF-100 coincides with the grafical representation of the stopping power ratio.

For reason of comformity with current litterature the energy dependence of LiF-7, with reference to rads in teflon (figure 3) is converted to its energy dependence with reference to rads in air (figure 4).

The mutual distance between the grains within a teflon matrix is approximately equal to the average range of secundary electrons with an energy of 400 keV. At energies greater than 400 keV, the possible influence of surrounding grains on the charged particle equilibrium flux generated in teflon can be neglected; the stopping power ratio of both materials does not differ greatly at energies above 400 keV. If there is any influence it should tend the resulting stopping power ratio nearer to one.

The reproducibility of the response and the degree of absolute accuracy of the calibration are illustrated by the experimental data (cfr. figure 1 and 2).
For $CaSO_4$-Mn[16] special attention was given to the diagnostic X-ray energy region where for different KVp settings and added filters the response is given at the corresponding affective energies.
The administered doses and irradiation times are kept constant, fading corrections are accounted for .

The experimental results obtained with LiF-100 ribbons in the diagnostic X-ray region and at 84 keV effective are shown in figure 1, together with the dose response value obtained with 20 MeV electron beam incident on a perspex phantom. At the position of the thermoluminescent material the electron energy is reduced about 15.3 MeV. At this energy the experimental value shown on the graph is taken at a dose of 10^4 rad. An experimental value at a lower dose, within the linear sensitivity region, could not be established, due to the limitations of the transfer instrument at the linear accelerator.

As the experimental error on the dose response data for LiF-7 is greater than the difference between the theoretical stopping power ratio curve and the μ_{en}/ρ - ratio curve, the experimental results are irrelevant. these results are not inserted in the grafical representation.

2) Dose response

For LiF-7 the experimental dose response data, expressed in rad in teflon, for an 8.3 keV effective X-ray spectrum and for cobalt-60 gamma radiation in the region from 10 rad to 10^6 rad are shown in figure 5. For cobalt-60 the experimental curve can be extended down to 10^{-2} rad, from 10^2 rad down to 10^{-2} rad the sensitivity remains constant. The constant sensitivity ratio in the linear region is taken equal to the ratio predicted by the cavity theory, for, a small error in the energy measurement at 8.3 keV eff. gives rise to a great uncertainty concerning the attenuation correction factor applied to the calibration. If the attenuation correction is evaluated at 8 keV and at 10 keV, it appears that the theoretical value at 8.3 keV lies between the, for 8 keV attenuation , and the for 10 keV attenuation corrected experimental value.

The dose response measurements based upon the evaluation of the maximum of the glow curve did not differ from those based upon the evaluation of the integrated area. Exception is made in the saturation region where they cross each other. This effect is explained by the reduction of the integrated area due to the fixed read out time.
In the superlinear region a high temperature part is observed which increases at higher doses. If not stated otherwise doses are evaluated using the integrated area.
In figure 6 dose response curves for LiF-100 for cobalt-60 and 15.3 MeV electrons from 10^2 to 10^6 rad are given. For Co-60 radiation a constant sensitivity was observed from 10^{-2} to $3 \cdot 10^2$ rad. The sensitivity curve is derived from the dose response curve, and is given in figure 7.

3) Rate dependence

At the present state of the investigation the results on the rate dependence of the thermoluminescent material do not allow any conclusive statement.

Discussion

From the experimental and theoretical results the grain size dependence of the thermoluminescent response is evident, particularly for $CaSO_4$-Mn were the effect is striking. The numerical values of the calculated stopping power ratios are of course dependent on the input data used in the Burlin equation. This may explain the difference in shape of our curves, for gamma ray energies higher than 50 keV, compared to those published by Chan and Burlin[2].
This fact does not alter our conclusions since most of our measurements were performed at energies below 50 keV effective.

In the comparison of theory and experiment two approximations are made :

- the experimental results obtained with continuous X-ray spectra characterised by a given effective energy are compared with the corresponding theoreticaly predicted values for monoenergetic gamma rays .
- the results for a teflon matrix with a distribution of grain sizes is compared with the theoretical values for the mean grain size, however upper and lower limits are given.

The grain size dependence may explain the discrepancies in the experimental results on energy dependence shown by Attix[17].
Insufficient information on grain sizes and experimental conditions does not allow to compare these data with the theoretical predictions of the cavity theory. The selection of grain sizes during the preparation process of the thermoluminescent dosemeters could lead to the production of dosemeters with a definite response within an appropriate energy region.

The 10 % smaller response of LiF for high electron energies deduced from our experiments are in agreement with the measurements of Crosby[18]. This reduction can only partially be explained by the 4 % smaller response predicted by our cavity calibrations.

Acknowledgements

The authors are indebted to Prof. Dr. J.L. Verhaeghe, director of the " Centrale Dienst voor Fysische Controle" and of the " Natuurkundig Laboratorium " of the Ghent State University, and to Prof. Dr. C. Palerents of the "Fakulteit Landbouwwetenschappen" for the use of the ^{60}Co irradiation facility.
Two of the authors, G. Eggermont and A. Janssens, are gratefull to their sponsor, the Interuniversity Institute for Nuclear Sciences, Belgium.
We acknowledge A. Masood (Bhabha Atomic Research Centre, Bombay) for his helpfull advice and collaboration.
We also want to thank the linear accelerator group together with the technical staff for their assistance.

References

1. G.D. Zanelli, Phys. Med. Biol., 13 , 393-399 (1968)
2. F.K. Chan, T.E. Burlin, Health Physics, 18, 325-332 (1970)
3. T.E. Burlin, Brit. J. Radiol., 39, 727-734 (1966)
4. T.E. Burlin, F.K. Chan, Int. J. Appl. Rad. Isot., 20, 767-775 (1969)
5. L.V. Spencer, F.H. Attix, Rad. Res. , 3 , 239-254 (1955)
6. E. Storm, H.I. Israel, LA - 3753 (1967)
7. L.V. Spencer, V. Fano, Phys. Review, 93 , 1172-1181 (1954)
8. L. Pages, E. Bertel, H. Joffre, L. Sklaventis, CEA-R-3942 (1970)
9. NBS Handbook 79 , 46 (1961)
10. NBS Handbook 85 ; 8-10 (1962)
11. Z. Katz, A.S. Penfold, Rev. Modern Phys., 24 , 28-44 (1952)
12. J.S. Laughlin, in Rad. Dosimetry, F.H. Attix, E.Tochilin ed., 2, 99(1969)
13. A.A.P.M. (SCRAD), Phys. Med. Biol., 11 , 505-520 (1966)
14. T.E. Burlin, F.K. Chan, Int. J. Appl.Radiat. Isot., 22, 73-83 (1971)
15. R. Jacobs et al, to be published
16. G. Eggermont et al, to be published
17. F.H. Attix, Health Physics, 15, 49-56 (1968)
18. E.H. Crosby, P.R. Almond, R.J. Shalek, 11, 131-132 (1966)

Webb

Your curve for 1.4 μm grain size of $CaSO_4$:Mn in teflon did not show a flat energy response. What grain size would you need to have to get the uniform response in the diagnostic region you just indicated was possible?

Fowler

How far can you go towards achieving a flat response (i.e. independent of photon energy) in the low keV range by choosing the grain size distribution? Can you reduce the response of LiF at 30 keV by 30%, for example, so as to eliminate its energy dependence altogether?

Eggermont

Although we concluded that a flat TL response in a limited energy region could be achieved by approiate choice of grain size distribution, up till now we have not made any calculations on this matter. With much smaller grain sizes ($\ll$ 1 μm) the response will approach unity, but this might be limited by practical difficulties.

Suntharalingam

In one of your slides you indicated that the response per rad for 15 MeV electrons was about 10% lower than for Co-60 gamma radiation. On another slide showing the TL response as a function of dose, where you compared 15 MeV electrons and Co-60 gamma radiation, it appeared that there was closer agreement at certain doses. Does this imply that the energy response is also a function of dose?

Eggermont

Over the dose region considered the experimental decrease in energy response varies between 0.88 and 0.92. This range in efficiency is well within the experimental error. The dose response at the doses you are referring to includes a greater experimental inaccuracy due to limitations of the transfer instrument of the linac at low dose rates. We have reached no definite conclusion on the agreement between theory and experiments for electrons, and the

problem will be studied again with a more sensitive transfer instrument in the linear TL region. However, I see no reason why a dose dependence of energy response should exist.

Carlsson, C.

With Co-60 gamma radiation the dose distribution within your grains depends on the direction of the incident photons as shown by Dutreix and Bernard. The Burlin formula neglects this effect of electron scattering. For this reasr : your normalization of experiments and calculations at 1.25 MeV may be questioned.

Eggermont

We agree that the Burlin theory in its actual form is not yet sufficiently refined. In our opinion the corrections for low-Z materials are negligible and within the large experimental error.

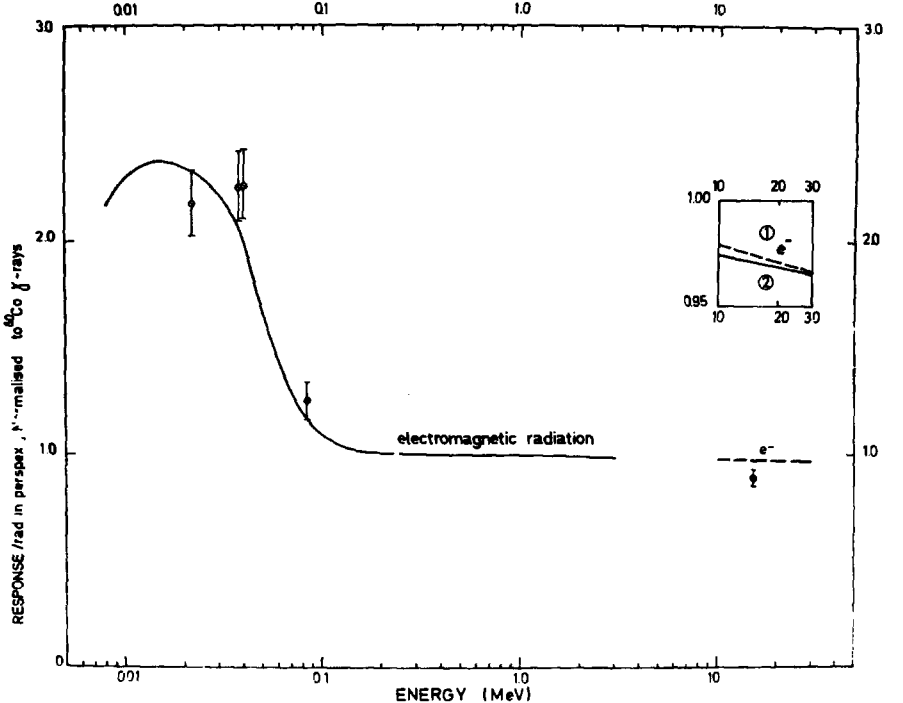

Fig. 1 Calculated Relative Energy Response of LiF-100 in Perspex (normalised to ^{60}Co). Sample thickness : 0.89 mm
Electrons : 1 average pathlength
2 thickness pathlength

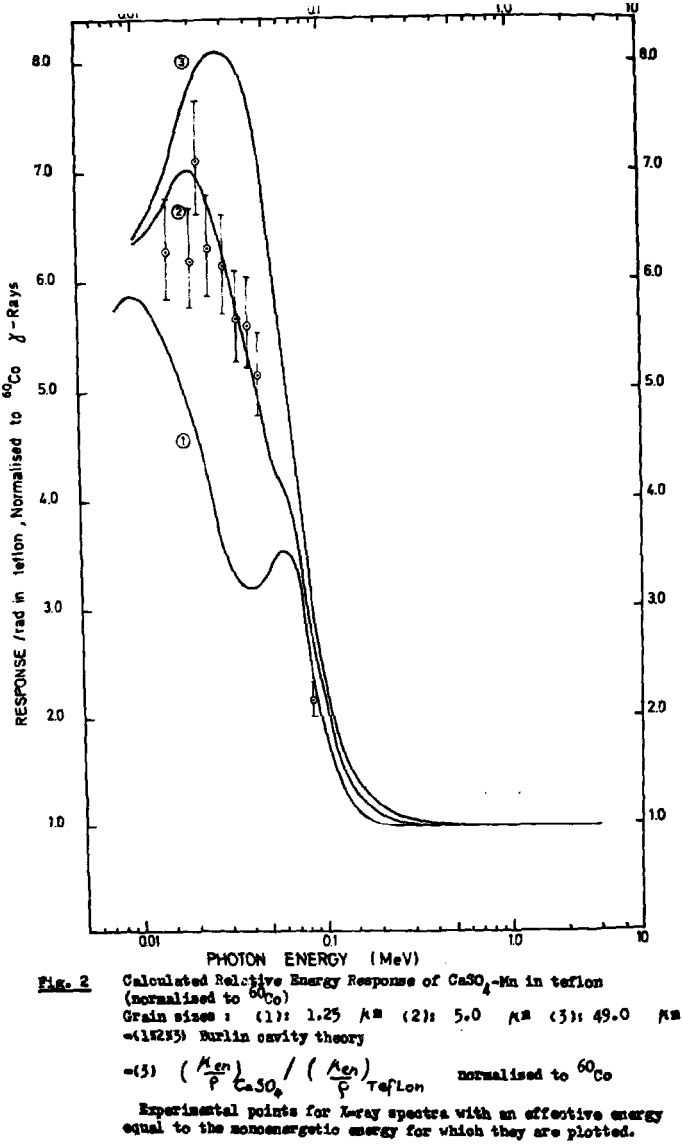

Fig. 2 Calculated Relative Energy Response of $CaSO_4$-Mn in teflon (normalised to ^{60}Co)
Grain sizes : (1): 1.25 μm (2): 5.0 μm (3): 49.0 μm
=(1)(2)(3) Burlin cavity theory

=(3) $\left(\frac{\mu_{en}}{\rho}\right)_{CaSO_4} / \left(\frac{\mu_{en}}{\rho}\right)_{Teflon}$ normalised to ^{60}Co

Experimental points for X-ray spectra with an effective energy equal to the monoenergetic energy for which they are plotted.

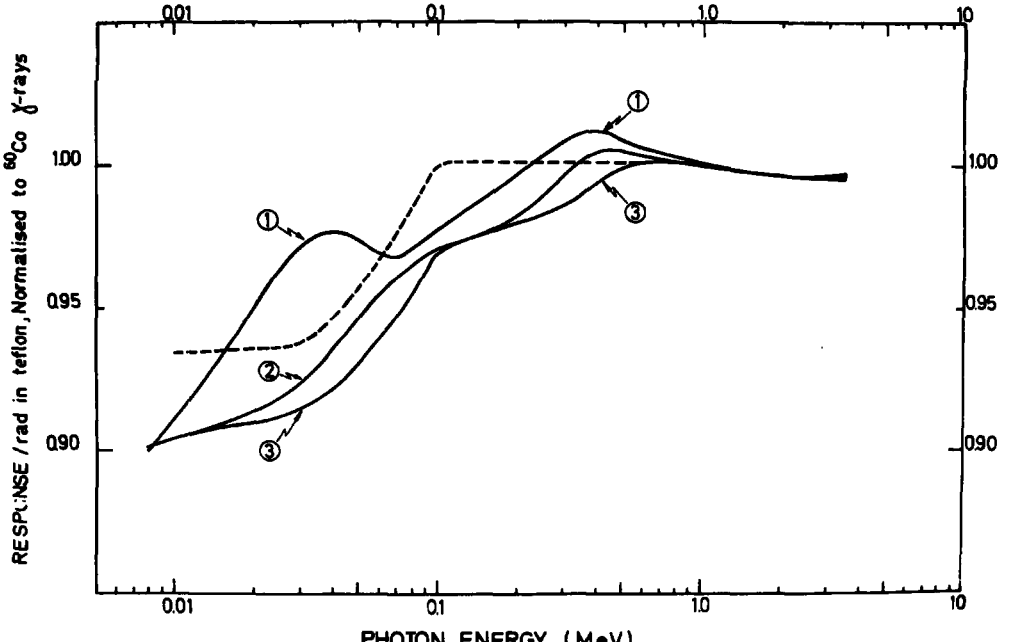

Fig. 3 Calculated Relative Energy Response of LiF-7 in Teflon (normalised to ^{60}Co for rad in Teflon).
Grain sizes : (1): 1.4 μm (2): 12.0 μm (3): 56.0 μm
—: Burlin Cavity Theory
---: $\left(\frac{\mu_{en}}{\rho}\right)_{LiF} / \left(\frac{\mu_{en}}{\rho}\right)_{air}$ normalised to ^{60}Co.

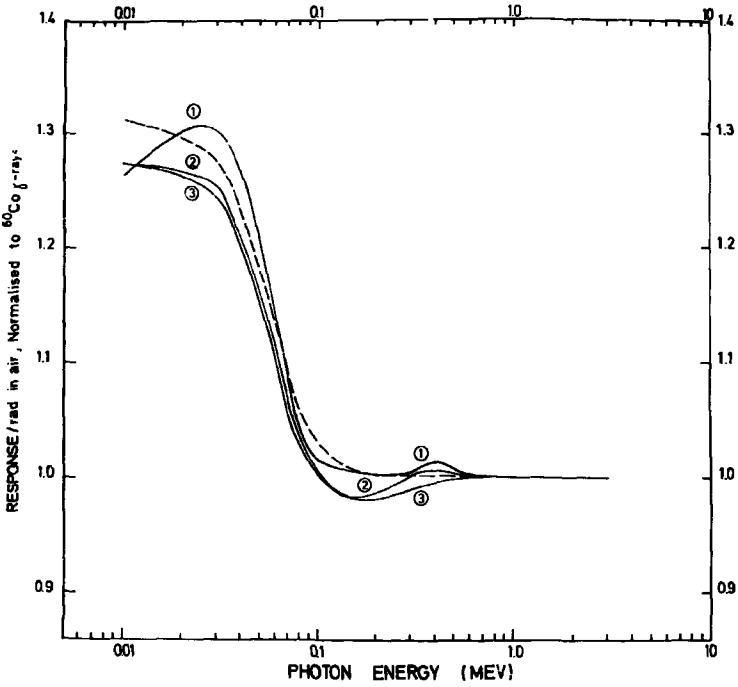

Fig. 4 Calculated Relative Energy Response of LiF-7 in Teflon (normalised to ^{60}Co for rad in air).
Grain sizes :
(1) : 1.4 μm
(2) : 12.0 μm
(3) : 56.0 μm
— : Burlin Cavity Theory
— : $\left(\frac{\mu_{en}}{\rho}\right)_{LiF} / \left(\frac{\mu_{en}}{\rho}\right)_{Teflon}$ normalised to ^{60}Co.

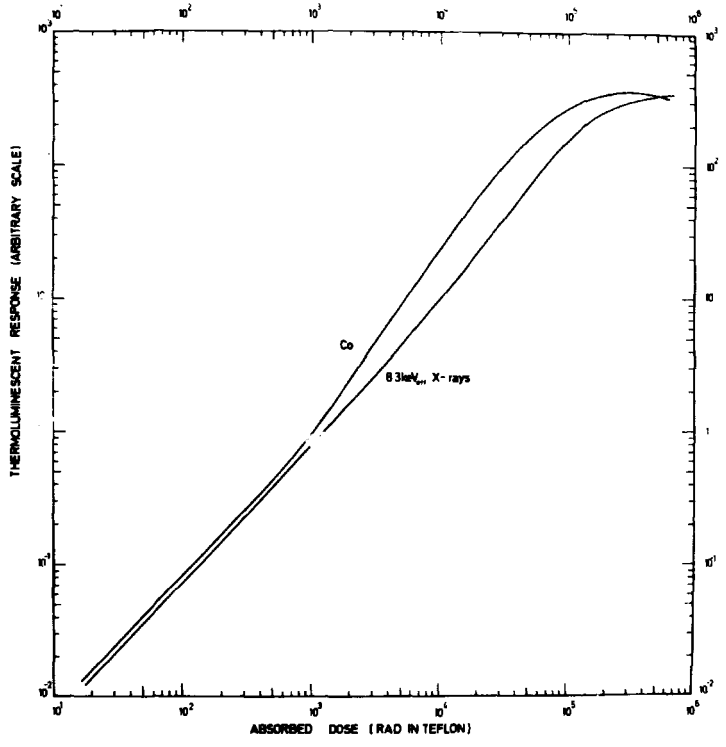

Fig. 5 Dose Response Curve of LiF-7 for ^{60}Co and 8.3 keV eff. X-rays .

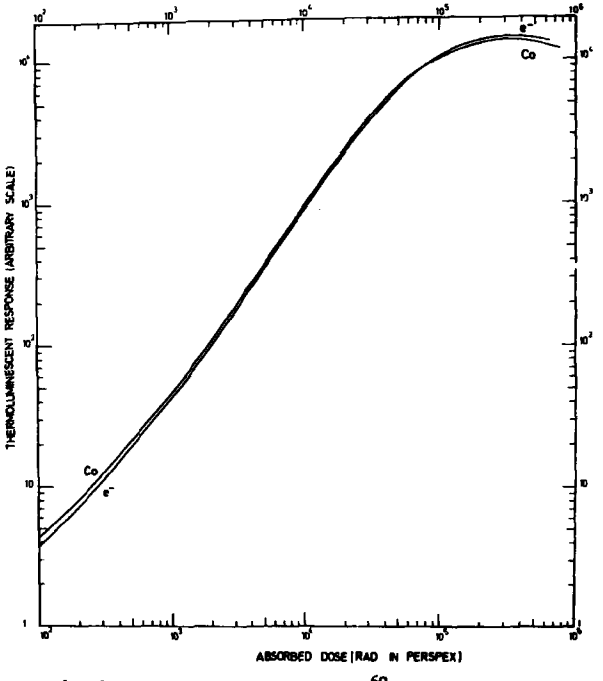

Fig. 6 Dose Response Curve of LiF-100 for ^{60}Co and 15.3 MeV electrons.

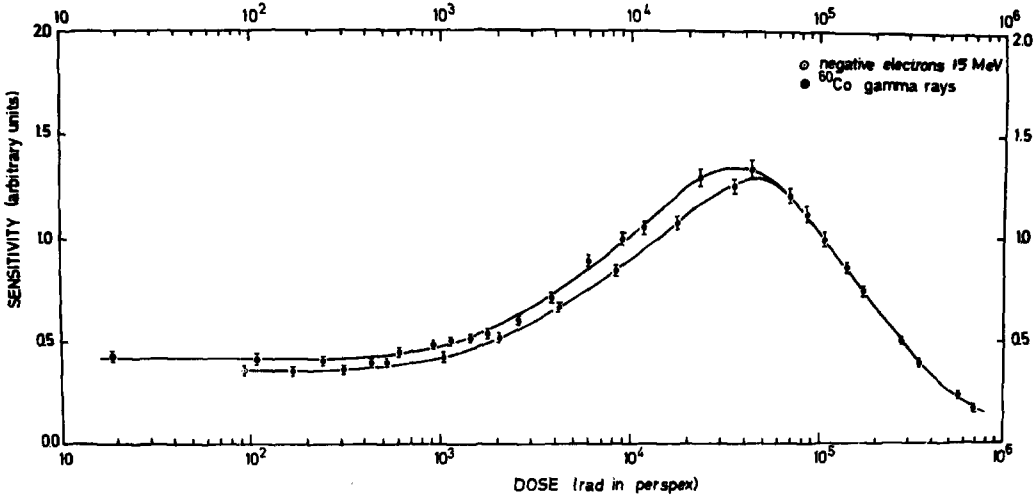

Fig. 7 Sensitivity Curve of LiF-100 for ^{60}Co gamma rays and 15 MeV electrons.

On the Non-Linearity and LET Effects of the Thermo-Luminescence Response

Toshiyuki Nakajima
Division of Physics, National Insitute of Radiological Sciences
9-1, 4-chome, Anagawa, Chiba-shi, Japan

Abstract

A releasing probability change model has bee proposed through investigation of the properties of LiF glow curve. In this work, it is mathematically discussed on the releasing probability change model for the problems of the thermoluminescence response. It has been revealed that this model can qualitatively explain these problems better than other models.

Introduction

Recently, thermoluminescence dosimeter has been widely utilized in the radiation dosimetry. However, it has been found the following phenomena by many of investigator;

(1) transformation of the glow curve due to the irradiating dose of low LET radiation,[1]
(2) absorbed energy independence of the glow curve of the phosphor irradiated with high LET radiation,[2]
(3) dependence of thermoluminescence response on the absorbed energy or LET,[3]
(4) decreasing non-linearity of the response with increasing the LET of irradiating radiation,[3]
(5) influence of exposure on the energy dependence of the phosphor,[4]
(6) dependence of sensitization factor on either the absorbed energy or LET of the post- and test-radiations,[5]

To explain the dose dependence and LET effects of the sensitivity of the phosphor, Cameron and his co-workers, and Attix et al. proposed the competing trap model and track model, respectively.[5,6] But these models have not been satisfactory to explain these phenomena. Recently, it has been proposed a model through investigation of the experiment which has been designed to measure the transformation of the glow curve due to the energy absorbed in the phosphor.[1]

This paper reports the result of mathematical analysis of the this model on the above phenomena.

Notations

A: number of electron produced by irradiation per unit energy which the phosphor absorbed,
D: the energy absorbed in the phosphor,
I_i: the thermoluminescence yields due to electron released from trapping level, E_i,
k: Boltzmann constant,
n_i: number of captured electron in the trapping level, E_i,
N_i: number of electron trapping level, E_i,
R: dose rate of irradiating radiation or absorbed energy rate,

s_i: frequency factor of the trapping level, E_i,
S: thermoluminescence response of post irradiated phosphor,
S_0: thermoluminescence response of the virgin phosphor,
t, t': irradiating period,
T_0: irradiating temperature,
T': maximum heating temperature,
β heating rate of phosphor,
δ_i: releasing probability of trapped electron in trapping level, E_i, at irradiating temperature,
ϵ_{ij}: intensity fraction of photon energy, j, in thermoluminescence emitted by releasing electron from trapping level, E_i,
γ_i: escaping probability from trapping level, E_i, at a given temperature,
σ_i: capturing probability of trapping level, E_i,
ξ_i: quantum efficiency of photo-detector for the emitted photon of energy, e_i,
θ_{ij}: transition probability of electron remained in the level, E_i, to E_j.

Theory

The radiation produces clusters of electron and hole along the track of energetic recoiled electrons. A concentration of these carrier in the cluster increases with increase of either LET of irradiating radiation or energy absorbed in the phosphor. Each trapping level near or in the cluster has a proper capturing probability of electron which contributes to thermoluminescence, and this probability of each trap varies with change in either the concentration of electron near or in the cluster, or the absorbed energy as a result of interaction between each other of the clusters.

Let us formulate a mathematical description of the model. According to Randall and Wilkins' model of thermoluminescence mechanism,[6] the thermoluminescence yield, I, is represented by followings;

$$I = \int \gamma n \, dt \qquad (1)$$

where dt and γ are defined as follows, $dt = dT/\beta$, $\gamma = s \exp(-E/kT)$.

Now, when their model applies to all the trapping levels in the phosphor, and when I is corrected with quantum efficiency of a photomultiplier tube and with a fraction of each emission in thermoluminescence, total light yields detected by the photomultiplier tube are represented as follows;

$$I_{all} = \sum_i I_i = \sum_i \sum_j \xi_i \, \epsilon_{ij} (n_i/\beta) \int_{T_0}^{T'} \gamma_i \, dT \qquad (2)$$

Now, if it is assumed that the ϵ_{ij} is unchanged against the absorbed in the phosphor and against LET of radiation, eq.(2) is proportional to the concentration or number of trapped electrons in the trapping levels. Therefore, it has need to know the concentration of the electrons in each trapping level in order to study the dose dependence on the response and so on.

Changes in the concentration of the trapped electron in each trapping level are given by eq.(3),

$$dn_i/dt = -\delta_i n_i + A(N_i - n_i)\sigma_i R . \qquad (3)$$

The boundary conditions can be given by the followings, $t = 0$, $n_i = 0$. The number of the trapped electron in each trapping level is presented by the following equation,

$$n_i = (\sigma_i A N_i R/(\delta_i + \sigma_i A R))(1 - \exp(-\sigma_i AR - \delta_i)t) \qquad (4)$$

If it is assumed that the number of the trapped electron, which is releasing from the trappling level, E_i, for irradiating period is very small, the concentration of the trapped electron is approximately given by eq. (5).

$$n_i \fallingdotseq N_i(1 - \exp(-\sigma_i A R t)), \qquad \text{as } \sigma_i A R t \ll 1$$

$$n_i \fallingdotseq \sigma_i A N_i R t = \sigma_i A N_i D \qquad (5)$$

When the phosphor is heated from T to T' with the dosimetric reader, the dosimetric thermoluminescence light yields, I_d, are presented by the following,

$$I_d = \sum_j \sum_i K_{ij} D \sigma_i \qquad (6)$$

where K_{ij} is $A\xi_i\epsilon_{ij} N_i \int_T^{T'} (\gamma_i/\beta)\, dt$.

It may be revealed that when the experimental results of the phenomena mentioned in the Introduction are mathematically expressed, σ_i in LiF phosphor is characterized by the followings;

$$(\partial \sigma_i/\partial D)_{\text{high LET}} \simeq (\partial \sigma_d/\partial D)_{\text{high LET}} \simeq 0, \qquad (7)$$

$$(\partial \sigma_i/\partial D)_{\text{low LET}} > (\partial \sigma_d/\partial D)_{\text{high LET}} \simeq 0, \qquad (8)$$

in case of low irradiation dose range,

$$(\partial \sigma_i/\partial D)_{\text{low LET}} \simeq (\partial \sigma_d/\partial D)_{\text{low LET}} \simeq 0, \qquad (9)$$

in case of high dose region,

$$(\partial \sigma_i/\partial D)_{\text{low LET}} > (\partial \sigma_d/\partial D)_{\text{low LET}} \simeq 0. \qquad (10)$$

Let us consider various phenomena of the response in LiF thermoluminescence dosimeter.

(1) Non-Linearity of Response

In case of irradiation of low dose with lower LET radiation, the cluster has lower concentration of electron created in the phosphor and scarcely interact with each other, because each track is so far separated from each. Accordingly, a value of σ_i is independent of the absorbed energy within some ranges. Now, if the response is defined as I_d/S, the dose dependence of the response is represented as follow,

$$(\partial S/\partial D)_{\text{LET}} = \sum_j \sum_i K_{ij} (\partial \sigma_i/\partial D)_{\text{LET}} \qquad (11)$$

In this case, eq.(11) from eq.(9) is nearly equal to zero. The response is independent of the absorbed energy. On the other hand, in case of the high doseregion of low LET radiation, the eq.(11) from eq.(10) is larger than zero. Accordingly, the sensitivity of the phosphor irradiated with low LET radiation becomes to reveal the non-linearity.

Let us supplement on σ_i from Carlsson's results in addition in eqs. (7), (8), (9) and (10). Namely, it is follow;

$$(\partial\sigma_i/\partial(\mathrm{LET}))_D \;/\; (\partial\sigma_d/\partial(\mathrm{LET}))_D > 1. \qquad (12)$$

in these equations, σ_d is of the dosimetric trap and σ_i is of the non-dosimetric deep trap.

In case of irradiation with higher LET radiation, eq.(11) from eqs. (7) and (12)is approching to zero with increasing LET of radiation. Therefore, the dependence of the response on the absorbed energy decreases with increasing LET.

(2) Dependence of Energy Dependence on Dose

In general, the energy dependence of the response is given by a ratio between thermoluminescence responses, S_X and S_{Co}, of the phosphors irradiated with X- and ^{60}Co gamma-rays, respectively.

$$S_X/S_{Co} = \sum_j \sum_i K_{ij}\,\sigma_i \;/\; \sum_j \sum_i K'_{ij}\sigma'_i \,. \qquad (13)$$

The dose dependence of the energy dependence is considered by followings;

$$(\partial S_X/\partial D)/(\partial S_{Co}/\partial D) = \sum_j \sum_i K_{ij}\,(\partial\sigma_i/\partial D)/\,K'_{ij}(\partial\sigma'_i/\partial D) \qquad (14)$$

In the energy range of 150 keV or below, LET of X-rays is larger than ^{60}Co gamma-rays. Accordingly, a function F(D) is an increasing function due tc eqs. (7),(8) and (9),

$$dF(D) = (\partial\sigma_i/\partial D)_{Co} - (\partial\sigma_i/\partial D)_X \qquad (15)$$

Therefore, it may be reaveled that eq.(13) is a decreasing function of the exposure.

(3) Sensitization Factor of LiF Phosphor

Author reveales that the cause of the sensitization factor and the of changes in the sensitivity of the phosphor due to repeated uses is a radio-stimulated thermoluminescence due to the trapped electrons in the non-dosimetric deep trapping levels.[1] Therefore the sensitization factor, S/S_0, is given by the followings;

$$Y = S/S_0 = 1 + \Big(\sum_{k=0} \sum_{j=0} \sum_{i=i+1} K_{jk}\,\theta_{ij}\,N_i(1-P_i)\sigma_i\,D_p\,/D_t\Big)/S_0 \qquad (16)$$

Where P_i is releasing probability of trapped electron due to annealing. In eq.(16), the second term is presented the radio-stimulated thermoluminescence yields of the non-dosimetric deep trapping levels.

Dose dependence of the sensitization factor, Y, is given by the followings;

$$(\partial Y/\partial D_p) = \sum_{ijk} K_{jk}\,\theta_{ij}\,N_i(1-(P_i/D_t S_0))(\sigma_i + D_p(\partial\sigma_i/\partial D_p)) \qquad (17)$$

where D_p and D_t are post radiation dose and test radiation dose, respectively.

In case of low LET radiation, eq.(17) from eq.(10) is an increasing

function of the dose, but in case of irradiating of high LET radiation eq. (17) from eqs. (7) and (12) decreases with increasing LET of post radiation. These result may reveal that mechanism for the sensitization factor can be explained by the releasing probability change model.

References

1. T. Nakajima, Radiation Physics Research, 3, No. 2, 15-22 (1970).
2. C.A. Carlsson and G.A. Carlsson, Proc. 2nd Intern. Conf. on Lumin. Dosim., 302-309 (1968).
3. J.R. Cameron and D.W. Zimmerman, USAEC Report COO-1105-113(part-1) (1966).
4. W.R. Hendee, G.S. Ibbott and D.B. Gilbert, Intern. J. Appl. Radiat. & Isot., 19, 431- 436 (19 (1968).
5. N. Suntharalingam and J.R. Cameron, Phys. Med. Biol., 14, 397-410 (1969).
6. J.T. Randall and M.H.F. Wilkins, Proc. Roy. Soc., (London) A184 366-389 (1945).

On the Sensitivity Factor Mechanism of Some Thermoluminescence Phosphors

Toshiyuki Nakajima

Division of Physics, National Institute of Radiological Sciences,
9-1, 4-chome, Anagawa, Chiba-shi, Japan

Abstract

The sensization factor of Mg_2SiO_4(Tb) and LiF is studied. It is obtained that the factor diminishes with increasing annealing temperature, and is dependent on linear energy transfer of both the previous and test radiations and that the sensitization factor of the sensitized phosphor with radiation of higher LET is greater than un-sensitized one even in the low dose region of the previous dose. The sensitization factor phenomena of LiF and Mg_2SiO_4 phosphors are caused by the radio-stimulated thermoluminescence of electron and hole captured in the deeper trapping levels.

Introduction

It has been reported that sensitivity of LiF TLD phosphor, annealed at low temperature after irradiation, increases with decrease of the annealing temperature, and that one of causes of changes in the sensitivity is radio-stimulated thermoluminescence of trapped electron in deep non-dosimetric traps.[1] On the other hand, Cameron and his co-workers have found the sensitivity factor phenomena in LiF phosphor which are similar to the sensitization of the annealed phosphor after irradiation, and have tried to explain them with the competing trap model.[2] But mechanism for the sensitivity factor and sensitization of the annealed phosphor after irradiation is not yet clarified.

The present experiment was made to obtain information on the mechanism for the sensitization (sensitivity) factor of LiF and Mg_2SiO_4(Tb) phosphors.

Experiments

Powdered Mg_2SiO_4(Tb) phosphors, enclosed in a glass capsule of about 15 mm length and 2 mm in dia, and powdered TLD-100 LiF phosphor were used in this experiment. The sensitization of Mg_2SiO_4(Tb) phosphor has been especially investigated.

The sources of γ-ray radiation were both 2000 curie ^{137}Cs and ^{60}Co units designed for the radiation theraphy. The X-ray radiation of 38 keV was obtained from a machine designed for the theraphy. The exposure to the phosphor was measured with Victoreen condenser chamber, Rad Con chamber or Fricke dosimeter according to the order of irradiating dose.

After irradiation at room temperature and subsequently thermal treatment

at the temperature from 300 °C to 500 °C, the phosphors were irradiated with a test radiation and subsequently their thermoluminescence yields were measured to obtain the sensitization factor with a Dai Nippon Toryo TLD Reader of model 1200 as a TLD reader.

Experiment on radio-stimulated thermoluminescence from the irradiated phosphor is undertaken to obtain some information on the mechanism for the sensitization factor. The radio-stimulated thermoluminescence is obtained by following processes:

1) The phosphor is irradiated at room temperature with 10^4 or 10^5 R of γ-rays from ^{60}Co source and sensitized.
2) The irradiated and sensitized phosphor is thermally treated at 300 °C or 350 °C for one hour.
3) Both the treated and virgin phosphors are irradiated again with either X-ray or γ-rays to compare the glow curves between them.
4) The irradiated phosphors are heated with a constant heating rate of 10 °C/min and its glow curves are recorded.

Results

1) Dependence of S/S_0 on Annealing Temperature

Fig. 1 presents the changes in the sensitization factor of Mg_2SiO_4(Tb) phosphor, irradiated with one R of the test radiation, as a function of annealing temperature and as a parameter of the previous and sensitizing irradiation dose.

As can be seen in Fig. 1, it is observed that the sensitization factors diminish with increasing the annealing temperature regardless of the sensitizing irradiation dose. However, a tendency of the deterioration of the sensitization factors markedly varies with the sensitizing irradiation dose. In case of the phosphors which are thermally treated at a relatively lower temperature, the sensitization factor of the phosphor, irradiated with high dose of the sensitizing radiation, is very large and is greater than that irradiated with lower dose.

In fig. 2, presents also the dependence of the sensitization factor of Mg_2SiO_4(Tb) phosphor as a function of the given dose of sensitizing radiation and as a parameter of annealing temperature. From Fig. 2, also, the sensitization factor of the annealed phosphor at higher temperature is smaller than that at lower temperature.

2) Dependence of S/S_0 on Irradiation Dose of Sensitizing radiation

Effect of sensitizing irradiation dose on the sensitization factors of Mg_2SiO_4(Tb) phosphor is observed.

Fig. 3 shows the changes in the sensitization factor of Mg_2SiO_4(Tb) phosphor, as a function of the sensitizing irradiation dose.

Curve A in Fig. 3 is the changes in the sensitization factor of the phosphor irradiated with the sensitizing radiation of 38 keV X-rays and curve B is of γ-rays from ^{60}Co source.

In case of using the γ-rays for the sensitizing irradiation, the sensitization factor is nearly equal to unit value of one in the sensitizing dose range from 3 R to about 100 R, but it gradually increases with increasing the sensitizing dose.

On the other hand, the sensitization factor of the sensitized phosphor with the radiation of 38 keV X-rays is greater than the unit value in the low dose region of the sensitizing irradiation. This fact reveals that the sensitivity of these treated phosphors with higher LET radiation is greater than the un-treated one even in the low dose region of the sensitizing irradiation. However, a gradient of the 38 keV X-ray irradiated sensitization factor on the sensitizing dose was smaller than that of the ^{60}Co γ-ray factor. In the sensitizing dose region of 600 R or over, the X-ray sensitization factor was

smaller than that γ-ray factor.

It is obtained from this result that, in the region of low sensitizing irradiation dose, difference in linear energy transfer(LET) of the sensitizing radiation brings about the different sensitization factor of the phosphor. But, Cameron and his co-workers have reported that difference in LET of the sensitizing radiation dose not bring about the different sensitization factor.

3) Dependence of S/S_0 on Test-Irradiation Dose

Fig. 4 presents the changes in the sensitization factor of Mg_2SiO_4(Tb) phosphor as a function of the test radiation dose. The crystal was thermally treated at 350 °C for one hour after irradiated with 10^4 R of either γ-rays or X-rays. In fig. 4 the vertical axis reveals a thermoluminescence yield divided by the test radiation dose. Curve A is the dependence of the sensitization factor of the γ-ray irradiated phosphor on the test irradiation dose of γ-rays from ^{137}Cs source, after irradiation of 38 keV X-ray. Curves B and C show the changes in the sensitization factor of the sensitized phosphors with ^{60}Co γ-rays due to different LET of the test radiation.

As shown in curves B and C of Fig. 4, in case of the different LET of the test radiation, the sensitization factor is different from each other even though the phosphor is irradiated with the sensitizing radiation of the same LET. Furthermore, it is obtained from curves A and B of Fig. 4 that, in case of the different LET of the sensitizing radiation, although the LET of the test radiation is same, the factor differs from each other.

In case of the former results, when the phosphor is irradiated with the test radiation of higher LET, the sensitization factor is nearly equal to one in the dose region from one roentgen to about 50 R. But after reaching the maximum value at 300 R, the factor decreases with increasing the test radiation dose. On the other hand, in case of the latter, it is observed that when the phosphor is irradiated with the test radiation of same low LET, the sensitization factor of the sensitized phosphor with the radiation of higher LET is greater than that of lower LET.

4) Radio-Stimulated Thermoluminescence as Mechanism for the Factor

It has been found difference of the sensitization factor of LiF phosphor due to irradiation of different LET radiation. But the cause on the difference is not yet clarified.

Experiment has been undertaken to obtain some information on the causes of this difference.

Fig. 5 shows a glow curve of the Harshaw TLD-100 LiF irradiated with 10^4 R after annealing at 300 °C for 30 min in the atmosphere of 10^{-2} mm Hg vacuum. In general, the peaks which appear in the temperature region from room temperature to about 300 °C, are used for the dosimetry. Accordingly, the glow peaks in the region of 300 °C or over is not used for the dosimetry and the trapped electron which contributes to these glow peaks remains in the phosphor. Actually, the glow peak is observed from the annealed LiF and Mg_2SiO_4(Tb) at about 300 °C and 400 °C, respectively, after irradiation.

To obtain the sensitization factor, the phosphor has been thermally treated at 350 °C or below for one hour. But it is clear from Figs. 5 and 6 that the annealing temperature is not suitable for releasing the trapped electrons in all trapping levels of the phosphor.

Figs. 7 and 8 show the effects of the re-irradiation on the remained electron captued in the deeper traps.

It is known that photo-stimulated thermoluminescence is emitted from the irradiated crystal, when it is heated after illumination at lower temperature than the irradiated temperaure. The photo-stimulated thermoluminescence has been reported to be caused by the photo-stimulation of the deeper trapped electron due to illumination.[1] As can be seen in curve of Figs. 7 and 8, the dosimetric glow peaks from the sensitized phosphor are greater than that from

the un-sensitized one. Especially, all glow peaks of the sensitized Mg_2SiO_4 (Tb) phosphor were higher than the un-sensitized one.

These results may reveal that when the phosphor which involves the electron captured in the trapping levels, is irradiated again, the re-excited electrons with radiation is re-trapped in the shallow trapping levels. Accordingly, the glow peak height from the sensitized phosphor is composed of the intrinsic and the radio-stimulated heights. Namely, it is concluded that the phenomena of the sensitization is caused by the radio-stimulated thermoluminescence due to re-trapping the remained electrons in the deeper traps into the shallow traps.

Discussion

The experimental results described in the present work has been provided information that should help in explaining the causes of the sensitization. The causes of the sensitization phenomena can be explained as follows;

When the thermoluminescence phosphors are excited with ionizing radiation. many of the electron are trapped at the trapping levels. Now, if the trapped electrons in the trapping levels between E_0 and $E_i(>E_0)$ are released by thermal treatment, the electrons in the levels of $E_j(>E_i)$ will remain in the phosphor.

When the remained electrons in the deeper trapping levels E_j are excited again with irradiation the radiation, the electron of E_j transfer into the trapping levels below E_i. The transfered electrons contribute to the thermoluminescence for the dosimetry. Therefore, the gross dosimetric thermoluminescence yield for the dosimetry is the sum of the intrinsic thermoluminescence yield due to irradiation and the radio-stimulated thermoluminescence yields.

Next, causes on the different sensitization factor due to different LET of both test and sensitizing radiations will be discussed.

To obtain the relative glow peak heights from the glow curve, the glow curve is recorded through heating the irradiated phosphor with heating rate of 10 °C/min. When the crystal of LiF is irradiated with γ-rays, its relative glow peak heights are changed with increasing the absorbed dose, as can be seen in Fig. 9. The relative heights in the higher temperature region —— the non-dosimetric peak temperature region —— increase with the absorbed dose.

The behaviour of the glow peak heights has been found in the Mg_2SiO_4(Tb) phosphor, also. As abovementioned, if the cause on the sensitization factor is due to the radio-stimulated thermoluminescence, it will be easily understood that the sensitization factor of the phosphor with higher dose of the sensitizing radiation is greater at lower annealing temperature than that with lower dose.

On difference in the sensitization factor due to different LET of the sensitizing radiation, it will be explained by following;

The radio-stimulated thermoluminescence yields are increased with the concentration of the trapped electron which stores in the non-dosimetric deep traps of the sensitized phosphor. According to the Carlsson's results,[3] in case of irradiation of high LET radiation, the relative concentration of the trapped electron between the deeper and shallow traps is scarcely dependent on the dose.

On the other hand, in case of low LET radiation, as shown in Fig. 9, the relative concentration of the trapped electron in each trap increases with the absorbed energy. Therefore, after annealing, the relative concentration of the trapped electron which remained in the traps is influenced by both LET and absorbed energy of the sensitizing radiation. If the absorbed energy of the phosphor due to irradiation of the sensitizing radiation is a constant, the concentration will be increased with increasing the LET. Therefore, the sensitization factor of the phosphor with the higher LET of the test radiation

is greater than that with the lower LET. If the LET of the sensitizing radiation is a constant, the concentration per dose increases with increasing the absorbed energy, as can be seen in Fig. 9. Therefore, the sensitization factor increases with the dose of the sensitizing radiation

Conclusion

The sensitization factor has been found to be diminished with annealing temperature, and to be differed with changing the LET of both sensitizing and test radiations. Furthermore, it is obtained that in the low dose of sensitizing irradiation the factor of the sensitized phosphor with 38 keV X-rays is greater than that of the un-sensitized one.

It may be concluded that the sensitization factor phenomena are caused by the radio-stimulated thermoluminescence due to re-exciting the trapped electrons remained in the deeper trapping levels. Various phenomena in the sensitization of the phosphor response have been found to be easily understood by the radio-stimulated thermoluminescence and our model for the non-linear response of the phosphor.

Acknowledgment

The author is indebted to Dr. Y. Yamamoto, of the Tokyo Metropolitan Isotope Research Centers, for helpful discussions on the interpretation of the results. Grateful acknowledgement is also due to Miss I. Taneichi for her assistance of experiment

References

1. D.W. Zimmerman, C.R. Rhyner and J.R. Cameron, Health Physics, 12, 525 - 531 (1966)
   T. Nakajima, Health Physics, 16, 509 - 51 (1969)
2. N. Suntharalingam and J.R. Cameron, Phys. Med. Biol., 14, 397-410(1969)
3. C.A. Carlsson and G.A. Carlsson, Proc. 2nd Intern. Conf. on Lumin. Dosim., 302-309 (1968)

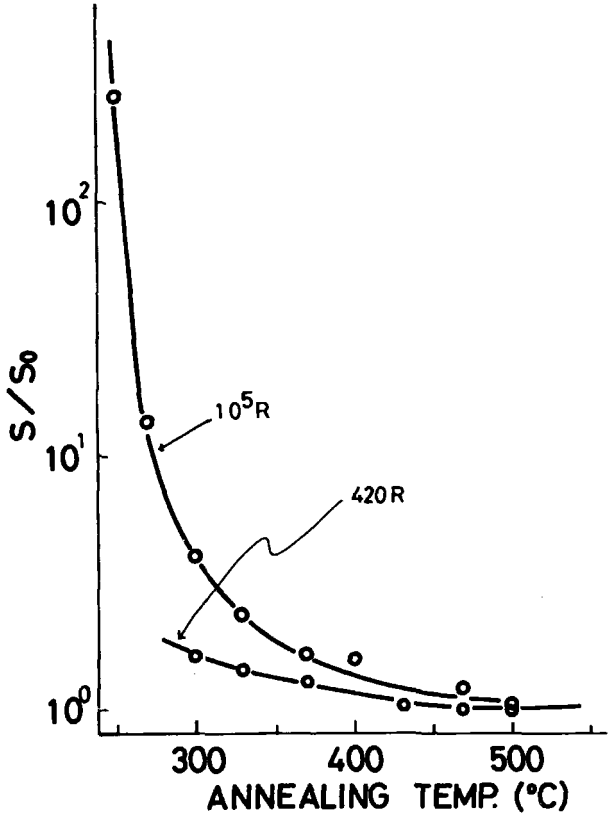

Fig. 1. Effect of annealing temperature on the sensitization factor of Mg_2SiO_4(Tb) phosphor as a parameter of the sensitizing irradiation-dose(These phosphors were thermally treated one hour after irradiation of gamma-rays from ^{60}Co)

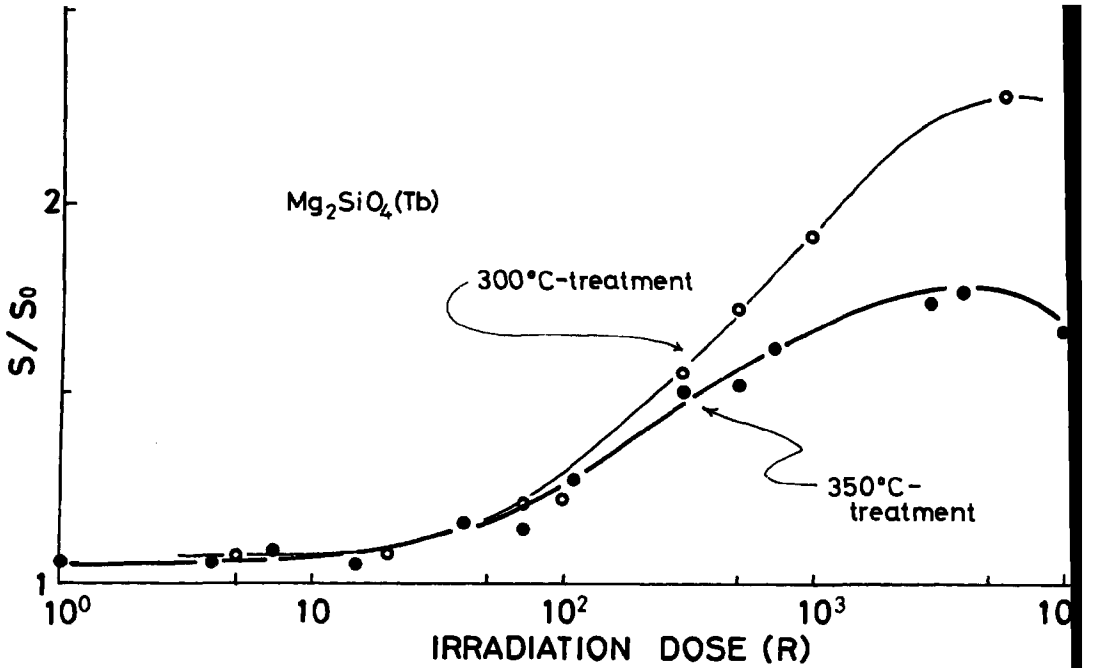

Fig. 2. Changes in the sensitization factor of $Mg_2SiO_4(Tb)$ as a function of the sensitizing irradiation dose and as a parameter of annealing temperature

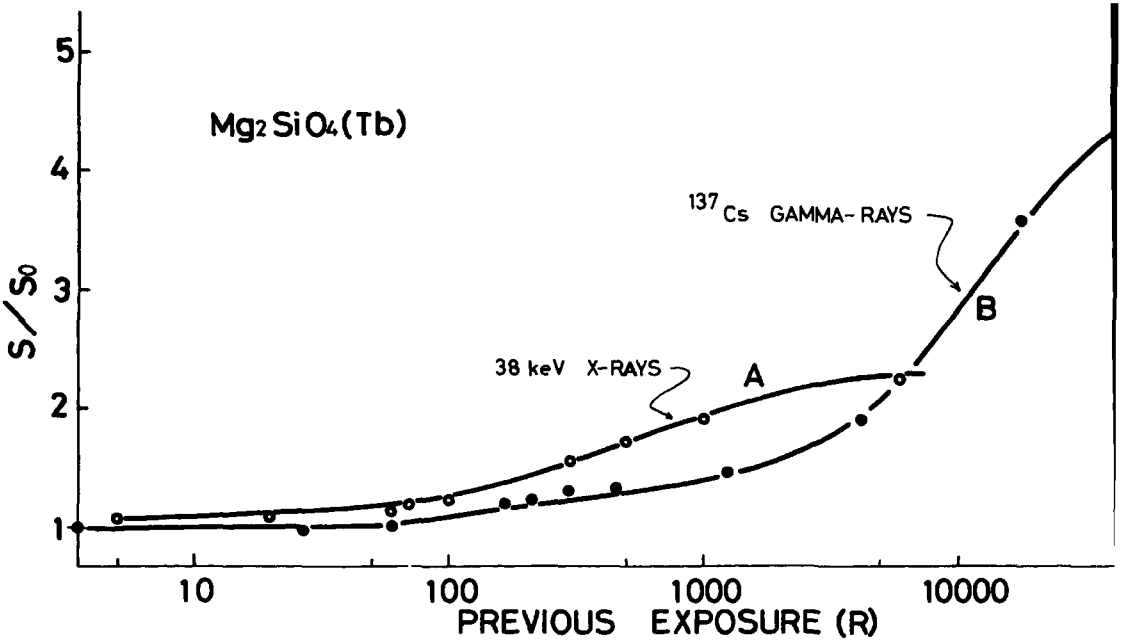

Fig. 3. Changes in the sensitization factor of Mg_2SiO_4(Tb) as a function of the sensitizing irradiation dose and as a parameter of the LET of the sensitizing radiation

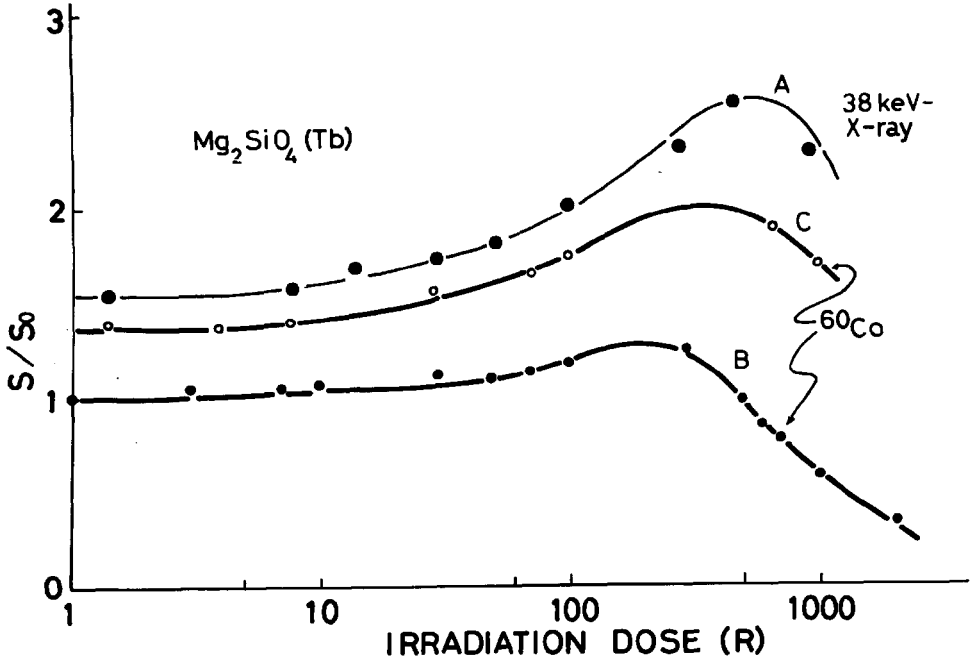

Fig. 4. Influence of the test irradiation dose on the sensitisation factor of $Mg_2SiO_4(Tb)$(A: the test radiation is gamma-rays of ^{137}Cs after irradiation of 10^4R X-ray and subsequently annealed for one hour at 350°C, B: the test radiation of 38 keV is used after gamma-ray irradiation of 10^4R, C: the test radiation of ^{137}Cs gamma-rays is used after gamma-ray irradiation of 10^4 R).

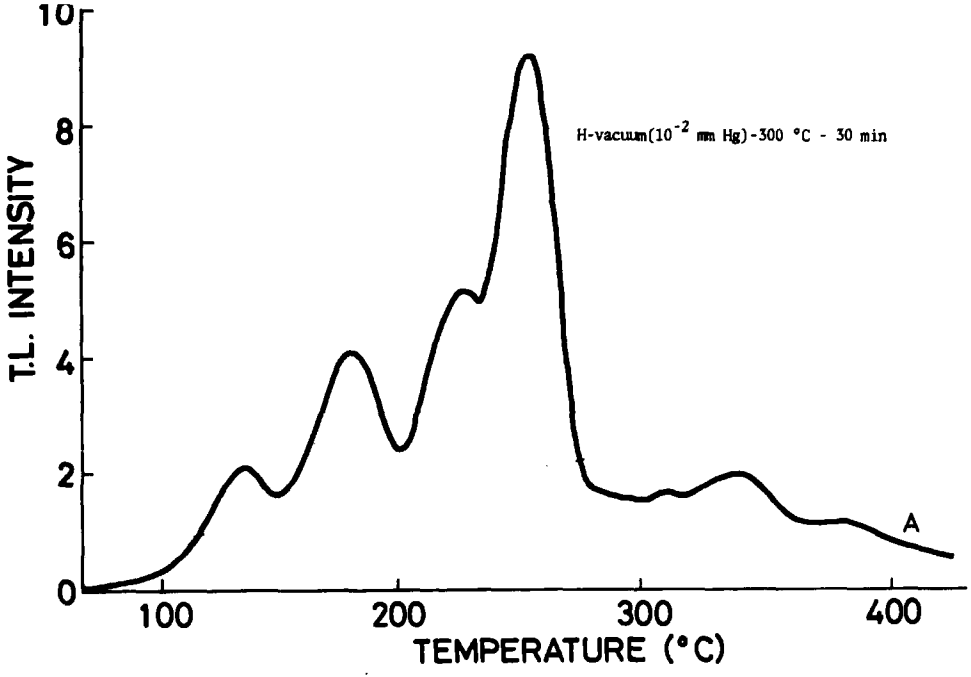

Fig. 5. Thermoluminescence glow curve of Harshaw TLD-100 LiF irradiated with 10^4 R after thermal treatment at 300 °C for 30 min in vacuum of 10^{-2} mm Hg

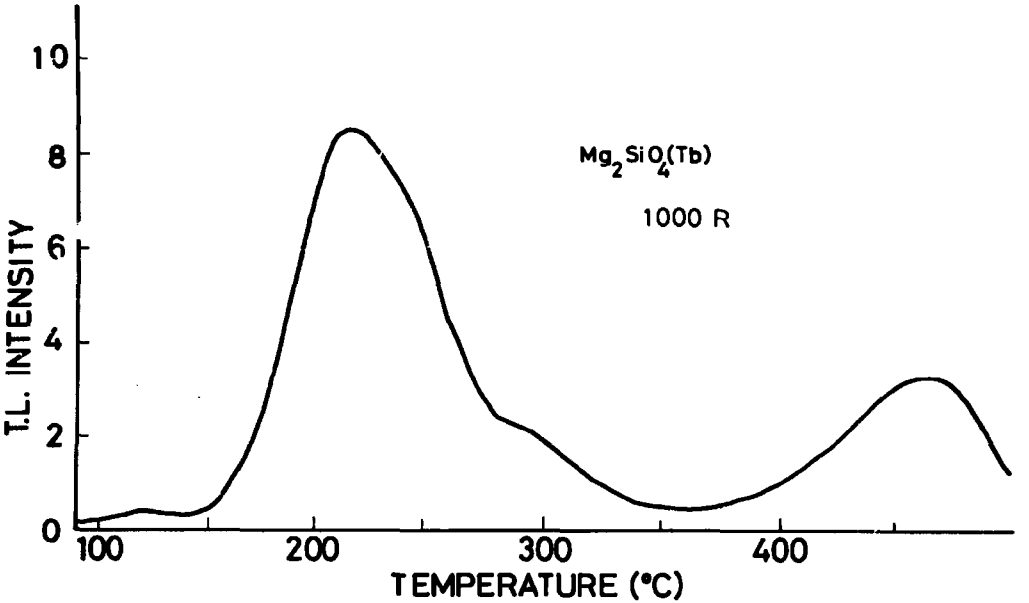

Fig. 6. Thermoluminescence glow curve of the Mg_2SiO_4(Tb) phosphor irradiated with 10^3 R

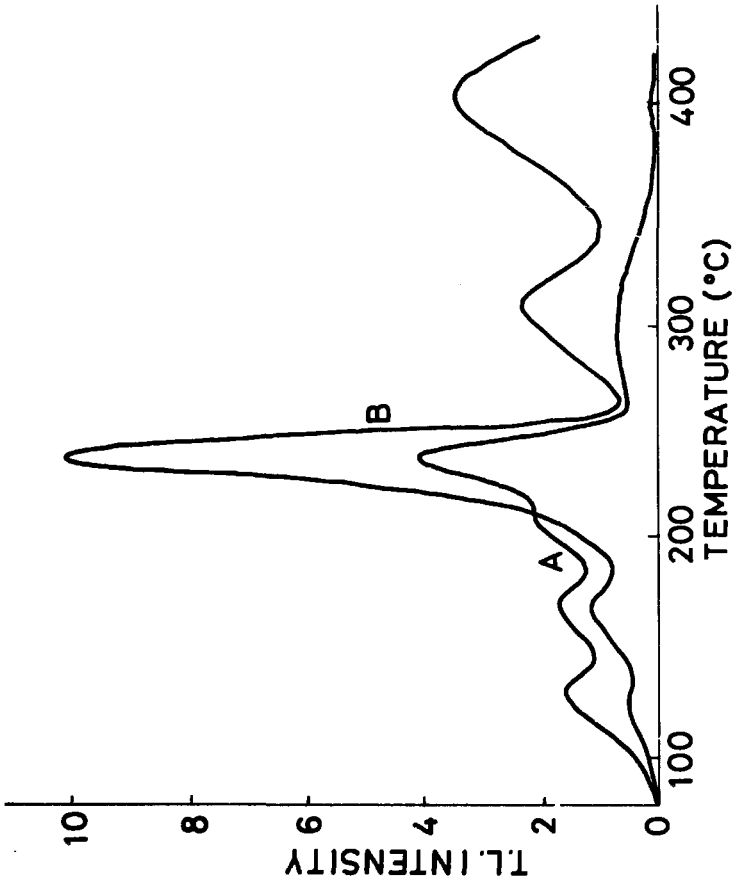

Fig. 7. Radio-stimulated thermoluminescence of TLD-100 LiF(curve A: the virgin of the crystal irradiated with 10^3 R after thermal treatment at 300 °C for one hour in argon gas, B: irradiated with 10^3 R after irradiation and sensitization with 10^5 R and subsequently annealing at 300 °C for one hour in argon gas)

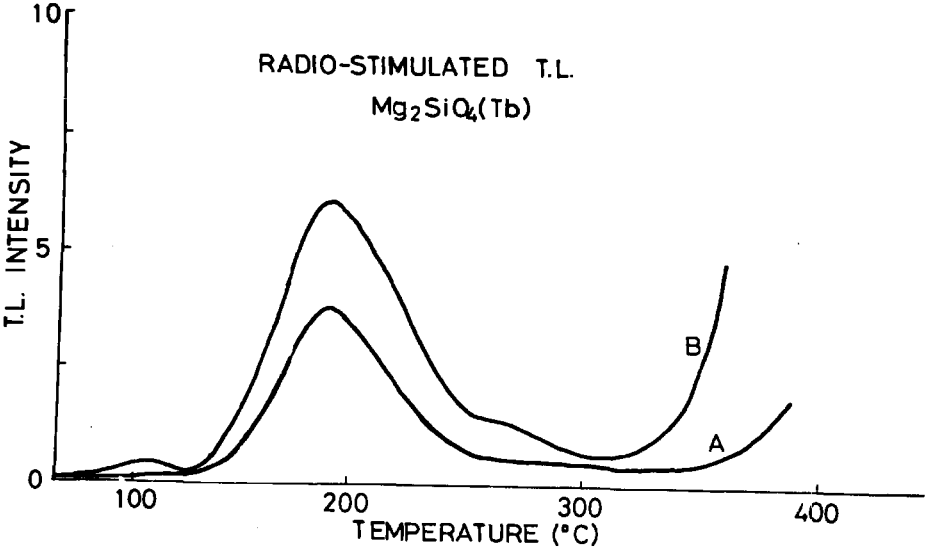

Fig. 8. Radio-stimulated thermoluminescence of $Mg_2SiO_4(Tb)$ (curve A: the virgin crystal irradiated with 10^3 R, B: with 10^3 R after irradiation and sensitization with 10^4 R, and subsequently annealing at 400 °C for 30 min)

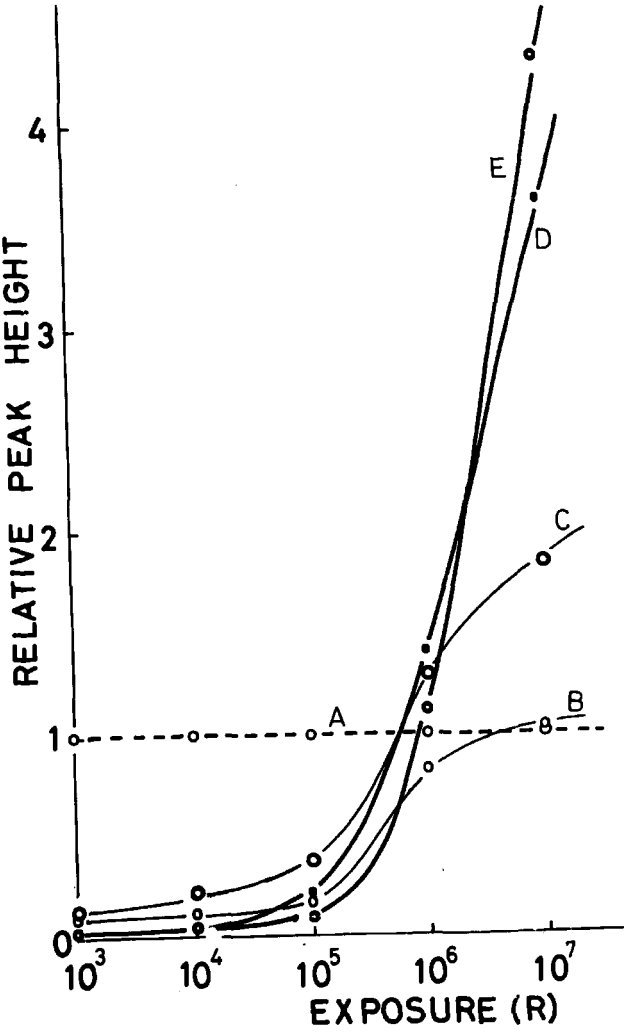

Fig. 9. The ratio between each glow peak height and 250 °C one in TLD-100 LiF phosphor as a function of absorbed energy(A: glow peak at 250 °C, B: at 310 °C, C: at 340 °C, D: 370 °C, and E: at 400 °C)

The TSEE Response of Ceramic BeO covered with Different Absorbers During Gamma and X-Ray Irradiation

by

E. Rotondi - T. Suppa

Lab. Dosimetria e Standardizzazione
C.N.E.N. - C.S.N. Casaccia
Roma (Italy)

Abstract

Owing to the very thin layer involved in exoemission process, the response of a TSEE detector is largely influenced by the material used as cover during γ and X rays irradiation.

In this paper a study was conducted on the TSEE response of ceramic BeO covered with materials of different atomic number such as aluminium and gold.

For X rays of 66 keV effective energy, the response with gold cover is 18 times higher than with aluminium. With a gold cover the response to X rays is much higher than to cobalt. It is also shown that the simultaneous use of two BeO detectors covered respectively with aluminium and gold can be utilized for evaluating the low energy X ray component in an unknown field of photon radiation. It has been observed the diffusion of the gold in the BeO produces the same effect of covering the BeO with gold layer during irradiation.

INTRODUCTION

The interactions of photons with the materials covering TSEE detectors give rise to many electrons, which reach the sensitive layer and contribute to the exoemission phenomenon.

At photon energies where the photoelectric process predominates,

this contribution varies strongly with the atomic number.

This paper is mainly concerned with the response variations produced by covering ceramic BeO with gold or aluminium during irradiation.

Moreover, measurements have been carried out with gold impregnated samples, to investigate whether the gold diffused in the BeO increases the response enhancing the exoemission probability or giving rise to more electrons available to be trapped.

1. EXPERIMENTAL

The measurements have been carried out on both bare and gold plated samples of sintered ceramic beryllium oxide[1], Thermalox 995 (discs 0.9 cm in diameter and 0.5 cm thick).

The apparatus, reported elsewhere[2] consisted of a gas flow Geiger counter provided with a linear heating rate system.

To obtain a good thermal annealing the BeO was maintained, before being used, at 600°C for 20 minutes. Each reading was terminated at 350°C and the sample was reused without annealing.

The irradiations have been performed with Co^{60} and X rays of 66 keV effective energy.

2. RESULTS AND DISCUSSION

2.1. BeO bare sample - Co^{60} irradiation

During the cobalt irradiation the BeO discs have been covered with either an aluminium or gold layer of thickness 600 mg/cm^2.

The exoemission curves reported in Fig. 1 are relative to 1 R exposure, the curve 1 refers to the sample covered with gold, the curve 2 to that covered with aluminium. The corresponding integral counts are 19000 and 16000, with standard deviation σ = 6%.

The results show that at the cobalt energy the TSEE response is rather insensitive to the different Z of the covers. Indeed in this case Compton interactions and pair production are predominant and the mass energy absorption coefficient varies slowly with the atomic number.

2.2. BeO bare sample - X rays irradiation

For low energy X rays the situation is quite different since the

photoelectric process, which is strongly energy and atomic number dependent, predominates.

In Fig. 2 the results obtained with BeO samples covered respectively with 10 mg/cm^2 of aluminium and gold are reported. The exposure was 50 mR, the curve 1 (integral counts 36000, σ = 6%) corresponds to the sample covered with gold, the curve 2 (integral counts 2000, σ = 6%) to that covered with aluminium. The response with gold is 18 times higher than that with aluminium, in good agreement with mass energy absorption coefficient ratio of the two metals at the considered energy.

Comparing X rays and cobalt results and taking into account the different exposures involved, it follows that the response to X rays is higher than to cobalt. This effect is greatly increased when using gold as a cover, pointing out the strong energy dependence introduced by the presence of a high Z material during the irradiation.

From the above considerations the possibility arises of using the energy and Z dependence to evaluate the low energy X rays component in an unknown field of photon radiation.

The measurements carried out in this connection have been reported in Fig. 3. The BeO sample, covered in turn with aluminium and gold, was irradiated with 1 R of cobalt plus 50 mR of X rays. The curve 1 refers to the sample covered with 10 mg/cm^2 of gold, the curve 2 to that covered with 10 mg/cm^2 of aluminium. The difference between the two curves is due essentially to the 50 mR of X rays component since 1 R of cobalt gives in both cases approximately similar contributions, as seen before.

2.3. Gold Plated Sample

The BeO discs were plated with 50 µg/cm^2 of gold and heated for two hours at 600°C to achieve the diffusion of the gold in the BeO.

Concerning the cobalt irradiation the gold plated samples give the same response as bare ones. The gold diffusion in the BeO does not produce any change in the sensitivity.

For X rays, 1 R exposure, the response of the gold plated sample was three times higher than the bare one, as shown in Fig. 4.

To investigate whether the increase in the response can be attributed entirely to the photon interaction with gold, the following experiment was performed.

The bare and plated samples were covered with a gold layer of 10 mg/cm^2 thick and exposed to 50 mR of X rays. The results obtained are shown in Fig 5 and it can be seen, that the response of the two samples is very

similar.

Therefore we may conclude that the difference in the response observed in Fig. 4 is only due to the photoelectric process which takes place in the 50 $\mu g/cm^2$ of gold diffused in the sample.

In speculating whether or not the gold diffusion process modifies the physical properties of the sensitive layer, we can say, as far as our experiment is concerned, that if changes occur they do not influence the exoemission process.

References

1) K. Becker, J.S. Cheka, K.W. Crase, R.B. Gammage - Advances in Physical and Biological Radiation Detectors.
IAEA Vienna 25 - 35 (1970).

2) E. Rotondi, F. Bordoni.
CNEN-RT/FI 7 - 15 (1970).

Fowler

Do you know whether the diffusion of the gold occurs efficiently at 600°C? Why did you choose this temperature?

Rotondi

I cannot give an answer about the efficiency of the diffusion, but, as reported by other investigators, it is likely that diffusion takes place at least into the sensitive layer. The temperature of 600°C has been chosen to conform with the thermal treatment used for annealing of the bare samples. Different temperature treatments would introduce sensitivity changes not related to gold diffusion in the BeO.

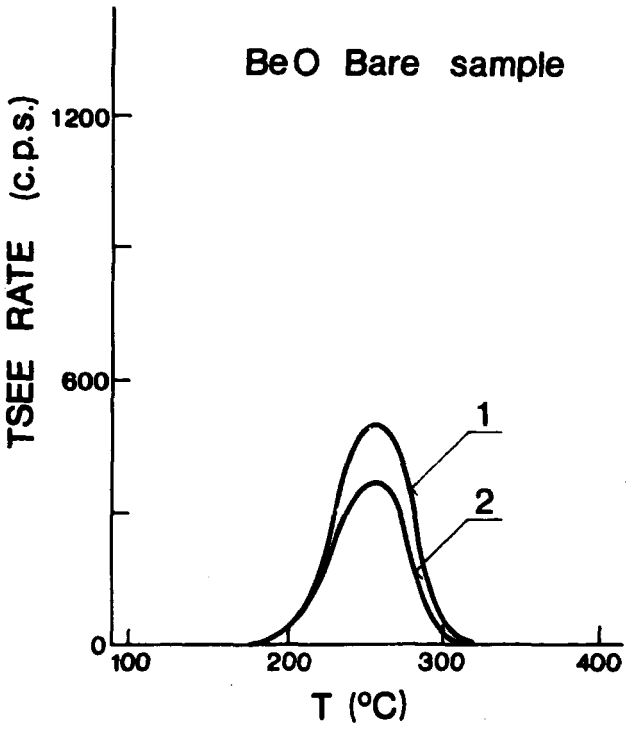

Fig. 1 Response to cobalt, exposure 1 R.
1 - gold cover 600 mg/cm^2
2 - aluminium cover 600 mg/cm^2

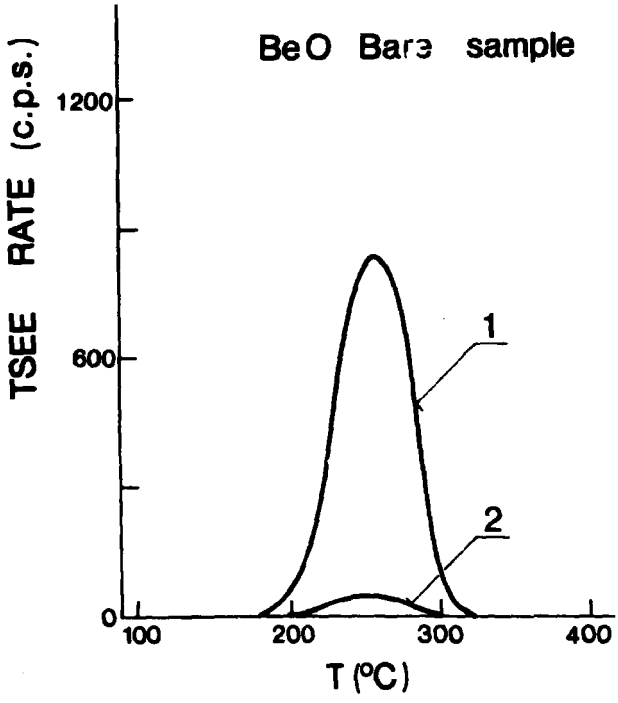

Fig. 2 Responce to X rays, exposure 1 R
1 - gold cover 10 mg/cm^2
2 - aluminium cover 10 mg/cm^2

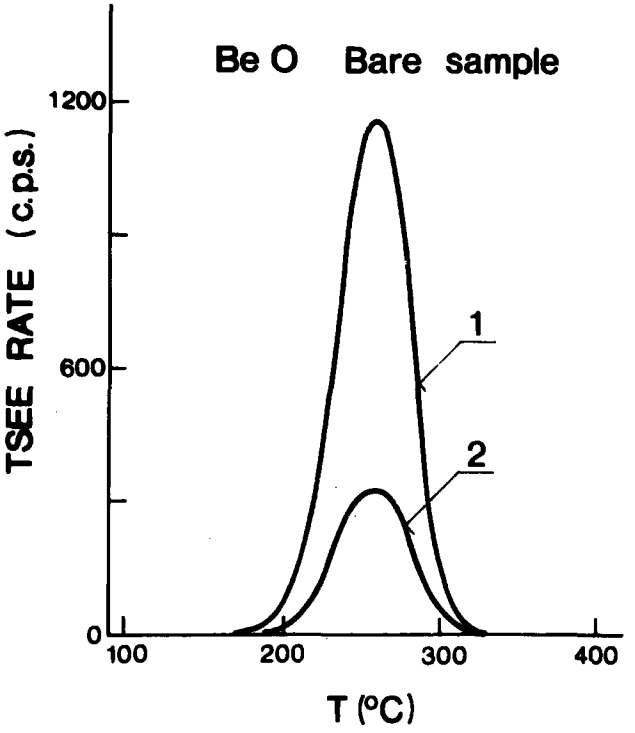

Fig. 3 Response to 1 R of cobalt plus 50 mR of X rays:
1 - gold cover 10 mg/cm^2
2 - aluminium cover 10 mg/cm^2

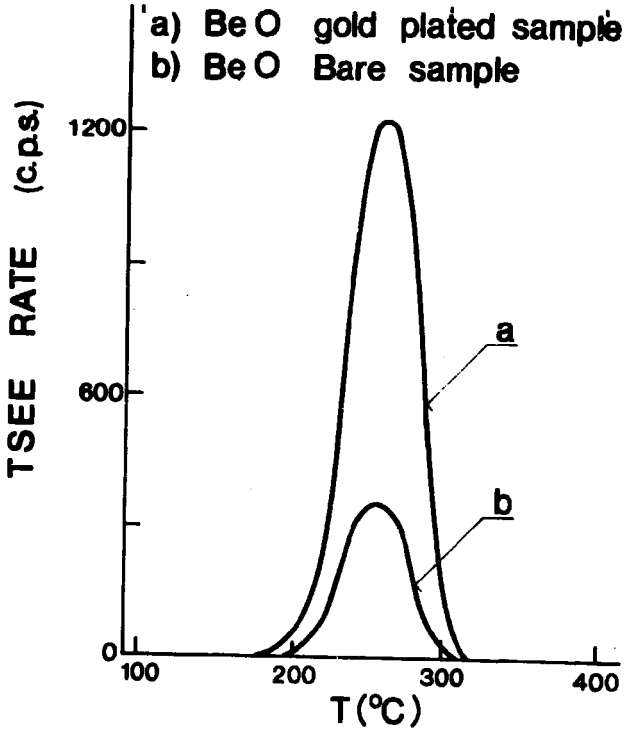

Fig. 4 Response to X rays, exposure 1 R.
a - gold plated sample
b - bare sample

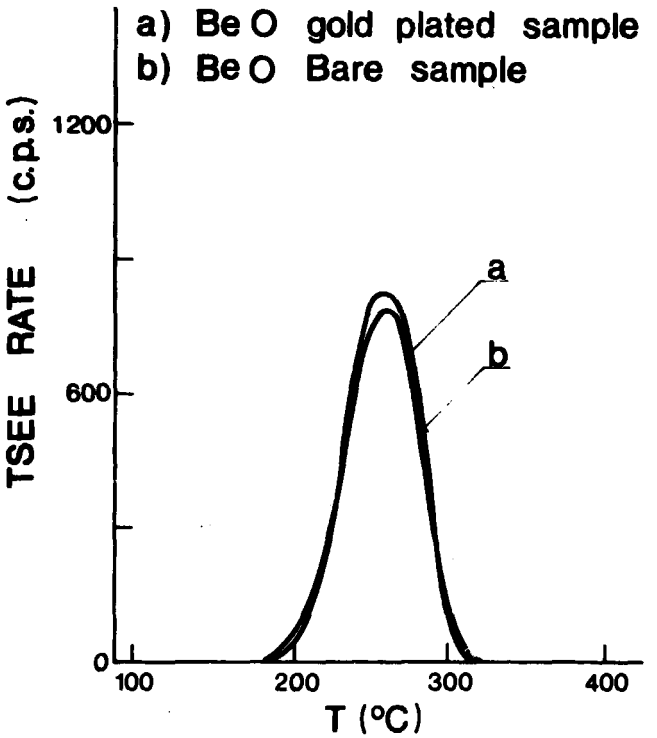

Fig. 5 Response to X rays, exposure 50 mR, gold cover 10 mg/cm^2:
a - gold plated sample
b - bare sample

Low Temperature Monitoring Using Thermoluminescent Materials

by

Robert D. Jarrett, J. Halliday and J. Tocci

U. S. Army Natick Laboratories
Natick, Massachusetts

Abstract

Organoleptic testing of radappertized foods has shown that acceptability is highly correlatible with irradiation temperature. In general, irradiation temperatures in the region of -30°C yield the most acceptable product. Thus, a requirement has been generated, particularly in commercial applications, for a dosimeter capable of being used in radiation field mapping and production dose monitoring at these temperatures.

Of the various dosimetry systems considered for this application, a thermoluminescent system shows the most promise. Samples of the commercially available materials were subjected to a screening and evaluation procedure to determine their applicability. The results of this study are discussed including calibration data for these thermoluminescent materials for gamma irradiations at various temperatures. For example, a sample of TLD-100 in its loose powder form yields values twenty to forty percent lower when irradiated at -196°C than when irradiated at 25°C. Such results show the potential usefulness of thermoluminescent materials but point to the critical dependence of the calibration function on temperature.

A standard procedure for "reading out" thermoluminescent materials is discussed. This procedure involves, among its other features, a ten minute annealing period at 100°C prior to readout. This was found necessary in order to eliminate a number of low energy traps that contribute to spurious results.

Again, for commercial radio-sterilization applications, a suitable total dose range is necessary. The potential applicability of certain high dose (in the megarads region) materials is discussed. For example, our evaluation of Isomet LiF in both its single crystal and loose powder forms will be contrasted with results on this material as reported by Tochlin.

This paper demonstrates the requirement for a low-temperature dosimetry system and evaluates the presently available thermoluminescent materials

(both commercially available or those in a developmental stage) with respect to their potential for meeting this requirement.

General Introduction

In numerous applications of ionizing radiation there exists the need for a dosimetry system with a rather specialized set of properties - the capability of measuring doses in the megarad region and at sub-zero centigrade irradiation temperatures. It is the intent of the present work to explore the applicability of thermoluminescent materials in fulfilling this dual requirement. The development of a satisfactory readout technique and some of the more significant pitfalls encountered are discussed. Several selected thermoluminescent materials are evaluated and discussed relative to their "ambient" and low temperature dose response.

This work was performed using the irradiation facilities of the U. S. Army Natick Laboratories, Natick, Massachusetts, U. S. A. The Irradiation Laboratory has a nine kilowatt electron linear accelerator capable of producing 12 MeV electrons, three Cobalt-60 sources (1.5 megacuries, 35 kilocuries, and 7 kilocuries) and a 200 kilocurie Cesium-137 source. All gamma irradiations were made using the two smaller Cobalt-60 research irradiators which have dose rates of 4.4 kilorads and 0.56 kilorads per second.

Introduction

The basic phenomenon underlying thermoluminescent dosimetry (TLD) is the freeing of trapped electrons by thermal stimulation. A plot of the intensity of the light emitted by the luminescent material as a function of its heat treatment is the familiar "glow" curve. Since the heat treatment involves a temperature-time relationship, the glow curve and hence the results of a thermoluminescent dosimeter reading must be considered relative to the mode of heat treatment. A large number of temperature profiles are possible; three basic types are illustrated in Figure 1. The first type (Figure Ia) features a preheat rate from A to B followed by the primary heating rate from B to C. A second type (Figure Ib) involves only the primary heating rate from A to C. A more versatile type (Figure Ic) inserts an annealing plateau between the preheat part of the cycle and the commencement of the primary heating. In all cases C represents the maximum temperature achieved and is usually the point where the integration of the light output is terminated.

The basic commercial instrument used was the Harshaw Model 2000 Analyzer (I). It was operated in the temperature range 40°C to 410°C using various primary heating rates. Samples of the thermoluminescent powder were dispensed onto the heating pan and then subjected to the desired temperature profile.

Post Irradiation Annealing

It has been suggested (2) that annealing the material for 10 minutes at 100°C after irradiation and before reading the samples would improve the results. This improvement is based upon the fact that heating at 100°C would greatly reduce or remove the traps below that temperature and give a reliable base line. We evaluated the effectiveness of this annealing procedure by dispensing a sample of irradiated TLD-100 powder into the heating pan of the reader and observing the output signal of the photomultiplier tube as a function of time when the sample was heated to and held at 100°C. It was observed that the signal approached a constant value after 8.5 minutes.

These results demonstrate that if the sample is held at 100°C for 10 minutes the base line is stable and any inaccuracy in timing would have a negligible effect.

Based upon the fact that post annealing stabilized the base line we modified our reader to allow post annealing to be performed in the reader as typified by Figure Ic. It is possible to vary the post annealing temperature (B) to any value and the annealing time (B to B^1) to any period. These modifications also allowed us to reduce the post anneal time to less than 10 minutes as the samples are now held for an exact time which eliminates the inaccuracies which would be involved in heating the samples in an oven for less than 10 minutes and transferring them to the reader. For most of the results reported we used this procedure with an annealing time of 0.5 minutes. It should be noted that the coulomb meter operates only during the period B^1 thru C. An additional advantage in using this readout procedure is that the temperature of the pan and sample, prior to the start of readout, has less effect on the peak height and integrated charge values. Therefore, we improved the readout reproducibility with this heating procedure.

As is obvious from the preceding description of an optimum readout technique, an integrated peak area as well as peak height(s) is a useful parameter in correlating luminescence with dose level. Based upon the standard error of ten readings at a given dose it was, in fact, determined that the integrated charge (output from the photomultiplier tube) gave the more reproducible results. The standard error using peak height measurements was approximately 5% as contrasted to a value of 2% using integrated charge measurements. The doses used for the evaluation were in excess of ten kilorads.

There are several effects observed incidental to the heat treatment which might lead to instrumental artifacts. These involve mainly the composition and pre-history of the heating pans and the contribution of infrared radiation at the higher temperatures.

During the course of these studies we were supplied with experimental type heating pans from Harshaw. While evaluating the usefulness of these pans at high readout temperatures we observed a rather impressive effect on our readings as a result of pan condition. This effect was observed by making a number of readings using irradiated TLD powder, that had been heated in an oven at 100°C for 10 minutes, in both new and used pans. The readings showed that the condition of the heating pan can affect the peak height values by as much as 35 percent and the integrated charge values by as much as 25 percent. Calibration curves made with the different pans had the same general shape but were displaced by various amounts.

According to the procedure described by Webb (3), the best readout procedure is that which integrates the total area under the glow curve peaks but excludes the rising contribution occuring at high temperatures. This artifact at the end of the glow curve is attributable to the emission of infrared radiation from the phosphor and pan. Hence, the optimum readout conditions for the higher dose levels must be compromised in order to minimize the contribution of this effect.

When quantative comparisons are made between glow curves, particularly when certain peaks are to be identified and compared, the calibration of pan temperature indicating device is crucial. A convenient alternative to the use of calibrated thermocouples is a paper thermometer (4). These devices are available in ten degree (centigrade) increments and may be conveniently placed directly on the pan. Gross errors in the pan temperature may be

quickly discovered using these thermometers.

TLD Materials Evaluated

Various thermoluminescent materials were evaluated with respect to their fulfillment of part of the dual dose range-irradiation temperature requirement. In addition to regular lithium flouride (LiF Harshaw TLD-100), the dose response of lithium borate ($Li_2B_4O_7$:Mn), isomet lithium flouride, strontium fluoride and lead fluoride was studied.

The thermoluminescence powders were dispensed into gelatin capsules 5 x 15 mm) for irradiation. Each capsule contained sufficient powder for seven readings. Exposed powder was dispensed in 28 mg. lots into the built-in heating pan for analyzing the radiation induced thermoluminescence.

The capsules of powder were irradiated to the desired doses in electron equilibrium shields using one of the Cobalt-60 irradiators previously mentioned. Doses were based on chemical dosimetry using the Fricke dosimeter (G value = 15.6)

Most of the low temperature irradiations were conducted at -40°C using cold nitrogen gas to regulate the temperature of the irradiation chamber. The several comparisons made at 196°C were achieved by irradiating the samples immersed in liquid nitrogen.

Lithium Florido - TLD-100

This material is one of the most researched and used thermoluminescent materials available. We therefore initiated our studies using this material and observed many interesting phenomena. Our first temperature response studies showed that the loose powder samples irradiated at -196°C gave results that were twenty to forty percent lower than samples irradiated at 25°C. These studies were over the limited dose range of 10^3 to 5 x 10^4 rads. To evaluate the temperature response in a temperature range more nearly approaching that to be used in radappertized foods we selected -40°C. It is observed in Figure 2 that in the dose range from 10^3 to 3 x 10^5 rads the integrated charge values of samples irradiated at -40°C are sixteen to thirty percent lower than similar samples irradiated at 25°C. Above 3 x 10^5 rads it appears that radiation damage to the crystal is more pronounced in the 25°C samples as evidenced by the reduced response. The peak height values differ quite considerably between the two temperatures as shown in Figure 3.

Lithium Borate

Two commercial forms of lithium borate were evaluated for their usefulness at doses greater than 10^3 rads and at two temperatures 25° and -40°C. They are loose powder and Conrad's teflon disks.

The powdered lithium borate was treated prior to irradiation by baking for 15 minutes at 300°C. The irradiated samples were annealed in an oven at 100°C for 10 minutes and read out with nitrogen gas purging the sample. The response curves of this material (Figure 4) show that it may be used into the megarad range depending upon the accuracy required in the dose measurement. The difference in response between samples irradiated at the two temperatures is approximately $\pm$ 6% of an average value. This is approximately equal to the standard deviation of our peak height readings and three times the standard deviation of our integrated charge readings.

The lithium borate teflon disks show the lowest sensitivity to irradiation temperature of any of the systems we tested (figure 5). All the integrated charge values for these disks between 10^3 and 3×10^6 rads were within the normal fluctuation of readings. Above 3×10^6 rads the 25°C samples give more light output per rad than the samples irradiated at -40°C.

Isomet Lithium Fluoride

In our search for a high dose phosphor we obtained a sample of the Isomet LiF suggested by Goldstein (5). This material was reported to be usable in the megarad range and to have a high temperature peak between 400 and 450°C. Tochlin reported (6) reading out 16 mg samples by preheating the sample to 350°C to erase the earlier dominant peak, and then reheating the samples to read out the 450°C peak. We irradiated samples in the megarad range and using Tochlin's procedures tried without success to locate the 450°C peak. We tried using a fast heating rate of approximately 40 C° per second and a slow rate of approximately 7 C° per second. The maximum temperature peak we were able to locate was at approximately 340°C (figure 6).

It was observed from the glow curves that the height of the 340°C peak was a function of the irradiation dose, while the lower temperature peaks remained relatively constant. Following the reasoning previously stated with regard to annealing the low energy traps, the samples were dispersed onto the heater pan and rapidly heated to 240°C. They were held at this temperature for 0.5 minutes and then heated to a temperature maximum of 390°C at a rate of 5°C per second. Figure 7 shows response curves we obtained for samples irradiated at 25° and -40°C, using the peak height values at the 340°C peak and the integrated charge values above 240°C. These curves show that there is considerable effect on the response of this material as a function of the irradiation dose. In the dose range of 10^5 to 3×10^6 rads, the samples irradiated at 25°C response is approximately four times that of similar samples irradiated at -40°C. It is noteworthy that using the above procedure this material is a potential high dose phosphor. Our main concern is the availability of similar material in the future.

In an effort to put the phosphor in a form which would be more usable than the loose powder we had Tyco Laboratories (7) grow single crystals .125 x .25 x 1.5 inches. These crystals were made by the continuous growth method (8,9) which allows the dimension of the crystal to be controlled independent of the growth rate. The glow curves for these single crystals might indicate that the concentration of the impurities in the original Isomet crystal are modified by the crystal growth method. It was observed that the main response peak to irradiation dose in these crystals is at 150°C in contrast to peak position at 340°C in the loose powder.

While we were not successful in our initial attempt to incorporate the Isomet material into single crystals that had a megarad dose response, Tyco's growth process shows two potential areas for development. First they are able to control the impurities in the growth crystals under some conditions so that they can conceivably dope the crystals. Secondly, these crystals are very transparent and could be grown in shapes which would allow the crystals to be read spectrophotometerically as well as thermally. These crystals' dose response resembles more the TLD-100 results than the original Isomet powder results. Figure 8.

Strontium and Lead Fluoride

Samples of strontium fluoride and lead fluoride were obtained from

Harshaw as materials that might be useful in measuring doses in the megarad range. These samples were irradiated with dose between 0.5 and 7 megarads and evaluated using Harshaw's standard readout procedure of heating to 100°C rapidly and then to temperature maximum using a lower heating rate. The results obtained were negative in that there was no appreciable change in the thermoluminescence as a function of dose.

Conclusion

These studies re-emphasize the importance of careful control of the readout equipment, especially the condition of the heater pan. It may be advisable to maintain a calibrated phosphor that is read periodically to assure that the pan has not degraded to a point that it is giving erroneous readings. In order to reduce the background, calibrations should be made for each phosphor using the optimum set of reader conditions. It has been demonstrated that an improved readout procedure is obtained by holding a sample at an annealing temperature in the reader (without integrating the signal) for a predetermined time and then continuing the heating at a fixed rate while integrating the signal. The reproducibility of the readings is improved in this manner and the contribution from the low energy traps is reduced or eliminated.

Commercially available TLD material may be used at low irradiation temperatures provided they are calibrated at the temperature. More studies need to be conducted to determine the decrease in response as a function of temperature.

References

1. Harshaw Chemical Company, Cleveland, Ohio

2. R. A. Arnold, private comm.

3. G. A. Webb, J. Sci. Instr. 44 (1967)

4. Paper Thermometer Co., 10 Stagg Dr., Natick, Mass. 01760

5. N. Goldstein, E. Tochlin, and W. G. Miller, Health Physics 14, 159-162 (1968)

6. E. Tochlin, private comm.

7. Tyco Corporate Technology Center, Waltham, Mass.

8. H. E. LeBelle, A. I. Mlavski, Material Research Bull. 6, 571 (1971).

9. H. E. LeBelle, ibid, 581 (1971).

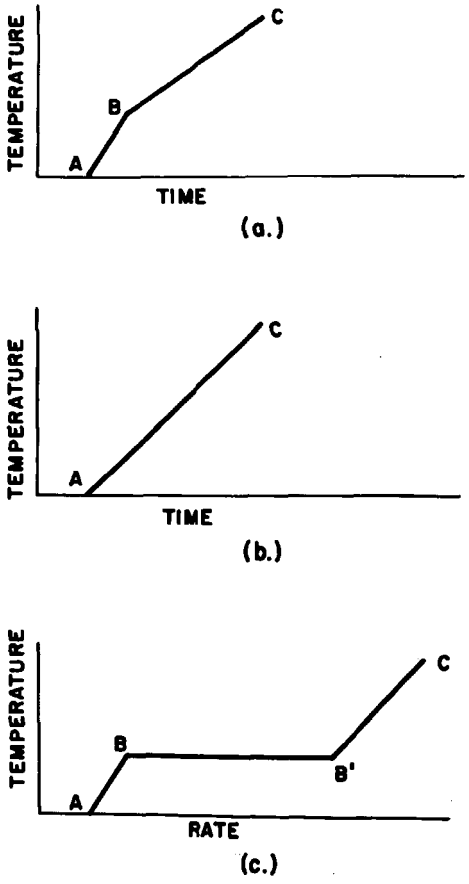

Figure 1. Three basic heating profiles used in evaluating the thermoluminescence properties of materials.

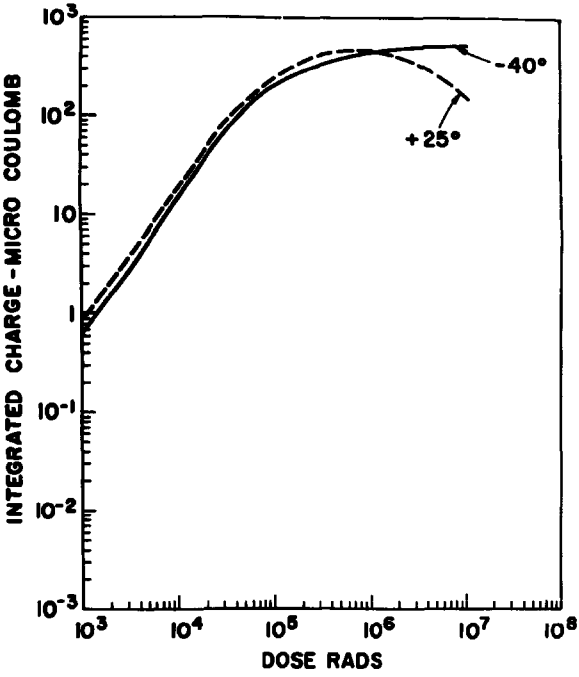

Figure 2. Response curve of LiF-TLD-100 as a function of irradiation temperature.

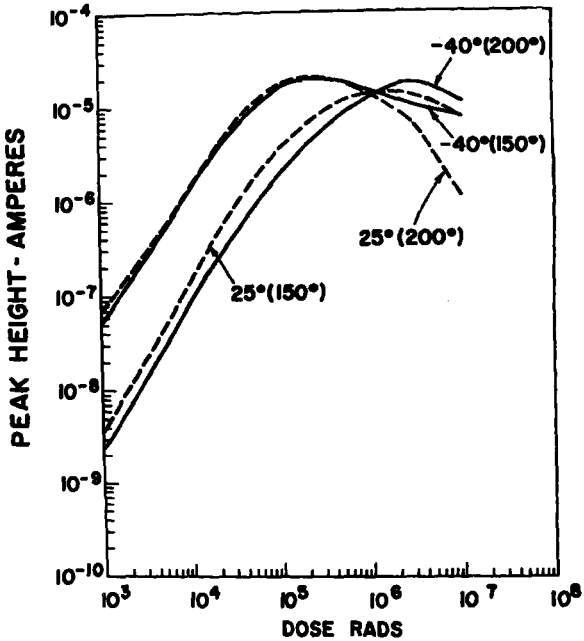

Figure 3. LiF-TLD-100 peak height measurements read at two temperatures (150° and 200°C) as a function of irradiation temperature.

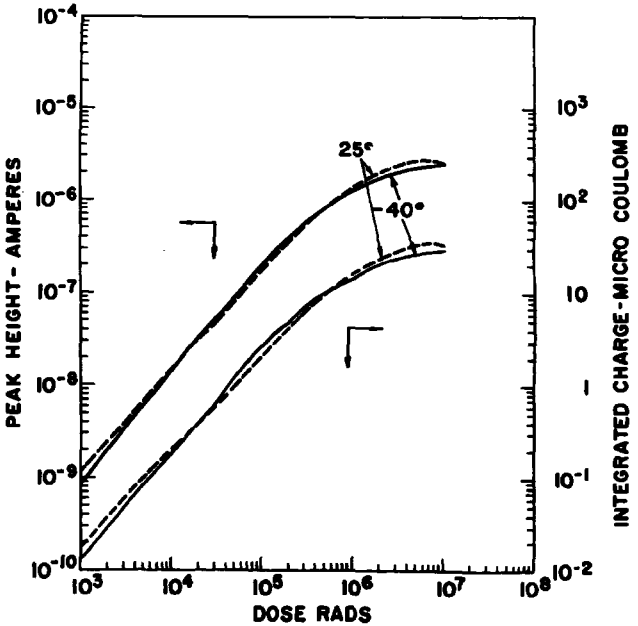

Figure 4. Peak Height and integrated charge values for samples of $Li_7B_4O_7$ irradiate between 10^3 and 10^7 rads at 25° and -40°C.

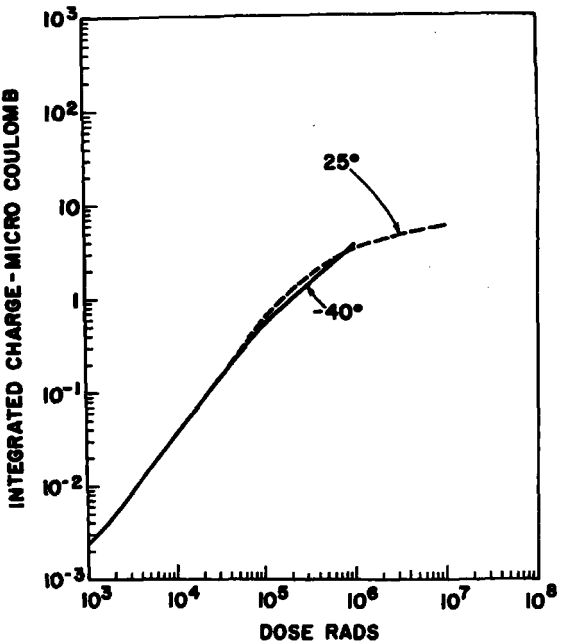

Figure 5. Response curve of teflon disks impregnated with lithium borate when irradiated at 25° and -40°C.

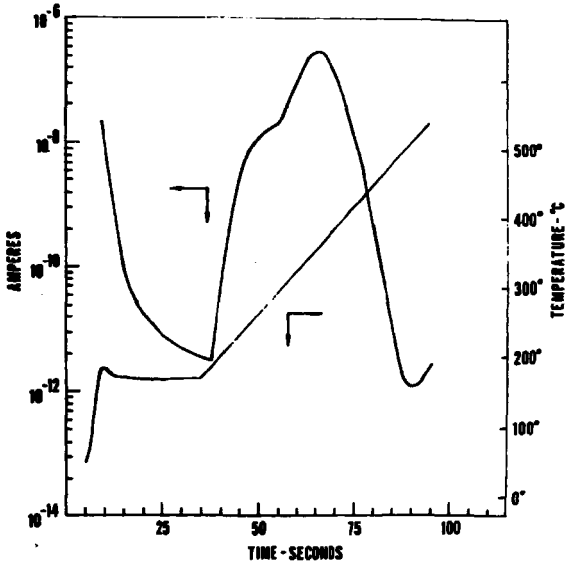

Figure 6. A sample of Isomet LiF loose powder preheated to 170°C and held for 30 seconds, then heated to a temperature maximum of 530°C at a rate of 6 degrees per second.

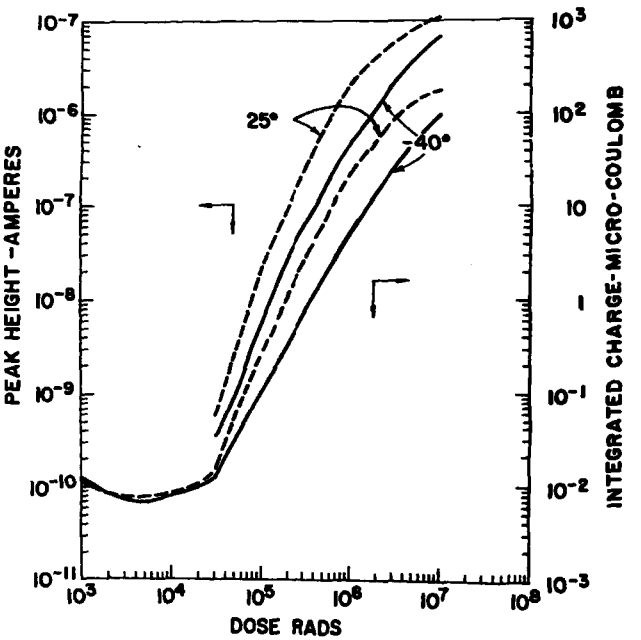

Figure 7. Calibration curves of Isomet LiF loose powder irradiated at -40 and 25°C.

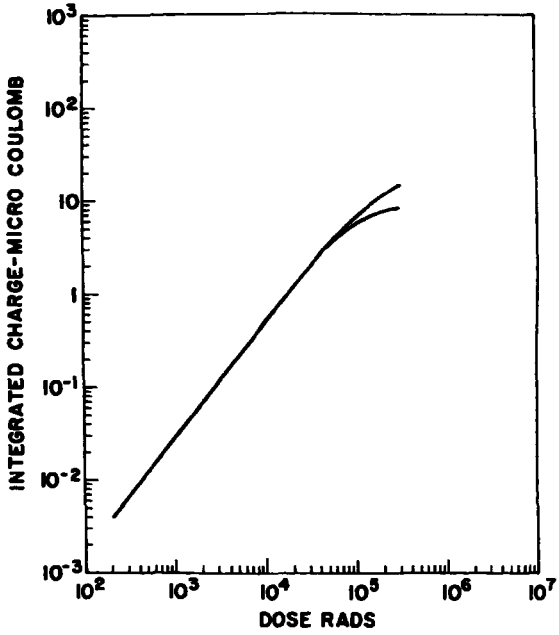

Figure 8. Response curves of Tyco LiF crystal. Lower curve is for a sample which was cycled by irradiating to a dose, then after readout, reirradiating to the next higher dose. Upper curve is the response curve of virgin crystals irradiated to the same doses.

Dependence of the Response of LiF TLD 100 Powder, Incorporated in Silicone Rubber, on Grain Size

by

P.Bassi, G.Busuoli, A.Cavallini, L.Lembo
Laboratorio Fisica Sanitaria, C.N.E.N., Bologna

and

O.Rimondi
Istituto di Fisica dell'Università, Bologna

Abstract

The response as a function of energy of a detector for electromagnetic radiations made up of LiF TLD 100 powder incorporated in silicone rubber has been calculated and measured. It has been shown that the response is due not only to the atomic composition of LiF, silicone rubber and the respective percentages by weight, but also to the mean weight diameter of the incorporated powder. Within the errors, the measurements fit the calculations which show that the crucial parameter is the mean weight diameter of the powder. In practice, if the mean weight diameter of the powder is larger than 70-80 μm, the detector has a response almost similar to that of the LiF TLD 100 used alone.

I. Introduction

A thermoluminescence powder, incorporated in silicone rubber or other materials, makes it possible to prepare even very thin radiation detectors for various uses in dosimetry [1]. These detectors have a response as a function of the electromagnetic radiation, determined by the kind of powder (LiF: Mg, $Li_2B_4O_7$: Mn, etc.), the kind of binder (silicone rubber, teflon,

etc.) and the respective percentages by weight. Moreover, the response depends also on the grain size of the powder [2]. In this research the dependence of the response on the various parameters has been calculated and measured with particular reference to the geometric parameter (the grain size of the powder).

II. Method of Calculation

The calculated energy dependence ($S = \frac{(\mu_{en}/\rho)_{medium}}{(\mu_{en}/\rho)_{air}}$) [3] of LiF TLD 100 (curve a), of silicone rubber (curve c) and of a homogeneous mixture: LiF plus silicone rubber, 30% and 70% by weight respectively (curve b) are shown in Fig.1. The silicone rubber RTV-615 used in this work is produced by the General Electric Company and it has the following composition by weight: C=31.3%, N=7.3%, O=21.9%, Si=38.7%.

The experimental response of the detector, made up of LiF and silicone rubber (30% and 70% by weight respectively), does not fit the curve b) calculated for the homogeneous mixture, because, as has been said, it depends also on the grain size of the powder. A homogeneous mixture means that the LiF molecules are homogeneously distributed among those of silicone rubber. The detector response may be correlated to the curves of Fig.2 or Fig.3. These curves have been calculated with two different approximations, but, in both cases, bearing in mind the powder grain size. The ordinate gives the ratio $\bar{H}$ between the energy actually absorbed by the powder grains, and the energy they would absorbe if they stayed in a homogeneous medium, i.e. in LiF. The $\bar{H}$ values have been normalized to that of Co-60. The parameter is the diameter D of the powder grains. The larger the diameter, in comparison with the range of the electrons arising in the medium, the more the ratio approaches unit value, i.e. the response of the loose powder. In other words the energy absorbed in the grains may be subdivided into two components: one imparted by the electrons generated in the silicone rubber and entering the grain, the second imparted by the electrons arising in the same grain. When the grain size increases, in comparison with the electron range, the first component becomes much lower than the second. Obviously, by keeping constant the grain diameter and varying the radiation energy, we have the former or the latter situation; this accounts for the bell shape of the curves of Fig.2 and Fig.3. The calculations have been made with J.L.Howarth's [4] method, because of its simplicity [5-6]. The Howarth method gives the dose distribution inside a spherical grain. The distribution function is:

$$H(x) = 1 + \Sigma_i K_i G_i \qquad (1)$$

where, H (x) is the ratio between the dose actually absorbed at the point P that has a distance x from the spherical grain surface and the dose there would be at P, if the grain were surrounded by LiF only (homogeneous medium). The sum is extended to any group i of electrons having initial energy T_i; G_i is a geometric factor that depends on T_i and x; K_i is a function of the mass energy absorption coefficients of the two mediums.

The mean value of H (x), within a grain, corresponds to the detector experimental response. The mean value is expressed by

$$\bar{H} = \frac{1}{D} \int_0^D H(x)\, dx \qquad (2)$$

Dependence of the Response of LiF TLD 100 Powder, Incorporated in Silicone Rubber, on Grain Size

by

P.Bassi, G.Busuoli, A.Cavallini, L.Lembo
Laboratorio Fisica Sanitaria, C.N.E.N., Bologna

and

O.Rimondi
Istituto di Fisica dell'Università, Bologna

Abstract

The response as a function of energy of a detector for electromagnetic radiations made up of LiF TLD 100 powder incorporated in silicone rubber has been calculated and measured. It has been shown that the response is due not only to the atomic composition of LiF, silicone rubber and the respective percentages by weight, but also to the mean weight diameter of the incorporated powder. Within the errors, the measurements fit the calculations which show that the crucial parameter is the mean weight diameter of the powder. In practice, if the mean weight diameter of the powder is larger than 70-80 μm, the detector has a response almost similar to that of the LiF TLD 100 used alone.

I. Introduction

A thermoluminescence powder, incorporated in silicone rubber or other materials, makes it possible to prepare even very thin radiation detectors for various uses in dosimetry [1]. These detectors have a response as a function of the electromagnetic radiation, determined by the kind of powder (LiF: Mg, $Li_2B_4O_7$: Mn, etc.), the kind of binder (silicone rubber, teflon,

etc.) and the respective percentages by weight. Moreover, the response depends also on the grain size of the powder [2]. In this research the dependence of the response on the various parameters has been calculated and measured with particular reference to the geometric parameter (the grain size of the powder).

II. Method of Calculation

The calculated energy dependence ($S = \frac{(\mu_{en}/\rho)_{medium}}{(\mu_{en}/\rho)_{air}}$) [3] of LiF TLD 100 (curve a), of silicone rubber (curve c) and of a homogeneous mixture: LiF plus silicone rubber, 30% and 70% by weight respectively (curve b) are shown in Fig.1. The silicone rubber RTV-615 used in this work is produced by the General Electric Company and it has the following composition by weight: C=31.3%, N=7.3%, O=21.9%, Si=38.7%.

The experimental response of the detector, made up of LiF and silicone rubber (30% and 70% by weight respectively), does not fit the curve b) calculated for the homogeneous mixture, because, as has been said, it depends also on the grain size of the powder. A homogeneous mixture means that the LiF molecules are homogeneously distributed among those of silicone rubber. The detector response may be correlated to the curves of Fig.2 or Fig.3. These curves have been calculated with two different approximations, but, in both cases, bearing in mind the powder grain size. The ordinate gives the ratio H between the energy actually absorbed by the powder grains, and the energy they would absorbe if they stayed in a homogeneous medium, i.e. in LiF. The H values have been normalized to that of Co-60. The parameter is the diameter D of the powder grains. The larger the diameter, in comparison with the range of the electrons arising in the medium, the more the ratio approaches unit value, i.e. the response of the loose powder. In other words the energy absorbed in the grains may be subdivided into two components: one imparted by the electrons generated in the silicone rubber and entering the grain, the second imparted by the electrons arising in the same grain. When the grain size increases, in comparison with the electron range, the first component becomes much lower than the second. Obviously, by keeping constant the grain diameter and varying the radiation energy, we have the former or the latter situation; this accounts for the bell shape of the curves of Fig.2 and Fig.3. The calculations have been made with J.L.Howarth's [4] method, because of its simplicity [5-6]. The Howarth method gives the dose distribution inside a spherical grain. The distribution function is:

$$H(x) = 1 + \Sigma_i K_i G_i \qquad (1)$$

where, H (x) is the ratio between the dose actually absorbed at the point P that has a distance x from the spherical grain surface and the dose there would be at P, if the grain were surrounded by LiF only (nomogeneous medium). The sum is extended to any group i of electrons having initial energy T_i; G_i is a geometric factor that depends on T_i and x; K_i is a function of the mass energy absorption coefficients of the two mediums.

The mean value of H (x), within a grain, corresponds to the detector experimental response. The mean value is expressed by

$$\bar{H} = \frac{1}{D} \int_0^D H(x)\, dx \qquad (2)$$

All the calculations have been made with the computer. First of all, in order to test the computer program, the marrow dose in spherical bone cavity 50 μm in diameter has been calculated. The results obtained for a 50 KeV electromagnetic radiation is 2.4 rad/R. F.W.Spiers gives 2.28 rad/R [5] for the same situation. The slight difference is probably due to the different choice of the parameters employed (*).

The H values of Tab.I have been calculated by supposing that the LiF grains are spherical and the binder boundless. In other words the distance between one grain and the nearest one is larger than the maximum electron range, whatever the radiation energy. However this is not the actual situation. The order of magnitude of the mean distance between the grains may be evaluated by supposing,to make calculations easier,that the grains are cube shaped (side D) and arranged at the lattice points of a simple cubic space lattice of side L.

It results:

$$L = D\sqrt{\frac{1}{\rho_s}\left(\frac{\rho_f\, p_s}{p_f} + 1\right)} \qquad (3)$$

where ρ_s=1, p_s= 70%, ρ_f=2.6, p_f=30% are the densities and the percentages by weight of silicone rubber and LiF respectively. In this case L = 2.6 D. When L is shorter than the electron range, the electrons emerging from a grain may reach the neighbours. This situation may be approximated by supposing that the LiF grains are embedded in a homogeneous mixture (LiF plus silicone rubber, 30% and 70% by weight respectively) instead of the silicone rubber only. These calculations are shown in Fig.3 or Table II. Both figures 2 and 3 show that the influence of the grain size begin to be important when the diameters are lower than 40 μm.

III. Measurements and Discussion of the Results

The detectors have the shape of a disc 7.5 mm in diameter and 0.9 mm thick. All the discs have the same percentage of LiF (30% by weight). The preparation method is described in a previous paper [1]. Two sets of detectors have been used, the first with grains having a mean weight diameter $\bar{D}_1$ = 6 μm and the second $\bar{D}_2$ = 70 μm. The mean weight diameter [7] is defined by

$$\bar{D} = \sqrt[3]{\frac{\Sigma_i\, n_i\, D_i^3}{\Sigma_i\, n_i}} \qquad (4)$$

where n_i is the number of particles having diameter D_i.

The incorporated powder was extracted from the commercial powder by means of calibrated sieves. The powder is not monodispersed and the size distribution was measured in the following way. A layer of LiF particles, laid on a slide, was photographed throught a microscope (Fig.4). The

(*) The values of all the parameters employed and the computer program will be published in a CNEN internal report.

particle diameters were measured on the photographs by means of a Zeiss particles analyzer TGZ 3 [8]. The size distribution is shown in Table III. From this table and the curves of Fig.2 or Fig.3 it is possible to calculate the response H_g of the detector (for a certain energy of the radiation) by means of:

$$H_g = \frac{1}{m} \Sigma_i \, m_i \, H_i \qquad (5)$$

where: m_i is the total mass of the particles having a diameter that ranges in the i-th interval, $m = \Sigma_i \, m_i$, H_i is the ordinate of the curve having the parameter corresponding to the i-th interval.

The detectors were exposed to Co-60, to filtered X-rays and to fluorescence X-rays. The caracteristics of the beams are shown in Tab.IV and Tab.V. The exposure measurements were made by means of a cavity chamber, calibrated in comparison with the standards of other European Laboratories [9]. The exposure measurements with the cavity chamber are accurate to within a few percent. The exposure at the various energies was about 10 R.

Before irradiation the detectors were annealed at 300°C for 10 min,then at 100°C for two hours. After irradiation, before the reading, the detectors were kept at 100°C for 10 min. The reading was taken with a Harshaw 2000. The maximum heating temperature was 260°C and the heating time 60 sec.

The results of the first set of detectors are shown in Table VI. The experimental values (column B) are normalized to that of Co-60. The error is the standard deviation of the ratio. Column C shows the ratio between the values of column B and column F (LiF calculated energy dependence). The LiF TLD 100 energy dependence has been calculated with the atomic composition given by C.G.Klick et al.[10]. The H_g values calculated with reference to the curves of Fig.2 and Fig.3 are shown in column D and E respectively. As may be seen the detector response (column C) stays between the values of column D and E, as foreseen by the previous considerations.

As further proof of the results of Table VI the detectors were exposed to fluorescence X-rays. These measurements are shown in Table VII and confirm the previous ones.

The results of the detectors, with large grains ($\bar{D}_2 \approx 70$ μm), are shown in Tab.VIII. As can be seen the response fits the calculated values within the experimental errors. Also for this set, the experimental results are normalized to the respective value of Co-60, so as to account for the large rise in light yield of LiF with the increase of the particle sizes [11]. The light yield of $\bar{D}_1$ and $\bar{D}_2$ detectors to Co-60 is respectively 10 + 1 and 28 + + 1.6 arbitrary unit per R. The light yield would also depend on the radiation energy but, at least in our case, this effect is contained within the experimental errors.

In conclusion the previous calculations and measurements show that the determining parameter of the detector response is the mean weight diameter of the powder, whereas the LiF percentage affects the detector sensitivity only.

From the practical point of view the results suggest the criterion for choosing the most convenient size distribution of the powder to be incorporated in silicone rubber. In other words, if the mean weight diameter of the powder is larger than 70-80 μm , the detector has a response as a function of energy almost similar to that of LiF used alone.

ACKNOWLEDGEMENT

The authors gratefully acknowledge the assistance of Mr.I.Maganzani who wrote the computer program used for the calculations.

REFERENCES

1 - P.Bassi, G.Busuoli, A.Cavallini, O.Rimondi, Giornale di Fisica Sanitaria e Protezione contro le Radiazioni, 13 n.4, 276-281, 1969.

2 - -ICRU, International Commission on Radiological Units and Measurements, Handbook 78 NBS, pg.6, 1959.

3 - F.H.Attix, Health Physics, 15, 49-56, 1968.

4 - J.L.Howarth, Radiation Research 24, 158-183, 1965.

5 - F.W.Spiers, in F.H.Attix and E.Tochlin "Radiation Dosimetry" Vol.III pg.840, Academic Press 1969.

6 - F.W.Spiers, Br.J.Radiol. 39, 216-211, 1966.

7 - R.D.Cadle "Particle Size" pg.30, Chapmann & Hall. 1965.

8 - F.Endter and H.Gebauer, Optik, 97-101, 1965.

9 - G.Busuoli, A.Cavallini, L.Lembo, Giornale di Fisica Sanitaria e Protezione contro le Radiazioni, 15, n.1, 28-32, 1971.

10 - C.C.Klick et all., Journal Applied Physics, 38, 3867-3874, 1967.

11 - G.D.Zanelli, Phys. Med. Biol.13, 393-399, 1968.

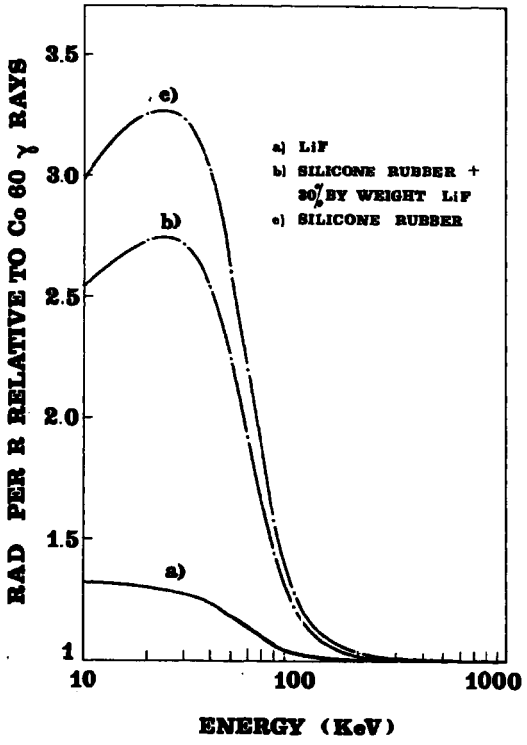

Fig.1

Fig.1 - Energy dependence of LiF (curve a), of a homogeneous mixture: silicone rubber plus LiF (curve b) and silicone rubber alone (curve c).

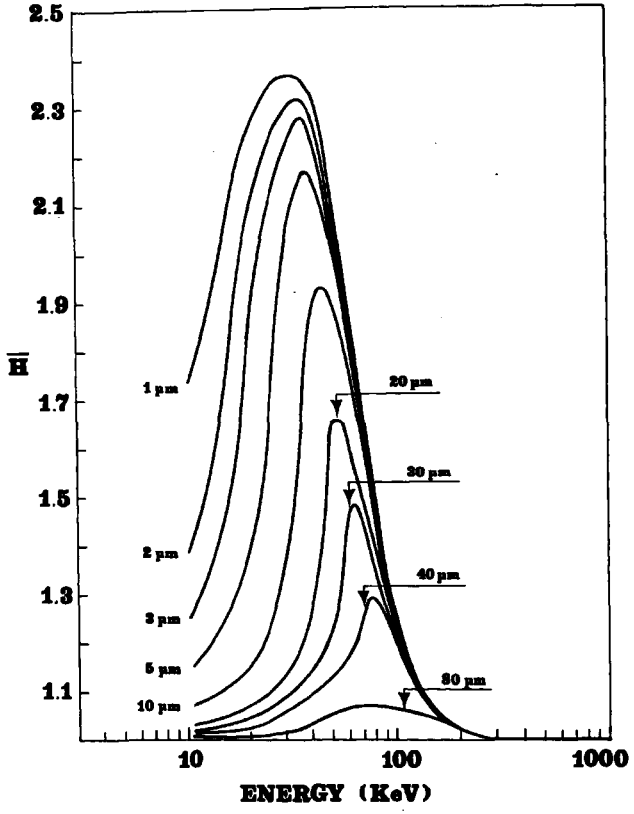

Fig 2

Fig. 2 - LiF powder incorporated in silicone rubber.
Calculations performed for spherical interface.

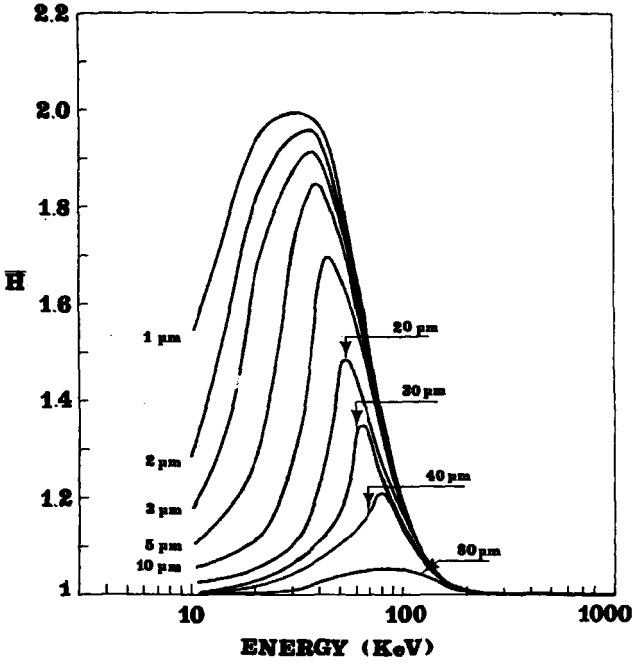

Fig.3

Fig. 3 - LiF powder incorporated in a homogeneous mixture of LiF and silicone rubber. Calculations performed for spherical interface.

Fig. 4 Photograph of the LiF powder.

Fig. 4 - Photograph of the LiF powder.

TABLE II:

Grain Size Distribution

POWDER D_g = 6 μm			POWDER T_c = 70 μm		
$D_i - D_{i+1}$ (μm)	$n_i / \Sigma n_i$ (%)	$n_i / \Sigma n_i$ (%)	$D_i - D_{i+1}$ (μm)	$n_i / \Sigma n_i$ (%)	$n_i / \Sigma n_i$ (%)
1.00 - 2.04	3.1	0.1	7.45 - 26.75	9.5	0.04
2.04 - 3.02	25.9	2.2	26.75 - 43.30	2.8	2.3
3.02 - 4.10	25.3	5.6	43.30 - 57.10	8.1	3.7
4.10 - 5.09	13.9	6.5	57.10 - 65.40	12.9	5.0
5.09 - 6.79	15.0	11.4	65.40 - 73.70	16.3	9.2
6.79 - 7.52	7.4	10.2	73.70 - 81.95	13.8	9.3
7.52 - 9.15	5.4	14.8	81.95 - 90.25	10.8	11.2
9.15 - 11.12	1.7	9.0	90.25 - 98.50	9.7	13.2
11.12 - 13.53	1.7	20.3	98.50 - 106.8	6.7	17.6
13.53 - 17.56	0.3	6.5	106.8 - 117.9	2.3	5.3
17.88 - 22.78	0.3	14.2	117.9 - 147.0	0.1	32.2

TABLE IV

Filtered X-Rays (a)

Excit.Volt. (KV)	Current (mA)	Filter (mm)	H.V.L. (mm)	Eff. En. (KeV)
20	10	1.0 Al	0.3 Al	15
37	10	4.0 Al	1.6 Al	26
70	10	7.0 Al	4.1 Al	36
85	10	8.0 Al	5.8 Al	42.5
100	10	9.0 Al	6.6 Al	46
120	10	1.0 Cu + 0.9 Al	0.91 Cu	61
150	10	1.63Cu + 1.02 Al	0.97 Cu	77
200	10	3.07Cu + 1.03 Al	1.93 Cu	103
400	10	37.15Cu + 0.92 Al	6.99 Cu	200

(a) The homogeneity factor (ratio between the second and the first H.V.L.), ranges between 1.1 and 1.2 for all the beams

TABLE V

Fluorescence X-Rays

Target	E_{ab} Ch. (Ref)	Excit. Volt. (kV)	Primary Beam Filter (mm)	Fluorescence Beam Filter (mm)
Mo	17.76	45	0.2 Al	0.15 Al
Sn	25.04	65	0.15 Co	0.15 Al
Ba	32.98	85	0.3 Co	0.25 Al

TABLE VI

Response to Filtered X-Rays of the Powder of Mean Weight Diameter $\bar{D}_w$ 6 µm

Eff. Energy (keV)	Exp. Response per Roentgen	D / F	$\bar{D}_g$		Energy Dependence
A	B	C	D	E	F
25	1.08 ± 12%	1.42 ± 12%	1.42	1.08	1.29
42.5	2.09 ± 12%	1.63 ± 12%	1.62	1.63	1.22
61	1.65 ± 12%	1.39 ± 12%	1.77	1.68	1.13
77	1.68 ± 13%	1.16 ± 13%	1.47	1.36	1.07
Co^{60}	1.00 ± 10%	1.00 ± 10%	1.00	1.00	1.00

TABLE I

R Values for LiF in Silicone Rubber

D / En. KeV	1 u	2 u	3 u	5 u	10 u	20 u	30 u	40 u	80 u
10	1.73	1.37	1.22	1.14	1.07	1.04	1.02	1.02	1.01
20	2.26	2.10	1.88	1.36	1.15	1.07	1.04	1.02	1.01
30	2.38	2.26	2.20	2.01	1.35	1.14	1.09	1.06	1.01
40	2.34	2.30	2.25	2.16	1.89	1.26	1.15	1.11	1.04
50	2.24	2.11	2.09	2.06	1.91	1.64	1.21	1.14	1.06
60	1.90	1.89	1.87	1.86	1.78	1.60	1.49	1.17	1.07
80	1.48	1.47	1.47	1.46	1.44	1.40	1.34	1.29	1.07
100	1.25	1.25	1.25	1.25	1.24	1.22	1.21	1.19	1.07
200	1.03	1.02	1.02	1.02	1.02	1.02	1.02	1.02	1.02
300	1.01	1.01	1.01	1.01	1.01	1.01	1.01	1.01	1.01
400	1.00	1.00	1.00	1.00	1.00	1.00	1.00	1.00	1.00
500	1.00	1.00	1.00	1.00	1.00	1.00	1.00	1.00	1.00
600	1.00	1.00	1.00	1.00	1.00	1.00	1.00	1.00	1.00
800	1.00	1.00	1.00	1.00	1.00	1.00	1.00	1.00	1.00
1000	1.00	1.00	1.00	1.00	1.00	1.00	1.00	1.00	1.00

TABLE II

R Values for LiF in Homogeneous Mixture (LiF + Silicone Rubber)

D / En. KeV	1 u	2 u	3 u	5 u	10 u	20 u	30 u	40 u	80 u
10	1.53	1.27	1.17	1.10	1.05	1.02	1.02	1.01	1.01
20	1.92	1.80	1.65	1.25	1.11	1.05	1.03	1.02	1.01
30	1.99	1.93	1.87	1.74	1.26	1.10	1.06	1.04	1.01
40	1.98	1.95	1.91	1.85	1.55	1.19	1.11	1.08	1.03
50	1.83	1.87	1.79	1.76	1.66	1.47	1.15	1.10	1.04
60	1.66	1.65	1.63	1.61	1.57	1.44	1.25	1.13	1.05
80	1.36	1.35	1.34	1.34	1.32	1.29	1.25	1.21	1.05
100	1.18	1.18	1.18	1.18	1.17	1.16	1.15	1.14	1.05
200	1.02	1.02	1.02	1.02	1.02	1.02	1.02	1.02	1.02
300	1.00	1.00	1.00	1.00	1.00	1.00	1.00	1.00	1.00
400	1.00	1.00	1.00	1.00	1.00	1.00	1.00	1.00	1.00
500	1.00	1.00	1.00	1.00	1.00	1.00	1.00	1.00	1.00
600	1.00	1.00	1.00	1.00	1.00	1.00	1.00	1.00	1.00
800	1.00	1.00	1.00	1.00	1.00	1.00	1.00	1.00	1.00
1000	1.00	1.00	1.00	1.00	1.00	1.00	1.00	1.00	1.00

TABLE VII

Response to Fluorescence X-Rays of the Powder of Mean Weight Diameter $\bar{D}_w$= 6 μm

Energy (keV)	Exp. Response per Roentgen	A / F	$\bar{N}_g$		Energy Dependence
A	B	C	D	E	F
17.8	1.50 ± 14%	1.21 ± 14%	1.19	1.15	1.31
25.6	1.79 ± 11%	1.39 ± 11%	1.42	1.28	1.29
33.0	1.82 ± 12%	1.44 ± 12%	1.64	1.46	1.26
Co^{60}	1.00 ± 10%	1.00 ± 10%	1.00	1.00	1.00

TABLE VIII

Response to Filtered X-Rays of the Powder of Mean Weight Diameter $\bar{D}_w$= 70 μm

Eff. Energy (keV)	Exp. Response per Roentgen	B / F	$\bar{N}_g$		Energy Dependence
A	B	C	D	E	F
42.5	1.32 ± 8%	1.03 ± 8%	1.03	1.03	1.22
77	1.16 ± 9%	1.07 ± 9%	1.08	1.08	1.07
103	0.96 ± 9%	0.92 ± 9%	1.06	1.06	1.03
Co^{60}	1.00 ± 6%	1.00 ± 6%	1.00	1.00	1.00

Scarpa

Does the grain size used in the mixture affect also the mechanical properties of the mixture?

Rimondi

Yes. It would be more convenient to use small grains because the grains would then be more homogeneously distributed, and the mixture would be more compact.

Manufacture of Uniform, Extremely Thin, Thermoluminescence Dosimeters by a Liquid Moulding Technique

by

Geoffrey A. M. Webb and George Bodin
Teledyne Isotopes, Westwood, N.J.

Abstract

A technique is described for preparing uniform thin thermoluminescence dosimeters. It is shown possible to fabricate dosimeters containing 30% by weight phosphor as thin as 15 microns with a standard deviation in weights of only 3.6%. In larger sizes the measured standard deviation of a batch of dosimeters was generally 3 to 4%.

The silicone polymer before curing has a viscosity high enough to maintain the phosphor in suspension but low enough to enable it to be poured and moulded easily. After curing it is a tough elastic solid able to withstand readout and 300°C annealing. The optical transmission is nearly 100% and it has a similar refractive index to most common phosphors. The efficiency and minimum detectable doses for different compositions with different phosphors are given. The low specific gravity of the silicone binder enables dosimeters to be made with a lower effective thickness for a given physical thickness. A 20 micron $CaSO_4$:Dy - Silicone dosimeter is only 2.1 mg/cm^2 effective thickness.

Introduction

Thermoluminescence dosimeters provide potential sources of solid state Bragg-Gray Cavity Chambers for radiation research. The major difficulty in their use has been the manufacture of uniform, high sensitivity dosimeters thin enough to not perturb the surrounding electron equilibrium but robust enough to be handled.

The thinnest dosimeter available at present is the Phosphor-Teflon "Ultra-thin" dosimeter[1]. These have been shown to agree well[2] with the Solid State Cavity Chamber theory developed by Burlin[3]. They have also been used in interface dosimetry by Schulz[4].

The phosphor-Teflon dosimeters are manufactured by microtoming from a solid bar of phosphor-Teflon of the appropriate diameter (normally 6mm). This technique can produce dosimeters of 20 micron nominal thickness but the variations in thicknesses between dosimeters is very great and necessitates weighing and correcting each reading to a normalized weight. The production is also very laborious and results in a very high unit cost for the dosimeters. A disadvantage of Teflon as a carrier in this instance is the relatively poor light transmission. Since each dosimeter contains only about 0.3 mg of phosphor it is obviously desirable to get as much light out as possible.

Most of the problems of variation among a batch of dosimeters seemed to us to be attributable to the manufacturing technique of machining from a solid so we have investigated a new technique which enables sheets of material to be manufactured directly to the required thickness. The dosimeters then merely have to be punched to the appropriate diameter which is a trival task.

Nakajima[5] described thin dosimeters of phosphor in a silicone matrix but his dosimeters could not be made extremely thin because of the relatively high viscosity of his material. In addition the finished dosimeters were brittle and hard to handle. We have manufactured dosimeters using a silicone elastomer which has a low viscosity before curing and which produces a flexible dosimeter which is very tough. The object of this paper is to report on the manufacture and properties of the dosimeter. No measurements using the dosimeters as cavity chambers or in interface dosimetry have been carried out.

2. Manufacture of Dosimeters by Liquid Moulding

In preparing the phosphor powder for manufacture of dosimeters, some preliminary screening must be carried out. Since the suspension of powder in the silicone is directly formed to the required thickness, phosphor grains of a larger diameter than this thickness should be removed by sieving. It might be expected from the results of Zanelli[6] with LiF that use of phosphor with maximum grain size of 15 micron would cause a significant reduction in light output compared with the normal "fine" powder ranging up to 75 micron grain size used in manufacture of phosphor-Teflon dosimeters. The results for $CaSO_4$:Dy did not show this reduction (see section 7).

The preparation of the compound follows the following steps

1. Mix silicone polymer with correct proportion of curing agent in a clean container.

2. Add phosphor powder in the correct proportion by weight and mix thoroughly.

3. Deaerate the mixture by reducing pressure to less than 20 mm for 15 to 20 minutes

4. Pour mixture into mould taking care not to introduce air bubbles. The moulds used have generally been optically flat glass plates with a spacer of the correct thickness on the lower plate. Excess material is placed inside the spacer which has a gap to allow this excess to escape during pressing.

5. Press on the top mould. This is another optically flat glass plate which is pressed down to touch the spacer all round.

6. Cure at room temperature for 7 days or at elevated temperature e.g. 100°C for 1 hour.

7. Punch out dosimeters of the appropriate diameter.

For making relatively thick dosimeters no support material has been used. For very thin dosimeters, however, the handling is much improved by placing on the lower mould under the spacer a metal foil (0.001" Aluminium). The elastomer bonds with the foil during curing and the foil imparts more rigidity enabling cutting and handling to be carried out more readily. The foil can be removed before use or left in place. In most of this work it was left in place as it appears to assist the heat distribution during heating for readout and also makes the very thin dosimeters more convenient to handle.

Dosimeters have been manufactured by this technique in thickness from 0.02 mm to 0.5 mm, containing percentages from 0.60% by weight of $CaSO_4$:Dy phosphors.

3. Physical Characteristics of Phosphor-Silicone Dosimeters

The main physical property made use of during the manufacturing process is the viscosity of approximately 3500 centipoise. This is sufficiently high to hold the powder in suspension with no observable settling out, but low enough to enable the mixture to be poured and moulded with relative ease.

After curing the silicone elastomer becomes a tough transparent solid, with a slightly "tacky" surface. The transmission of visible light is almost 100% in the thicknesses we are considering and the refractive index of 1.4 is very close to the indices of most thermoluminescence phosphor materials. The material is non-conducting electrically and a relatively poor thermal conductor.

The resistance to temperature is not very great, however it can withstand temperatures of 300°C in an oven for periods of 2 hours with no apparent deterioration. Higher temperatures can cause the material to turn brittle and crack. In addition dosimeters have been put through many readout cycles without affect. The material is therefore capable of withstanding the temperatures necessary for readout and annealing of all common phosphors. The readout cycle with anneal described in another paper at this meeting[1] is ideally suited for these dosimeters as the post-readout anneal of 20 seconds at 305°C proves to be optimum in zeroing the dosimeter without causing thermal damage.

The dosimeters are insoluble in water and resist attack by most common solvents.

4. Readout Technique

Most of the results in this paper were obtained on Teledyne Isotopes Model 7100TS reader. This uses a constant heater current through a resistive heating element for a fixed time and integrates and displays the light emission. The temperature ar` glow curve were displayed on a dual channel recorder. The reader was se_ up for minimum contribution from residual thermoluminescence and incandescence emission.

Since the phosphor-silicone dosimeters are slightly tacky they tend to stick to the heater tray and provide good thermal contact. In the case of the very thin dosimeters these were generally left on their Aluminium backing for irradiation and readout. It was found that as long as the metal touched the heater in two or three places the thermal conductivity was good enough to provide uniform heating.

In the newer model 7300 reader[7] which has a ramp and hold heating pattern the heating characteristics should be even better.

5. Thermoluminescence from the Silicone

In some earlier dosimeters using Silicone materials the limiting property at low levels was the inherent luminescence of the Silicone itself. In the material we are using there seems to be no inherent luminescence property. Irradiation of discs made from pure silicone elastomer with no phosphor to 100 R did not produce any increase in signal above background. Irradiation of the same discs to laboratory fluorescent lighting also produced no detectable signal increase over discs stored in darkness. The sensitivity was such that a signal from a 5 mR exposure of a similar dosimeter containing 30% by weight $CaSO_4$:Dy would have been detectable.

6. Light Output Efficiency

The increased light output efficiency was measured by comparison with standard $CaSO_4$:Dy Teflon dosimeters containing the same quantities of the same phosphor. The results show that the light output per mg of phosphor from the Phosphor-Silicone dosimeter is approximately 3 times that from an equivalent Phosphor-Teflon dosimeter. This is directly attributable to the improved optical characteristics of the silicone matrix.

This result can be used in two ways for standard dosimeters. If performance is the objective then the increased signal/noise ratio permits lower minimum detectable levels. If cost reduction is the objective then the same performance can be obtained with one third of the phosphor content, resulting in lower costs.

For thin dosimeters the phosphor cost is insignificant and performance improvement is the only criterion.

7. Effect of Phosphor Loading

To test the effect of different phosphor contents on detection efficiency and mechanical strength of the dosimeter, the phosphor content was varied from 0 to 60%. Figure 1 shows the relative sensitivity corrected for dosimeters of different weights after exposure to the same dose as a function of phosphor content.

Although results have some variability the light output is roughly proportional to the loading.

Even for 60% loadings the phosphor does not interfere with the mechanical properties of the silicone.

A further test was the effect of different phosphor grain sizes on the efficiency. Figure 2 shows the results normalized to light output per unit dose per unit mass of phosphor for dosimeters with different maximum grain sizes. It can be seen that the marked fall in efficiency observed by Zanelli[6] for grain sizes below 20 microns is not observed in these circumstances.

8. Uniformity of Production

One advantage of the production process is the much closer tolerance on thickness which can be obtained. Since the dosimeters are punched to exactly the same diameters a good check on the thickness is the weight of the dosimeter. Actual measurements of thickness are difficult as the silicone is elastic and compresses rather easily.

Table 1 shows the standard deviation of weights obtained in several batches of dosimeters of different types

TABLE 1. Standard Deviations of weights and measured thermoluminescence of different batches of Phosphor-Silicone Dosimeters.

Phosphor Loading %	Thickness (microns)	Standard Deviation Weight (%)	Standard Deviation of Signal Corrected for Weights (%)
20%	75	1.8%	1.7%
20%	15	3.6%	2.8%
30%	75	2.5%	2.0%
30%	75	1.7%	1.8%
30%	50	1.5%	1.0%
40%	75	0.8%	0.5%

Table 1 also shows the results of the measured thermoluminescence signal from different batches of dosimeters. The results show the excellent reproducibility of dosimeters produced by this technique. The production batches were generally small (50-100 dosimeters) and the batch to batch variation can be anticipated to be worse than the results shown in Table 1.

9. Minimum Detectable Dose

There are several definitions of this but one which is acceptable is three times the Standard deviation of the background from unirradiated dosimeters.[8] Table 2 shows the results according to this definition for minimum detectable dose for phosphor-Silicone dosimeters. Similar results for some phosphor-Teflon dosimeters are included for comparison.

TABLE 2. Comparison of minimum detectable doses for phosphor-Teflon and phosphor-Silicone dosimeters.

Dosimeter	Matrix	Phosphor %	Content mg	Minimum Detectable dose mR
D-$CaSO_4$:Dy-0.4	Teflon	30	30	0.5
UT-$CaSO_4$:Dy	Teflon	30	0.3	45
75 micron $CaSO_4$:Dy	Silicone	30	3.0	1.5
15 micron $CaSO_4$:Dy	Silicone	30	0.27	20

10. Application to extremity Dosimetry

The current interest in accurate skin dosimetry[9] and the excellent results obtained by Marshall and Docherty[10,11] using 40 micron thick LiF-Teflon dosimeters suggest the possibility of using LiF-Silicone dosimeters for this purpose. The increased light output should enable doses as low as 10 to 20 mRad to be detected. The effect of the Silicone binder on the energy dependence of the phosphor would have to be investigated before this application could be pursued In this connection it is interesting to conjecture whether a material with an inherent under-response such as Lithium Borate(Mn) in a Silicone matrix would result in a dosimeter with relatively good energy response characteristics. A further advantage of Silicone as a binder is a considerable reduction in the effective thickness in mg/cm^2 for a phosphor-Silicone dosimeter of the same measured thickness as a phosphor-Teflon dosimeter. Table 3 shows the comparison of measured thickness, weight and effective thickness for the two dosimeter types. The difference is due to the low specific gravity of the Silicone (1.02) compared with Teflon (2.7)

TABLE 3. Comparison of measured and effective thickness for phosphor-Silicone and phosphor-Teflon dosimeters

Dosimeter	Diameter	Thickness	Weight	Effective Thickness
$CaSO_4$:Dy Teflon	12.0 mm	0.4 mm	100 mg	90 mg/cm^2
$CaSO_4$:Dy Teflon	6.0 mm	20 micron	1.25 mg	4.5 mg/cm^2
$CaSO_4$:Dy Silicone	11.0 mm	0.4 mm	53 mg	43 mg/cm^2
$CaSO_4$:Dy Silicone	11.0 mm	20 micron	2.6 mg	2.1 mg/cm^2

This decrease in effective thickness for a given physical thickness is an advantage when attempting skin dosimetry. For example a 40 micron thick Phosphor-Silicone dosimeter under a 2 mg/cm^2 window is an almost perfect replica of the basal layer skin depth found[9] in recent measurements for the trunk.

11. Conclusions

The preparation and properties of a new Phosphor-Silicone dosimeter type have been described. It has been shown that it is possible to fabricate dosimeters as thin as 15 micron with a standard deviation in weight of only 3.6%. In larger sizes the measured standard deviation of a batch of phosphor Silicone dosimeters was generally 3 to 4%.

The principal advantage of the silicone binder in manufacture is its viscosity which is high enough to maintain the phosphor in suspension but low enough to enable it to be poured and moulded easily.

After curing the dosimeter is a tough elastic solid. The optical transmission is almost 100% and the refractive index is suitable for optimum light collection from the phosphor.

The lower specific gravity of the Silicone matrix enables dosimeters to be constructed with a lower effective thickness for a given physical thickness. For example a 20 micron thickness dosimeter of $CaSO_4$:Dy-Silicone is 2.1 mg/cm^2 compared with 4.5 mg/cm^2 for a 20 micron $CaSO_4$:Dy-Teflon dosimeter. This capability has potential for more precise skin dose measurements than hitherto possible.

References

1. B. E. Bjarngard and D. Jones. Symp on Solid State and Chemical Radiation Dosimetry in Med. and Biol. IAEA Vienna (1966)

2. T. E. Burlin and F. K. Chan British J. Radiol 40 556 (1967)

3. T. E. Burlin British J. Radiol 39 727 (1966)

4. R. J. Schulz Proceedings of the Conference "Microdosimetry" Ispra (1967)

5. T. Nakajima Int. J. Appl. Radn. and Isotopes 19 789 (1968)

6. G. D. Zanelli Phys. Med. Biol 13 No. 3 393 (1968)

7. G. A. M. Webb and H. P. Phykitt 3rd Int. Conf. on Luminescence Dosimetry Riso (1971)

8. B. E. Bjarngard and D. Jones Phys. Med. Biol 13 No. 3 461 (1968)

9. Mrs. J. T. Whitton, J.R. Harvey, J.D. Everall, E. Galabova and M. Meek Proceedings I.R.P.A. Congress Brighton, England (1970)

10. J. A. B. Gibson, M. Marshall and J. Docherty. Symposium on New Dev. in Physical and Biol. Radn. Detectors Vienna (1970)

11. M. Marshall and J. Docherty Phys. Med. Biol. 16 No. 3 503 (1971)

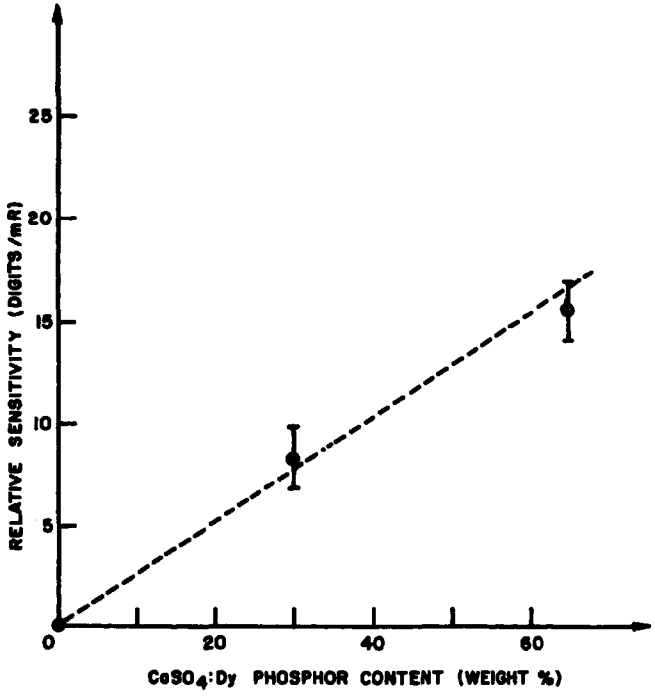

Figure 1. The relative sensitivity corrected for dosimeters of different weights as a function of phosphor content for $CaSO_4$:Dy - Silicone dosimeters.

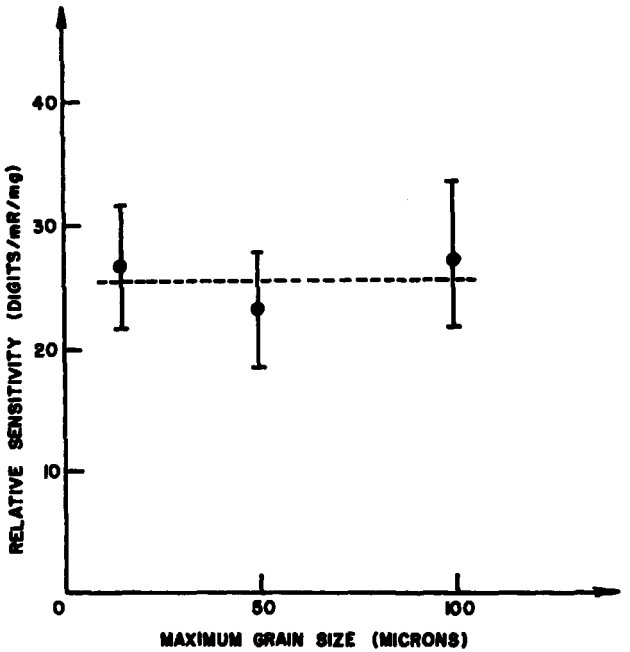

Figure 2. Relative sensitivity of $CaSO_4$:Dy - Silicone dosimeters for different maximum phosphor grain sizes.

Suntharalingam

Is the uniformity of response of these newly fabricated dosimeters the same as the ± 3.5% you stated for the uniformity of weight in the fabrication?

Webb

Full information is given in the paper on the uniformity of radiation response. A typical figure for 15 μm dosimeters is ± 3% after correction for weight variation or ± 6% with no corrections applied.

The Consistency of the Dosimetric Properties of ^{7}LiF in Teflon Discs over Repeated Cycles of Use

T.O. Marshall and K.B. Shaw

National Radiological Protection Board

South Eastern Centre

Clifton Avenue, Belmont,

Surrey, U.K.

and

E.W. Mason

National Radiological Protection Board

Scottish Centre

9, West Graham Street,

Glasgow, C.4,

U.K.

Abstract

A series of anneal and read-out conditions has been applied to ^{7}LiF in teflon discs in order to determine the feasibility of using this thermoluminescent device as the basis of a personal dosemeter for routine whole-body monitoring. It has been demonstrated with six different read/anneal combinations that, with the discs protected from light, little fading occurs and a sufficiently constant sensitivity and an acceptable background can be maintained over numerous cycles of use for average doses up to 1 rad per cycle. Of the six read/anneal combinations some involved the conventional high plus low temperature anneal conditions but in other combinations these anneals were replaced by high and low temperature holds introduced into the read cycle. It still remains to be demonstrated, however, that the performance observed does not deteriorate under operational conditions.

1. Introduction

This paper is an interim report on an investigation being carried out in order to determine the feasibility of using ^{7}LiF in teflon discs as the basis of a personal dosemeter for routine whole-body monitoring. In considering the suitability of such a dosemeter the cost must be taken into account, not only that of the dosemeter itself, but also the cost of processing it. Thus the dosimetric material must either be inexpensive or be capable of repeated use. The price of LiF discs is, at present, such that they must be capable of being used at least 25 times if they are to form an economically

viable basis of a 2 element dosemeter. The aim of the study was, therefore, to see if a combination of anneal and read cycles could be specified which would give rise to little fading and to a constant sensitivity and an acceptable background over at least 25 cycles of use.

2. Experimental programme

The programme included four anneal conditions based on the recommendations of the manufacturers of the discs and on procedures in current use or being tried in various laboratories. The anneal conditions chosen were:-

A_1 - 400°C for 30 mins, followed by 80°C for 16h

A_2 - 300°C " " " " " " " "

A_3 - 80°C for 16h

A_4 - No pre-irradiation anneal.

Similarly a range of read cycles were chosen. Each read cycle can be split into four parts and the following conditions were chosen for each part.

(i) Pre-read treatment R_{1---} low temperature trip* (130°C)

or R_{2---} low temperature hold** (130°C for 15s before trip)

(ii) Heating rate R_{-1--} 10°C/s

or R_{-2--} 20°C/s

(iii) High temperature trip R_{--1-} 260°C

or R_{--2-} 290°C

(iv) Post read-out treatment R_{---1} Nil

or R_{---2} High temperature hold (at trip temperature for 15s)

The anneal conditions A_1 and A_2 are typical of those in current use in a number of laboratories. Conditions A_3 and A_4 have been suggested by other authors[1] with the idea of keeping the anneal process as simple as possible, thereby reducing processing costs. In the case of anneal A_3 the high temperature anneal is replaced by a high temperature hold in the read cycle while in the case of A_4, the high and low temperature anneals are replaced by the high and low temperature holds respectively in the read cycle. The combination of anneal and read cycles which were investigated are shown in Table 1.

*Low and high temperature trips are the temperatures between which the signal is integrated.

**A temperature hold refers to a period in the read cycle during which the temperature is held constant.

The signal was integrated between the low and high temperature trips or holds as appropriate.

The study was split into four parts to observe:-

(i) The variation of background

(ii) The consistency of sensitivity

(iii) The degree of fading

(iv) The useful disc life.

It was intended that each read/anneal (RA) combination would be subjected to the individual parts of the study in the order indicated. Failure to provide satisfactory results for any part would eliminate the RA combination concerned from the remainder of the study. However, more of the RA combinations than expected proved to be satisfactory so that the programme had to be reduced where possible. Details of the modifications made are given in Section 5 Results.

3. Experimental method

3.1. The variation of background

Ten new discs were allotted to each RA combination investigated and the experiment was carried out as follows in each case:-

Anneal	
Read 1 (prior to dose)	B_0
Anneal	
Dose	D (1 rad)
Read 2 (post dose)	S
Anneal	
Read 3 (1st Background)	B_1
Anneal	
Read 4 (2nd Background)	B_2
Anneal	
Read 5 (3rd Background)	B_3

The experiment was thus designed to give information on the sensitivity of the system from the values of S and the magnitude and constancy of the background from the values of B_1, B_2 and B_3 for each combination. It was recognised that, for a combination to be acceptable, it must enable a threshold dose of a few tens of mrad to be maintained. This necessitates a very low background or a very constant one which is independent of dose history.

3.2. The consistency of sensitivity

Ten new discs were allotted to each RA combination being investigated; each batch was subjected to the following:-

Anneal

Dose (1 rad)

Read (S_1)

Anneal

Read background (B)

Anneal)
Dose (1 rad)) Repeat three times to obtain S_3, S_4 and S_5
Read dose (S_2))

After the second anneal the background was read for comparison with the values obtained in the previous experiment. The consistency of the sensitivity of the discs was obtained from the values of S_1 to S_5. A particular RA combination was considered satisfactory at this stage provided the values of S showed no systematic change in sensitivity exceeding ± 15% about the overall mean sensitivity.

3.3. The degree of fading

New discs were taken for each RA combination undergoing this experiment and were annealed and exposed to a dose of 1 rad. These were read over a period of 28 days, a standard light source being used to check the stability of the reader. A particular RA combination was considered satisfactory provided the fading did not exceed 10% over the 28 days.

3.4. The useful disc life

This experiment was similar to the sensitivity experiment described in 3.2 but involved a larger number of cycles (at least 25). The effects of different dose levels and of cleaning the discs by means of washing were also to be observed. The discs were also to be examined at various stages during the experiment to observe discolouration or any other form of deterioration.

Thirty-six new discs were allotted to each of the RA combinations under investigation. These were split into two batches of 18, one to be washed and the other unwashed. These were further divided into batches of 9, one to be exposed to low doses and the other to high. At each irradiatic stage, 3 discs in the low dose batch were exposed to each of the following doses: 0, 100 and 500 mrad. Doses chosen for the high dose batch were 0, 500 and 2,500 mrad. The discs in the high and low dose batches were randomly chosen for exposure to the prescribed doses; the average dose per cycle was 200 mrad in the low dose batch and 1,000 mrad in the high. The washing procedure was simply agitation in methanol for approximately a minute after which

the discs were allowed to dry. The washing procedure was carried out prior to each anneal.

The experimental procedure was as follows:-

Anneal

Dose

Read

It was intended that this should be repeated at least 25 times or until, for some reason, a particular RA combination was found to be unsatisfactory and therefore eliminated from the experiment.

4. The sensitivity to light of ^{6}LiF in teflon discs

Initially an attempt was made to carry out the background experiment taking no precautions to prevent exposure of the discs to light. The RA combinations being investigated at that stage were those involving both high and low temperature anneals, i.e. A_1 and A_2. The backgrounds observed were high and variable and such that a dose threshold of a few tens of millirads could not be maintained. Light effects were suspected and simple experiments, in which the behaviour of discs handled in normal light conditions was compared with that of discs handled in subdued light conditions (i.e. under photographic safe lights), showed that the backgrounds were almost entirely due to the sensitivity of the discs to light. Some of these experiments were repeated with discs of pure teflon and similar counts were observed, indicating that the light sensitivity is mainly due to the teflon.

Several methods of eliminating the effect were tried. The only satisfactory method was that of handling the discs in total darkness or in subdued light. Under these conditions the signal increased linearly with radiation dose and the backgrounds were at or near zero so that a dose threshold of a few tens of mrads could easily be maintained. A possible compromise solution was obtained with a post irradiation anneal of 15 mins at 130°C. This was found to reduce the sensitivity by a factor of about 2 but the response remained linear and the backgrounds were sufficiently constant to be subtracted. Discs handled in normal and subdued light conditions are compared in Table 2 and the behaviour of discs exposed to light and then subjected to a post irradiation anneal of 15 mins at 130°C are shown in Table 3. It can be seen from Table 2 that it would be difficult to maintain a dose threshold below 100 mrad if the discs are not protected from light.

At this stage the possibility of investigating the light effect in detail was considered as well as the possibility of designing a system for personal dosimetry in which the discs could be handled in subdued light conditions. It was decided, as a monitoring system designed to keep the discs in subdued light conditions was feasible, to re-start the study taking precautions to prevent exposure of the discs to light.

5. Results

The main feature of the study was the experiment to determine

the useful disc life; the other three experiments were included in order to eliminate quickly unsatisfactory RA combinations. It is sufficient, therefore, to comment merely on the findings of the "background", "consistency of sensitivity" and "fading" experiments and to give detailed results only on the useful disc life experiment.

5.1. RA combinations involving anneal conditions A_1 and A_2

RA combinations R_{1121}/A_1, R_{1211}/A_1, R_{1121}/A_2 and R_{1211}/A_2 were investigated using a disc reader designed at the Atomic Energy Establishment, Winfrith[2]. In this reader a disc, when being read, is clamped between upper and lower elements which are heated electrically. The lower element is a nichrome block and the upper a nickel mesh. The temperature of the lower element is monitored by means of a thermocouple and controlled electronically. The reader is housed in an air-conditioned room and the temperature of the photomultiplier tube is controlled by means of a water-cooled fridgistor in order to stabilize its gain and dark current.

All four RA combinations were subjected to the background experiment (Section 3.1). In all cases the values of B_0 to B_3 were at or near zero indicating that a threshold dose of a few tens of mrads could easily be maintained.

All four combinations were next subjected to the consistency of sensitivity experiment (Section 3.2) which showed that the sensitivity in all cases was sufficiently constant to continue with the remainder of the study. However, it was decided that, with the effort available, the number of combinations subjected to the "fading" and "useful disc life" experiments should be limited to two. Those chosen were R_{1121}/A_1 and R_{1211}/A_2. Both were subjected to the fading experiment and, in each case, the fading observed over 28 days was less than 10%.

During the "useful disc life" experiment there was an interval of 1 to 3 days between each cycle and 31 cycles were carried out in all. As indicated in Section 3.4, the discs were divided into washed and unwashed groups, each group being subdivided further into high and low dose batches. However, no significant differences in the behaviour of washed, unwashed, high and low dose batches were observed. Therefore, the readings of all the discs for a given cycle and RA combination have been combined and expressed as counts per mrad. These are shown plotted against cycle number in Figure 1 for RA combinations R_{1121}/A_1 and R_{1211}/A_2. Error bars corresponding to one standard deviation are also shown. The counts for zero dose were practically zero in all cases as observed in the background experiment.

After completing the 31 cycles both sets of discs appeared to be in good condition. Discolouration was only slight and the indications were that many more cycles could have been successfully carried out. The optical density was measured at intervals throughout the experiment. The values stayed reasonably constant with cycle number at densities of about 0·5 and 0·7 for R_{1121}/A_1 and R_{1211}/A_2 respectively.

The sensitivity of the discs was found to be a factor 2 greater for R_{1121}/A_1 than for R_{1211}/A_2, the overall mean sensitivities indicated by the dotted lines in Figure 1 being 1·44 and 0·71 cts/mrad respectively. This enhanced sensitivity is due mainly to the different

anneal conditions as the consistency of sensitivity experiment showed only a marginal increase in the sensitivity for combination R_{1121}/A_2 over R_{1211}/A_2, i.e. 0·91 cts/mrad as compared with 0·71 cts/mrad. The higher value associated with the A_1 anneal could, to some extent, be due to the lower optical density of the discs annealed at 400°C.

The dotted lines in Figure 1 show the overall mean sensitivities for the two RA combinations concerned. The scatter of the points (the mean value for each cycle) about the overall mean shows no systematic change in sensitivity with cycle number. The random spread of the individual means about the overall mean is less with the 400°C anneal; the standard deviation expressed as a percentage of the overall mean sensitivity is 3% whereas it is 7% in the case of the 300°C anneal. The spread in the values for each cycle is also less for the 400°C anneal; σ is typically 6% whereas it is 9% in the case of the 300°C anneal.

5.2. RA combinations involving anneal conditions A_4

RA combinations R_{2112}/A_4, R_{2212}/A_4, R_{2122}/A_4 and R_{2222}/A_4 were investigated using a powder reader designed by the Atomic Energy Establishment, Winfrith[3], which had been modified to take discs. The planchet was shaped for discs and a nickel mesh was welded to it to form an upper heating element. When being read discs are positioned in the planchet and beneath the nickel mesh, both of which are heated electrically. The temperature of the planchet is monitored by means of a thermocouple and controlled electronically. The photomultiplier tube is cooled by means of an air-cooled fridgistor in order to stabilize its gain and dark current.

All four combinations were subjected to the background experiment. The values of B_0 to B_3 (Section 3.1) obtained were higher than observed with the RA combinations involving anneal conditions A_1 and A_2. This was thought to be due to the behaviour of the reader and not the discs since, to obtain a sensitivity in the region of 1 ct/mrad, it was found necessary to select a high PM tube EHT setting with a resulting increase in the dark current. However, the values of B_0 to B_3 were approximately constant such that a threshold of a few tens of mrads could be maintained.

At this stage it was decided that a maximum of two RA combinations could be subjected to the disc life experiment. Combinations R_{2112}/A_4 and R_{2222}/A_4 were chosen as these represent the two extremes of the read cycles under consideration. Both these combinations were taken successfully through the "consistency of sensitivity" experiment. It was considered sufficient to subject combination R_{2112}/A_4 to the "fading" experiment which it completed satisfactorily. The experiment was of particular interest because it enabled a comparison to be made of combinations in which the 80°C anneal is replaced by the 130°C 15 s hold.

The "useful disc life" experiment was carried out without including the washing procedure since the results presented in Section 5.1 showed that this was unimportant. However, the high and low dose batches were again employed but again no differences in the behaviour of the two groups were observed. Therefore, the readings of all the discs for given cycles and RA combinations have been combined and

expressed as cts/mrad. These are shown plotted against cycle number in Figures 2 and 3 for combinations R_{2112}/A_4 and R_{2222}/A_4 respectively for the 25 cycles completed. Error bars corresponding to one standard deviation are also shown. The counts for zero dose were high and varied from day-to-day. This was thought to be due to the high PM tube EHT setting and not to the discs. The background remained sufficiently constant throughout a given day for a dose threshold of a few tens of mrads to be maintained. There was also very little difference between the zero dose reading for the high and low dose groups. At the end of the experiment the discs were in good condition and the indications were that more cycles could have been carried out.

The dotted lines in Figures 2 and 3 show the overall mean sensitivities of the two combinations concerned. The scatter of the points (the mean value for each cycle) about the overall mean shows no systematic change in sensitivity with cycle number in Figure 2, i.e. for R_{2112}/A_4. Superficially it appears that the sensitivity indicated in Figure 3 is less constant than that of Figure 2 but the change in sensitivity is not sufficient to be considered serious as far as a personal dosemeter is concerned.

The mean σ values for the spread in the readings for individual cycles was 8% and 9% for R_{2112}/A_4 and R_{2222}/A_4 respectively. The σ values for the spread in the mean values for individual cycles about the overall means was 6% and 9% for R_{2112}/A_4 and R_{2222}/A_4 respectively.

5.3. RA combinations involving anneal conditions A_3

Experience with RA combinations involving anneal conditions A_1, A_2 and A_4 showed that the preliminary experiments could be dispensed with in the case of anneal condition A_3, and RA combinations R_{1122}/A_3 and R_{1112}/A_3 were chosen for the "useful disc life" experiment. The discs were read-out with the modified powder reader (Section 5.2) but the PM tube EHT setting was lowered as much as possible to reduce the dark current. It was adjusted such that the sensitivity of the discs was about 0·5 cts/mrad which was considered sufficient for personal monitoring purposes. This experiment is still in progress but so far 16 cycles have been completed.

The washing procedure of the "disc life" experiment was dispensed with but the high and low dose batches were retained. There was again no difference in the behaviour of the high and low dose batches so that the readings were combined and the results expressed as cts/mrad. These are shown plotted against cycle number in Figure 4 for R_{1122}/A_3 and R_{1112}/A_3. Error bars corresponding to one standard deviation are also shown.

The variation of the mean values for zero dose for the high and low dose groups are shown in Table 4 for R_{1112}/A_3. The values are reasonably constant from day-to-day, with the exception of cycle number 8, and practically equal for the high and low dose batches. These results support the idea that the high and variable zero dose or background readings obtained with the A_4 anneal were probably due to the reader and not the discs. Residual backgrounds are governed to a large extent by the high temperature treatment in the read/anneal cycles. In this respect RA combinations involving anneal conditions

A_3 and A_4 are identical in that this is limited to a high temperature hold in the read cycle.

The dotted lines in Figure 4 show the overall mean sensitivities. The scatter of the points about the overall mean shows no systematic change in sensitivity with cycle number so far. The mean σ values for the spread in the readings for individual cycles were 9% and 12·5% for R_{1112}/A_3 and R_{1122}/A_3 respectively. The σ values for the spread in the mean values for individual cycles about the overall mean was 5·5% and 8% respectively.

6. Discussion

Table 5 compares the performance of the RA combinations investigated. The second column gives the mean σ value for the individual cycles and is included to give an indication of the spread in the values of a given batch of discs. The third column gives the σ values for the spread of the means of the individual cycles about the overall mean and is included to give an indication of the useful life of the discs.

Combination R_{1121}/A_1 gave the best results but there was little to choose between the performance of the others. All combinations investigated are considered suitable for personal monitoring and it is important to note that the discs were still in good condition at the end of the experiment. Moreover, improvements in the design of the read-out unit would almost certainly improve the results.

The study is still in progress as not all the RA combinations in Table 1 have been investigated but, at this stage, there is no reason to suppose that the remaining combinations will not prove satisfactory. However, there are some reservations. The anneal-dose-read cycles were carried out over regular intervals of a day or so, which would not be the case in practice. At least a week would normally lapse between the anneal and the beginning of the issue period. The dosemeter would then be worn for about 1 month before being read-out. There may also be some deterioration in performance under operational handling conditions. Thus, the study will be concluded with an experiment simulating conditions met in practice. This will include some dosemeters issued to personnel for wearing alongside their present dosemeters.

The choice of RA combination should depend upon the type of service being operated. Although the best results were obtained with anneal conditions A_1, this includes a 400°C high temperature anneal and is not easy to carry out in practice since teflon undergoes a phase change at approximately 320°C. It could, however, be used where small numbers of individual discs are concerned. RA combinations involving A_4 dispense with the conventional anneal procedures but reduce the throughput of the reader. Thus, for very large services an RA combination involving A_2 may be preferred. Clearly, a multiplicity of satisfactory RA combinations could now be specified. The one chosen should, of course, be optimised for the particular service envisaged. What has been demonstrated here is that, subject to the reservation referred to in the previous paragraph, the conventional high and low temperature anneals can be replaced by high and

low temperature holds in the read cycles while maintaining a sufficiently constant sensitivity, acceptable background and little fading over at least 25 cycles of use for average doses up to 1 rad per cycle.

7. Conclusions

The experiments described have shown that six of the twelve RA combinations given in Table 1 could be used with lithium fluoride in teflon discs to form the basis of a personal dosemeter for routine whole body monitoring. The other six combinations have not been investigated so far but the work reported here suggests that these will also prove satisfactory. The choice of read and anneal cycles should depend on the type and size of personal monitoring service envisaged. It still remains to be demonstrated, however, that the performance observed does not deteriorate under operational conditions.

Acknowledgements

The work reported here was part of the technical development programme of the National Radiological Protection Board. The authors are grateful to Mr. E.E. Smith for his support and help in preparing the manuscript and to Dr. G.S. Linsley, Mrs. G. Flinn and Mr. S.N. Sketchley for their assistance in carrying out the experimental work.

References

1. G. Portal, H. Francois, and P. Blanchard, Reemploi Sans Regeneration du LiF Radiothermoluminescent, CEA-R-3746 (1969).

2. K.E.G. Perry, Reading Equipment for Thermoluminescent Dosimetry, AERE-R607 (1968).

3. K.E.G.Perry and E. George, An Experimental System for Thermoluminescent Dosimetry, AERE-R411 (1965).

Table 1

Combinations of anneal and read cycles

Anneal conditions	Read cycles
A_1	R_{1121} R_{1211}
A_2	R_{1121} R_{1211}
A_3	R_{1112} R_{1212} R_{1122} R_{1222}
A_4	R_{2112} R_{2212} R_{2122} R_{2222}

Table 2

Comparison of discs handled in dark and sunlight

Dose	Count	
	Discs kept in dark	Discs exposed to several hours sunlight
Background	0, 1, 1, 1, 0	116, 146, 176, 214, 100
20 mrad	12, 15, 16, 12, 15	204, 110, 147, 117, 102
100 mrad	93, 86, 89, 97, 107	170, 265, 152, 160, 193
1000 mrad	1087, 1013, 989, 991, 1017	989. 1036, 1039, 983, 912

Table 3

Effect of post irradiation anneal at 130°C for 15 min

Dose	Count	Mean Count	Mean - background
Background	18, 15, 13 10, 4, 6	11	-
20 mrad	26, 25, 26 23, 21, 25	24	13
50 mrad	39, 30, 43 35, 40, 46	39	28
100 mrad	64, 54, 66 64, 67, 74	65	54
1000 mrad	585, 608, 513 508, 590, 511	553	542

Table 4

Backgrounds (zero dose readings) for R_{1112}/A_3

Cycle Number	Mean background readings (etc.)	
	Low dose batch	High dose batch
1	29	28
2	33	33
3	35	39
4	35	38
5	32	36
6	35	33
7	31	34
8	1	5
9	31	34
10	31	31
11	32	32
12	35	38
13	36	36
14	31	29
15	30	30
16	30	31

Table 5

Relevant σ values for the various RA combinations

RA combinations	σ values as % of appropriate mean sensitivity	
	Mean σ for individual cycles	σ for spread of means of individual cycles about overall means
R_{1121}/A_1	6%	3%
R_{1211}/A_2	9%	7%
R_{1112}/A_3	9%	5·5%
R_{1122}/A_3	12·5%	8%
R_{2112}/A_4	8%	6%
R_{2222}/A_4	9%	9%

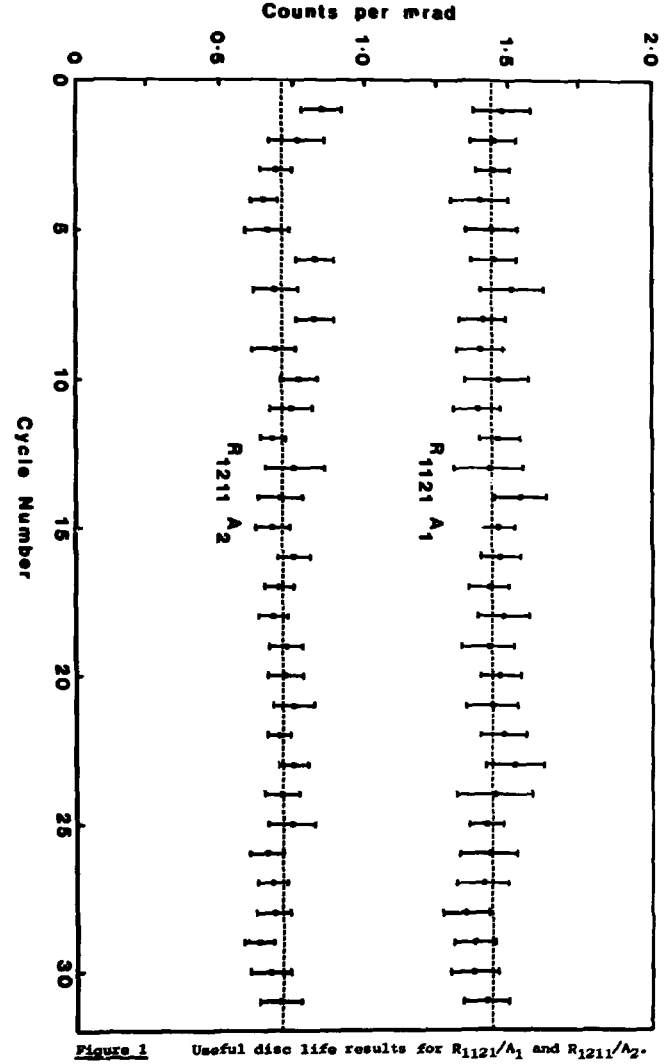

Figure 1 Useful disc life results for R_{1121}/A_1 and R_{1211}/A_2.

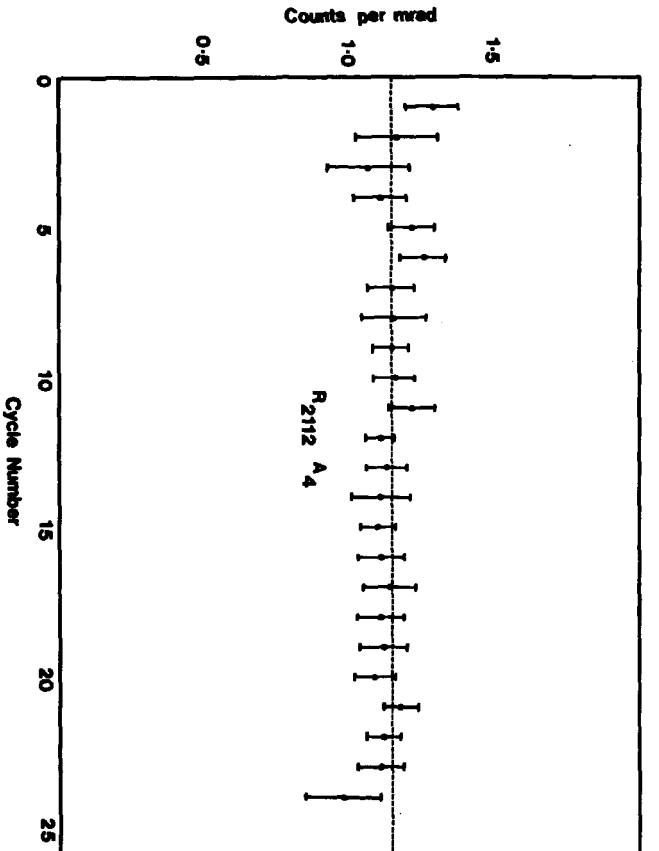

Figure 2 Useful disc life results for R_{2112}/A_4.

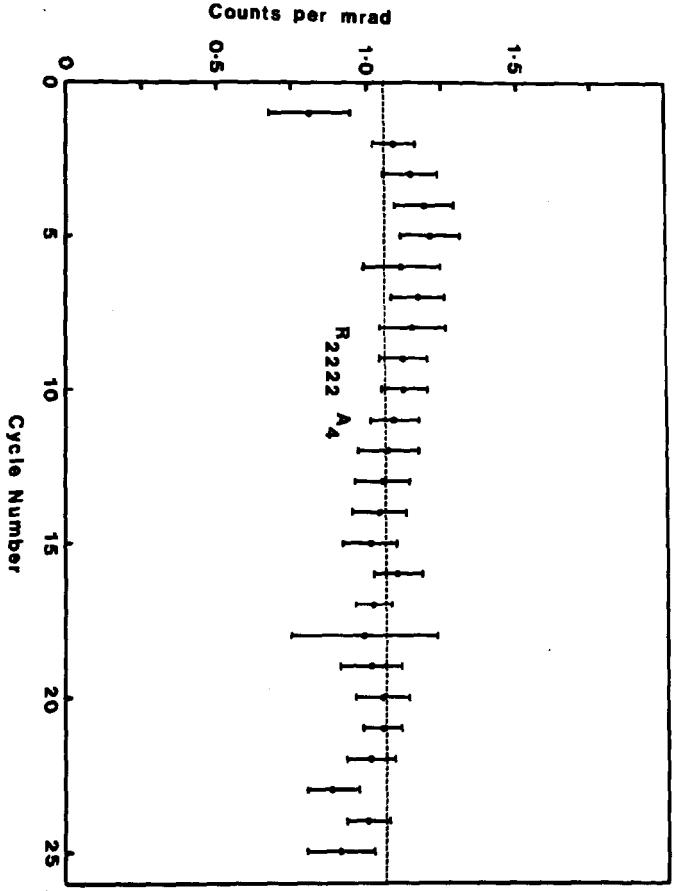

Figure 3 Useful disc life results for R_{2222}/A_4.

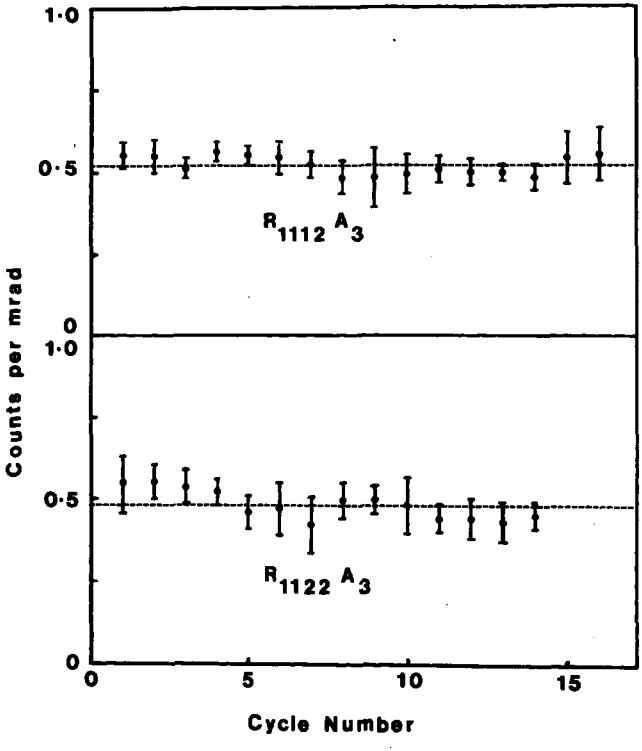

Figure 4 Useful disc life results for R_{1122}/A_3 and R_{1112}/A_3.

Suntharalingam

It is well known that teflon has a softening point close to 330°C. Could you please tell us how you have been able to carry out the 400°C annealing for the teflon disc dosimeters you described? Are these dosimeters different from those commercially available?

Marshall

We used the commercially available discs. They do soften during the 400°C annealing, which means that they have to be supported and kept separate on a flat plate during the process. Our discs were supported in one of the annealing stacks manufactured by D.A. Pitmann Ltd.

Webb

First a comment on the previous question. As the manufacturer of the LiF-teflon discs we are aware of the 400°C annealing possibility, but it must be used with care as the dosimeters may turn brown if they are heated under pressure, and also the large change in optical density must be kept the same for all dosimeters of a batch. With regard to the lifetime of the dosimeters we have taken them through one hundred readout and annealing cycles in a reader with preheating and annealing with a standard deviation of sensitivities of $\pm$ 3%.

Influence of Size of CaF_2:Mn Thermoluminescence Dosimeters on ^{60}Co Gamma-Ray Dosimetry in Extended Media

by

Margarete Ehrlich

National Bureau of Standards, Washington, D.C. 20234, U.S.A.

Abstract

Absorbed-dose distributions were measured in CaF_2:Mn TLD of thicknesses between 0.5 and 3.5mm, irradiated with an essentially plane-parallel beam of ^{60}Co gamma rays in media of aluminum (homogeneous case), polystyrene, copper, and lead. Change of average absorbed dose with dosimeter thickness was deduced from the dose distribution. Since dosimeter sizes were of the order of secondary-electron ranges, total energy absorption was found to be critically affected by interface effects, which caused a loss of linearity of energy absorbed with dosimeter thickness for polystyrene and lead. A relatively strong asymmetry in the absorbed-dose distributions was found near front and rear interfaces, absorbed dose being ~ 10 percent higher in front for polystyrene, and ~ 15 and ~ 30 percent lower for copper and lead, respectively. Comparisons of relative experimental values of average absorbed dose for different dosimeter thicknesses with values computed according to Burlin's scheme (which does not consider front-rear asymmetries) were not conclusive for polystyrene and lead, since the assumptions regarding the electron spectrum at the dosimeter site proved to be critical for polystyrene, and the assumptions regarding the photon spectrum critical for lead. For copper, there was agreement to within the limits of experimental reproducibility.

Introduction

Detailed information on the distribution of absorbed dose in the vicinity of interfaces between media of different atomic compositions has been obtained in the past with thin ion chambers with opposite walls consisting of different materials[1,2], with suitably embedded sheets of Perspex,[3] of anthracene in gelatine,[4] or of radiochromic-dye dosimeters[5]. The ionization method requires precision equipment and measurements. The

thin-film method is simple and capable of furnishing dose distributions of high spatial resolution, but it is insensitive, requiring megarads of absorbed dose. Also, when solid systems are used for the dosimetry of x or gamma rays, dosimeter dimensions often are comparable to the range of the secondary electrons produced by the photon interaction in the dosimeter proper and in its immediate surroundings. As a consequence, it is no longer possible to deduce absorbed dose from Spencer-Attix theory,[6] and the observable effects are small. Nevertheless, by computing absorbed dose by means of Burlin's extension of cavity theory,[6] Chan and Burlin,[3] and Ilić-Popović,[4] obtained good agreement with experiment for dosimeter thicknesses comparable to secondary-electron ranges, even when the difference in atomic number between dosimeter material and medium was large. They employed ^{60}Co gamma-ray irradiators delivering high dose rates in cylindrical geometries. This limits the generality of their results, since the influence of directional effects known to exist at interfaces[1,2] is removed. Burlin's theory, too, is formulated for diffuse radiation incidence, but this fact is not stated explicitely.

This paper deals with studies of absorbed-dose distributions and average absorbed dose as a function of dosimeter dimensions, employing hot-pressed CaF_2:Mn thermoluminescence dosimeters (TLDs) in media irradiated in a plane-parallel geometry. Burlin and Chan's earlier work with TLDs was inconclusive because of lack of reproducibility.[7] However, when properly calibrated, some TLDs are comparable in reproducibility to Perspex, but are more sensitive by orders of magnitude; therefore, they should lend themselves well to interface studies in a plane-parallel geometry, which is easier to obtain with a weaker radiation source. Also, since TLD materials of different atomic number (Z) are available, they could be used in the future to simulate both the higher-and the lower-Z sections of the interface.

Experimental Setup

The experiment was performed with individually calibrated hot-pressed CaF_2:Mn samples of dimensions 6.25mm x 6.25mm x 0.5mm. Readout was accomplished with a linear heating ramp extending from about 100 to 400 degrees C, and the heating time was chosen so as to produce essentially complete annealing during a single readout. Both glow curves and integral readings were obtained. Most of the data presented here are based on integral readings over a preselected temperature interval. The relative standard deviation for a series of individual readings was about 0.8 percent.*

Figure 1 shows the irradiation geometry. In order to achieve a configuration suited for comparison of the experimental data with future theoretical results for a semi-infinite geometry, the individual TLD samples were pressed into cutouts in the center of 5cmx5cm aluminum sheets of the same thickness as the dosimeter samples. Stacks of these TLD-loaded sheets

* The TLD reader used for most of this work was designed for variable-temperature "on" and "off" gating of an analogue-to-digital converter, which furnished the number of pulses (counts) proportional to the area under the portion of the glow curve between pre-selected minimum and maximum temperatures. With this arrangement, number of counts was found to be more reproducible than peak height.

could be sandwiched between layers of polystyrene, aluminum, copper, or lead, and irradiated with a nearly plane-parallel beam of ^{60}Co gamma radiation of a cross section large in comparison to the lateral extension of the medium. On the side facing the source, the layers were approximately equal in thickness to the range of the most energetic secondary electrons produced in the medium; the layers in back of the aluminum sheets were at least ten times as thick. Since the average Z of CaF_2 is approximately equal to that of aluminum, the TLD-loaded aluminum sheets sandwiched between layers of aluminum may be considered to constitute a homogeneous block.* A single TLD-loaded aluminum sheet, or stacks of two, four, or seven sheets were used, providing a range of dosimeter thicknesses from 0.5 to 3.5 mm (corresponding to mass per unit area from about 0.16 to 1.12 g/cm^2). In order to simulate a semi-infinite geometry in the case of TLD-loaded aluminum sheets in a polystyrene medium (constituting an assembly essentially equivalent to bone in tissue), a block of larger lateral dimensions (30cm x 30cm) was used as well, again in conjunction with a beam of a cross section larger than the irradiated block.

Results

a- Absorbed-Dose Distributions

The measurements furnish information on the response of individual (0.5 mm thick) dosimeter samples placed inside different blocks of extended media, in stacks of varying thickness; or, if one thinks of each stack as one dosimeter, they furnish information on the response distribution over dosimeter depth. Figure 2 shows CaF_2:Mn TL response for the stacks of different thicknesses contained in polystyrene, copper, or lead blocks, relative to the response of the singly exposed samples in the same media. For the homogeneous case of TLD in aluminum, the response across the dosimeter stack was constant to within a relative standard deviation of 0.8 percent.** Therefore, since the TL response is known to be proportional to absorbed dose over wide ranges of electron and photon energies,[8,9] these response distributions reflect the absorbed-dose distributions within the dosimeter stacks. The values shown in figure 2 for each step represent an average of several readings (five in most cases; in some only three or four). Most of these measurements did not reproduce to better than ± 3 to ± 5 percent of the values shown. In view of the 0.8 percent relative standard

* It may be noted here that, because of differences in mass fractions, equal average atomic numbers do not necessarily result in equal stopping powers and attenuation coefficients. However, since measurements in aluminum revealed no interface effects, one must conclude that, for the present experiment, an aluminum medium containing CaF_2:Mn dosimeters may be considered homogeneous.

** For the relatively large source-to-dosimeter distance (~ 150cm) and the small stack depth employed (3.5mm or less), inverse-square reduction in dose and beam attenuation over the dosimeter thickness were smaller than 1 percent.

deviation of individual dosimeter readings and of stack-dosimeter readings in the homogeneous case, this is a relatively large error. Data from the two series of experiments performed with the large polystyrene blocks, in which components could be more precisely assembled, were within ± 2 percent of the indicated values. This suggests that contact and alignment of the individual components of each block assembly are rather critical in this type of experiment, and that one could improve reproducibility by a more careful experimental design.

In spite of the larger-than expected uncertainties, the experiment yielded information on dose distribution in the dosimeters which is of some interest. In figure 2, in which relative TL response (absorbed dose) is shown as a function of order number of the samples in stacks of different thicknesses embedded in the media of different average Z, a definite front-rear asymmetry of the distributions is apparent near the interfaces. The dosimeter layers in the rear are seen to read higher than in front by as much as 15 percent for copper and 30 percent for lead, while, in the case of polystyrene, the front layer shows a reading about 10 percent higher than the rear layer. One may note that absorbed dose at any given depth in the 30cm x 30cm polystyrene block is about 10 percent higher than in the 5cm x 5cm block, but the trend of absorbed dose with depth is not very different. A qualitative analysis of this effect is possible if one assumes that, relative to CaF_2, electron back scattering prevails over forward scattering in copper and lead, while, in polystyrene, only forward scattering is of importance.

These results confirm earlier findings obtained with ionisation chambers[1,2], and suggest that, in a general cavity theory, the angular distribution of the secondary electrons may have to be taken into account. They also suggest that, if TLD powder is used in a cavity of a medium of different atomic number, considerable non-uniformity in the readings of equal aliquots of powder may occur, unless the powder is thoroughly mixed prior to readout, or is contained in a TLD-equivalent capsule of suitable thickness. For a bone-equivalent dosimeter material in a soft-tissue medium, these non-uniformities could amount to more than 10 percent.

b- Average Absorbed Dose in Dosimeter Stacks of Different Thicknesses

By adding the readings of all dosimeters in a given stack, the results of the measurements also may be used to obtain information on total energy absorption, proportional to total response of dosimeters of varying thickness irradiated in extended media of different Z,* and of average absorbed dose, proportional to response per unit mass ("specific response"). This procedure was used to arrive at the data shown in figure 3 from those of figure 2. In figure 3, specific TL response (proportional to average

* The quantities obtained by this summation procedure would be proportional, for instance, to the total response of TLD powder, filling cavities of varying size inside the different media, or to the response one would obtain with solid TLD blocks of the different thicknesses, if self-absorption of the luminescence were negligible.

absorbed dose in CaF_2:Mn embedded in the different media) is plotted as a function of dosimeter thickness, relative to the specific response of the thinnest dosimeter used (the single 0.5mm sample). The solid straight line through unity represents the ideal response for the homogeneous case, for which average absorbed dose is not a function of dosimeter size. In the copper medium, average absorbed dose is seen to be essentially equal to that in the homogeneous case (the points straying about this line by no more than the experimental error). In polystyrene and lead, average absorbed dose decreases as the size of the dosimeters is increased. While, for polystyrene, the downward trend with increasing thickness is within the limits of experimental reproducibility, its consistency suggests that it may be real. For lead, the decrease in average absorbed dose amounts to almost 20 percent.

Comparison with Theory

In order to examine whether the asymmetry effects demonstrated in figure 2 materially influence the trends of average absorbed dose with dosimeter size shown in figure 3, absorbed dose was computed following Burlin's approach,[6] which does not take asymmetry effects into account. Absorbed dose in the TLD stacks (representing cavities comparable in size to the range of secondary electrons) was computed as

$$D \propto d\,(\bar{s})^{TLD}_{med} + (1 - d)\,(\bar{\mu}_{en})^{TLD}_{med}\,, \qquad (1)$$

where $0 \leq d \leq 1$, and the symbols $\bar{s}$ and $\bar{\mu}_{en}$ are ratios of average stopping powers and energy-absorption coefficients. Since it was intended to compare the results of the present computations with those of other authors[3,4], it was important to make comparable choices for the values of d, $\bar{s}$, and $\bar{\mu}_{en}$. Using the (not-too-realistic) expression suggested by Burlin, d values from 0.25 to 0.03 were obtained for dosimeters ranging in thickness from 0.5 to 3.5mm.* In the limit of d = 1 (small cavity), eq 1 is to furnish absorbed dose according to Spencer-Attix theory; therefore, the value for $\bar{s}$ has to be computed for a cavity small compared to secondary-electron ranges. Conversely, in the limit of d = 0, eq 1 is to furnish the absorbed dose in a cavity large compared to secondary-electron ranges; therefore, the $\bar{\mu}_{en}$ values are to be taken for the photon spectrum at the cavity site in the absence of a cavity.

Neither Chan and Burlin nor Ilić-Popović state their assumptions regarding cavity size (and associated electron-energy cutoff) for their Spencer-Attix-type computations of the relative stopping-power values. Therefore, it was decided to compute the two limiting cases of (1) electrons having the average energy of the initial Compton- and photoelectrons, and (2) electrons having an equilibrium slowing-down spectrum (cavity size infinitesimal). Similarly, the values for the ratio of energy-absorption

* Since, in the present experiment, the dosimeter material essentially was semi-infinite, the average electron-track length appearing in the expression for d was computed as 1.2 times the dosimeter thickness; the factor 1.2= 1/0.8 is the one suggested by Spencer and Attix.

coefficients were computed for the cases of (a) a pure ^{60}Co gamma-ray spectrum, as assumed by Ilić-Popović,[4] and (b) the spectrum measured by Costrell[10], which was the one assumed by Chan and Burlin[3].* The electron-stopping powers used were those of Berger and Seltzer,[11] the electron slowing-down spectra those of McGinnies[12], and the energy-absorption coefficients those of Hubbell, published by Evans.[13]

The computations resulted in four sets of absorbed-dose values for each dosimeter thickness. Depending on the medium used, these values were rather insensitive either to the choice of the electron spectrum or the photon spectrum, or both. Therefore, in figure 3, only the sets resulting in the largest trends are shown (broken lines). The values not plotted would agree with these lines to within 1 or 2 percent.

For copper, for which neither the choice of stopping powers nor energy-absorption coefficients was critical, the plotted case(1a) is seen to agree with the experimental data to within the relatively large limits of experimental error. Since, for copper, the choice of d is not too critical either (the two extreme dose values for d = 1 and d = 0 being within ± 6 percent), one must conclude that, within the limits of experimental error, asymmetry effects are unimportant.

For polystyrene, the choice of stopping powers proved to be critical. The plotted trends for the cases (1a) and (2a) are seen to bracket the experimental trend. Therefore, for drawing any conclusions from the trend of experimental and computed data, a decision would be required on how best to compute the stopping-power term in eq 1.

For lead, on the other hand, the choice of energy-absorption coefficients was critical. The plotted trend for case (1a) is seen to coincide with the experimental data, although, from preliminary spectral measurements, it is known that the ^{60}Co gamma-ray beam employed is not free of scattered radiation. The Costrell spectrum (1b) is seen to produce a considerably larger trend. Therefore, for drawing any conclusions from either agreement or disagreement between computed and experimental trends, a more precise knowledge of the photon spectrum at the site of the cavity would be required.

* Because of the plane-parallel beam geometry chosen for the present experiment and the shallow depth in the medium chosen as the site of the dosimeters, there is reason to assume that our photon spectrum at the dosimeter site was purer than that of Chan and Burlin, and not more degraded than that of Ilić-Popović. For this reason, the energy-absorption coefficients computed for the selected gamma-ray spectra are considered to represent upper and lower limits.

References

1- J. Dutreix, A. Dutreix, M. Bernard, Phys. Med. Biol. 1, 69 (1962).

2- C.L. Wingate, W. Gross, G. Failla, Radiology 79, 948 (1962).

3- F.K. Chan, T.E. Burlin, Brit. J. Radiol. 43, 54 (1970).

4- J. Ilić-Popović, Int. J. appl. Radiat. Isotopes 22, 457 (1971).

5- W.L. McLaughlin, in Manual on Radiation Dosimetry, N.W. Holm, R.J. Berry, editors, Marcel Dekker Inc., New York (1970).

6- T.E. Burlin, in Radiation Dosimetry I, F.H. Attix, W.C. Roesch, editors, Academic Press, New York and London (1968).

7- T.E. Burlin, F.K. Chan, Br.J. Radiol. 40, 556 (1967).

8- M. Ehrlich, R.C. Placious, Health Physics 15, 341 (1968).

9- P.R. Almond, K. McCray, Phys. Med. Biol. 15, 335 (1970).

10- L. Costrell, Health Phys. 8, 261 (1962).

11- M.J. Berger, S.M. Seltzer, NASA SP-3036, National Aeronautics and Space Administration, Washington, D. C. (1966).

12- R.T. McGinnies, National Bureau of Standards Circular 597, U. S. Government Printing Office, Washington, D.C. (1959).

13- R.D. Evans, in Radiation Dosimetry I, F.H. Attix, W.C. Roesch, editors, Academic Press, New York and London (1968).

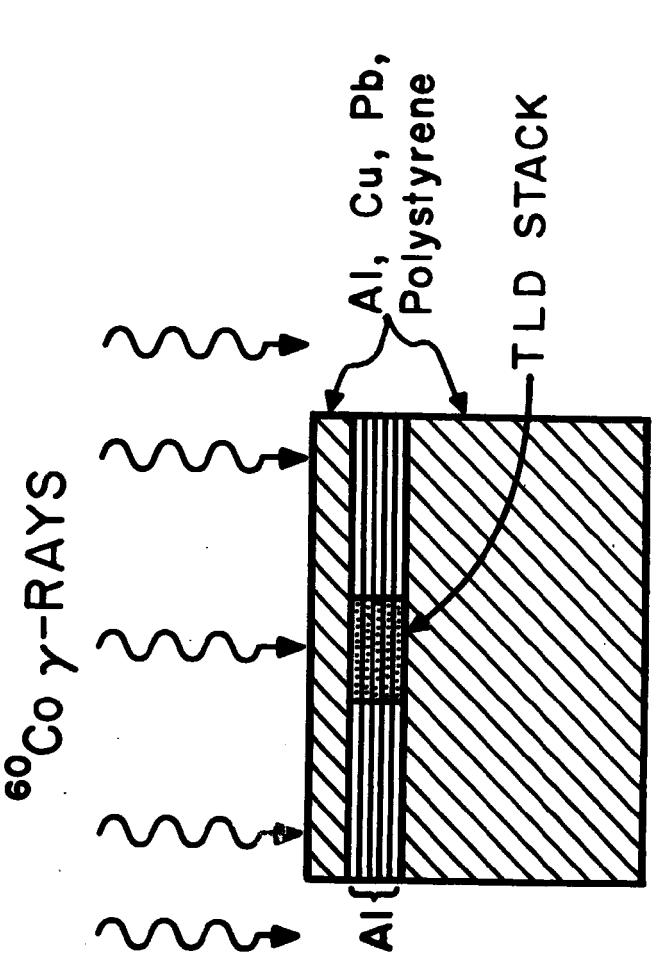

Fig. 1 Irradiation geometry

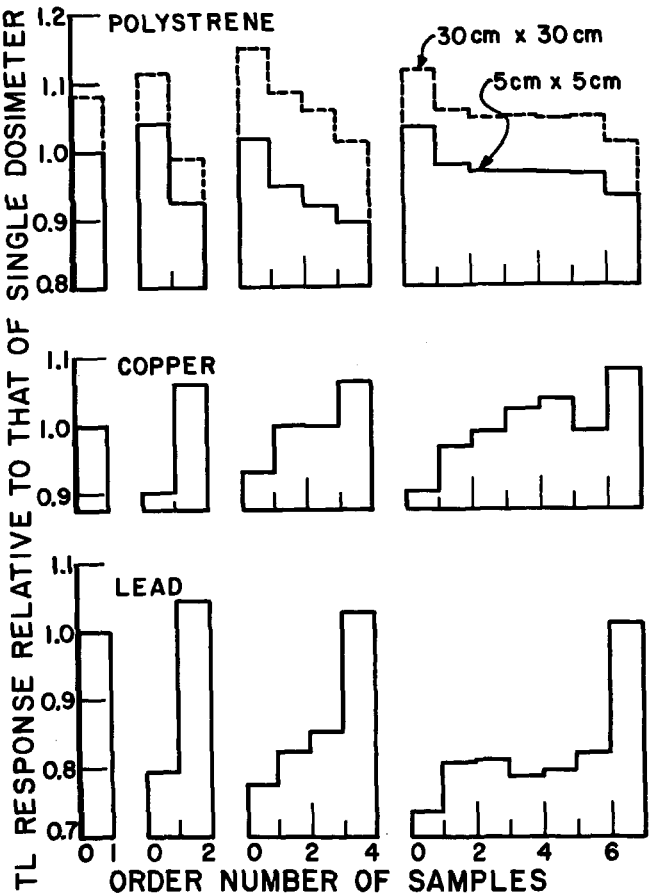

Fig.2 TL response distribution (absorbed-dose distribution) relative to that of singly exposed dosimeter in medium of 5cm x 5cm cross section. Abscissa: Order number of 0.5mm samples in stacks. Radiation incident from left. Each step represents an average of several measurements, straying by up to ±5 percent (solid lines) and ±2 percent (dashed lines).

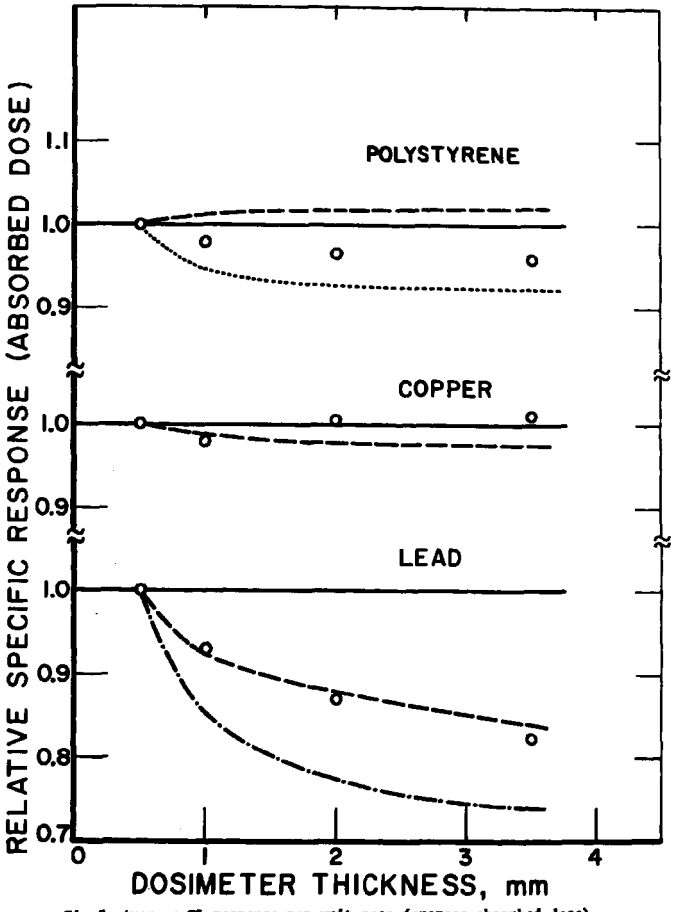

Fig. 3 Average TL response per unit mass (average absorbed dose) relative to that of singly exposed dosimeter; solid lines -- homogeneous case. Response estimated from Burlin's extension of cavity theory; dashed lines -- pure ^{60}Co gamma-ray spectrum, average initial electron energy (case 1a); dotted line-- pure ^{60}Co gamma-ray spectrum, equilibrium slowing-down electron spectrum (case 2a); dash-dotted line-- Costrell ^{60}Co gamma-ray spectrum, average initial electron energy (case 1b).

Puite

Will you also extend these experiments into the X-ray region? In my opinion, this would be very valuable.

Erhlich

I plan an extension to high-energy electrons, but not to low-energy X-rays. An extension into the X-ray region would require very thin dosimeters.

Exoelectronic Properties of Al_2O_3-solids

by

G.Holzapfel and E.Chryssou

Physikalisch-Technische Bundesanstalt, Berlin, Germany

Technical University of Athens, Phys.Lab.I, Athens, Greece

Abstract

Besides BeO-materials, Al_2O_3-solids seem to be appropriate to TSEE dosimetry. The exopassive γ-modification changes continuously to the stable and exoactive α-modification between 800°C and 1200°C. For powder materials as well as for ceramics and single crystals an intense double glow peak around 450°C is characteristic and may be correlated to electron traps within a thin oxygen-deficient cubic surface layer which is mismatched to the underlying hexagonal bulk material. This peak may be convenient especially for high temperature dosimetry and another double peak around 250°C for ordinary TSEE dosimetry.

Introduction

In integrating solid state dosimetry Berylliumoxide (BeO) has been most frequently used as TSEE material [1]. Mixtures of Berylliumoxide and graphite powders (BeO/C) seem to be more effective than nonconductive BeO-ceramics with respect to radiation response linearity and reproducibility. On the other hand, dispersed materials like powders are sometimes dangerous to handle because of the toxidity of BeO. Therefore, non-toxic

TSEE materials with low effective atomic number are investigated now. Despite of apparent lower chemical stability, Aluminumoxide (Al_2O_3) is believed to be a promising TSEE material.

Al_2O_3-Modifications

Among the different Al_2O_3-modifications

$$Al_2O_3 \cdot 3H_2O \xrightarrow[150^oC]{} Al_2O_3 \cdot 1H_2O \xrightarrow[300^oC]{} \gamma\text{-}Al_2O_3 \xrightarrow[1000^oC]{} \alpha\text{-}Al_2O_3$$

only the anhydrous γ- and α-phases are stable in the temperature range of TSEE dosimetry (200 - 600°C). The transformation $\gamma \rightarrow \alpha$-$Al_2O_3$ around the 1000°C annealing temperature is detected by X-ray diffraction techniques and correlated to measurements using well-known TSEE-glow curve techniques [2,3]. "Pure" γ-Al_2O_3 (MERCK 1095) is totally transformed to α-Al_2O_3 by annealing in air at 1200°C. After this treatment different charges of MERCK-material, some of them fabricated recently and others years ago, always show an identical six-glow-peak arrangement with a remarkably intense high-temperature double peak around 450°C, Fig.1. Annealing temperatures below 1200°C produce a mixed γ/α -Al_2O_3 material. The α-Al_2O_3 glow curve is only lowered in the semilogarithmic graph of Fig.1 but not essentially changed in shape. That means, γ-Al_2O_3 is nearly exopassive and rather acts as a matrix for the strongly exoactive α-Al_2O_3 modification which seems to be present in seeds already in the initial "pure" γ-Al_2O_3 material with the lowest glow curve in Fig.1.

Nature of Traps

In order to get some information on the nature of electron traps in α-Al_2O_3 we analyzed the glow spectrum according to the method of Balarin and Zetzsche [3,4]. In table 1 the normalized glow peak locations, T_{max} ($1^oC/S$), and the term data (activation energy E and frequency factor K_o) of the peaks at moderate temperatures are listed. The strongly overlapped high temperature peak could not be evaluated exactly up to date. The frequency factors reach values close to the Debye-frequency of the bulk material. From that we exclude traps in sorption layers which generally exhibit much lower frequency factors [3,5].

Since TSEE is an effect in the surface region, the atomic structure of the disordered surface is of major importance. Several authors [6,7] have suggested that the traps in Al_2O_3 consist in oxygen vacancies (F-centers). Recently, from low energy electron diffraction (LEED-) studies on α-Al_2O_3 single crystals [8] it was concluded that by annealing at high temperatures, especially with Al- or Si-contamination, the surface structure is changed chemically within a few atomic layers from hexagonal Al_2O_3 to cubic Al_2O or AlO, Fig.2. This stable and very thin overlayer is strongly mismatched to the underlying hexagonal bulk material. Therefore, a multitude of lattice defects within the range of exoemission depth of some 100 Å is expected which may act as electron traps.

Al_2O_3-Single Crystals

Evidence for the existence of this kind of electron traps

is given from our experiments on Al_2O_3-single crystals, Fig.3. Single crystals, grown at our institute and annealed after preparation at 1200°C exhibit only a high temperature double peak. The structure at moderate temperatures in the glow curve of polycrystalline material is missing. After producing fresh surfaces which never have seen high temperatures, by smashing the same single crystal in a ball mill the high temperature double peak disappears and a pronounced emission is raised at moderate temperatures. But, additional annealing of the fresh surfaces at 1200°C regenerates the high temperature emission obviously by restoring the discussed thin surface layer.

Al_2O_3-Ceramics

The glow curve of Al_2O_3-ceramics (MRC Superstrate 7800) Fig.4, does not undergo a change by smashing and successive annealing. Especially, the high temperature glow peak is always present. This can be explained because ceramics consist of sintered grains which have been mechanically treated and heated already during fabrication, i.e. smashing does not really produce new surfaces and the discussed exoactive surface overlayer may be inherent to the ceramic material.

Potential Applications in TSEE Dosimetry

Starting from powder materials we notice first that by proper annealing at temperatures between 800°C and 1200°C, see Fig.1, the sensitivity can be adjusted to values within three orders of magnitude. This procedure is more effective than diluting the exoactive material by foreign exopassive admixtures. Those admixtures may be preferably applied for varying the effective

atomic number.

Dose response linearity and reproducibility of dose measurements depend on the conductivity of the material. We observed that the emission on the high temperature peak around 450°C in the glow curve of Al_2O_3 powders, ceramics and single crystals, Fig.5, is much less impaired by this effect than the emission at moderate temperatures. Evidently, increasing conductivity above 300 - 400°C eliminates disturbing surface charging.

When powder materials with conductive exopassive admixtures (graphite) are used the double peak around 250°C may be convenient for the main dose read out and the double peak around 450°C for dose information storage only. However, rugged solids like ceramics and single crystals without conductive additives may also be applicable, especially for high temperature dosimetry. In this case, the intense high temperature double peak around 450°C has to be used for the main read out.

References

1. K.Becker, J.S.Cheka, and R.B.Gammage, Proc.Third Internat. Symp. Exoelectrons, PTB-Mitteilungen 80, 334 (1970)
2. E.Chryssou, and G.Holzapfel, to be published in phys.stat. sol. (a)
3. G.Holzapfel, Z.angew.Phys. 29, 107 (1970)
4. M.Balarin, and A.Zetzsche, phys.stat.sol. 2, 1670 (1962)
5. G.Holzapfel, and R.Nink, phys.stat.sol.(a) K 181 (1970)
6. L.Grunberg, and K.H.R.Wright, acta physica austriaca 10, 375 (1957)

7. T.Lewowski, acta physica polonica 20, 161 (1961)

8. T.M.French, and G.A.Somorjai, J.Phys.Chem. 74, 2489 (1970)

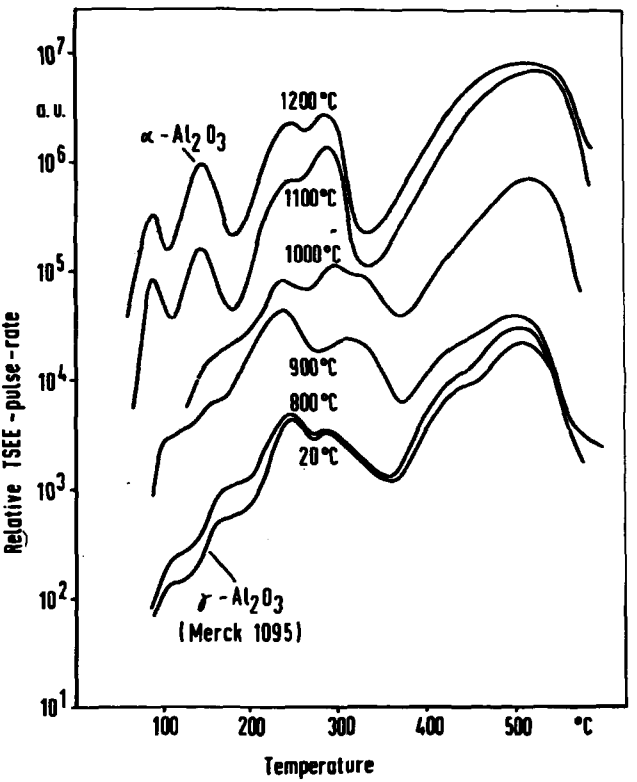

Fig. 1 TSEE glow spectra of Al_2O_3 recorded parallel to the γ - α phase transformation between 800°C and 1200°C. Parameter: Annealing temperature. Annealing time: 4 hours. Normalized to equal X-ray doses, approx. 10 R.

Heating rate of glow curve recording: 0.34 °C/s

Table 1

T_{max} (1°C/s) °C	E eV	K_0 s^{-1}
105	0.9_4	$3 \cdot 10^{11}$
161	1.2_0	$6 \cdot 10^{12}$
267	1.5_1	$6 \cdot 10^{12}$
313	1.6_6	$1 \cdot 10^{13}$

Table 1 Term data of electron traps in γ/α -Al_2O_3

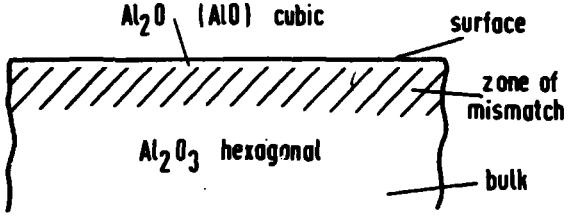

8) T.M. French and G.A. Somorjai

Fig. 2 Al_2O- or AlO-overlayer on α-Al_2O_3-single crystal, see Ref. 8.

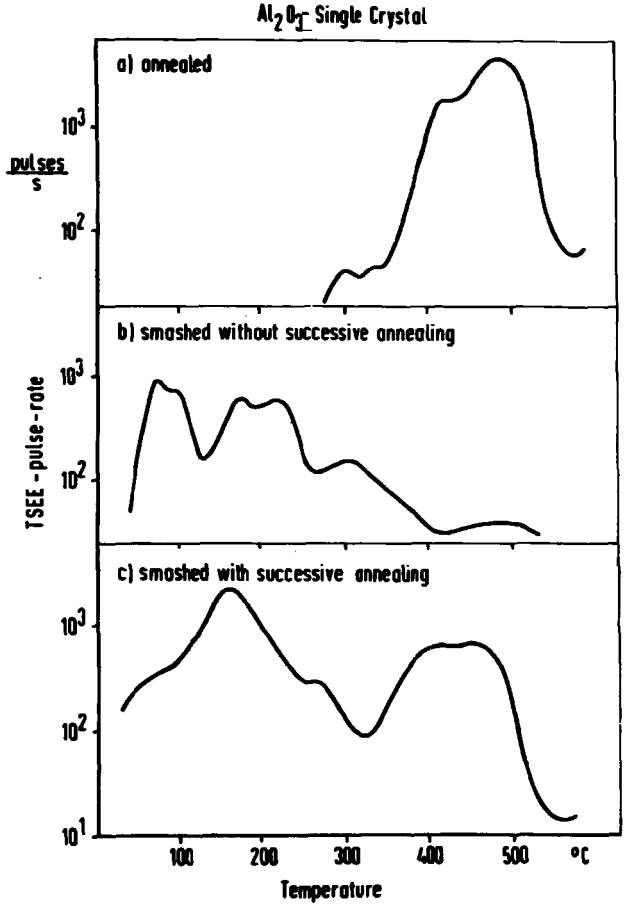

Fig. 3 TSEE glow spectra of solid and dispersed Al_2O_3 - single crystals. Heating rate: 0.34 °C/s. Annealing temperature: 1200°C. Annealing time: 4 hours.

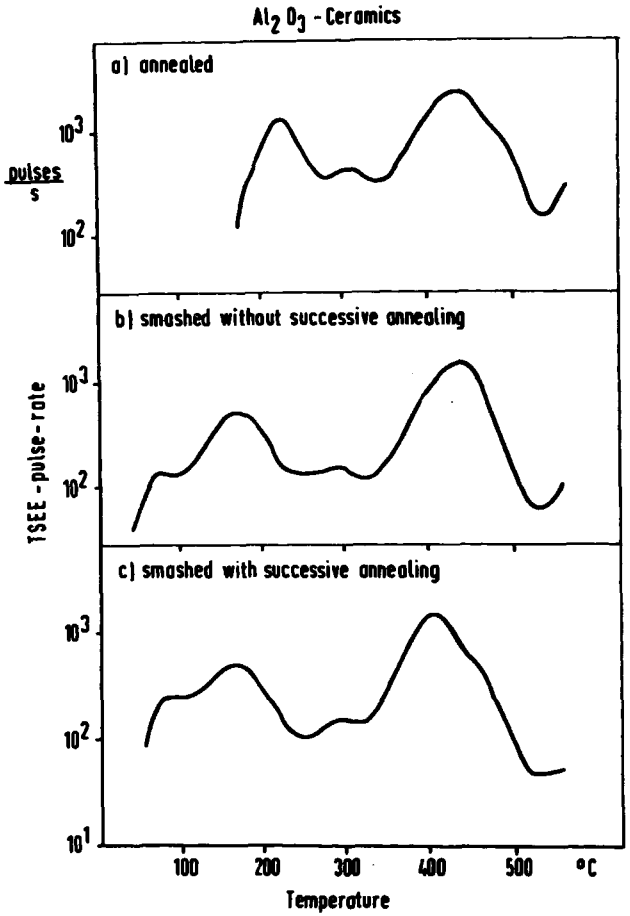

Fig. 4 TSEE glow spectra of solid and dispersed Al_2O_3-ceramics. Heating rate: 0.34 °C/s. Annealing temperature: 1200°C. Annealing time: 4 hours

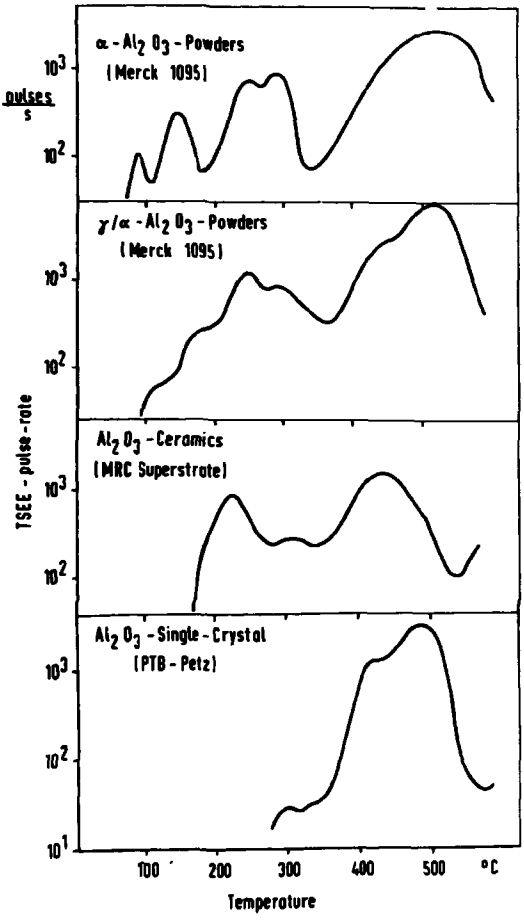

Fig. 5 TSEE glow spectra of different Al_2O_3-materials. Heating rate: 0.34 °C/s.

Rotondi

You mentioned that a TSEE material for dosimetry purposes must be characterized by a low atomic number. I should like to remark that the electron build-up available for trapping in the sensitive layer is largely dependent on the encapsulating or covering material during irradiation.

Holzapfel

Yes, you are right. TSEE seems to be less dependent on the effective atomic number, at least in the thin sensitive surface region. But it is probably preferable to use low-Z material also for TSEE in order to get correlation with the related and well-established phenomenon of TL in dosimetry.

Third International Conference on Luminescence Dosimetry

Risø, Denmark

October 11-14, 1971

Chemically, Thermally and Radiation-Induced Changes in the TSEE Characteristics of Ceramic BeO[1]

by

R. B. Gammage, K. Becker, K. W. Crase, and A. Moreno y Moreno
Health Physics Division
Oak Ridge National Laboratory
Oak Ridge, Tennessee 37830

Abstract

Of the materials studied so far at ORNL, some commercial ceramic beryllium oxides (Brush Thermalox 995) exhibited the most promising properties for practical TSEE dosimetry. It has been found that a pronounced TSEE peak at ~325°C in this material is closely associated with the presence of SiO_2 in the emitting surface. The peak can be destroyed and an unusual "self-excitation" effect induced by removal of the SiO_2. Both effects are reversible by restoring the initial SiO_2 concentration in the surface. Heat sensitization (optimum sensitivity is obtained by several hours of preheating at 1400°C), can be related to the phase diagram of the BeO-SiO_2 system, in particular the formation of phenacite (Be_2SiO_4). Of several other potential activators, only Li^+ was shown to have a pronounced effect in increasing the high temperature peaks at ~450 and ~550°C. The sensitivity can be optimized at a diffusion temperature of 1000°C.

Unlike X, beta and gamma radiation, high doses of heavy particles create semipermanent changes in the TSEE peak ratios. In BeO:Si, bombardment with 10^{10} rad or more of 200 keV deuterons, for example, destroys most of the silicon traps. Annealing at 950°C increases the TSEE peak at ~450°C, which disappears after further annealing at 1400°C. A brief interpretation of these effects is given.

---

[1]Research sponsored by the U.S. Atomic Energy Commission under contract with the Union Carbide Corporation.

[2]Visiting scientist, University of Mexico, Mexico D.F.

Introduction

It has been pointed out in previous publications[1-3] that a commercial ceramic Beryllium oxide, which is made in different sizes and shapes under the trade name of Thermalox 995 by the Brush Beryllium Company, is superior in its dosimetric properties to all other materials which we investigated so far. It is the purpose of this paper to summarize the results of some recent studies concerning the effect of various parameters on the characteristics of this material. In particular, we will describe attempts to optimize the sensitivity and stability of the radiation response by heating, activation, and/or exposure to a high flux of heavy ions.

Heat Treatment

In the following experiments, usually ceramic disks 12.4 mm in diameter have been used and evaluated, after exposure to ~100 mR of gamma radiation, in a gas-flow GM counter at a heating rate of 1°C/sec. Heating of these disks to temperatures exceeding ~800°C for several hours in air prior to exposure resulted in an increase of sensitivity. If the sensitivity after four hours of heating is plotted as a function of temperature (Fig. 1), a sharp peak at 1400°C results. The same maximum sensitivity can be obtained if a sample is first heated to 1500°C, followed by heating to 1400°C. Preheating not only increases the sensitivity, but also increases the reproducibility of the reading from about ± 20% standard deviation to about 5% for the same group of disks.

This heat sensitization, resulting in a hydrophobic surface, is partially reversible when the surface equilibrates with water. Still, a substantial increase of sensitivity by about a factor of four remains, indicating that only traps in the immediate surface region are affected by the interaction with water. No chemically induced fading can be observed in sensitized and equilibrated samples at storage temperatures up to 100°C. Of course, dehydration and hydration are completely reversible processes. It is interesting to note

that heat sensitization and hydration only affects the main TSEE peak at ∿325°C* (Fig. 2), leaving the smaller high-temperature peaks at ∿450 and ∿535°C (not resolved in Fig. 2) unaffected.

Silicon Activation

The TSEE curve of Thermalox 995 which contains as a main impurity 0.2% silicon, has been compared (Fig. 3) with that of another, purer preparation of the same ceramic which contains thirty times less Si (Thermalox 998). Not only is the characteristic peak at ∿325°C lacking in the purer material, but the reproducibility of the readings is much less and a strange, non-radiation induced TSEE signal is observed during multiple reading cycles ("self-excitation"). This effect has some similarity to the "cold cathode discharge" as observed in ceramic Al_2O_3, MgO and BeO.[4]

An electron microprobe analysis shows that the actual surface concentration of Si, in particular at growth steps and grain boundaries, is even higher than in the bulk of Thermalox 995, averaging about 1% of silicon. In order to remove the SiO_2 without affecting the BeO, samples have been etched with hydrofluoric acid.[5] By this treatment, the dominant TSEE peak at ∿325°C (Fig. 4) could be eliminated without affecting the smaller high temperature peaks. The material becomes very similar in behavior to the Thermalox 998 with its much lower Si content.

The peak at ∿325°C can be fully restored by impregnating the surface with SiO_2 again (a 350 Å layer of silicon was vacuum deposited onto the etched surface, oxidized and diffused into the BeO at 1400°C). Etching and reimpregnation are reversible. In the insensitive 998, silicon coating, oxidation and heat treatment at 1400°C also induced as expected a strong TSEE peak at ∿325°C, thus making it almost identical to the 995.

*All temperatures given are those measured by a thermocouple at the bottom of the sample; due to the thermal gradient in the sample, the actual temperature of the emitting surface layer is lower.

A thin layer of silica itself does not give appreciable TSEE signals. Self-excitation also occurs and disappears as the Si-concentration in the surface is changed. One concludes that it is the presence of silicon in BeO which gives rise to strong exoelectron emission at ∿325°C.

For an explanation of the role of silicon and the effects of heat treatment, reference should be made to the phase diagram[6] for bulk BeO-SiO_2 (Fig. 5): There is a eutectoid at 1560°C, below which 99% is composed of BeO and 2 BeO·SiO_2 (phenacite). Above 1560°C and below the eutectic temperature (1670°C), the phenacite decomposes to solid BeO + solid SiO_2. Solid BeO + liquid form above the eutectic point. It appears necessary for SiO_2 to be in the form of 2 BeO·SiO_2 to act as a TSEE "activator", because the production and decomposition of phenacite appears to coincide with the increase and decrease of the TSEE peak at ∿325°C.

One can speculate why silicon is such a good activator. BeO is one of the few oxides crystallizing in the wurtzite structure. The small size of the beryllium ion (0.31 Å radius) and the nearly perfect packing of the anions suggests that BeO might be relatively free from substitutional impurities. Si^{4+} (0.41 Å) is a particularly suitable candidate for substitution because of its closeness in size to the Be^{2+} ions and its preference for tetrahedral coordination. It is suggested that within the exoelectron emitting region, substitutional Si^{4+} in place of Be^{2+} acts as an electron trap giving rise to the ∿325°C TSEE peak because of its excess positive charge with respect to the normal lattice sites. We do not know, however, whether the Si trap is located in the BeO, the phenacite, or in the interface region between both.

Other Activators

Experiments are being carried out with modified BeO/SiO_2 systems, in particular with ceramics containing larger amounts of SiO_2, and with ceramics to which other low-Z metal oxides have been added with or without the presence of SiO_2. So far, it appears that an increase of SiO_2 by a factor of two further

increases the sensitivity, but that additions of MgO, Al_2O_3 and CaO have only relatively little influence on the sensitivity. Work with some high-Z activators such as Ti and Mn is also in progress, but has not yet lead to substantial results.[7]

So far, distinct success in influencing the TSEE spectra with other elements than Si has only been achieved by diffusing Li^+ into the BeO.[8] Lithium activation has the effect of increasing the intensity of the TSEE peaks at ∿450 and ∿535°C up to 50 and 20 fold, respectively, without affecting the peak at ∿325°C, if the Li activation is carried out at 1000°C (Fig. 6). The exoelectron trap is probably an oxygen vacancy formed to preserve charge neutrality during substitution of Be^{2+} by Li^+. Unfortunately, the Li-induced TSEE response is somewhat erratic, which makes it unlikely that lithium activation has much practical value for dosimetry. Perhaps lithium imparts hydrophilic character to the surface because of its highly polar character, thus making the surface-doped BeO more prone to chemical attack by atmospheric constituents.

Radiation Effects

It can be speculated that heavy particle exposure should be effective in creating oxygen vacancies which act as in lithium doping. Indeed, exposure to more than 10^4 rad of alpha radiation also increased the high temperature TSEE peak at ∿535°C. BeO 995 detectors, after sensitization at 1400°C, were also exposed to high fluences of deuterons (about 7×10^{11} to 2×10^{15} d/cm^2, corresponding approximately to doses of 10^6 to 10^{10} rads in BeO). Subsequent exposure to gamma radiation resulted in TSEE curves differing significantly from those obtained prior to deuteron bombardment (Fig. 7). A deuteron fluence of 10^{14} d/cm^2 caused the peak at ∿325°C to be reduced in intensity by a factor of approximately 2.3×10^3, a peak intensity at ∿450°C to be slightly enhanced and the ∿535°C peak to be of greatly reduced intensity.

To study the effect of annealing on sensitivity and peak ratios, the radiation-damaged samples were heated at temperatures between 650° and 1400°C for one hour. The results are summarized in Fig. 8. The ∿450°C peak increases to maximum intensity at 950°C. At this point, sensitivities of $\sim 10^3$ counts/mR/cm^2 are obtained. Obviously, a peak at ∿450°C is not subject to thermal fading at storage temperatures up to 200 to 250°C, making this material suitable for dose measurements at high ambient temperatures. The peak at ∿535°C is not much affected by the deuteron bombardment. The ∿325°C peak which was severely reduced in intensity as a result of deuteron bombardment begins to grow back at 1000°C until at 1400°C the original intensity is fully restored.

The intensity changes in the ∿325°C peak can be explained as follows: During deuteron irradiation at currents of ∿10 μA, severe near-instantaneous heating and cooling occurs on a localized scale within the range of the deuteron (<1 μ), resulting in at least partial decomposition of the phenacite and the associated exoelectron activity.

Radiation damage centers such as interstitials, vacancies, or clusters of such are most likely giving rise to the increase in the ∿450°C peak intensity. After annealing at 900°C, a defect cluster is probably causing the ∿450°C peak intensity to be enhanced further. Even after annealing of the radiation damage centers at 1000°C and higher, there remains evidence for the presence of a new defect complex, because a weak TSEE peak is introduced at ∿400°C. It is possible that the highest TSEE peak (∿535°C) is linked to single oxygen vacancies such as might be expected from lithium doping or low dose charged particle irradiation.

Acknowledgments

The authors would like to thank other members of the TSEE team, in particular J. S. Cheka and J. S. Nagpal, as well as numerous other colleagues at ORNL for experimental assistance and valuable discussions.

References

1. K. Becker, J. S. Cheka and R. B. Gammage, Proc. Int. Symp. Exoelectrons, PTB-Mitt. 80, 335 (1970).

2. K. Becker, J. S. Cheka, K. W. Crase and R. B. Gammage, Paper SM 143/37, IAEA Symp. on New Radiation Detectors, Vienna 1970.

3. K. W. Crase, K. Becker and R. B. Gammage, ORNL-TM, in press (1971).

4. D. W. Mayer, Proceed. 5th. Nat. Conf. Electron Tube Techniques, Pergamon Press 1961, p. 70.

5. R. B. Gammage, K. W. Crase and K. Becker, Health Phys., in press.

6. E. M. Levin, C. R. Rolskins, and H. F. McMurdie, Phase Diagrams for Ceramists, Am. Ceramic. Soc., Columbus 1964.

7. J. S. Nagpal and J. S. Cheka, unpublished.

8. A. Moreno y Moreno, J. S. Cheka, R. B. Gammage, J. S. Nagpal and K. Becker, ORNL-TM, in press.

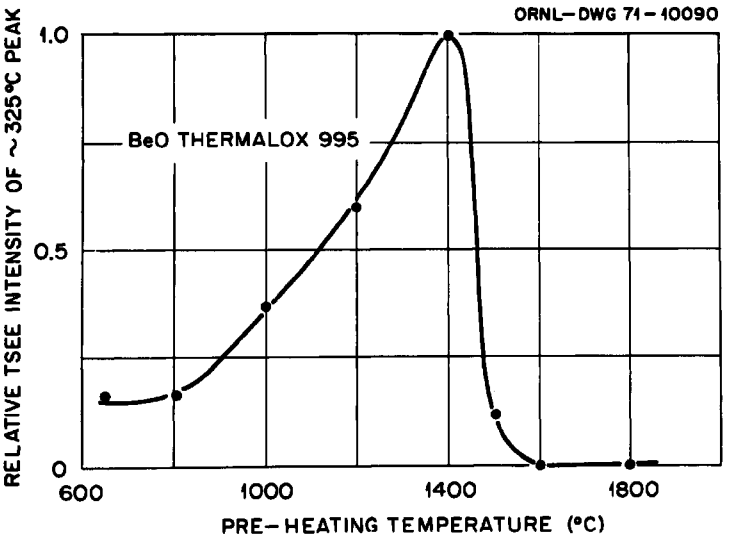

Fig. 1. Relative TSEE emission of the ~325°C main peak of ceramic BeO (Thermalox 995) as a function of the temperature at which the samples have been preheated for four hours.

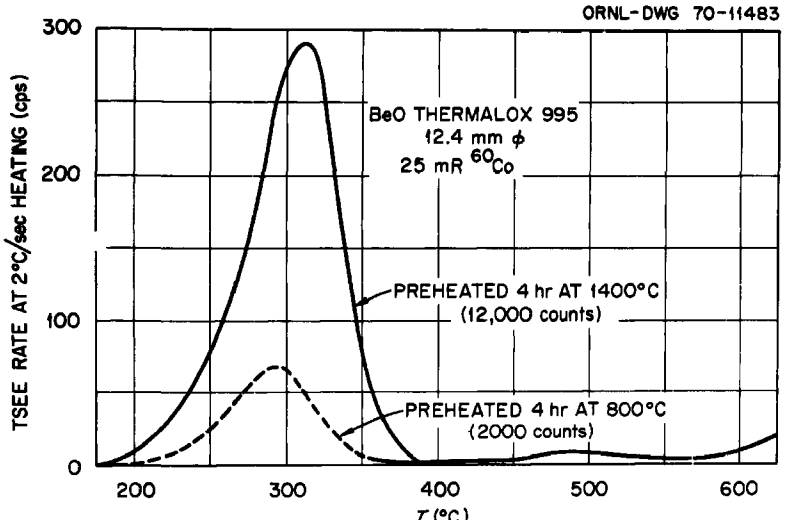

Fig. 2. Effect of heat pretreatment on the TSEE curve of Thermalox 995.

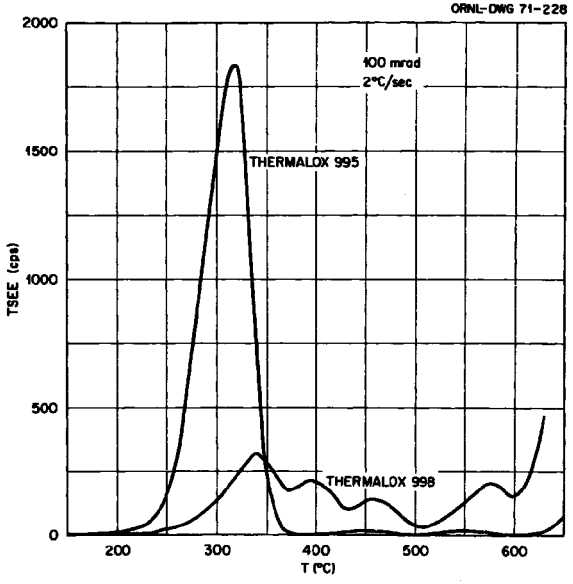

Fig. 3. TSEE curves of untreated BeO Thermalox 995 and 998.

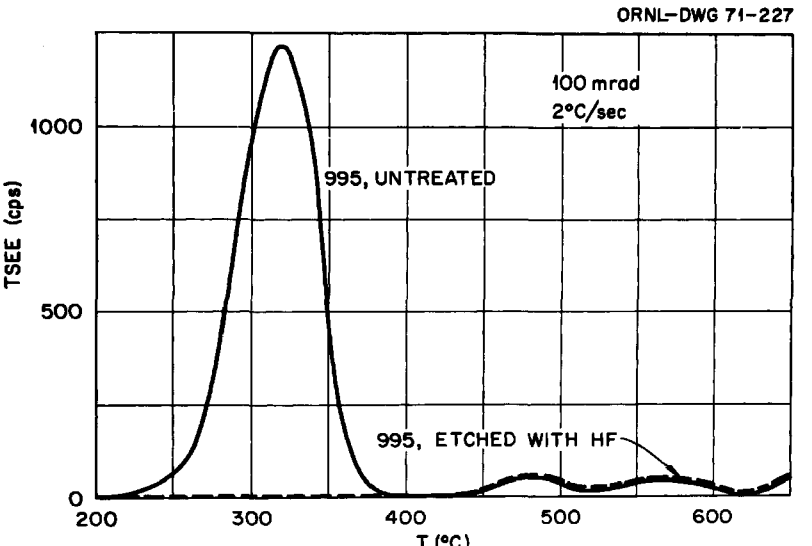

Fig. 4. TSEE curves of BeO Thermalox 995 before and after etching for several seconds in 40% HF.

ORNL-DWG 71-6876

R.A. MORGAN AND F.A. HUMMEL, *J. AM. CERAM. SOC.*, 32 [8] 255 (1949)

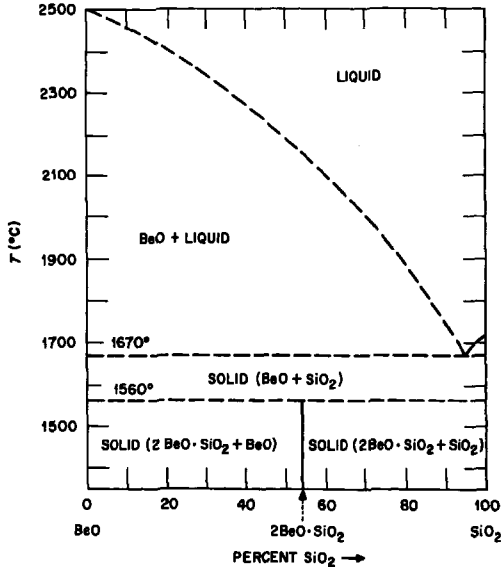

Fig. 5. Phase diagram of $BeO-SiO_2$ (after ref. 6).

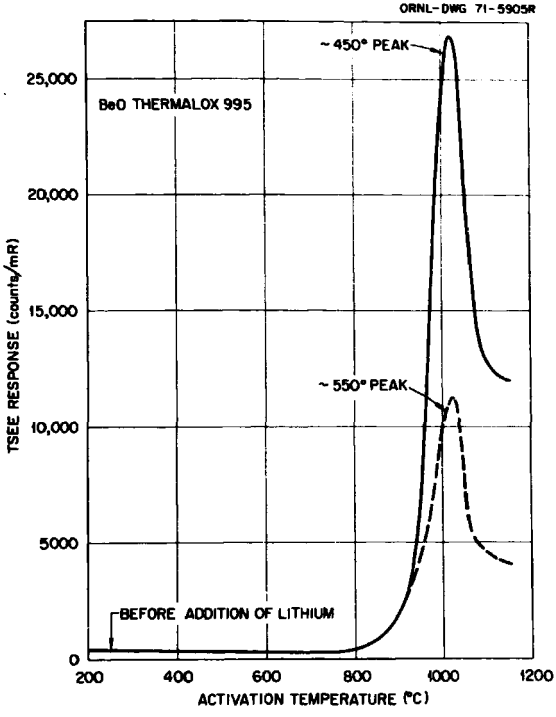

Fig. 6. Increase of the high-temperature TSEE peaks in BeO Thermalox 995 as a function of the temperature at which Li^+ is diffused into the material.

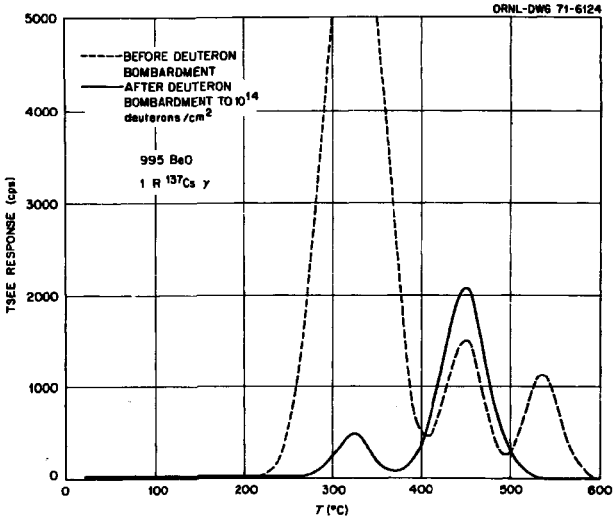

Fig. 7. Effect of 10^{14} deuterons/cm^2 irradiation on the TSEE curve of Thermalox 995 BeO (heating rate 1°C sec.).

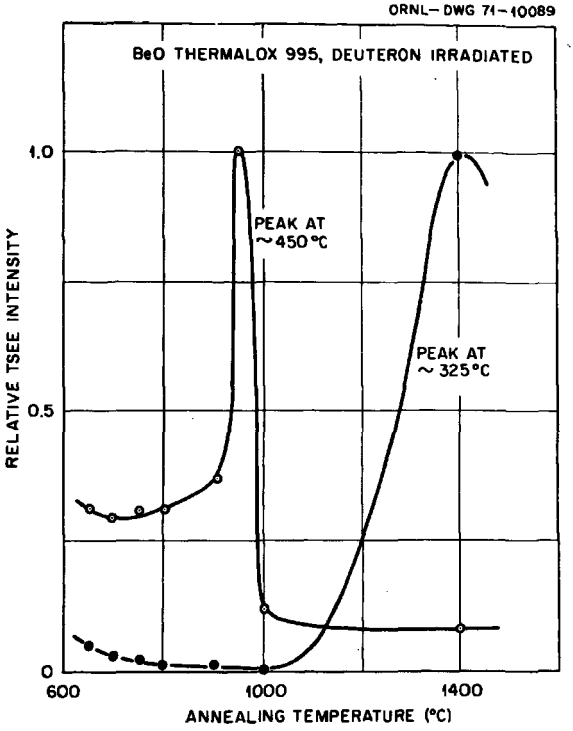

Fig. 8. Relative peak intensities in deuteron irradiated Thermalox 995 BeO, normalized for the ~325°C peak after 1400°C treatment and the ~450°C peak after heating at 950°C, as a function of post-irradiation annealing temperature.

Attix

What heat treatment was used for the Thermalox 998 discs?

Becker

Neither of the two samples compared in figure 3 got any heat treatment.

Exoelectron Dosimetry with Oxide Mixtures

by

M. Euler, W. Kriegseis, and A. Scharmann
I. Physikalisches Institut der Universität Giessen, Germany

Abstract

Results describing the dependence of the thermally stimulated exoelectron emission (TSEE) of BeO on various oxide and silicate admixtures after high temperature pretreatment at 1100 °C are reported.

The intensity of emission is not affected by low concentrations of MgO, Al_2O_3, or SiO_2, but is reduced by high concentrations. A mixture of BeO+ZnO+2 SiO_2 was considerably more sensitive than all its components. Although during the heat pretreatment Be_2SiO_4 and Zn_2SiO_4 are formed, the increase of sensitivity is only correlated to the combination of ZnO and BeO. This could be concluded from a comparison of the individual TSEE-curves of the mixture - components and was verified by an investigation of the system BeO+ZnO.

BeO is one of the most suitable materials for TSEE - dosimetry due to its high sensitivity, chemical stability, and favourable fading characteristics. However, investigations of BECKER indicated, that as well the temperature of the emission maximum as the sensitivity of the available commercial BeO-powders and BeO-ceramics vary from each other [1].

The relative impure Thermaload - powder (Brush Beryllium Co.) yielded a considerably higher emission than the purer BeO-powder, produced by Merck. It can be assumed that the TSEE of BeO strongly depends on chemical impurities. After the diffusion of evaporated Au, Pd or Pt into ceramic samples, BECKER also observed increased sensitivity, which was explained by a reduction of the work function [1]. Apart from these experiments very little is known about the correlation of the TSEE of BeO with defined impurities. Therefore we investigated the TSEE of the rather pure Merck-BeO and its dependence on admixtures of various oxides. These experiments should enable the development of new substances with increased sensitivity compared to the materials so far available.

For our experiments the powder-mixtures of BeO with other oxides were heated for a few days at 1100 ^{o}C in Al_2O_3-vessels in a closed furnace. To avoid contaminations, we placed the Al_2O_3 - vessels in quartz tubes, which were open at one end. The substances were pulverized after the high temperature treatment and sedimented on graphite discs of 19 mm diameter and 0.8 mm thickness. These samples were pre-annealed for 30 minutes at 600 ^{o}C, and afterwards slowly cooled down to room temperature during 30 minutes, that no backround emission could be induced by quenching. They were irradiated by a 50 kV - X - ray tube (Dermopan, Siemens) or a ^{60}Co - source. The TSEE was measured in a high vacuum apparatus (heating rate 0.5 $^{o}K \cdot sec^{-1}$) by an open multiplier and a combination of amplifier, counter, and printer.

First we investigated mixtures, which contained one of the main impurities Mg, Al or Si of the Thermaload-powder. After doping with small amounts of MgO, Al_2O_3 or SiO_2we could not observe any important changes of the TSEE compared to the undoped heated

BeO-powder of Merck. Higher concentrations of oxide admixtures reduced the sensitivity as is pointed out for Al_2O_3 by fig. 1. This results was astonishing at least in the case of Al_2O_3. We had expected a remarkable increase of sensitivity, because EPR-investigations by DU VARNEY, GARRISON and HAREM[2] proved, that in Thermalox 995, a commercial ceramic BeO-material, Be^{2+} is substituted by Al^{3+}. The Al^{3+}-ions act as electron traps and thus should contribute to an increase of the concentration of exoelectron emission-centres. However, our negative results may be caused by the fact, that possibly the temperature of 1100 °C is not high enough for the substitution of a sufficient amount of Be^{2+} -ions by Al^{3+}. This may also be valid for the incorporation of Mg or Si.

We also investigated a mixture of ZnO+BeO (Merck) + 2 SiO_2, which was heated for 3 days at 1100 °C. X-ray diffraction analysis proved that it was mainly composed of Zn_2SiO_4 and Be_2SiO_4 after the heat treatment. Rests of BeO, SiO_2, and in a smaller degree of ZnO, were also present. Normally Be_2SiO_4 from BeO and SiO_2 is formed at temperatures not lower than 1500 °C. If ZnO is present, the conversion takes place already at 900 °C[3]. Our mixture is as sensitive as Thermaload. A comparison with the TSEE of Merck-BeO is presented in fig. 2. The broad main peak at about 280 °C indicates a substructure, and therefore can be assumed to be due to various electron emission centres. Probably the most active of these traps is not present in the original materials. At 280 °C neither ZnO nor BeO have maximum emission, only SiO_2 which is, however, far too insensitive to cause the observed increase of the emission current (fig. 3).

A correlation of the new emission centres to the silicates, which are formed during the heat pretreatment at 110 °C, can also be excluded. We compared the TSEE of the oxide-silicate-mixture to that of pre-annealed Zn_2SiO_4 (produced by van Baerle & Co) and Be_2SiO_4 (Prof. Bauer, Institut für Anorganische Chemie, TH Karlsruhe) (fig. 4). Doses of 300 R can hardly be detected with Zn_2SiO_4 (curve a). The TSEE-curve of the Be_2SiO_4 powder also exhibits an emission peak at 280 °C, but with lower intensity

than the oxide-silicate-mixture (curve b). After admixture of Zn_2SiO_4 this peak vanishes completly (curve c).

From all these results we concluded that the increased sensitivity of our silicate-oxide-mixture is due to the system of BeO+ZnO. This statement is verified by fig. 5. The TSEE-curve of a mixture of BeO (Merck) and ZnO, which was fired for 12 hours, is very similar to the Thermaload-curve in shape and intensity. After a longer heating period the maximum of emission shifts towards 280 °C. The peak of Be_2SiO_4 at this temperature is caused by rests of ZnO and BeO.

In fig. 6 the response of our silicate-oxide-mixture is plotted for exposures to various doses D of the radiation of a ^{60}Co - source. The values on the ordinate are proportional to the sum of counted TSEE-pulses in the temperature range of 250° - 350 °C. We did not receive linearity of the response, but a $D^{0.8}$ - relation. The upper and lower detection limit depend mainly on the electronic device and can be improved.

Our work on this subject is not yet finished. We recently discovered that a mixture of Thermaload + ZnO is even more sensitive than Thermaload itself. Further improvement also seems to be possible by optimizing the lenght of the heat treatment.

References

1) K. Becker, J. S. Cheka, and M. Oberhofer, Health Phys. 19, 391 - 403 (1970)

2) R. C. Du Varney, A.K. Garrison, and S.B. Harem, phys. stat. sol. (b) 45, 259 - 264 (1971)

3) G. R. Fonda, J. electrochem. soc. 95, 3o4 - 315 (1949)
A. P. Rice, J. electrochem. soc. 96, 114 - 122 (1949)

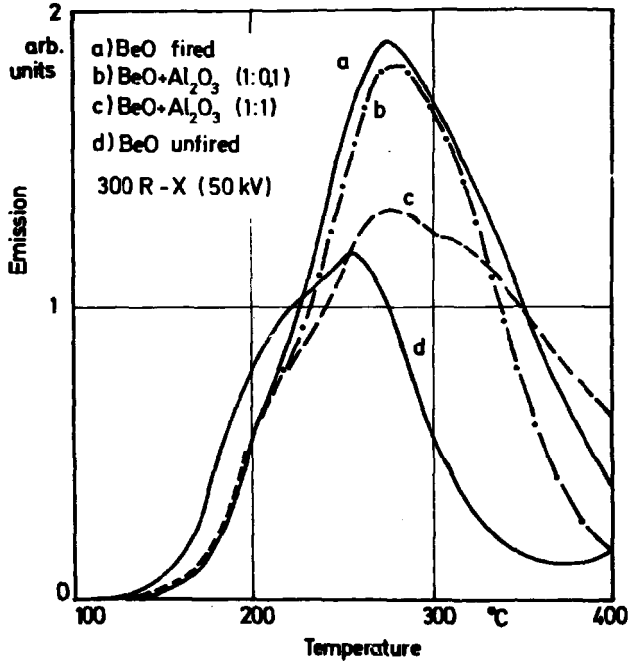

Fig. 1 : Dependence of the TSEE of BeO (Merck) on various admixtures of Al_2O_3

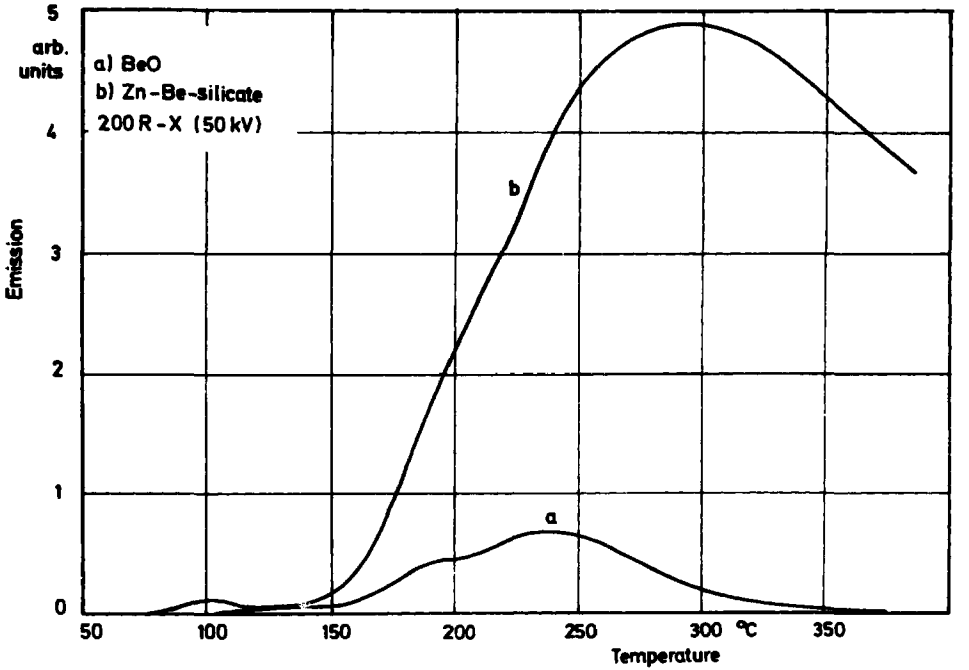

Fig. 2: TSEE of the mixture BeO+ZnO+2 SiO_2 compared to BeO

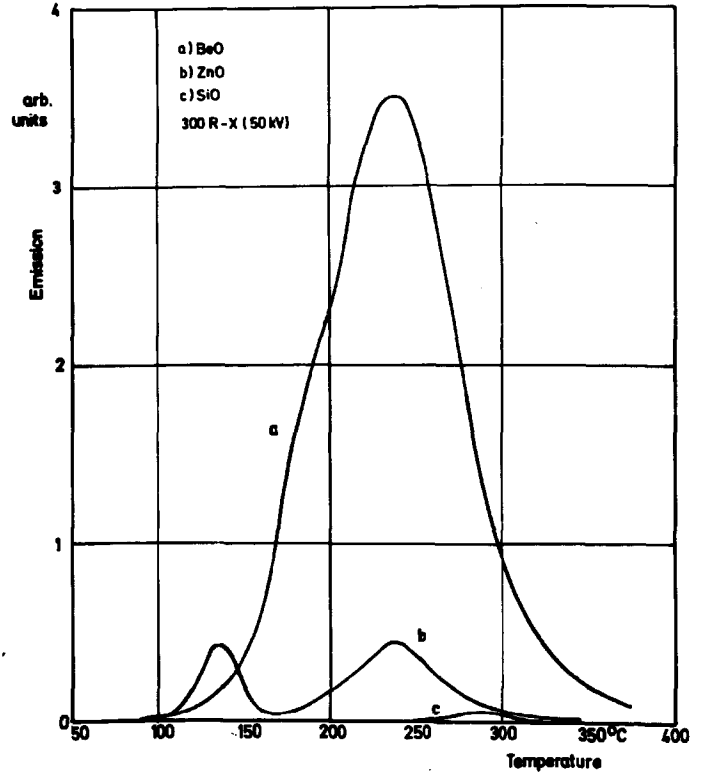

Fig. 3: TSEE of BeO, ZnO, and SiO_2

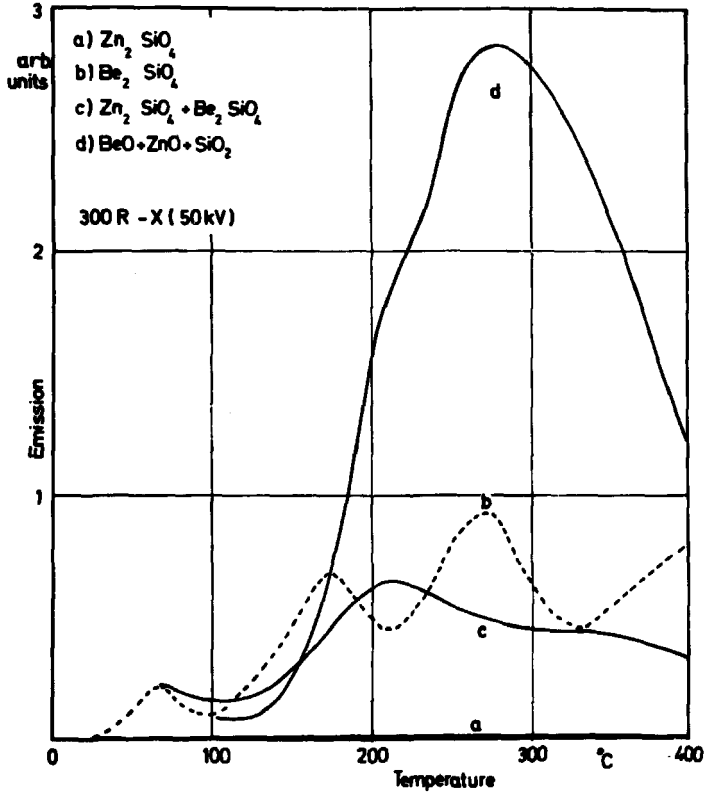

Fig. 4: TSEE of the mixture BeO+ZnO+2 SiO_2 compared to Zn_2SiO_4, Be_2SiO_4, and Zn_2SiO_4/Be_2SiO_4

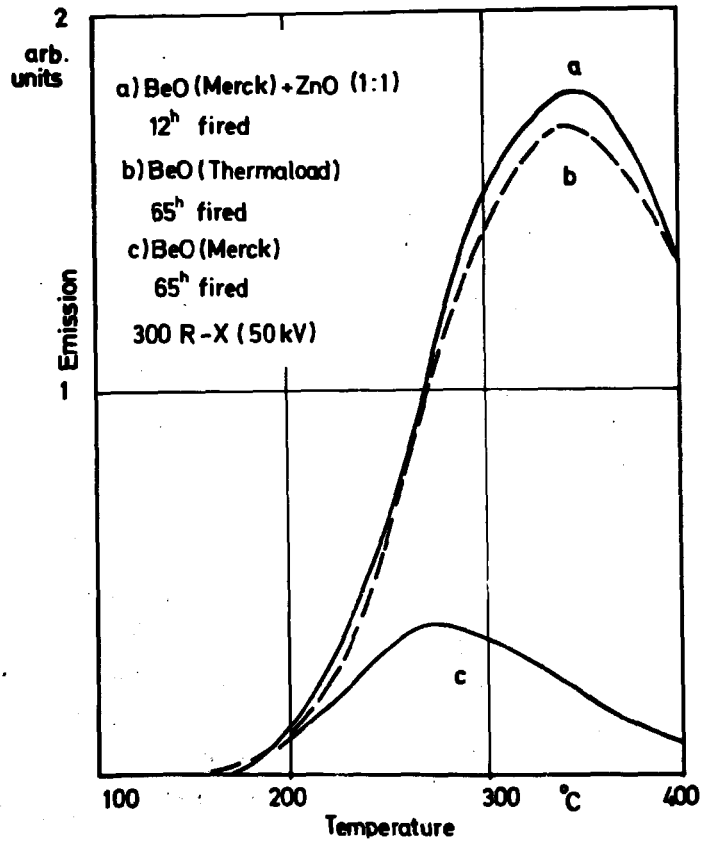

Fig. 5: TSEE of BeO+ZnO+2 SiO_2 and of Thermaload-powder after heat treatment of 12 hours

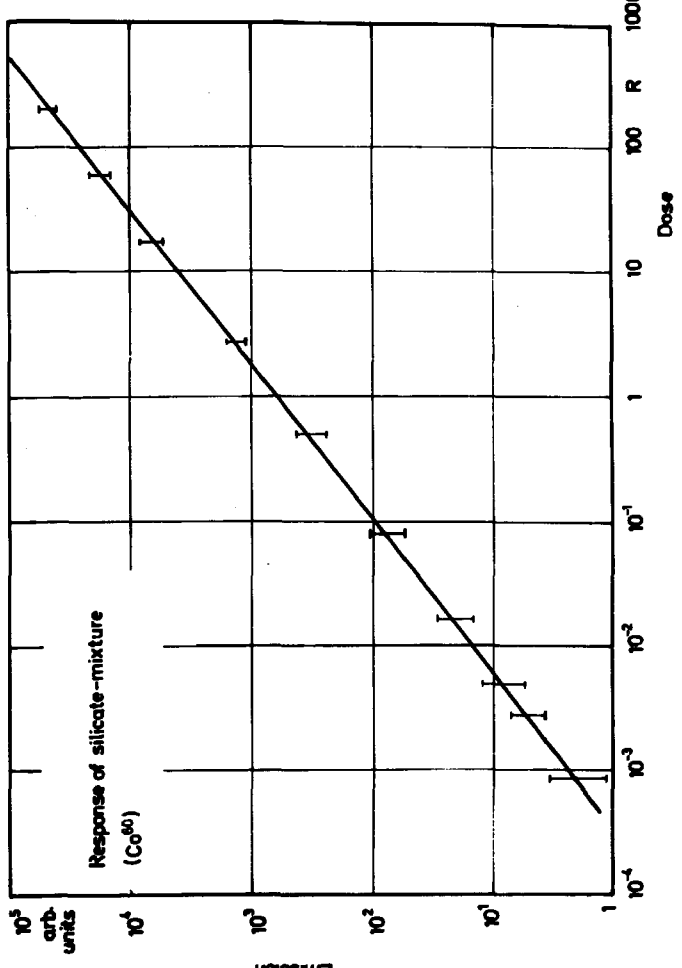

Fig. 5: Dose response of BeO+ZnO+2 SiO_2

Becker

It is obviously not only the chemical composition, but equally or even more important, other factors such as grain size, fine structure of the emission surface, etc. which affect the sensitivity of TSEE detectors. Did you by any chance study these parameters?

Kriegseis

Indeed TSEE is governed by even more parameters. One of the most important for a lot of materials is sorption, since it causes decisive changes of surface potentials. So far we did not examine any of these parameters, but we intend to investigate the influence of sorption. It is well known that at the surface of ZnO chemisorption of oxygen takes place. Therefore it may be possible that the high sensitivity of our BeO-ZnO-SiO_2 powder depends on the distribution of oxygen along the grain boundaries of the powder.

Holzapfel

Do you think that a better mixture of nondestructive BeO and conductive ZnO could improve the dose-response linearity?

Kriegseis

We did not observe any relation between dose response linearity and ZnO content. The ZnO-to-BeO mixing ratio mainly affects the sensitivity.

Low-Z Activated Beryllium Oxide as a High Sensitive Radiation Detector in TSEE·Dosimetry

D. F. Regulla, G. Drexler and L. Boros[+]

Institut für Strahlenschutz

Gesellschaft für Strahlen- und Umweltforschung mbH München,

D-8042 Neuherberg, Ingolstädter Landstr. 1, West-Germany

Abstract

To improve reproducibility and sensitivity of ceramic BeO used in TSEE dosimetry several coating and activation procedures have been described in literature based upon doping the matrix material with high-Z metals.

In order to avoid unwanted effects of the high-Z material such as reduction of tissue equivalency, a procedure of activating BeO with low-Z material has been developed. By this new activation technique the flat energy response of the matrix material could be maintained; moreover, a marked gain in sensitivity was attained. For multiple re-use of the detectors high reproducibility could be achieved by a preirradiation treatment based on "oxidation" and "hydration" of the detector surface.

The paper reports glow curves and sensitization factors achieved with BeO by the new activation technique as well as the technology of preparation of the detectors concerning the activation material, the activation procedure and optimum conditions due to thermal treatment and activation atmosphere. Furthermore, some results on the dosimetric properties of the low-Z activated BeO are presented, i.e. the relation between exposure and total counts, the conditions for dose-independent total output/exposure unit, the detection limits and the directional and energy dependences.

[+]Present address: Radiological Clinic of Medical University, Budapest, Üllői ut 78, Hungary

Introduction

Much work has been done up to now necessary for an application of the TSEE phenomenon of BeO to dosimetry. Especially, properties like sensitivity and reproducibility had to be improved.

KRAMER[1] first succeeded in reaching a linear dose-effect relation by adding non-emitting, electrically and thermally conductive material, for instance graphite to BeO. BECKER et al.[2,3] described promising results after metal impregnation with platinum, palladium and gold: These processes of coating and activating yielded remarkable gains in sensitivity, but there was found an over-sensitivity for low energy photons and, partly, a non-linear dose-effect relation. Own experiences confirmed data given by BECKER[2], that the sensitivity of ceramic BeO increases up to a factor of 7 by solely a thermal treatment of the detectors; however, we could not find the high reproducibility reported by him. We explained this poor reproducibility by dehydration and creation of hydrophobic detector surfaces. In this case, there should be an influence of ambient humidity, which has positively been proven for aluminium surfaces by RAMSEY[4], LINKE and MEYER[5].

Philosophy of Present Investigations

The possibility of an amelioration of detector properties by doping seems to be evident. In contrary to other authors, however, we assumed that this activation should be done with low-Z material because of better diffusion caused by compatible ionic radii of the activation and matrix material. Moreover, to avoid an over-sensitivity for low energy photons the atomic number of the activation material should be similar to Be. Due to these reasons we decided to investigate lithium as activation material.

Moreover, the oxidation and hydration of the detector surface has obviously major influence on the reproducibility of measurement. From literature study and experiment we learned that it is H_2O which plays an important part in the TSEE emission process, the adsorption of which obviously presumes an oxide layer. As for adsorbed oxygen our assumption agrees with explanations of HOLZAPFEL[6] and BECKER et al.[7].

In order to be independent of casual influences of ambient water vapour and oxygen, as well as of the counting gas atmosphere, we introduced a pre-irradiation treatment to the detectors consisting out of the following processes:

1) "Oxidation" in air at 400°C for 20 sec
2) Definite cooling down to room temperature
3) "Hydration" in water at room temperature for 2 min.

Technology of Li-Activation

BeO ceramic discs of the wellknown Brush Thermalox 995 type+ (dimensions: 10 mm dia. x 0,5 mm) and of Berylco type++ (purity: 96 %; dimensions: 6 mm dia. x 1,5 mm) has been used as basic material. For sensitization the lithium was applied as Li-dispersion in vaseline.

Already the virgin BeO emitts TSEE after exposure. However, by the activation process a gain in sensitivity by a factor 50 for Brush and a factor 200 for Berylco BeO could be achieved. Fig. 1 shows the glow curves of both detector materials used: The one of Brush BeO: Li has a single, gaussian shaped TSEE emission peak at about 300°C, the one of BeO: Li from Berylco shows two peaks at 360°C and 410°C, by contrast. These peak temperatures are high enough to exclude fading even at elevated irradiation and storage temperatures; moreover, for Brush BeO: Li there is no pronounced second glow peak at higher temperature found in Berylco BeO: Li and in some home-made BeO:C samples being strongly influenced by mechanical treatment and ambient conditions.

Fig. 2 shows the integral TSEE output against exposure of BeO: Li in comparison with data published by other authors. The TSEE intensity of BeO: Li turned out to be proportional to exposure in case of Brush BeO: Li from about 100 µR to 10 R, respectively to 100 R with a lower heating rate (1°C/s , not indicated in Fig. 2). It became evident that these detectors are even more sensitive than those doped with noble metal ions.

+ Manufacturer: Brush Beryllium Comp., Elmore, Ohio 43416, USA

++ Dealer: Deutsche Beryllium GmbH, 6370 Oberursel, W.-Germany

The lowest limit of detection has been achieved with Berylco BeO:Li which permitted the detection of exposures as low as 10 μR.

By reducing the relatively high background of our reading apparatus an extension of the lower limit of detection seems to be possible.

Preparation of Detectors

It has soon been found that activation has to be performed at elevated temperature. Fig. 3a demonstrates, that maximum sensitivity could resonance-like be attained by tempering the samples at 1000°C.

Activation at lower temperatures even reduces sensitivity if compared with the undoped material. The same is true for temperatures between 1000°C and 1200°C, above which sensitivity increases again. Looking to the optimum duration of the high temperature treatment it became evident that it must be applied by about 60 min (Fig. 3b) at which time maximum sensitivity has been found, agreeing somehow with BeO-Pd activation curves of BECKER[3]. Shorter or extented temper procedures at 1000°C reduce the TSEE sensitivity significantly.

Major influence to the dose dependence of the ratio total counts/exposure unit was found to arrive from the atmosphere during the high temperature treatment (Fig. 4). While this ratio decreased with increasing exposure in case of air, it kept constant for argon atmosphere.

Dosimetric Properties

It has been shown in Fig. 2 that the specific sensitivity of BeO:Li is about 10^7 counts/cm^2.R for Brush and 8×10^8 counts/cm^2.R for Berylco detectors. These sensitivities could not be reproduced, if the detectors were cooled down in the counting gas atmosphere after reading. Nevertheless, by this way of re-use the decreasing sensitivity seemed to approach asymtotically a new sensitivity level, which is about 20 % of the one after activation (Fig. 5), provided the ambient atmosphere remains constant.

After applying the above mentioned pre-irradiation-treatment of "oxy-hydration" to the detectors, however, a good reproducibility of the previous radiation sensitivity was achieved with a standard deviation of $\sigma \simeq 4.5$ % from the mean value over 15 readings.

The energy dependence was determined using heavily filtered X-rays from a 300 kV X-ray facility, and Co-60 gamma rays. All measurements were performed under conditions of electron equilibrium. From Fig. 6 it can be seen that only for low photon energies <30 keV the experimentally determined energy dependence of BeO:Li deviates slightly from the calculated one of pure BeO, because of the lower Z of Li (Z = 3) compared with Be (Z = 4). By adding a defined amount of high-Z material to BeO:Li the production of high sensitive, practically energy independent detectors seems to be possible. For comparison, Fig. 6 exhibits the energy dependence of BeO doped with noble metal ions and the one of the wellknown LiF TLD-100.

As for the free air directional dependence to Co-60 radiation the TSEE output/R of the Brush BeO:Li discs seems to increase by about 15 % for radiation incidence from backward, i.e. when the radiation passes the detector material before penetrating into the exoelectron emitting layer (Fig. 7).

All detector evaluations were performed with a two minutes reading cycle up to 400°C (heating rate: 10°C/s) with the detector not grounded. After reading the detectors were re-used without any long-term annealing procedure.

Summary

Ceramic BeO activated with Li turned out to be a high-sensitive radiation detector on TSEE basis characterized as follows:

1. Linearity: TSEE output proportional to exposure in the range investigated, i.e. between 10 µR and 100 R.
2. Sensitivity: 10^7 counts/cm^2.R (Brush) and 8×10^8 counts/cm^2.R (Berylco)
3. Reproducibility: Standard deviation $\sigma \simeq 4.5$ % with pre-irradiation treatment

4. Energy dependence: No influence of the doping material on the energy dependence of the matrix for photon energies > 30 keV.

As our detectors were evaluated electrically isolated on a silica plate the often described TSEE concept providing grounding of the detector for reproducible and dose-proportional measurements seems not to be suitable in case of BeO:Li, at least.

The stabilizing effect of the oxidation and hydration on the radiation sensitivity demonstrates the importance of the detector surface and of adsorbed surface layers on the emission mechanism of thermally stimulated exoelectrons.

References

(1) J. KRAMER: Z. angew. Phys. 20, 411 (1966)

(2) K. BECKER, J. S. CHEKA, K. W. CRASE and R. B. GAMMAGE: IAEA-Symposium on New Developments in Phys. and Biol. Rad. Detectors SM-143/37, Vienna, 23-27 Nov. 1970

(3) K. BECKER, J. S. CHEKA, K. W. CRASE and R. B. GAMMAGE: Proc. 3rd Int. Symp. on Exoelectrons at Physikalisch-Technische Bundesanstalt, Braunschweig, July 6-8. 1970

(4) J. A. RAMSEY: Surface Sci. 8, 313 (1967)

(5) E. LINKE and K. MEYER: Surface Sci. 20, 304 (1970)

(6) G. HOLZAPFEL: Diss. D 83, Techn. Univ. Berlin (1968)

(7) K. BECKER, J. S. CHEKA and M. OBERHOFER: Hlth. Phys. 19, 391 (1970)

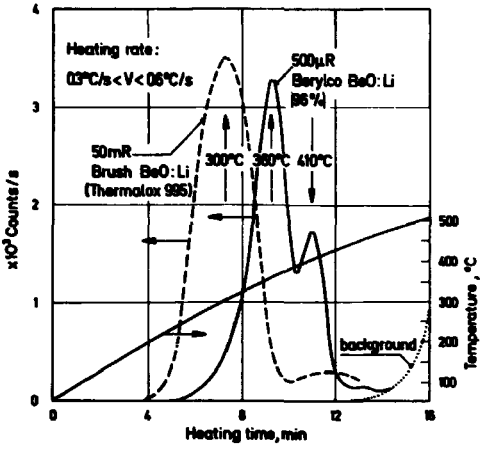

Fig. 1: TSEE glow-curves of BeO:Li

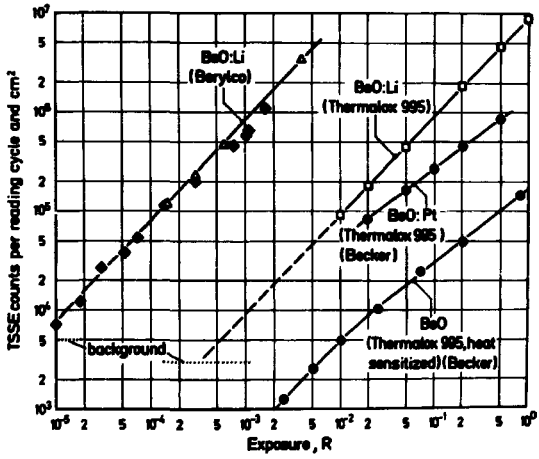

Fig. 2: TSEE sensitivity of BeO (Co-60)

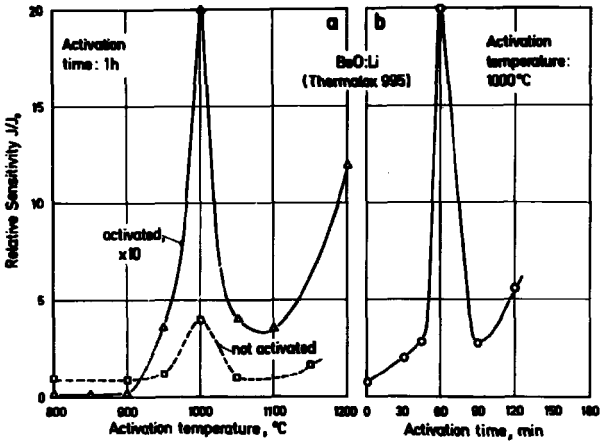

Fig. 3: Dependence of TSEE sensitivity of BeO:Li on magnitude and duration of the activation temperature

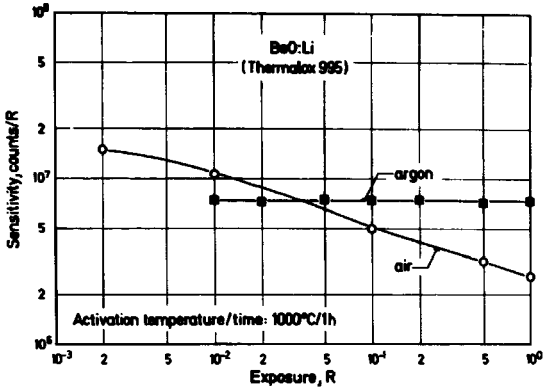

Fig. 4: Dependence of TSEE sensitivity of BeO:Li on activation atmosphere

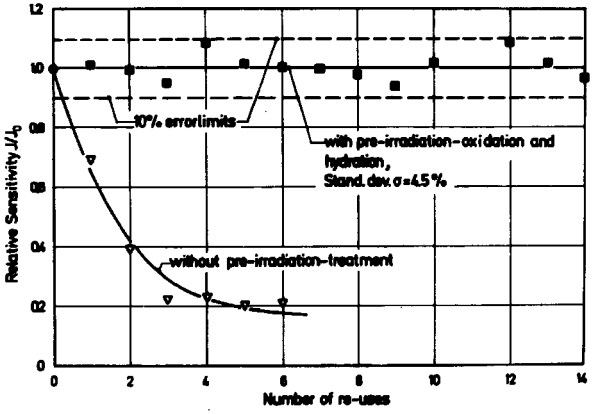

Fig. 5: Reproducibility of BeO:Li with and without pre-irradiation treatment between re-uses

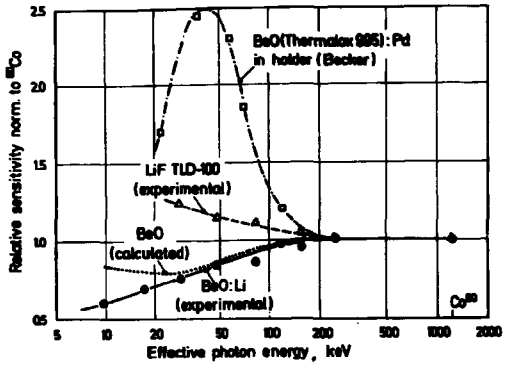

Fig. 6: Calculated and experimental energy dependence of different BeO compared with LiF TLD-100

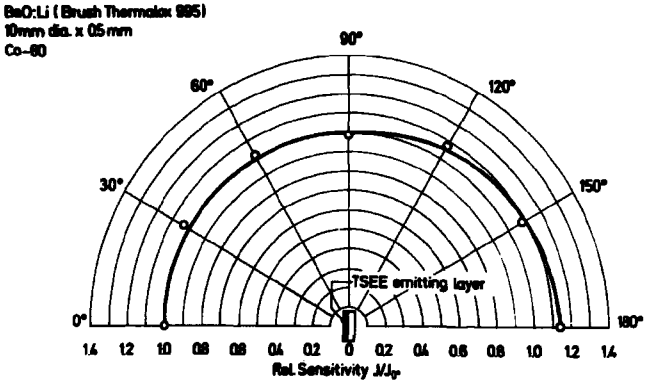

Fig. 7: Directional dependence of TSEE sensitivity of BeO:Li to Co-60 (free air exposure)

Becker

The effect of your water treatment appears to be simply a surface hydration, resulting probably in a tri-molecular layer of water molecules on a previously partially hydrophobic surface (see Becker et al., Symp. New Rad. Detectors, IAEA, Vienna 1970). Did you observe any changes in the TSEE curve as a result of the Li treatment as we did, and what are your diffusion procedures (we evaporated a $LiNO_3$ solution on the surface prior to heating)?

Regulla

I agree with your ideas about surface hydration. In order to justify these models experimentally we are going on with specific experiments. As for the TSEE glow curve it has not been affected by the Li activation. The Li treatment consisted of a covering procedure of the BeO disc surface with metallic Li dispersed in vaseline with a special iterative temperature programme up to 1000°C.

Scharmann

You suggested that the mechanism of Linke and Meyer (preparation of pure metal surfaces in UHV by water for oxidation) is also responsible for the results of your experiments. What is the explanation in your case: BeO in normal atmosphere + water?

Regulla

We did not assume identical mechanisms for our results and those of the mentioned authors at all, but we learnt by studying their papers that oxygen and water influence the TSEE output. This idea applied to our detectors enabled us to improve the reproducibility, rather poor so far. Furthermore, our experiments were primarily performed with an eye to dosimetry application, up to now without any special ambition to clarify the mechanism. However, since we have reproduceable results, the experiments are going to be extended in this direction, about which we shall publish later.

TSEE Dosimetry Studies

by

T. Niewiadomski

Institute of Nuclear Physics, Cracow, Poland

Abstract

An open window G.M. counter and a proportional counter for TSEE measurements were constructed. The G.M. gas flow counter with 0.1 mm Pt wire operates with 98% argon and 2% ethanol mixture. It works at 1720 V and gives 0.2 V pulses with 0.3 msec dead time and 40 cpm cold background. Pulses are amplified /50 dB/ and integrally counted or the count rate is recorded versus temperature. The counter is operated over a nickel sheet working as a heater, supplied by a controlled power supply giving precise linear heating rates between 0.1 and 5^{o}C/sec and temperatures up to 750^{o}C.

The proportional counter is a butane-propane flow counter operating at 4 kV. Its pulses are amplified /70 dB/ and recorded similar to those obtained from the G.M. counter.

Some dosimetric grade LiF powders were investigated for their TSL and TSEE phenomena. The influence of thermal and chemical treatment was investigated and some similarity with the properties of Mg doped phosphors was found.

Introduction

Recent developments in TSEE and the possibility of very low dose measurements aroused our interest in TSEE dosimetry. Two types of counters were constructed and some materials investigated. The first experiments performed showed that the application of the TSEE phenomenon in radiation dosimetry

must be preceded by fundamental investigations of the properties of exoemission. In our opinion, the main difficulty in this application is the high instability of TSEE output. Experience shows that the higher the sensitivity of the materials measured the greater appears to be the instability.

This paper describes our first TSEE investigation concerning LiF phosphors used for TL dosimetry. These phosphors exhibit relatively reproducible TSEE output, compared with BeO powders and BeO sintered disks.

G.M. Counter

The G.M. counter shown schematicaly in Fig. 1 is an argon /90%/ ethanol /2%/ flow counter with 0.1 mm Pt anode wire /2a/. The counter is operated over a nickel sheet working as a heater /3/ supplied by an electronic controlled power supply giving precise linear heating rates between 0.1 and 5°C/sec and temperatures up to 750°C. The heater is mounted in a drawer /5/ which allows the introduction of samples into the counter volume. The counter cathode is at +80 V accelerating potential with respect to the heater sheet. Without this potential the efficiency of exoelectron counting was 4 times lower. The count rate versus applied voltage as well as the dead time influence are given also in Fig. 1. A working voltage of 1720 V was chosen at which the pulse amplitude is about 0.2 V, the dead time about 0.3 msec, and the cold background 40 cpm. The pulses were amplified /50 dB/ and their count rate was integrated and registered on an XY recorder. The counter plateau measured with a C-14 source and with exoelectrons were practically at the same voltage. The counter was investigated with LiF:Mg,Ti sintered disks [1] which appeared to be suitable for this purpose, because of handling convenience and their sufficient TSEE output reproducibility. This counter operates very stably and all the subsequent measurements were performed with it.

Proportional Counter

This counter, shown schematicaly in the upper right part of Fig. 2, is similar to the proportional counter constructed by Attix [2]. Instead of methane, a butane-propane liquid mixture, produced for kitchen and tourist purposes was used as the counting gas. The optimal distance between sample

and anode loop centre is 25 mm. The application of the accelerating potential also gives some gain in exoelectron counting but not so significant as with G.M. counter. This is due to the much higher operating voltage, amounting to 4 kV, in this counter. The counter pulses are amplified by a bootstrap type head amplifier /30 dB/ and a main amplifier /40 dB/. The pulses are discriminated at the level of 2 V, and the count rate is registered on the XY recorder or counted. The counting rate characteristics given in the lower right part of Fig. 1 show the main advantage of this counter over the G.M. counter, i.e. a broad range of counting due to the short dead time of the counters. A low pulse amplitude /below 0.5 mV/ obtained from this counter is the main difficulty of its use and some care should be taken to reduce the noise. Hence the electronic heater supply containing two thyrystors was replaced by a mechanical one. The very narrow pulses produced by the thyrystors could not be filtered until the counter voltage had increased above 4.3 kV. The counter was investigated using the same LiF:Mg,Ti sintered disks. This counter is intended for further dose measurements and only a few TSEE count rate curves have been taken with it. The sensitivity of the counter is about twice that of the G.M. counter, but the curves obtained are quite similar. This means that neither of the counting gases introduce any changes in the crystal surface which would influence the TSEE curve of the phosphors investigated.

TSL and TSEE Investigations of LiF Phosphors

Two dosimetric grade LiF powders were investigated for connections between their TSL and TSEE phenomena. LiF:Cu,Ag [3], having a high single TL peak at about 120°C which may be used for TL dosimetry without any inter-operational annealing /its glow curve does not change either by read out heating or by high dose/, and LiF:Mg,Ti [4], exhibiting properties similar to those of the well-known TLD-100, were measured. Two other LiF phosphors, i.e. TLD-100 and LiF:200 Ti /OHR production/, have also partly been investigated. The differences occurring in the TSEE output of all the phosphors exhibiting the main glow peak at 200°C are of a little significance, and the results for LiF:Mg,Ti given below are also representative for TLD-100 and LiF:200 Ti.

The first experiment was carried out to investigate the thermal stability of the TSEE output. On the basis of Bohun's work [5], we expected the thermal

treatment to have great influence, because the phosphors used are of doped type. 10 mg of long stored />1 yr/ phosphor was put on a graphite disk /6 mm in diameter/, carefully cleaned and warmed out. This sample was irradiated up to a dose of 10 rads of Co-60 gamma radiation and promptly read-out, avoiding any strong light illumination of the sample. The irradiations and read-outs were repeated several times and several samples were used in order to avoid any incorrect interpretation due to the influence of external variables. The results shown in Fig. 2 allow the following conclusions to be drawn:

1. Both TSEE curves exhibit some similarity to the corresponding TL curves when the samples are heated for the first time, but the main TSEE peaks appear at slightly higher temperatures than the main TSL peaks.
2. Although the LiF:Cu,Ag TL output is about 10 times higher than that of LiF:Mg,Ti, the TSEE main peak amplitudes of both phosphors are nearly of the same size.
3. Besides the main peaks, other peaks appear also on both TSEE curves. They have no corresponding peaks on the TSL curves.
4. The amplitudes of the main TSEE peaks are reduced significantly as a consequence of first heating, but no new peaks are then formed.
5. Thermal annealing of LiF:Mg,Ti phosphor, restoring the "virgin" TL glow curve, does not influence the shape of two TSEE curve.
6. The "virgin" TSEE curve shape is not restored until the sample has been stored for at least two weeks.
7. Only one TSEE peak at about 300°C appears to be common in the two phosphors.

There is a question as to what part is played by the centres created by surface sorption or hydrolysis in TSEE output of LiF phosphors. The influence of the surface centres is shown on the "first heating" curve obtained when the phosphors are stored for few weeks. It seems that these centres are thermally unstable and are disintegrated during heating. But it is also possible that some internal changes occur during the heating as is the case in the TSL of most LiF phosphors.

In the next experiment we tried to influence the crystal surface by means of weak acids and alkalis. For this purpose the sample was moistened with a drop of HNO_3 solution /pH = 3/ or LiOH solution /pH = 9/, dried, and measured

on the next day. With reference to thermoluminescence it was confirmed that this influence is very weak, only a decrease in the 300°C peak on the LiF:Mg,Ti curve being observed after using the acid solution. Conversely, this influence on TSEE is more evident. The TSEE curve changes shown in Figs 3 and 4, are typical for all LiF phosphors exhibiting the main TL peak at 200°C. They may be summarized as follows:

1. Acid solution "stabilizes" the TSEE curve to some extent. The acidified sample may be read out several times without any remarkable TSEE curve change. The integrated exoelectron yield is slightly lower than that of the "virgin" sample.

2. After treatment of the sample with alkaline solution the TSEE output during the first read out increases but this increase disappears after the first heating.

These results suggest that the TSEE output enhancement of the "first" read out may be due to some LiOH groups adsorbed on the crystal surface during storage in air. These groups are thermally unstable.

There is an interesting fact, why during all these experiments no new peaks are formed? An explanation of this fact may be the supposition that the exoelectrons registered are emitted not by the surface defect, but that the heteromorphic structure defects adsorbed on the crystal surface diminish the work function in the places where they are created, and the emission of exoelectrons increases depending on the number of defects. The defects produced by acid are thermally more stable than those produced by alkali.

Unfortunately, the experiments performed in this work do not allow an exact explanation of what kind of surface phenomenon is responsible for the TSEE curve changes described. We are also unable to stabilize the TSEE output so well that the LiF phosphors could be used for dosimetry purposes.

Conclusion

The TSEE sensitivity of LiF powders allows doses higher than 0.1 rad to be read but the reproducibility of the read out of the same sample as well as that of different samples are unsatisfactory. Work is in progress to obtain a better knowledge of the TSEE properties of LiF and of some other materials.

Acknowledgement

Thanks are due to Dr. O.K. Daszkiewicz for constructing the electronic heating device.

References

1. T. Niewiadomski, M. Jasińska, E. Ryba, this Conference paper No 22.

2. P.H. Attix, Int. J. Appl. Rad. Isot. 22, 185, 1971.

3. T. Niewiadomski, Nukleonika 12, 281, 1967.

4. M. Jasińska, T. Niewiadomski, E. Ryba, Nukleonika 14, 995, 1969.

5. A. Bohm, P.T.B. Mitteilungen 80, 318, 1970.

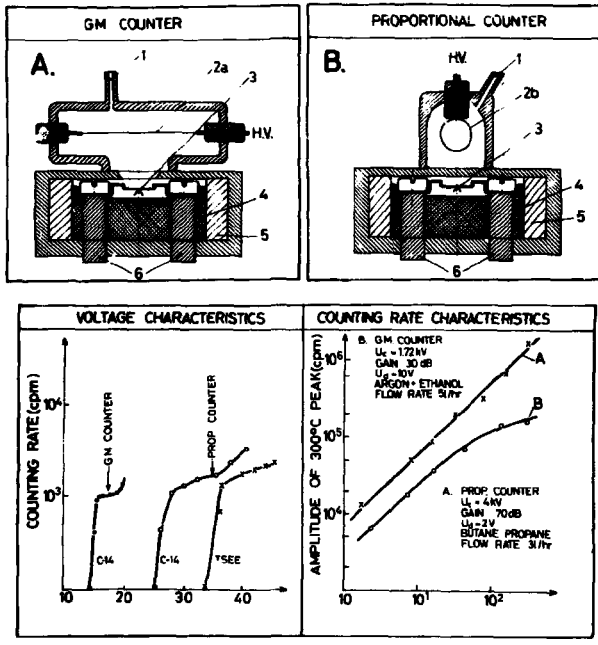

Fig. 1. Counters for TSEE and their characteristics.

1 - gas inlet, 2a - anode, 2b - loop anode, 3 - heater sheet with thermocouple, 4 - PTFE insulator, 5 - Al drawer, 6 - current conductors.

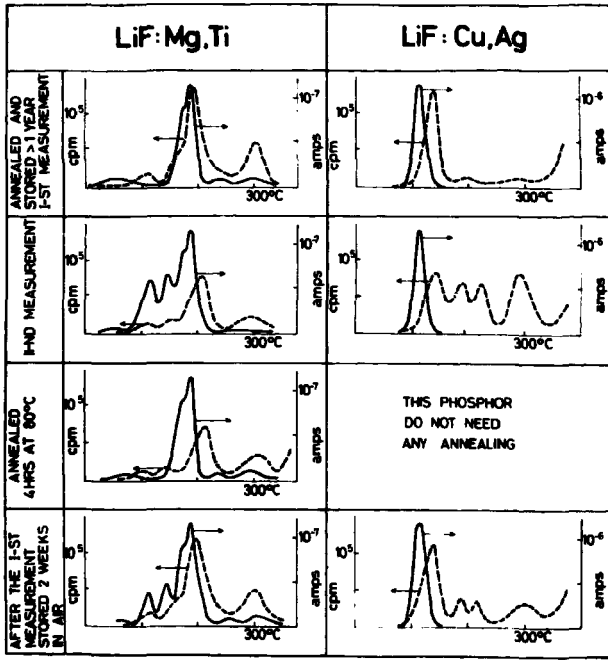

Fig. 2. Comparison of TSEE and TSL of two LiF phosphors with different history.

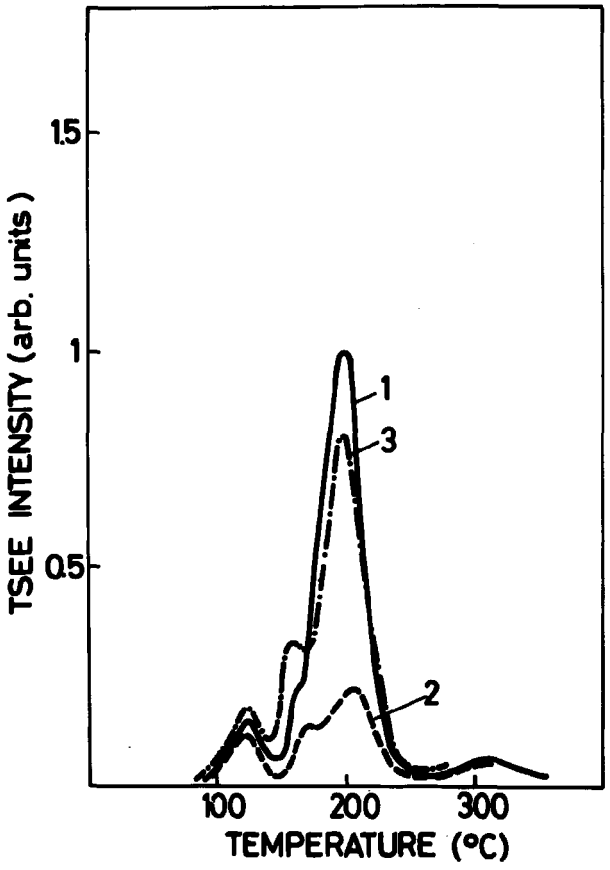

Fig. 3. Effect of HNO_3 solution /pH = 3/ on TSEE of LiF:Mg,Ti

1 - "virgin" curve, 2 - "stabilized" sample by several runs,
3 - acidified sample.

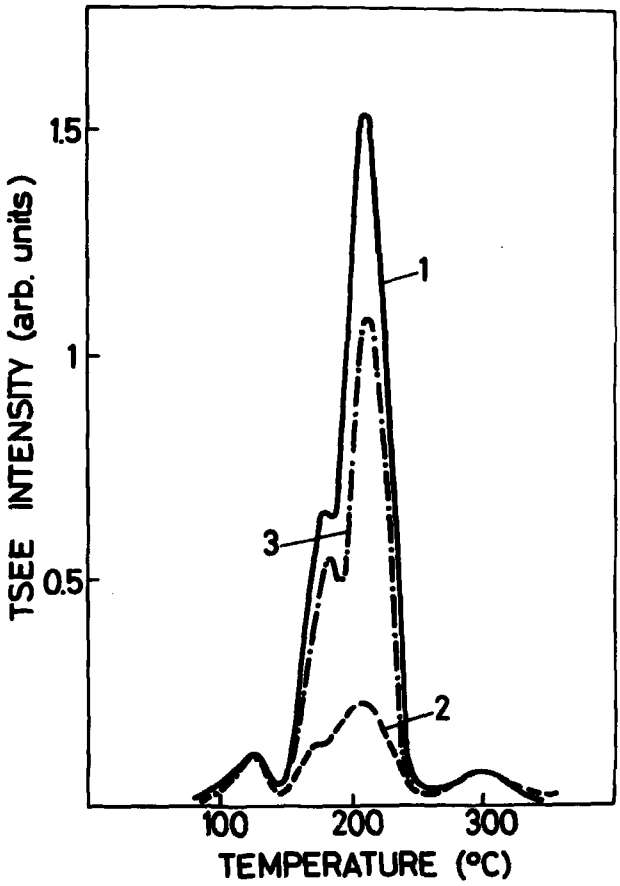

Fig. 4. Effect of LiOH solution /pH = 8/ on TSEE of LiF:Mg,Ti

1 - new sample treated with LiOH solution, 2 - "stabilized" sample by several runs, 3 - "used" sample treated with LiOH solution.

The Optical Stimulation of Exoelectron Emission

by

J. KRAMER
Physikalisch-Technische Bundesanstalt
Braunschweig, Germany

Abstract

Until now only the thermal stimulation has been applied to dosimetry with exoelectrons. Although more expensive, the optical stimulation has important advantages. It is also of great advantage for analysing the traps and determining the stimulation energies.

1. Thermal and optical stimulation

Up to now, when using exoelectrons for dosimetry, the thermal stimulation (TSEE) has almost always been applied. In view of our own experience, we too were not in favour of the optical stimulation (OSEE), as the dispersion of the measured values for TSEE was smaller and it was less expensive. The main reason for better results with TSEE is due to the fact that all electrons are emitted when an emission maximum is exceeded. With OSEE it is not possible with normal light sources to empty the traps completely in a reasonable time. Fig. 1 shows the difference between the two kinds of stimulation. To obtain better results with OSEE also, quantity and spectral distribution of the stimulating light must be kept constant in order to bring an equal percentage to emission. If the intensity of light is reduced, the counting time must be proportionally prolonged. The reduction of the light intensity is desired in order to adapt the emission rate to the counting capacity of the counter. For the reduction of the light intensity without changing the spectral distribution, neutral density filters are suitable which are available in the range of 1 to 10^{-5}. This method has the disadvantage that at large doses unbearably long counting times are required. To avoid this difficulty, the part of electrons used for measurement was kept so small that the optical bleaching is negligible. It is then possible, by equal counting time, to multiply the measured emission with the absorption factor of the neutral density filter without causing a great error. This procedure was chosen though it reduces the sensitivity. But it allows a quick evaluation for a wide dose range using only one G-M-counter.

2. Advantages and disadvantages of optical stimulation

The following 8 points may be regarded as advantages of OSEE:

1. The range of unknown irradiation dose can be determined by a first rough measurement without losing the information of the whole dosemeter.

2. The specific range of the used measuring method, e.g. G-M-counter, can be adjusted to the dose range by changing the light intensity with neutral density filters in order to have the best counting conditions and to enlarge the range of measurement.
3. A single dosemeter gives a series of values and a mean value of dose is easily determined.
4. Partial regions of the dosemeter can be covered by an absorber in order to get information about the type of irradiation.
5. Partial covering with polyethylene or similar materials enables a discrimination of γ-radiation and fast neutrons.
6. The OSEE-dosemeter is not heated; any thermally-induced changes of exo-sensitivity are excluded.
7. Manufacturing OSEE-dosemeters is very cheap, e.g. impregnated paper may be used. Therefore OSEE-dosemeters should be one-way dosemeters.
8. Because only a little part of excitation is used for the measurement, OSEE-dosemeters can be stored for a later checking.

A disadvantage must be mentioned, namely the lower sensitivity of OSEE-dosemeters. But very sensitive exo-dosemeters can be produced so that this disadvantage of OSEE should not be decisive for normal application. Another disadvantage is that it needs a device for controlling the light intensity. This, however, can easily be installed by common electronic means.

3. Conditions for optical stimulation

In contrast to TSEE, the following conditions have to be observed for OSEE:

1. The dosemeters must in every case show a linear dependence of the emission on the dose. As non-linearity arises by charges on the surface, the OSEE-dosemeter must have sufficient electrical conductivity. Non-linearity which, to our opinion, handicaps

the measurements also for TSEE, renders the application of neutral density filters by OSEE absolutely impossible, because a non-linearity depending on the dose also causes a non-linearity depending on the light intensity.

2. Certain substances, f.i. BeO, produce a spontaneous emission after intensive irradiation at room temperature without additional stimulation. This does not matter in the case of TSEE; but at the far lower emission by OSEE, mainly when neutral density filters are used, it must be taken into consideration either by leaving sufficient time after the irradiation, or by measuring the spontaneous emission and subtracting it from the OSEE.

4. Results using $SrSO_4$ and BeO

In fig. 2, the results using $SrSO_4$ and BeO are demonstrated. The influence of the spontaneous emission is indicated in the BeO-curve. All results of TSEE are found here: Large dose volume which is measured here solely with a G-M-counter; beginning of saturation of $SrSO_4$ and beginning of supra-linearity of BeO. The increase of the sensitivity by an intensive preradiation of BeO could also be observed. There is, therefore, no difference in the results using OSEE or TSEE.

5. Paper dosemeters

To profit by the advantages of OSEE over TSEE, special shapes must be chosen for these dosemeters. Tests have been carried out to use strips of paper as dosemeters. The strips were 20 x 60 mm^2. After irradiation they were covered by a lattice leaving 12 measuring places open which were evaluated step by step.

Even common commercial paper can be used as a dosemeter, because most paper, except newsprint and special paper, contain exo-sensitive substances as filling material. For fig. 3, paper with 3 % TiO and 2 % $BaSO_4$ has been used; the strips were

irradiated in the middle only. One obtains a great emission and sees the bleaching. Although these paper strips show local irregularities of sensitivity, they can even be used for measurements, because the 12 measured values give an only little dispersing mean value. For fig. 4, a block of 22 paper strips has been irradiated together. The absorption of the X-rays and the intensification of the excitation by a platin foil for the last paper strip can be seen.

This paper is, of course, not practicable. More suitable fillings will have to be used and sufficient electrical conductivity should exist. For these investigations, the paper was self-produced, or filter paper was spread with a layer consisting of $SrSO_4$, graphite and methanol. This paper is sufficiently sensitive, and linearity can be obtained as some examples on fig.5 show. Although these tests have been carried out with extremely simple means, the results are so promising that further tests are planned together with a paper factory. For practical use, two strips are welded into plastic foils and only taken out immediately before evaluation.

6. The optical stimulation for the analysis of traps

OSEE is not only advantageous in dosemetry but also to analyse traps for the determination of activation energies. Using wedge-shaped interference filters, the measurement is as simple as TSEE and does not take more time. The activation energies can be taken directly, while in the case of TSEE, this determination is more problematic because of experimental and theoretical reasons. The resolving power is better for OSEE, as can be seen in fig. 6. For the same evaluation time, the small maximum appears only at OSEE, while this can be obtained at TSEE only by very slow heating.

The optical stimulation offers great advantages for physical research and for the application of exoelectrons.

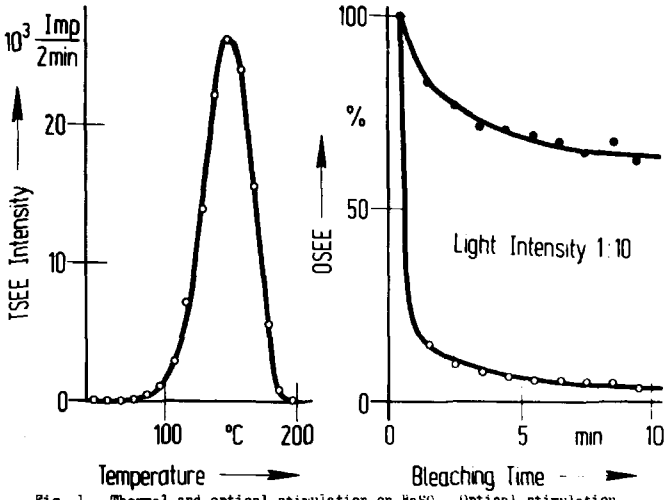

Fig. 1 Thermal and optical stimulation on $BaSO_4$. Optical stimulation without and with neutral density filter.

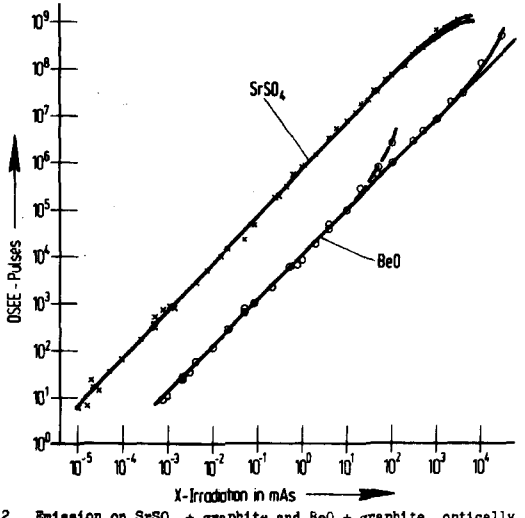

Fig. 2 Emission on $SrSO_4$ + graphite and BeO + graphite, optically stimulated with neutral density filters. The dashed part of the BeO-curve indicates the spontaneous emission X-rays 10 kV.

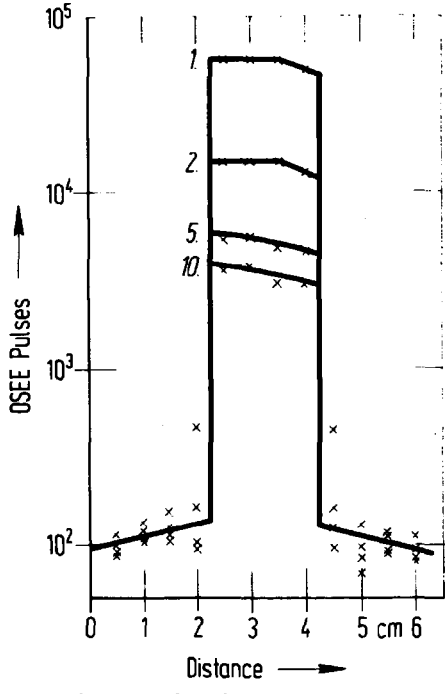

Fig. 3 Scanning of an irradiated paper strip. Paper with 3 % TiO_2 and 2 % $BaSO_4$. Ten times scanned.

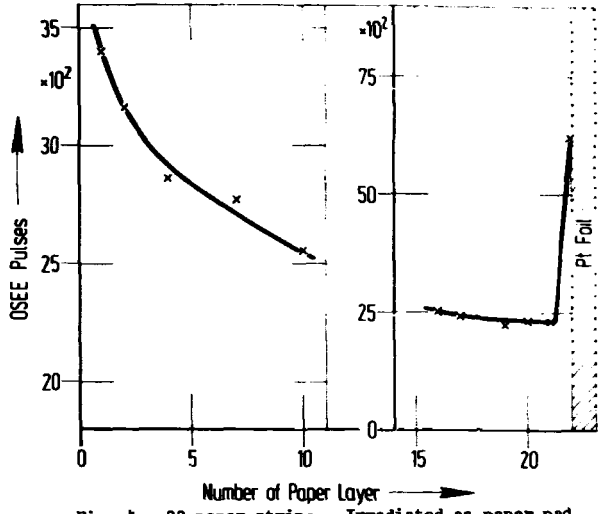

Fig. 4 22 paper strips. Irradiated as paper pad.

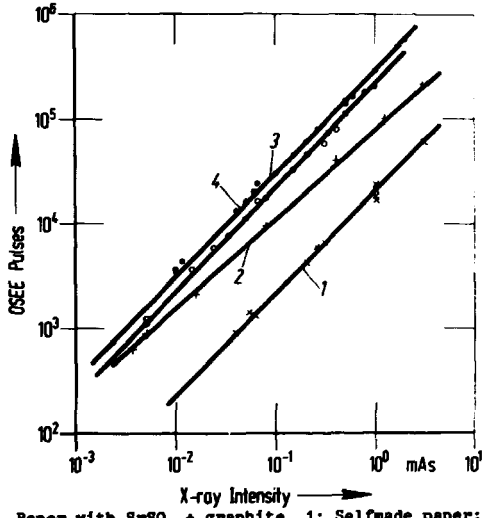

Fig. 5 Paper with $SrSO_4$ + graphite. 1: Selfmade paper; 2, 3, and 4: Filter paper covered with $SrSO_4$ + graphit and methanol.

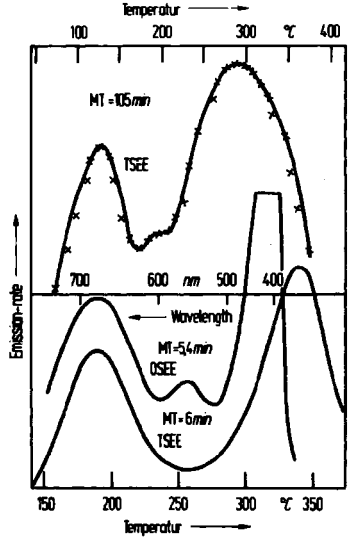

Fig. 6 $CaSO_4$ baked at 940 °C thermally and optically stimulated.

Spurny

It seems to us that commercial paper produced for reprographic purposes which has a ZnO surface layer should be a sensitive "paper dosimeter".

Characteristics of Selected Phosphors for Stimulated Exoelectron Emission Dosimetry

P. L. Ziemer, W. C. McArthur, V. L. McManaman, and G. D. Smith
Bionucleonics Department, Purdue University, Lafayette, Indiana, USA

Abstract

The sensitivity, linearity, reproducibility, fading and emission curve characteristics for thermally stimulated exoelectron emission were studied for reagent grade LiF, and CaF_2 powders. Readout was by means of a windowless proportional counter using an argon-methane gas mixture. Sample heating during readout was accomplished using a linear temperature programmer. A multichannel analyser operated in the multiscaler mode was used to obtain the emission curves.

A mixture of LiF with graphite gave improved precision but sacrificed sensitivity as compared to the pure powder. Pure CaF_2 powder was slightly more sensitive than LiF while a mixture of CaF_2 with graphite again resulted in a decrease in sensitivity. In all cases the sensitivity was effected by heat treatments prior to use. In the case of CaF_2, the emission curve characteristics were altered by such preheating.

The responses of the powders as a function of exposure were linear over only limited exposure ranges of up to 700 R for LiF/graphite and up to 300 R for CaF/graphite.

Both powders exhibited "fading" or loss of emission as a function of time after exposure. At room temperature, the fading for LiF was 30% in 6 weeks while for CaF_2 the decrease was about 25% in 122 hours.

Introduction

Since the time of Kramer's report[1] in 1957 indicating a linear relation between radiation dose and exoelectron emission in $CaSO_4$, a number of materials have been considered[2-7] for radiation dosimeters using thermally stimulated emission of exoelectrons (TSEE). Those materials which have received the most attention include LiF, BeO, $BaSO_4$ as well as $CaSO_4$. For practical dosimetry, LiF and BeO appear to hold much promise, due largely to their relative insensitivity to environmental influences. Other materials which have received limited attention include $SrSO_4$, CaF_2, BaF_2, and SrF_2.

In comparing studies reported in the literature, one notes conflicting data in some cases and lack of detailed data in other cases. For example, lithium floride was reported to have an emission peak at 135°C in one study[8] and at 210°C in another study[9]. These same publications reported fading rates of zero loss of emission for up to 10 days in dark storage at room temperature in the first case and 25% loss of emission in 5 hours at room temperature, in the second case.

In the present study, we initiated a systematic examination of $CaSO_4$, $BaSO_4$, LiF, and CaF_2 powders in an attempt to determine TSEE sensitivity, linearity, reproducibility, and emission curve characteristics. The $CaSO_4$ and $BaSO_4$ proved to be very difficult to work with as far as obtaining reliable and reproducible results. Hence the major portion of the study was confined to the two fluoride compounds.

Instrumentation

The detector was composed basically of a counting chamber and a stainless steel drawer which contained the dosimeter sample, heater and thermocouples. A stainless steel adapter plate was machined for a precision match between the counting chamber and drawer. The counting chamber and anode wire assembly were taken directly from a standard, commercially available, windowless gas flow detector.[a]

The loop shaped anode wire was attached to a high voltage connector which was mounted with screws to the top of the cylindrical counting chamber. The anode wire and connector assembly could thereby be quickly and easily removed for cleaning or replacement without disturbing other parts of the detector.

The heating element consisted of a disc-shaped array of nichrome ribbon strips which were electrically connected in series by spot welding. The nichrome heater was mechanically connected across two large copper leads which entered the drawer recess through a hole drilled from the back of the drawer up to the recess. Two iron-constantan thermocouples, one a control sensor for the linear temperature programmer and the other for temperature monitoring, were pressed firmly against the bottom of the nichrome heater by a small piece of mica which was reinforced with asbestos packing. A thin layer of mica was placed over the nichrome for electrical insulation from the dosimeter sample during readout. An aluminum disc 1.25 in. in diameter was placed over the mica and was electrically grounded. The dosimeter sample was then placed upon the aluminum disc for readout. The distance from the top of the anode loop to the powder surface measured approximately .69 in.

[a] Model 200A, Packard Instrument Company, LaGrange, Ill.

The block diagram in Figure 1 includes all the components of the complete counting system. The electronic components of the system consisted of a 0 - 3000 V high voltage supply [a] which was connected to the anode through a FET preamplifier[b]. Detector pulses of negative polarity were fed through a short length of cable into the preamplifier. Pulses of positive polarity from the preamplifier were then fed into an amplifier[c]. The amplified pulses were then sent into a single channel analyzer[c] operated in the integral mode and with zero lower level discrimination. The standard 6 V output pulses were then fed into a scaler[e] which was operated in conjunction with a timer[f]. The same standard pulses were also sent into the input of a 400 channel multichannel analyzer[g] which was operated in the multi-scaler mode. An external variable frequency pulser[h] provided the necessary negative pulses to advance the channels at a selected rate, normally 45 channels per min. TSEE curves could then be directly recorded photographically from the multichannel analyzer oscilloscope and through an X-Y plotter[i] and indirectly through a high speed parallel printer[j]. Also the integral count was displayed on the module scaler.

Heating of the dosimeter sample was controlled by a linear temperature programmer[k]. The nichrome heater was connected to the power output of the linear temperature programmer through a step down isolation transformer[l]. Control was obtained through the iron-constantan thermocouple held against the bottom of the nichrome heater. Heating rates from 2°C/min to 40°C/min could be selected by the dial setting, and faster rates could be obtained by connecting appropriate resistances across an external input jack. The linear temperature programmer could also be operated in an isothermal mode at any desired

---

[a] Model 446, Ortec, Oak Ridge, Tenn.

[b] Model 109PC, Ortec, Oak Ridge, Tenn.

[c] Model 451, Ortec, Oak Ridge, Tenn.

[d] Model 406A, Ortec, Oak Ridge, Tenn.

[e] Model 430, Ortec, Oak Ridge, Tenn.

[f] Model 482, Ortec, Oak Ridge, Tenn.

[g] Model 34-12B, RIDL, Nuclear Chicago Corp., Des Plaines, Ill.

[h] Model VP2E Varipulse, W. B. Johnson and Associates, Mountain Lakes, N.J.

[i] Model HR-97, Houston Instrument Corp., Houston, Texas

[j] Model H43562A, Hewlett-Packerd, Palo Alto, Calif.

[k] Model 326, Wilkens Instrument and Research, Inc., Walnut Creek, Calif.

[l] Model P6309, Chicago Standard Transformer Corp., Chicago, Ill.

temperature. A linear heating rate of 93°C/min was used in the LiF studies and 81°C/min in the CaF_2 studies. A second iron-constantan thermocouple also positioned beneath the nichrome heater provided temperature monitoring through a variable speed strip chart recorder[a].

Three different counting gases were checked for an optimum response. These gases included a mixture of 90% argon and 10% methane, pure methane, and a mixture of 79.05% helium and 0.95% isobutane. The helium/isobutane mixture gave an erratic response which appeared to be due to insufficient quench. A stable and reproducible response was obtained for pure methane, but no counting plateau occurred within the range of the high voltage supply. When used with a standard ^{204}Tl beta source, the argon-methane mixture gave an excellent characteristic curve with a plateau length of 500 V centering at 1775 V with a slope of 0.67% per 100 V. Characteristic curves were then obtained for both LiF and CaF_2 exoelectrons. For LiF exoelectrons, a very narrow "plateau" was observed having a width of about 100 V and located at about 2100 V. For CaF_2 exoelectrons, a narrow "plateau" only 50 V wide was observed at an operating voltage of 2250 V.

Dosimeter Preparation

The phosphors used in all cases were reagent grade powders obtained commercially.[b] Initially, all dosimeters were prepared by evaporating a thin layer of the powder from an acetone-powder slurry into a 1/2 inch diameter stainless steel planchet. It was found that this technique worked very well for pure LiF and for LiF mixed with graphite. In the case of CaF_2, the acetone plating method did not yield dosimeters having a reproducible response. It was found that for CaF_2 the best results were obtained by simply placing known weights of the loose powder directly into the planchets.

In the experiments described in the remainder of this paper, all LiF dosimeters were prepared by acetone plating prior to irradiation. For CaF_2, on the other hand, irradiations were carried out on the loose powder contained either on planchets or in vials. In the latter case the powder was transferred to planchets just prior to readout.

The thickness of the pure LiF powder in the planchets was 10.5 mg/cm^2. For mixtures of LiF and graphite in a 3:1 ratio, the thickness was 7.2 mg/cm^2. In the case of the CaF_2, the planchets were filled to a thickness of 14.8 mg/cm^2 for pure CaF_2, and 11.0 mg/cm^2 for mixtures of CaF_2 and graphite in a 3:1 ratio.

---

[a] Honeywell Electronik 194, Honeywell, Fort Washington, Pa.

[b] J. T. Baker Chemical Co. (LiF, Lot 33152; CaF_2, Lot 35904)

Irradiation Conditions

The exposures were carried out using a 1663 Ci ^{60}Co gamma irradiation facility. The irradiator was the panoramic beam type[a] located in the center of a shielded room with inside dimensions of about 4 meters X 4 meters. The planchets containing the powders were sandwiched between sheets of plexiglass in groups of 12 dosimeters. The plexiglass holders were positioned at a distance which provided an exposure rate of 100 mR/sec (a distance of approximately 2 meters from the source). The source was calibrated with a Victoreen R-meter.

Results

Lithium Fluoride

A group of typical emission curves for LiF, as recorded on the X-Y plotter, is shown in Figure 2. The main peak position corresponded to a temperature of 140° as determined by a thermocouple placed on the surface of the stainless steel planchet. A second higher temperature peak was observed at about 260° C but was not normally used since it was more convenient to limit the operating temperatures.

It was found that the sensitivity (counts per R) and the reproducibility of the LiF dosimeters could be altered in a number of ways. The addition of graphite to the LiF powder has been used by others to improve the reproducibility of exoelectron emission. In so doing, one sacrifices the sensitivity somewhat. For the detection system described, a mixture of LiF to graphite in a 3:1 ratio by weight and prepared by the acetone plating method resulted in dosimeters which gave a reproducible response with a standard error of the mean as low as 2%. In contrast, the precision of pure LiF fluoride dosimeter was 17% (standard error of the mean). Sensitivity was better for the pure powder, however, being 1200 counts/R for LiF for the system described as compared to 650 counts/R for the graphite mixture.

Preparation conditions play an important role in establishing the sensitivity of LiF dosimeters. To study this aspect, groups of dosimeters were preheated for a constant time at selected temperatures from 100° C to 800° C. The powders were heated for 15 minutes at a given temperature, allowed to cool to room temperature, plated in the planchets using acetone and then given a test exposure. For the LiF-graphite mixture, the greatest sensitivity resulted for powders heated at 450° C. For the pure LiF powder, the 380° C treatment gave maximum sensitivity. Using these two optimum temperatures, the heating times were then varied for groups of dosimeters. The sensitivity plotted as a function of heating time in both case indicated a broad peak which remained fairly flat

[a] Model 150 "Gammabeam", Atomic Energy of Canada, Ltd., Ottawa, Canada.

between 20 minutes and one hour. For convenience, a 30 minute treatment time was selected in the preparation of all subsequent LiF dosimeter powders in order to maximize the sensitivity. Figure 3 shows the heat treatment effect.

Predosing has been used in thermoluminescence dosimetry as a means of enhancing response. This technique has been suggested for increasing sensitivity of TSEE dosimeters also. To investigate this possibility, LiF was exposed to ^{60}Co gamma rays for total exposures in the range of 5×10^4 R to 3.5×10^8 R. The exposed powder was then annealed, prepared on planchets, and exposed to a small test exposure (13.2 R). No significant difference in exoelectron emission was observed for any of the powders treated with high exposure as compared to non-treated LiF.

Response as a function of total exposure was found to be dependent of the addition of the conducting material (graphite). Figure 4 indicates the response of both pure LiF and of the LiF-graphite mixture. For the pure powder, the response was linear over a range of about 100 mR to 100 R, while the mixture gave a linear response up to about 700 R.

Stability of the 140° C emission peak for LiF/C was reasonably good despite the low temperature of the peak. The fading of the peak over a period of about two months under typical room conditions (25° C temperature and 45% relative humidity) is shown in Figure 5. The fading reaches about 30% after 6 weeks. Storage at an elevated temperature (50° C) resulted in rapid fading with 50% loss of the peak within 10 hours.

Calcium Fluoride

The unsmoothed emission curve of a pure CaF dosimeter is shown in Figure 6. The two main peaks occurred at temperatures of 79° C and 115° C respectively. These temperatures were measured with a copper-constantan thermocouple which was placed directly into the powder of a dosimeter during temperature calibration runs.

As suggested previously, plating of the CaF_2 powder with acetone onto planchets did not produce dosimeters having reproducible response. Even the addition of graphite in this case did not solve the problem. The sensitivity of the CaF_2 dosimeters prepared in this way generally decreased with time following preparation. They also exhibited an increasingly erratic behavior for longer times after preparation. The absorption of water or atmospheric constituents could account for these effects. The best reproducibility was obtained by preparing dosimeters with loose powder taken directly from covered glass storage jars. Even in this case, care had to be taken to keep the dosimeters covered after preparation since sensitivity changes were observed for these dosimeters when they remained for prolonged periods in open air.

This effect was clearly demonstrated in an experiment in which groups of dosimeters (loose powder in planchets) were prepared and stored in open air. Control groups, prepared in a similar manner, were stored beneath a flat piece of lucite, essentially "sealing" the dosimeters from contact with the room air. At selected times after preparation, groups of 6 dosimeters were removed from storage, given a test exposure (13.1 R of ^{60}Co gamma irradiation) and immediately read out. The sensitivity of the covered dosimeters remained essentially unchanged in time (Fig. 7), while those stored in open room air showed a continual drop in sensitivity as a function of storage time.

The TSEE response of CaF_2 powder showed a dependence on preirradiation heat treatment as was the case for LiF. A study was made of the sensitivity of response as a function of heat treatment over a temperature range of 100° C to 1000° C. The procedure involved the heating of a 1 g sample of pure CaF_2 powder in a small crucible at the selected temperatures for a period of one-half hour. The maximum sensitivity, about 2000 counts/R, was obtained for powders heated at 200° C. (Fig. 8) An examination of emission curves indicated that this increase in sensitivity was not accompanied by any apparent changes in the emission curve structure with respect to unheated powder. However, the changes in sensitivity at the higher temperatures (300° C to 1000° C) very definitely involved changes in the emission curves. At 300° C, the 115° C peak was reduced while the 79° C peak was increased. Treatment at 350° C resulted in these two peaks being approximately the same height. Powder treated at 400° C showed a downward shift of the low temperature peak to a position corresponding to 69° C with both peaks remaining equal in height. Treatment at 460° C resulted in a decrease in height of the 115° C peak plus the appearance of a slight peak at the 178° C positions. Powder treated at 600° C showed a complete absence of the 115° C peak, but a new peak at 162° C was observed. The 700° C heating resulted in a substantial reduction in counts in all peaks with almost complete loss of the 69° C peak. Finally, the emission curves for the 900° C treatment showed the appearance of the 69° C peak, the 115° C peak, and a predominant 162° C peak. Typical emission curves for the 600° C and 900° C treatments are shown in Figures 9 and 10. It should be noted that for powders heated at 700° C and above, a solid mass formed which required grinding with a morter and pestle before the material could be used. Since pure CaF_2 has a melting point of 1360° C, the formation of the solid mass was probably due to one of the impurities present. The presence of $CaCl_2$, which has a melting point of 772° C, could perhaps be involved.

The response of CaF_2 as a function of exposure to ^{60}Co gamma radiation is shown in Figure 11. The pure CaF_2 exhibited a linear response for exposures between 25 R and 125 R. The CaF_2-graphite mixture gave a linear response between

40 R and 310 R.

An experiment was designed to observe the response of irradiated CaF_2 dosimeters as a function of time after irradiation (time fading). Due to the environmental sensitivity, a small quantity of CaF_2 powder was irradiated inside a small glass bottle. Dosimeters were prepared from this bottle and read out at selected times after irradiation. The response as a function of the time after irradiation is shown in Figure 12. A response decrease of approximately 19% within 32 hr and of approximately 25% within 122 hr after irradiation was due primarily to the 79° C temperature peak.

It has been known that TSEE dosimeters are light sensitive after irradiation. To have some quantitative information on this effect, CaF_2 dosimeters were exposed to normal room fluorescent lighting (approximately 100 foot-candles) for different lengths of time ranging from 1 min to 60 min. As shown in Figure 13, a 17% response loss occurred for a 5 min exposure and a 23% response loss occurred for a 60 min exposure. Essentially all the fading occurred within the first 5 min of light exposure and appeared to be characteristic of the 79° C temperature peak, since the peak heights of the 115° C peak remained constant. The general shape of the glowcurve remained essentially unchanged for exposures from 5 min to 60 min.

Discussion

The results obtained with LiF are generally in agreement with other published reports. The dosimetric properties of LiF were satisfactory with respect to reproducibility and sensitivity. Furthermore, such dosimeters were rather easy to handle and use, in that they were seemingly not affected by normal room environment such as exposure to air or humidity.

The CaF_2 presents some interesting questions and should be discussed in more detail. Due to the sparce amount of information available in the literature, any comparisons of the dosimetric properties of CaF_2 are extremely limited. The majority of the previous work on the TSEE of CaF_2 has been primarily concerned with glowcurve characteristics for various colorations, while the limited work of Sujak and Gierossynska[6] appears to provide the only available information on the TSEE dosimetric properties.

The decreasing sensitivity with increasing heating temperature is in disagreement with the findings of Sujak and Gierossynska who observed a sensitivity enhancement with increasing temperature from 27° C to 900° C. This apparent discrepancy might be explained by the fact that the powder used in the present work was not of the highest purity; whereas, the powder used by Sujak and Gierossynska was described as "pure." If indeed they did have high purity powder, they would not have experienced any diffusion of impurities with low melting points to the surfaces of the crystals. Consequently, on this basis a

sensitivity drop would not be expected. Their observed increased sensitivity could then possibly be related to the desorption of surface coatings at higher temperatures resulting in a reduced work function. Also their dosimeters were read out within 60 sec after irradiation; whereas, a time of 25 min elapsed between irradiation and readout in the present work. The significance of this is that, if the work function was indeed lowered by heating in the present work, there is a possibility that a rapid decay of the emission would appear as a lower sensitivity because of the longer time between irradiation and readout.

A particularly interesting observation associated with the experiment on radiation fading in time should be noted. As previously shown the sensitivity of CaF_2 dosimeters which stand uncovered in normal room air prior to irradiation decreases with time, and a cover over the dosimeters inhibits this loss of sensitivity. To circumvent the necessity for carefully controlling the exposure of the dosimeter surfaces to air during a long range fading study, dosimeters were prepared just prior to their readout from powder which had been previously irradiated inside a small glass bottle. The excellent reproducibility of dosimeters so prepared and read out points to the possibility of irradiating TSEE dosimeters in a manner similar to that of TL dosimeters. Small encapsulation tubes containing known weights of the sensitive material can be irradiated and emptied into a readout planchet. At least for CaF_2 it appears that such handling does not effect the response and that, contrary to other findings, a smooth undisturbed surface may not be a necessary requirement for reproducible TSEE dosimeters using CaF_2.

References Cited

1. J. Kramer, Acta Phys. Austriaca, 10, 392, (1957).
2. K. Becker, J. Cheke, and M. Oberhofer, Health Phys. 19, 391 (1970).
3. J. Kramer, Proc. Second Int. Conf. Luminescence Dosimetry (CONF-680920), 180, (1968).
4. W. Hanle, A. Scharmann, G. Seibert, and J. Siebert, Nukleonik 8, 129, (1966).
5. K. Becker, Proc. Second Int. Conf. Luminescence Dosimetry (CONF-680920), 200 , (1968).
6. B. Suyak and K. Gierosznska, Acta Phys. Austriaca 10, 427, (1957).
7. B. Sujak and S. Geisor, Acta Phys. Pol. 32, 541, (1967).
8. K. Becker, Health Phys. 16, 527, (1969).
9. M. Frank, P. Knoll, and F. Muller, Isotopenpraxis 2, 369, (1966).

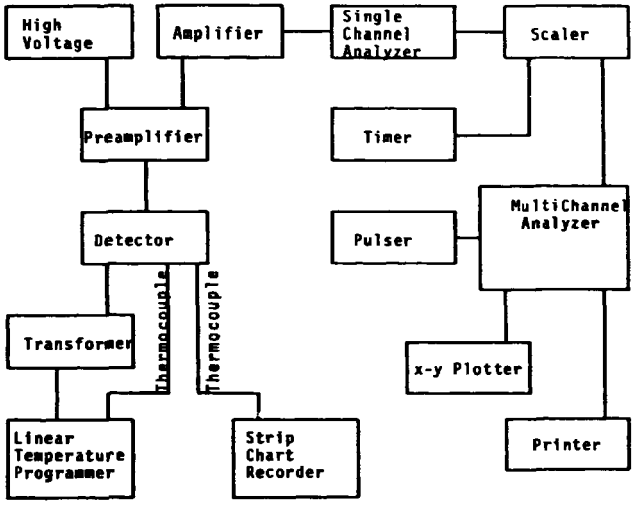

Figure 1. Block diagram of TSEE dosimeter readout system.

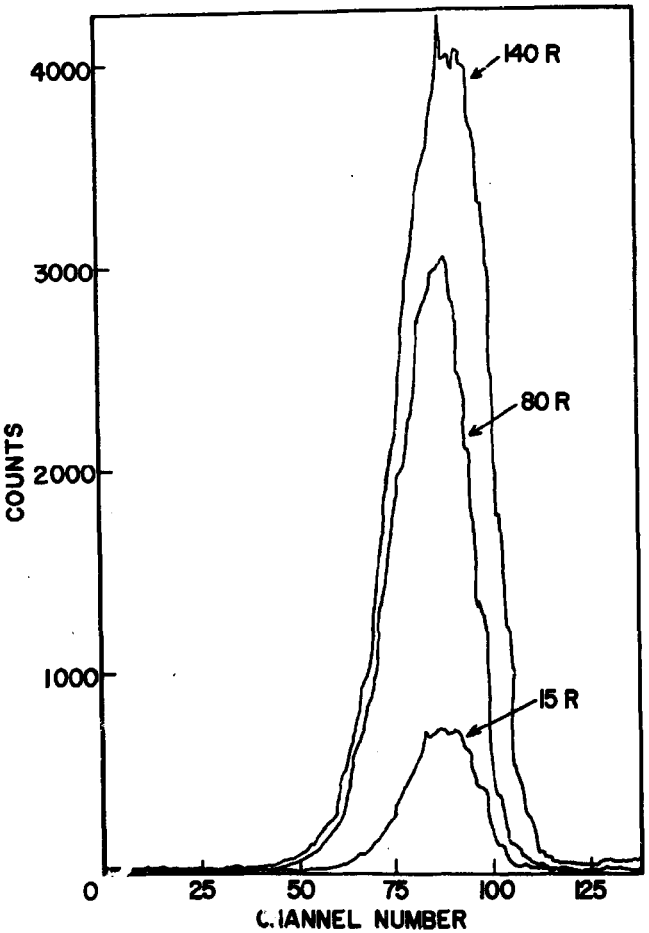

Figure 2. Exoelectron emission curves for LiF.

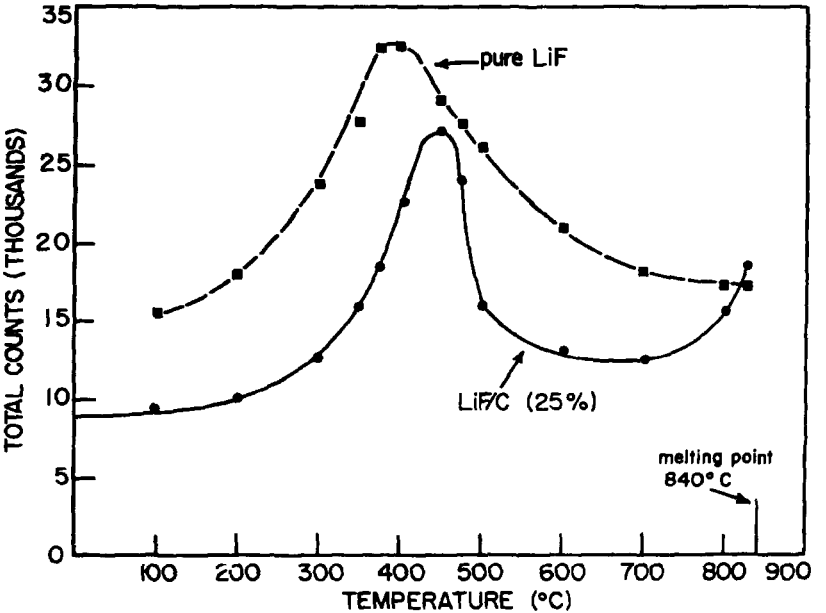

Figure 3. Sensitivity of Lithium Fluoride as a function of preheating treatment (15 minute heating times).

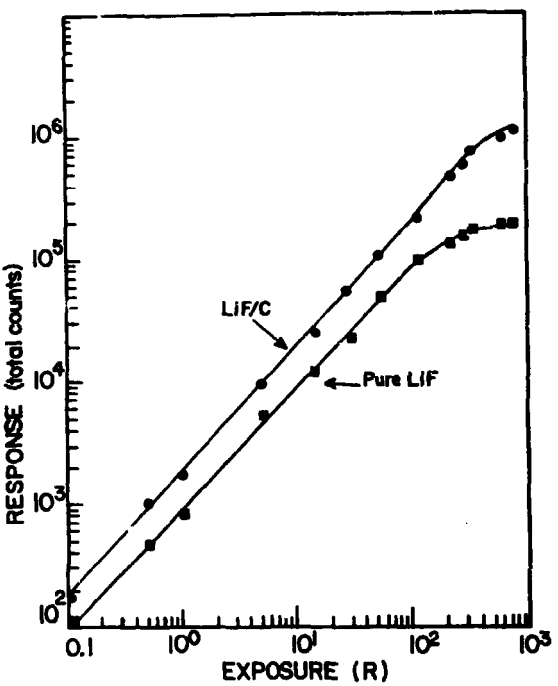

Figure 4. Lithium fluoride TSEE response as a function of exposure. (LiF/C pretreated at 450°C compared to untreated LiF)

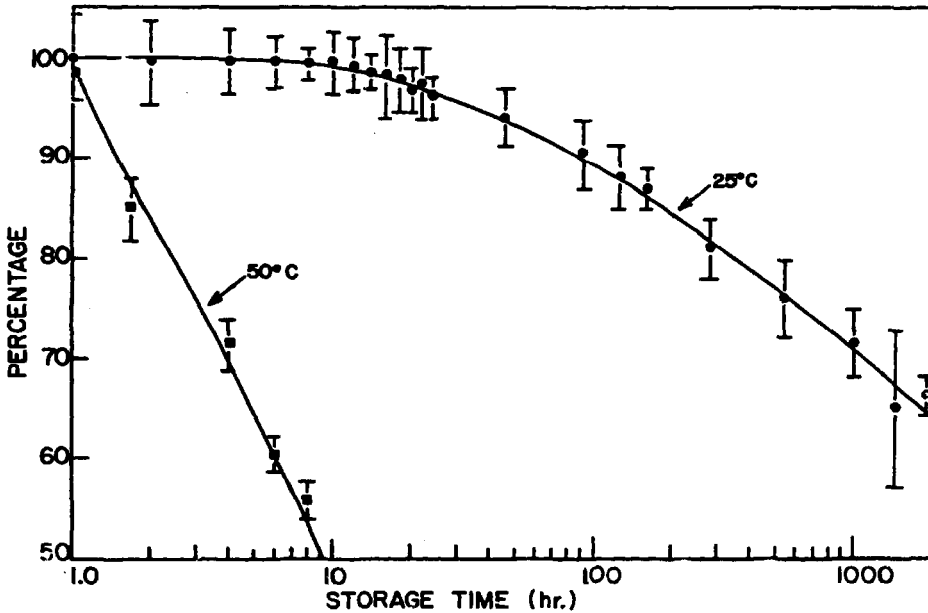

Figure 5. Fading of TSEE as a function of storage time and temperature for LiF.

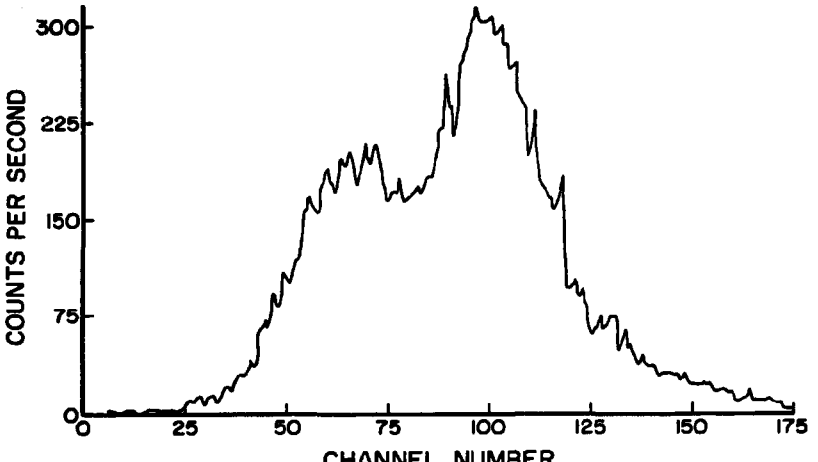

Figure 6. Exoelectron emission curve for CaF_2.

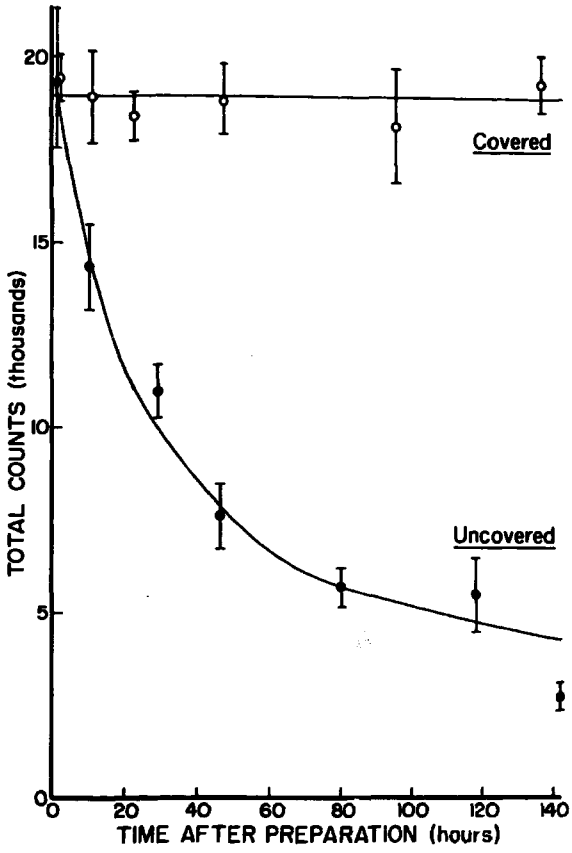

Figure 7. Sensitivity of CaF_2 dosimeters stored in air prior to irradiation.

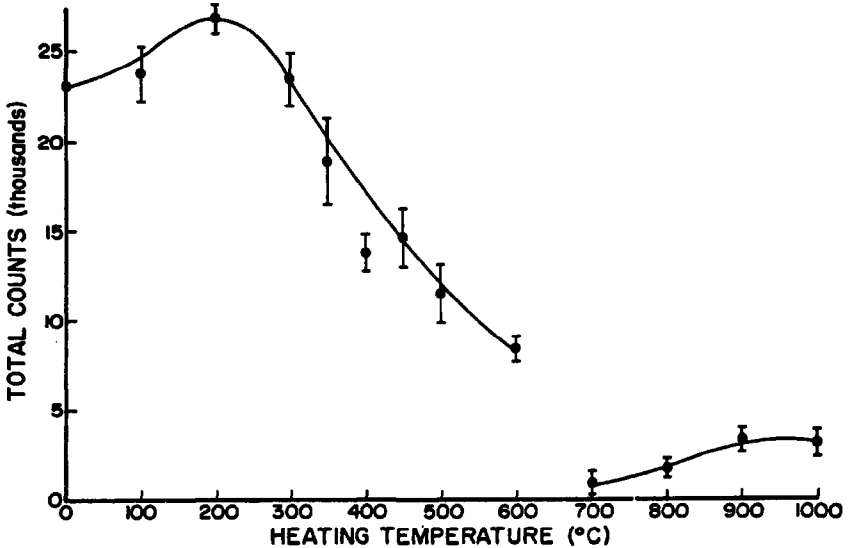

Figure 8. Sensitivity of CaF_2 as a function of pre-irradiation heat treatment.

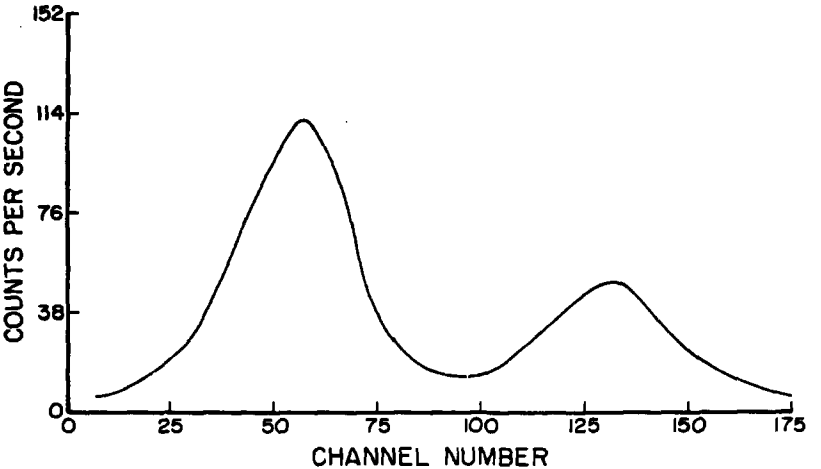

Figure 9. Emission curve of CaF_2 treated at 600°C prior to exposure.

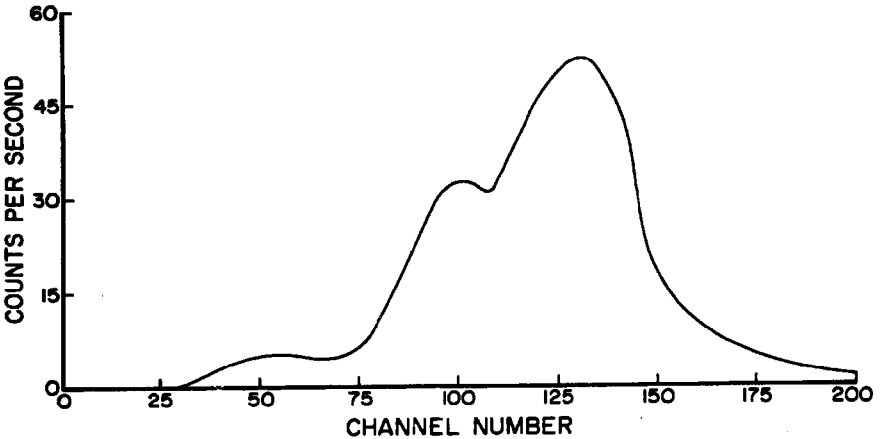

Figure 10. Emission curve of CaF_2 treated at 900°C prior to exposure.

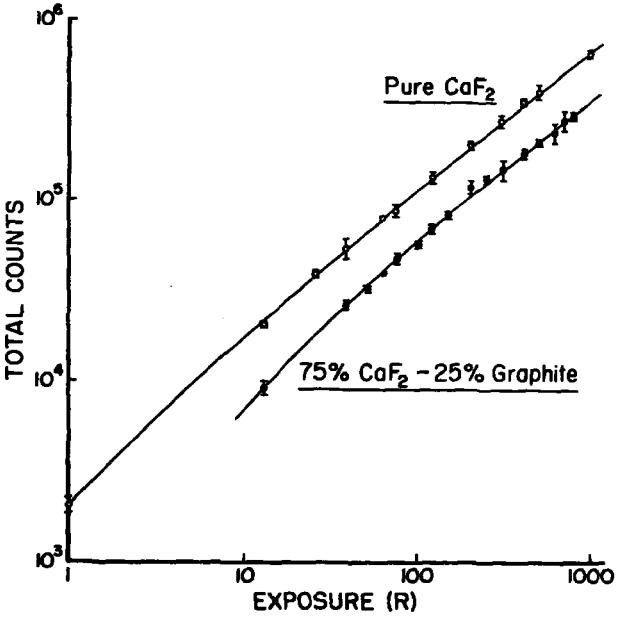

Figure 11. Calcium fluoride TSEE response as a function of exposure.

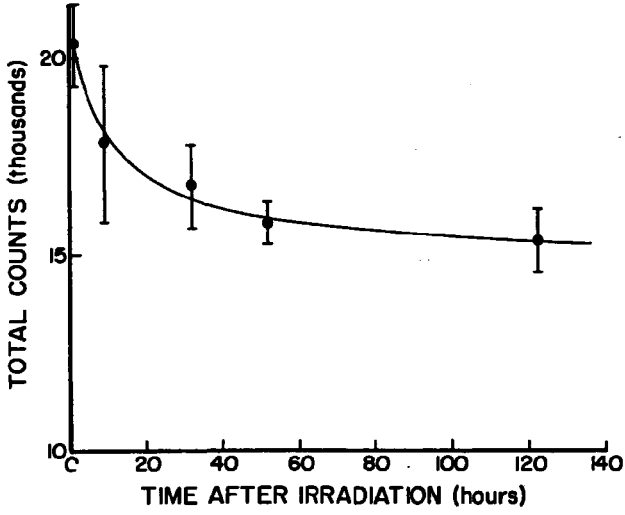

Figure 12. Calcium fluoride TSEE response as a function of time after gamma irradiation (storage in dark).

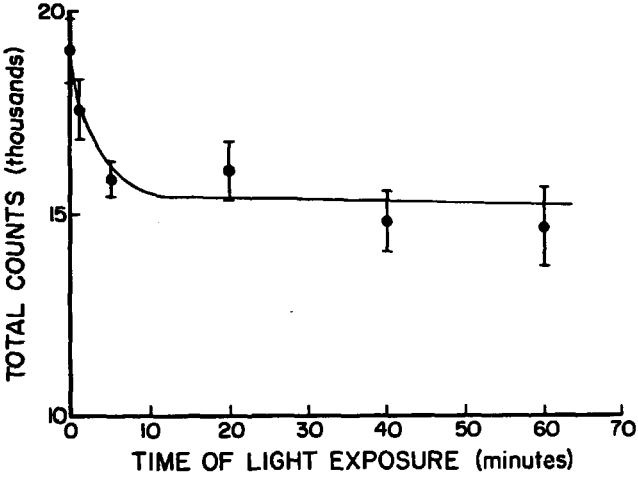

Figure 13. Calcium fluoride TSEE response as a function of light exposure time after gamma irradiation.

Problems in the Use of Proportional Counters for TSEE Measurements

L.D.Brown. Edwards Radiation Laboratories, North East London Polytechnic, Romford Road, London, E.15.*

Abstract.

It has been found that proportional counters designed for the detection of thermally stimulated exo-electrons must be operated at voltages above the end of the conventional plateau. Under these conditions difficulties have been experienced in eliminating occasional spurious readings. Methods have therefore been developed for producing geometrically stable samples suitable for repeated readout which have enabled some of the factors leading to variations in counter performance to be studied. These include the choice of counting gas, the gas flow dynamics, the counter head design and the effect of the heating cycle during readout.

The reader developed following consideration of these studies incorporates facilities for the recording and comparison of both thermoluminescent and exo-electron emission curves using a small multichannel analyser. TLD and TSEE reader heads can be quickly interchanged and samples can be re-irradiated in the reader without being removed from the heater cup.

Results reported show that it is desirable to avoid the use of extended anodes in the counter, that photo-electrons released as a result of sample thermoluminescence do not contribute significantly to exo-electron counts and that the simultaneous emission of more than one exo-electron appears to be usual.

Introduction

When it was decided to construct an exo-electron dosimeter reader at the North East London Polytechnic discussions were arranged with members of the Health Physics and Medical Division A.E.R.E. Harwell. As a result I was invited to make use of the TSEE reader constructed there by F.H.Attix and B.Hinchley in 1968 and subsequently described by Dr Attix.[1] Results reported in this paper are based partly on readings made at Harwell and partly on additional work at the Polytechnic where the reader described later in this paper was developed. The counting chamber in this second reader was designed with rather different geometry and for a considerable time work was proceeding concurrently in both centres in order to facilitate assessment of the importance of reader characteristics on the results obtained.

Although the relatively long dead time associated with geiger counters renders these unsuitable for the development of a wide range linear TSEE dosimetry system, proportional counters have so far been less widely used. Dr Attix's work at Harwell and the USNRL has shown not only that proportional counters can be used successfully but that they are more informative than geiger counters. They have therefore been used throughout the following work which has been carried out principally with

* Now at Dept. of Medical Physics, University of Aberdeen.

Conrad thermoluminescent grade lithium fluoride LiF-7 (referred to subsequently in this paper as TLD 7 to distinguish it from the reagent grade lithium fluoride which was also used for some observations) and beryllium oxide in powder form. Some observations have also been made with ceramic BeO discs obtained from Consolidated Beryllium Ltd. of Milford Haven. Problems arising from electrostatic effects at the surface of the discs during readout, which Dr Becker's group at Oak Ridge overcame by applying a thin evaporated metal film[2] appear to have been avoided in our work by pressing a fine earthed metal gauze firmly into contact with it.

Problems of Spurious Readings.

The early work showed discrepancies between repeated readings which exceeded normal statistical variations in the counts. This could be readily explained if for example the number of actual emission sites on the surface of the sample was very much smaller than the total number of electrons actually emitted, and was not regarded as of serious importance. A greater problem arose with between 5% and 10% of the samples which gave totally unexpected and apparently spurious readings. These were usually excessively large although occasional very low counts were also encountered. If a group of about 10 samples were dosed and read out several times in succession it would typically be found that on each run one of the samples gave a result incompatible with the others but that the sample concerned was not the same on different runs. Unexpectedly high counts were typically associated with very short bursts of counting during the readout cycle which appeared to be caused by counter instability. Low readings were thought to result from electrostatic effects associated with inadequate earthing of the samples. However alternative explanations were possible-low counts also followed the 'poisoning' of prepared samples by exposure to certain organic vapours such as those from plasticising agents[3] whilst high counts could be due to sample inhomogenity permitting a very few exceptionally efficient emission centres to occur. To decide conclusively whether these spurious results were due to sample or counter effects a twin programme of investigations was planned the aims of which were:-

(a) To develop samples which were geometrically stable and would give more closely repeatable readings.
(b) To study possible causes of spurious counting in the proportional counter head.

Sample Preparation.

The most widely reported methods of producing dosimeter discs from luminescent crystals are deposition on a planchet from a suspension in acetone[4] and binding with sodium silicate solution[5,6]. The former of these was not regarded as giving sufficient stability for reliably repeatable readout and the latter was found to produce a drastic loss in sensitivity. Alternative binding agents were therefore tested, the most satisfactory being a thin layer of polyimide thermocuring plastic in the form of Du Pont RK 692 Pyre ML varnish a sample of which was kindly supplied by the manufacturers. This material,unlike most alternatives tested, is suitable for repeated heat cycling at up to 600°C.

Samples evaporated under vacuum and deposited on stainless steel planchets were also used successfully. This process changed the emission curve for luminescent grade lithium fluoride to a form very close to that of the laboratory grade showing that the activators in luminescent grade material are not carried over in the evaporation process and hence indicating why evaporation has not so far proved successful for the preparation of thermo-luminescent dosimeters. (Figure 1.) The majority of the results reported here were however obtained with samples thermally fused to the planchet by heating to about 800°C for a few minutes. This technique can be used successfully with both graphite and stainless steel planchets although less accurate control of the heating process is required with the latter.

Figure 2 shows the TSEE response of some of these various samples.

Proportional Counter Design.

The reader constructed at Harwell used pure methane gas flowing through a hemispherical proportional counter fitted with a platinum wire loop anode. It had to be operated with an applied voltage greater than that corresponding to the end of the counting plateau plotted for a radioactive source- an effect previously observed by Campion when detecting single electrons in a proportional counter.[7] Apart from the problem of occasional spurious results this reader also showed a steady loss of sensitivity with use necessitating a regular increase in the operating voltage which was attributed to spark polishing of the wire. Consequently when the Polytechnic reader was developed it was decided to investigate the various factors which could affect counter sensitivity or stability. These included:-

(a) Counting chamber shape and nature of anode.
(b) Gas flow dynamics.
(c) The effect of the heating cycle on the gas gain.
(d) The choice of counting gas.
(e) The relationship between the pulse height spectrum from the counter and the energy spectrum of the emitted exo-electrons.

Initially a second counting chamber was developed with the same height as the original but only half the diameter. This was fitted with a needle point anode. (A Millward Number 3 Sharp hand sewing needle.) It was found to have closely comparable efficiency to the original chamber but to be less subject to instability. Unlike this original it could be used successfully with an argon-methane gas mixture as well as with pure methane. The plateau for a radioactive source was however shorter than for the original counter and the operating voltage required to detect single electrons came still further beyond the end of this plateau. Replacing this needle with a still more sharply pointed surgical needle led to the plateau being reduced to little more than a kink in the curve and was not found successful. Figure 3 shows a photo-micrograph of the tips of these two needles.

Although Roost et al[8] have reported that a counting chamber with a large height to diameter ratio is desirable to minimise photon induced spurious pulses, the Millward needle anode when fitted into the original counting chamber showed the same reduction in spurious pulses as observed with the second chamber.

This reduction was therefore clearly associated with the use of the needle anode and not with the difference in chamber geometry. Other anodes were subsequently tested including a straight wire anode, a special wire anode and mounting developed by Dr. Cairns at A.E.R.E. for X-Ray spectrometry[3], and a piece of razor blade. Figures 4-10 show the characteristic curves for background counts, radioactive source counts, and exo-electron counts obtained with these various anodes. The razor blade with a nominal radius of curvature at its edge of 0·03 μm. surprisingly required a higher operating voltage than 1/100 in. diameter wire anodes, thus tending to confirm the importance of surface irregularities in controlling the operating point for the latter. Due to the limited E.H.T. voltage available it could only be tested with the argon methane gas mixture for which it showed serious instability when counting exo-electrons. A similar problem with this counting gas has been reported by Dr Attix[1]. In our work it was found with all the extended anodes tested and was not entirely absent with these even when counting in pure methane. The needle anodes were however completely stable with both counting gases. It was concluded that this instability was associated with positive ion induced afterpulses associated with discharges at different points along the perimeter of the anode, and that the use of point anodes was desirable.

Both the volume and the direction of gas flow through the counter were varied. No change of sensitivity was detectable for variations of flow rate between 0·5 l/min. and 5 l/min. Reversing the direction of gas flow to carry emitted electrons away from the anode had only a marginal effect on the probability of them being detected. (Figure 11.) Possible effects of convection currents produced by heating of the chamber during readout were also shown to be small by inverting the reader head assembly and comparing readings obtained with the heater at the bottom and the top. (Figure 12.) Using a ^{14}C radioactive source and a hot wire source of thermal electrons it was found that, as expected a reduction in gas gain followed the change in density produced by heating the chamber during the readout cycle. This effect however was small (Less than 10% reduction in detection efficiency at 400°C.) and could not contribute to the spurious results which had been observed.

Finally the pulse height spectrum of the exo-electron induced pulses from the counter was studied. Measurements were carried out using pulses initiated by single thermal electrons from a hot wire, exo-electrons and ^{14}C beta particles. Results are displayed on Figure 13 and show that with both the single electron sources a wide range of pulse amplitudes exist although this is greater for the exo-electron pulses than for those initiated by thermal electrons. To determine the reason for this the reader was modified by the introduction of a negatively biassed grid to check the energies of the exo-electrons. Figure 14 shows that for TLD 7 their number falls off exponentially with increasing energy, virtually none having energies greater than 1 eV. (This graph also proves that the exo-electron counts recorded cannot have been produced by photo-electric emission from the counter wall following sample thermoluminescence.) The larger spread in pulse amplitudes observed for exo-electrons rather

than thermal electrons cannot therefore be explained by the former producing multiple ionization and is most readily accounted for by Attix's suggestion of multiple electron emission. From Figure 15 it can be seen that halving the electronic gain also halves the thermal electron count but only reduces the exo-electron count by about a third as much. This suggests that up to two thirds of the exo-electron counts are associated with the simultaneous emission of more than one electron.

To study the relative probabilities of multiple emission at different temperatures families of emission curves were prepared with different counter voltages (gas gains), amplifier gains, and discriminator bias settings. (Figures 15-17) In all cases it is seen that the larger emission peak (which for TLD 7 is the high temperature peak) is most quickly affected and therefore appears to contain the largest proportion of low amplitude pulses. With Harshaw TLD 100 Attix observed a similar effect but the large emission peak for this material was the low temperature one. Multiple emission therefore appears to be related to free electron carrier density in the crystal rather than to temperature.

Figures 18-20 show the reader developed during the course of this work. Its most important feature is that powder samples can be re-irradiated in the heater cup so that repeated readout of a sample in either TLD or TEEE mode is possible without disturbing it. This facility helps in the study of materials that cannot readily be prepared as solid rigid samples. Provision is also made for the incorporation of a small NIM multichannel analyser which can be used in multiscaling mode to obtain numerical values for the total emission in each peak.

Acknowledgments.

Thanks are due to the Head of the Health Physics and Medical Division, A.E.R.E., Harwell; the Governors of the North East London Polytechnic and the Science Research Council for supporting this work.

REFERENCES.

(1) Attix F.H. Int. J. App. Radn. & Isotopes 22 185 (1971)
A proportional counter for thermally stimulated exo-electrons.

(2) Robinson E.M., Oberhofer M. Health Physics 18 434 (1970)
A sensitive ceramic BeO TEEE dosimeter.

(3) Brown L.D. IRPA/6/70 and Health Physics 19 93 (1970)
The design of a TEEE dosimeter and a comparison of exo-electron emission sensitivity with thermoluminescent sensitivity for various phosphors.

(4) Becker K. Proc. 2nd. Int. Conf. Lum. Dosimetry, Gatlinburg 1968. Conf. 680920. p.200.
Some studies on radiation dosimetry by thermally stimulated exo-electron emission.

(5) Svercer V., Fowler J.F. Proc 1st. Int. Conf. Lum. Dosimetry, Stenford 1965. Conf. 650637. p.227
Spurious thermoluminescence and triboluminescence in LiF dosimetry powder.

(6) Kramer J. Proc. 2nd. Int. Conf. Lum. Dosimetry, Gatlinburg 1968. Conf. 680920. p.180.
Dosimetry with exo-electrons.

(7) Campion P.J.,Murray D.K. Int. J. App. Radn. & Isotopes. 18 204 (1967)
The detection of single electrons in pulse radiation detectors.

(8) Roost E.de, Bunck E., Spernol A. Int. J. App. Radn. & Isotopes 20 387 (1969)
Improvements in 4π β-γ coincidence counting.

(9) Cairns J.A.,Holloway D.F. Nuc. Insts. & Methods. 94 579 (1971)
A new proportional counter anode unit.

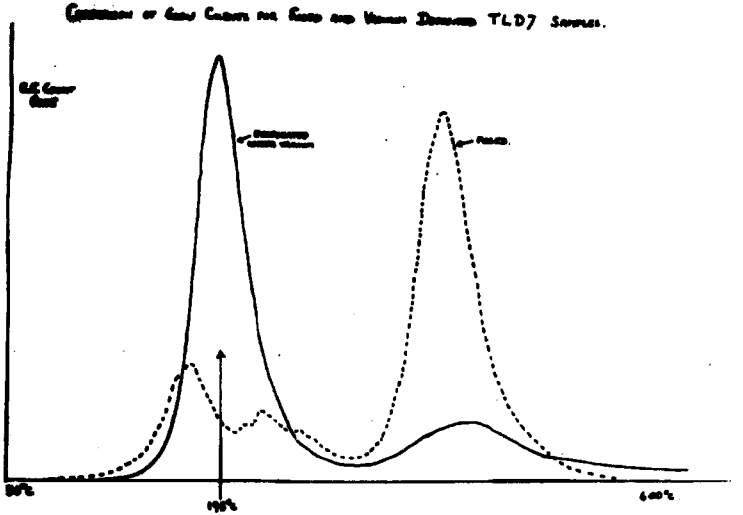

Figure 1. TSEE emission curves for fused and evaporated samples of Conrad TLD 7.

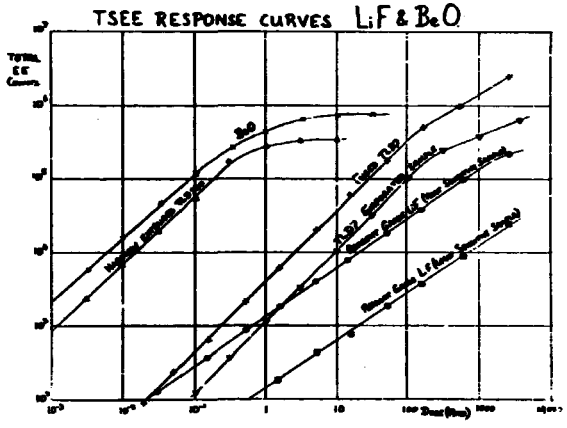

Figure 2. TSEE response of various samples tested.

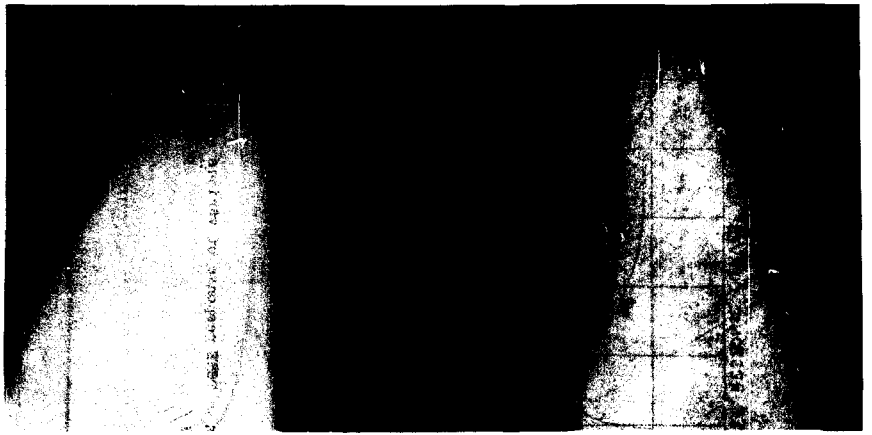

Figure 3. Photomicrograph of tips of needle anodes.

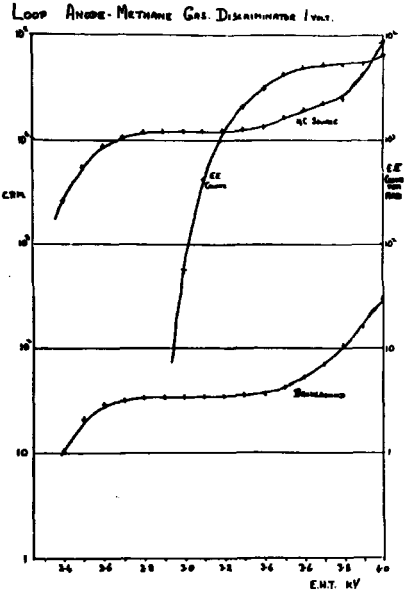

Figure 4. Characteristic curves for TSEE reader with loop anode and methane gas.

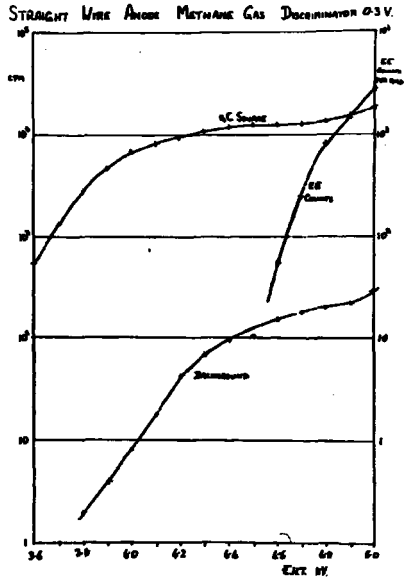

Figure 5. Characteristic curves for TSEE reader with straight wire anode and methane gas.

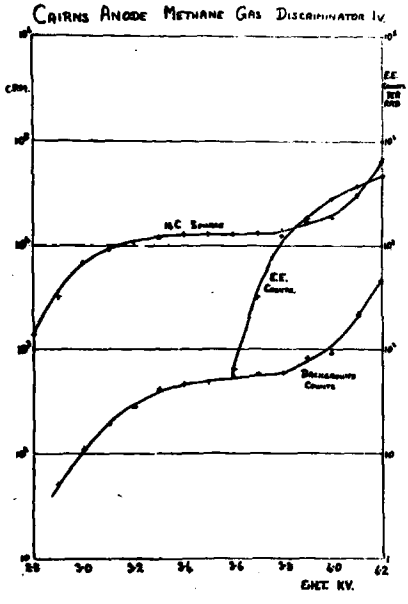

Figure 6. Characteristic curves for TSEE reader with Cairns anode and methane gas.

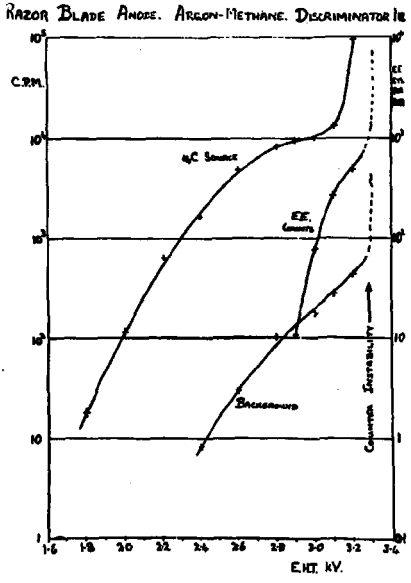

Figure 7. Characteristic curves for TGEE reader with razor blade anode and argon-methane gas.

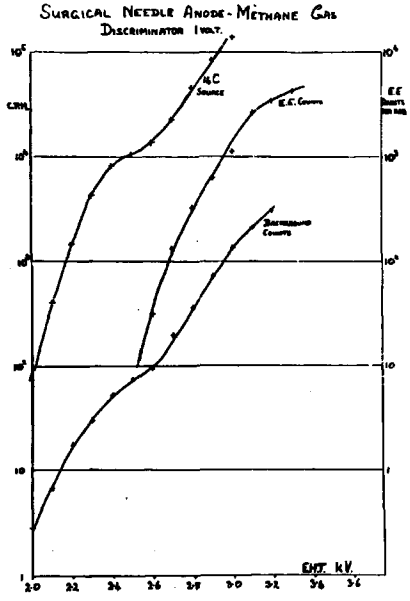

Figure 8. Characteristic curves for TSEE reader with surgical needle anode and methane gas.

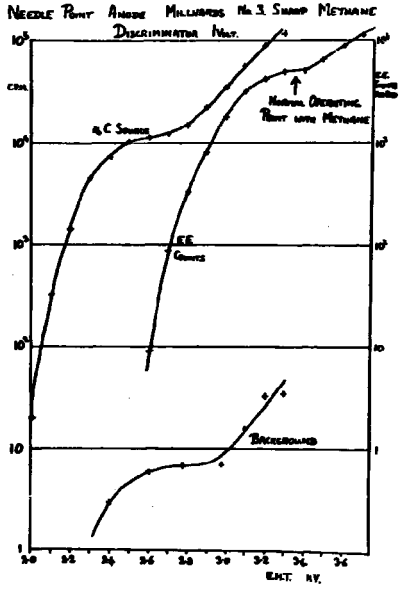

Figure 9. Characteristic curves for TSEE reader with Millward needle anode and methane gas.

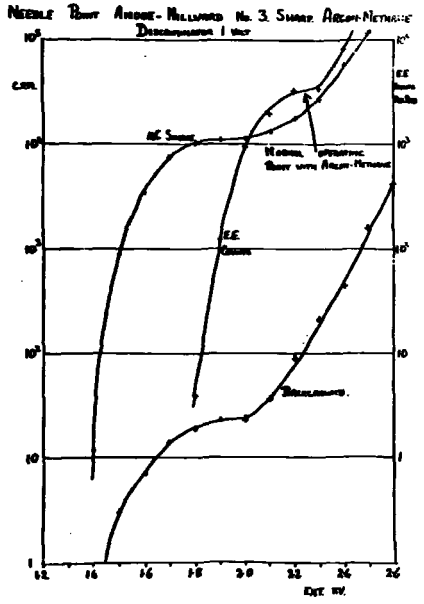

Figure 10. Characteristic curves for TSEE reader with Millward needle anode and argon-methane gas.

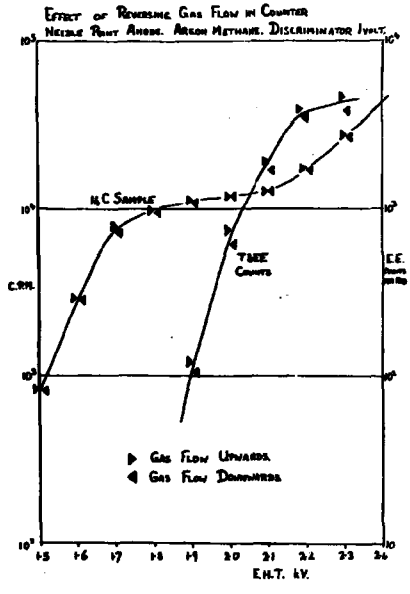

Figure 11. Effect of reversing gas flow in counter.

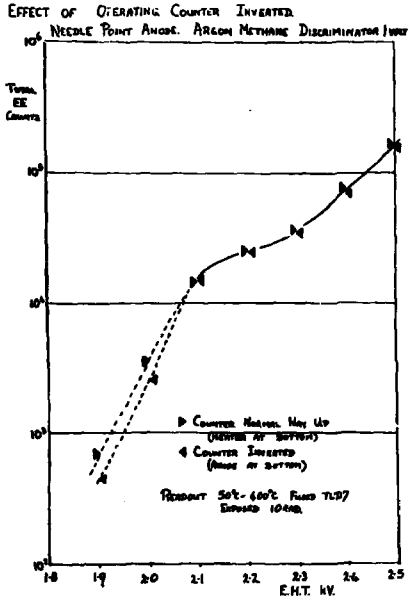

Figure 12. Effect of operating counter inverted.

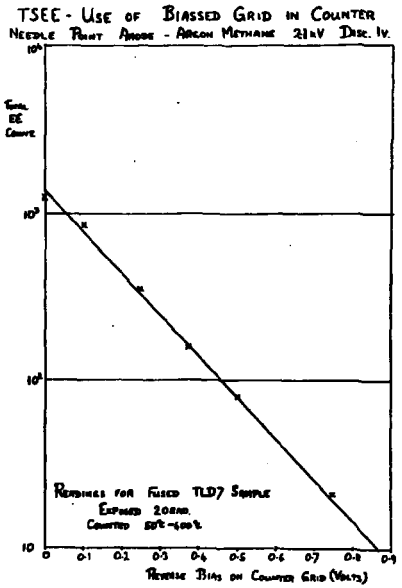

Figure 13. Effect of varying electronic gain.

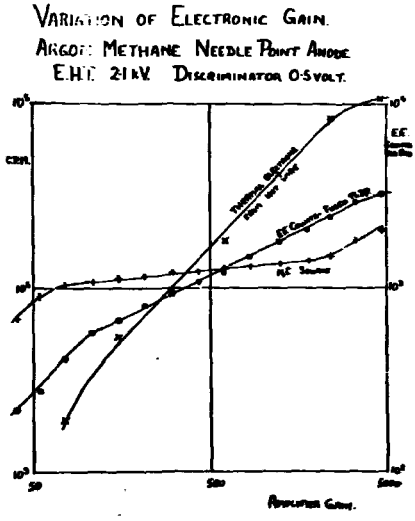

Figure 14. Use of biassed grid in counting chamber.

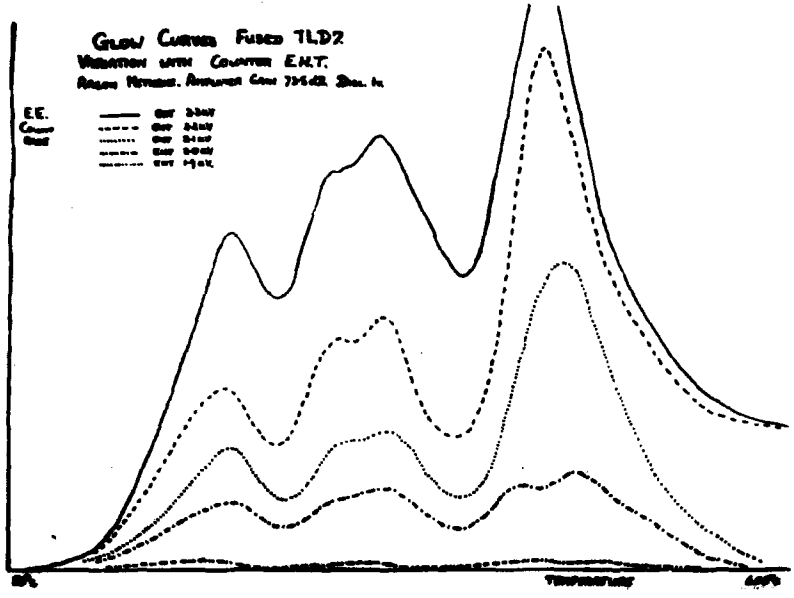

Figure 15. Comparative emission curves for different counter voltages.

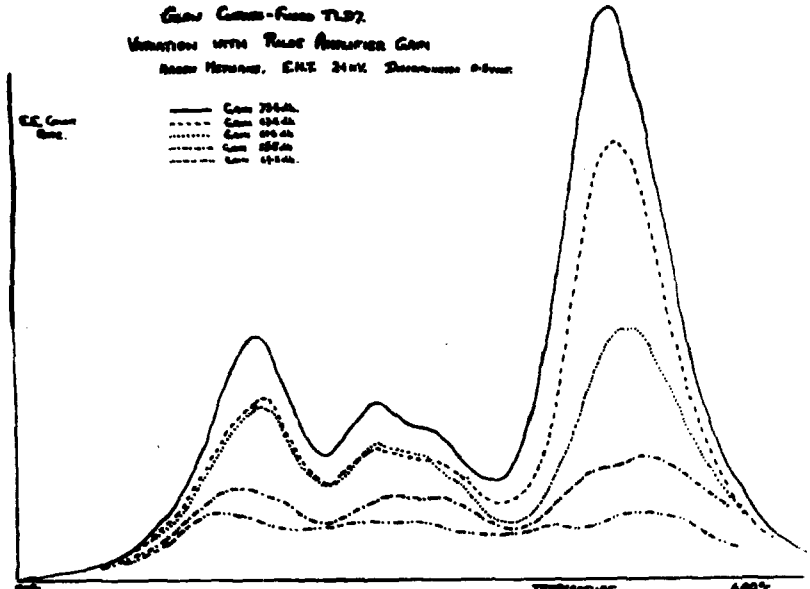

Figure 16. Comparative emission curves for different amplifier gains.

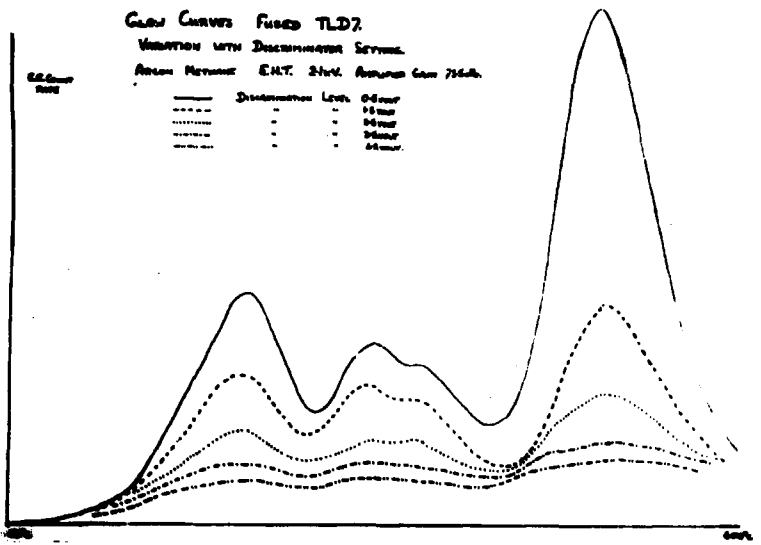

Figure 17. Comparative emission curves for different discriminator bias settings.

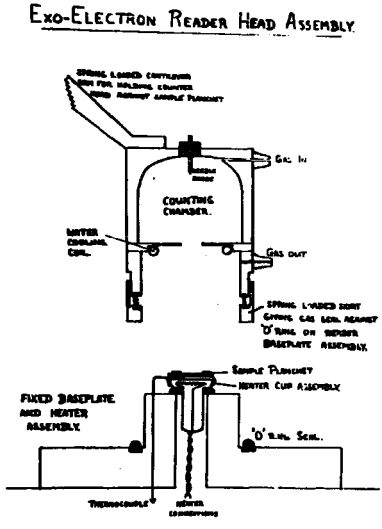

Figure 18. Counter head developed for TSEE reader. (Diagram.)

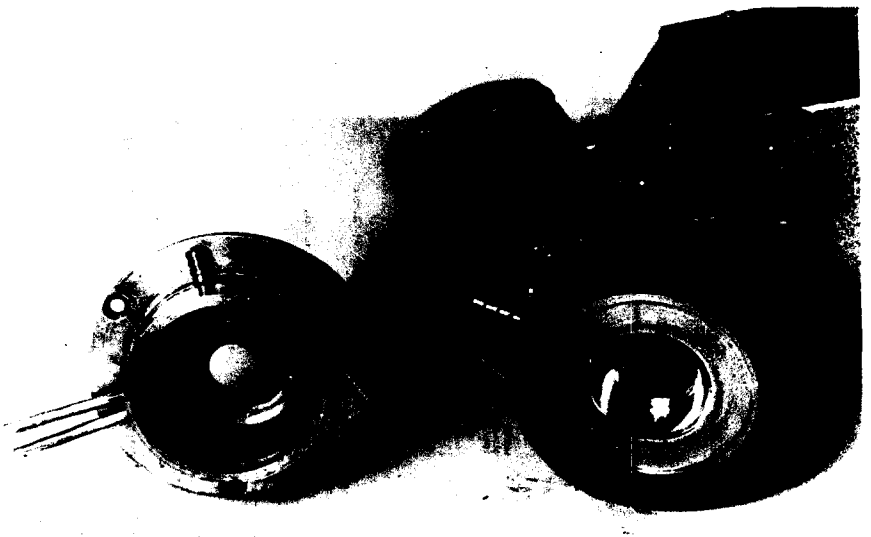

Figure 19. Photograph of counter head. (Dismantled.)

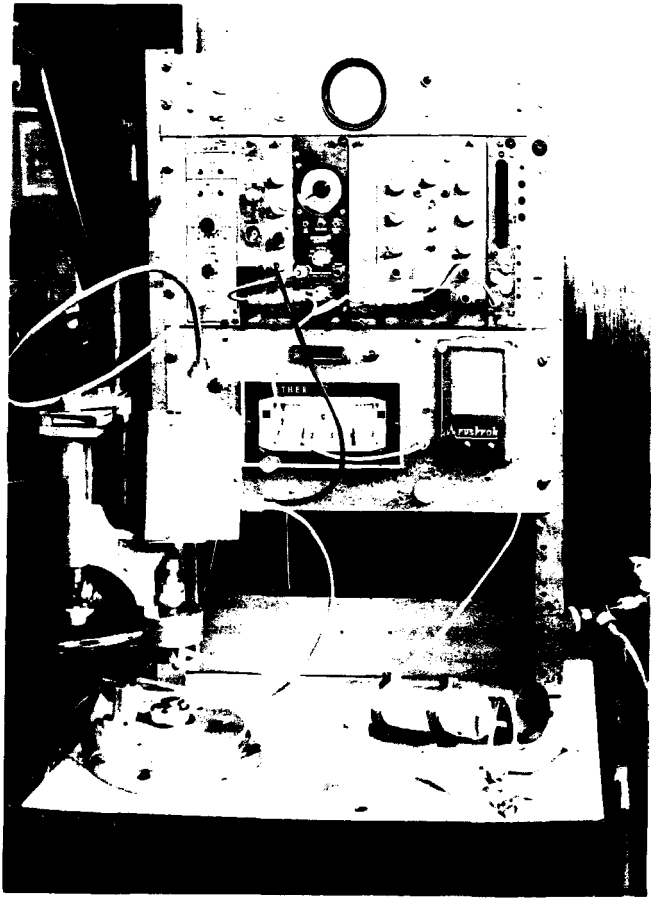

Figure 20. Photograph of complete TSEE reader.

Trapping Centers in CaF_2:Mn from Thermoluminescence and Thermally Stimulated Exoelectron Emission measurements on Undoped and Mn Doped CaF_2 Samples

by

K.J. Puite, Institute for Atomic Sciences in Agriculture, Wageningen, the Netherlands

J. Arends, Laboratory for Materia Technica, State University of Groningen, the Netherlands

Abstract

The trapping centers in CaF_2: 3 mole % Mn powder, which exhibits a single but composite thermoluminescence glow peak, have been investigated.

Simultaneous measurements of the thermoluminescence (TL) and thermally stimulated exoelectron emission (TSEE) from this powder were carried out using different post-irradiation annealing temperatures. Special precautions have been taken to prevent the light produced by the gas discharge during the TSEE measurements from interfering with the TL signal.

TL and TSEE data from single crystals and powdered samples of undoped CaF_2 and CaF_2 doped with 0.1 and 2 mole % Mn, a chemical analysis of the samples as well as optical density measurements have provided additional information.

The combined results indicate that both electron- and hole traps are present in CaF_2: 3 mole % Mn. The TL is mainly due to holes trapped at the Mn^{++} ions. The high temperature component of the composite TL glow peak and the TSEE peak are probably due to electrons trapped at trivalent rare earth ions, such as Y^{+++}, Ho^{+++}, Sm^{+++} and Tm^{+++}.

Introduction

The single TL glow peak of the TLD powder CaF_2: 3 mole % Mn does in fact consist of several unresolved peaks due to different types of trapping centers. This composite character of the glow peak has been shown previously by Schulman et al.[1] with a post-exposure annealing of the NRL CaF_2:Mn (Naval Research Laboratory, USA), while the possibility

of a second read out after UV exposure of already read out CaF_2:Mn from Philips (the Netherlands) has also given evidence for a complex character of the glow peak[2].

In an attempt to obtain information about the origin of the unresolved peaks simultaneous measurements of TL and TSEE on CaF_2: 3 mole % Mn (Philips) have been carried out. Special precautions have been taken to prevent the light produced by the gas discharge during the TSEE measurements from interfering with the TL signal.

The TL and TSEE data obtained have been compared with TL and TSEE data from undoped CaF_2 and CaF_2 doped with 0.1 and 2 mole % Mn. Furthermore optical density (OD) measurements on single crystals of these samples have been carried out. The combined measurements have resulted in some insight in the type of trapping centers, present in the CaF_2 samples, especially in the TLD powder CaF_2: 3 mole % Mn.

Methods

The apparatus for measuring the TL and TSEE signals simultaneously is shown in Fig. 1. The gamma irradiated powder was heated in three small holes which have a diameter of 0.9 mm each. A constant heating rate of 24°C/min was used with a thermocouple situated at a distance of 3 mm from the holes. The temperature at the position of the powder and the influence of the gas flow on the temperature at this position was determined with a second thermocouple in one of the holes. The temperature difference between the positions of the thermocouples was considerable e.g. at 250°C a difference of 15°C was measured both with and without a gas flow. A mixture of helium gas (98.7 %) and isobutane (1.3 %) was flowed through the counter, which was used in the GM region. A useful plateau could bs obtained up to an oven temperature of 500°C.

The TL signal was detected with a photomultiplier (type EMI 9656 R, super 11 cathode) on top of the counter. An optical filter (LCV, Baird Atomic) was used which only transmitted the spectral region of the maximum emission of CaF_2: 3 mole % Mn (485–515 nm). The TL signal proved to be distorted by the light arising from the gas discharges in the counter. To avoid this a chopper system has been used in order to decrease the high tension on the wire periodically by 200 V to stop the discharges. During this period, being 450 msec, only the TL signal was recorded. When the GM counter had reached its working potential of

1220 V again only the TSEE signal was recorded, also over a period of 450 msec (see also Fig. 1).

Results and Discussion

The peak temperatures of TL and TSEE for different read out procedures of the CaF_2 : 3 mole % Mn powder are shown in Fig. 2. The results of a post-irradiation annealing, where the powder was linearly heated up to different temperatures, are plotted. Due to the composite character of the TL glow peak a shift of the TL peak to a higher temperature is found when the maximum annealing temperature is increased. Apparently, the position of the TSEE peak is less influenced by this annealing. The difference between the TL and TSEE peaks seems to be at minimum $\sim 10^{\circ}C$. It should be noted that the estimated accuracy of the temperature measurements is $\pm 5^{\circ}C$.

In the same Figure the position of the TL and TSEE peaks, recorded during a second read out is given, when the gamma irradiated powder was first completely read out and afterwards exposed to UV light from a Philips HPLR mercury lamp. The UV transferred TL belongs to an electron trapping center.

The theory on the shift of the TL peak relative to the TSEE peak is complicated[3]. Although no direct relationship has been derived the following two effects play an important role:

a. a decrease of the luminescence intensity at higher temperatures, due to the increase in the number of non-radiative transitions compared to the number of radiative transitions. A measure of this so-called thermal quenching effect for the NRL CaF_2:Mn has been obtained by Gorbics et al.[4] by measuring the X-ray-excited radioluminescence as a function of the phosphor temperature.

b. the influence of the effective work function φ on the position of the TSEE maximum. φ is defined as the minimum energy needed for an electron located at the bottom of the conduction band to escape from the crystal surface. A value φ of 0.5 eV for CaF_2 has been reported by Bohun and Dolejsi[5] giving the best fit between their theoretical and experimental TSEE curves.

Further information on the type of trapping centers present in the CaF_2: 3 mole % Mn (Philips) powder could be obtained from optical density (OD) measurements on gamma irradiated single crystals of CaF_2, un-

doped and doped with 0.1 and 2 mole % Mn, from a chemical analysis of the CaF_2 samples and from TL and TSEE measurements of these samples.

The OD experiments were carried out at room temperature with a Unicam SP 700 recording spectrophotometer. Very pure CaF_2 can hardly be coloured by irradiation at room temperature. O'Connor and Chen[5] have demonstrated that an absorption at very high doses can often be ascribed to the contaminant yttrium Y^{+++}, which has the same ionic radius as Ca^{++}. From our samples the undoped CaF_2 of Materials Research Corporation[*1] (MRC) and the CaF_2: 0.1 mole % Mn from Semi-Elements[*2] both show the presence of yttrium, while in the crystals from MRC doped with 2 mole % of Mn the yttrium absorption is obviously influenced by the presence of Mn. A Vinor[*3] crystal, which is yttrium free, shows F-center absorption due to the presence of vacancies introduced by oxygen (Table 1).

A chemical analysis by neutron activation[*4] confirmed the presence of yttrium in the MRC and Semi-Elements samples. The Philips powder[*5] contained 0.03 ppm yttrium, while an Harshaw[*6] sample was contaminated with 0.7 ppm yttrium. The impurities which could be demonstrated eleven days after the end of the irradiation are collected in Table 2.

The peak temperatures of the TL and TSEE curves from the CaF_2 samples are shown in Table 3. Comparing the two MRC samples and the sample of Semi-Elements it is clear that the 310°C TSEE peak is due to the Y^{++} center. The TL peak for this center was found at $\sim$300°C. From the initial rise of the TL glow curve (neglecting thermal quenching) a trap depth E of 1.0 eV along with frequency factor s of 9×10^6/sec is obtained for the Y^{++} center in the undoped MRC sample. Substituting these E and s values in the equation derived by Holzapfel[6]:

*1. Materials Research Corporation, Orangeburg, New York 10962, U.S.A.
*2. Semi-Elements, Inc. Saxonburg, Pa. 16056, U.S.A.
*3. Vinor Laboratories, Medford, Mass. 02155, U.S.A.
*4. The chemical analysis was kindly carried out by Mr. P. Bruys from the Philips factories, Eindhoven, the Netherlands.
*5. Philips N.V., Eindhoven, the Netherlands.
*6. The Harshaw Chemical Co., Cleveland 6, Ohio, U.S.A.

$$\beta\ (E + \varphi)/kT_m^2 \approx s \exp\ (-E/kT_m)$$

with k = Boltzmann's constant, 8.61 x 10^{-5} eV/°K

β = heating rate

T_m = peak temperature of TSEE curve,

an E + φ value of 1.4 eV for the Y^{++} center of the 310°C TSEE peak is calculated. This would imply that the value of φ is probably $\sim$ 0.4 eV, in agreement with the value of 0.5 eV reported by Bohun and Dolejsi[5].

The thermal quenching effect measured by Gorbics et al.[4] and the influence of the work function are shown in Fig. 3. The TL glow curves of CaF_2: 3 mole % Mn have been 'corrected' for this thermal quenching while the TSEE curves have also been 'corrected' by dividing this signal by the factor exp (- φ/kT) with φ = 0.4 eV. The resulting peak temperatures are collected in Fig. 4 and show that the temperature difference between the positions of the T_L and TSEE peaks disappears when an increasing post-irradiation annealing temperature is used or when the powder is exposed to UV after being read out.

This indicates that only a part of the different types of trapping centers which contribute to the normal TL glow peak -probably the Y^{++} centers- also contribute to the TSEE peak. The remaining part of these centers are hole centers, in casu Mn^{+++} centers. The TL peak at 259°C occurring in CaF_2: 0.1 mole % Mn is probably due to these Mn^{+++} centers because no TSEE peak was observed in the neighbourhood of this temperature for gamma doses < 12 krad. At high gamma doses (5 Mrad), however, a TSEE peak has been observed at 263°C indicating that electrons may also be released in this temperature region. This effect occurs incidently and was found only twice in eight measurements. The Mn^{++} ions, present in the CaF_2:Mn samples, are probably situated at Ca^{++} ion lattice positions[7] and have an energy level of some eV above the valence band. The exact position of this level is not known. It is well known that the Mn^{++} ions can easily be converted into Mn^{+++} ions by trapping one hole.

Both the TL and TSEE peaks of the Philips powder are shifted to lower temperatures compared to the MRC samples doped with 2 mole % Mn, which have a high contamination of yttrium.

Furthermore Table 3 indicates the presence of F-centers already demonstrated in Vinor crystals with optical absorption measurements

(Table 1). Therefore, F-center type traps may be emptied in the temperature region of 150-170°C.

Conclusion

After irradiation of CaF_2: 3 mole % Mn (Philips) powder both Y^{++} and Mn^{+++} centers are expected to occur. The TL is mainly due to holes trapped at the Mn^{++} ions. The TSEE, which peaks at 292°C, the UV transferred TL, which peaks at 281°C and the high temperature components of the composite TL peak are associated with Y^{++} and probably with Y^{++} + Mn^{++} trapped electron centers, while also other divalent rare earth centers such as Ho^{++}, Sm^{++} and Tm^{++} might be present instead of Y^{++} centers.

Acknowledgements

The authors wish to thank D.L.J.M. Crebolder for his skilful technical assistance in constructing the apparatus. The discussions with K.H. Chadwick, H.P. Leenhouts and W.F. Oosterheert (ITAL, Wageningen) are gratefully acknowledged.

References

1. J.H. Schulman, R.J. Ginther, S.G. Gorbics, A.E. Nash, E.J. West, F.H. Attix, Int. J. appl. Radiat. Isotopes 20, 523 (1969).

2. K.J. Puite, Int. J. appl. Radiat. Isotopes 19, 397 (1968).

3. B.M. Nosenko and V.Ya. Yaskolko, Opt. i. Spektr. Suppl. 1, 117 (1963).

4. S.G. Gorbics, A.E. Nash and F.H. Attix, Int. J. appl. Radiat. Isotopes 20, 829 (1969).

5. J.R. O'Connor and J.H. Chen, Phys. Rev. 130, 1790 (1963).

6. G. Holzapfel, Phys. stat. sol. 33, 235 (1969).

7. J.M. Baker, B. Bleany, F.R.S. and W. Hayes, Proc. Roy. Soc. London, A 247, 141 (1958).

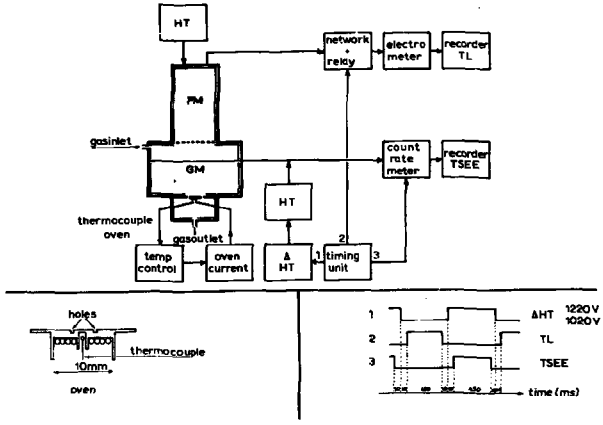

Fig. 1 Apparatus for simultaneous measurement of TL and TSEE.

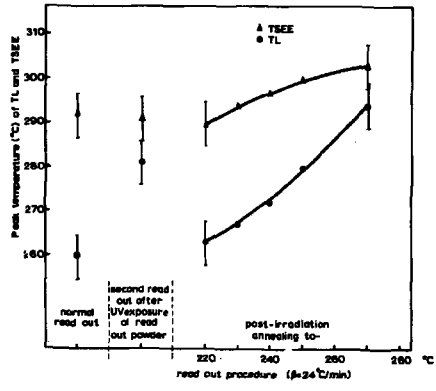

Fig. 2 TL and TSEE peak temperatures of CaF_2: 3 mole % Mn (Philips) using different read out procedures.

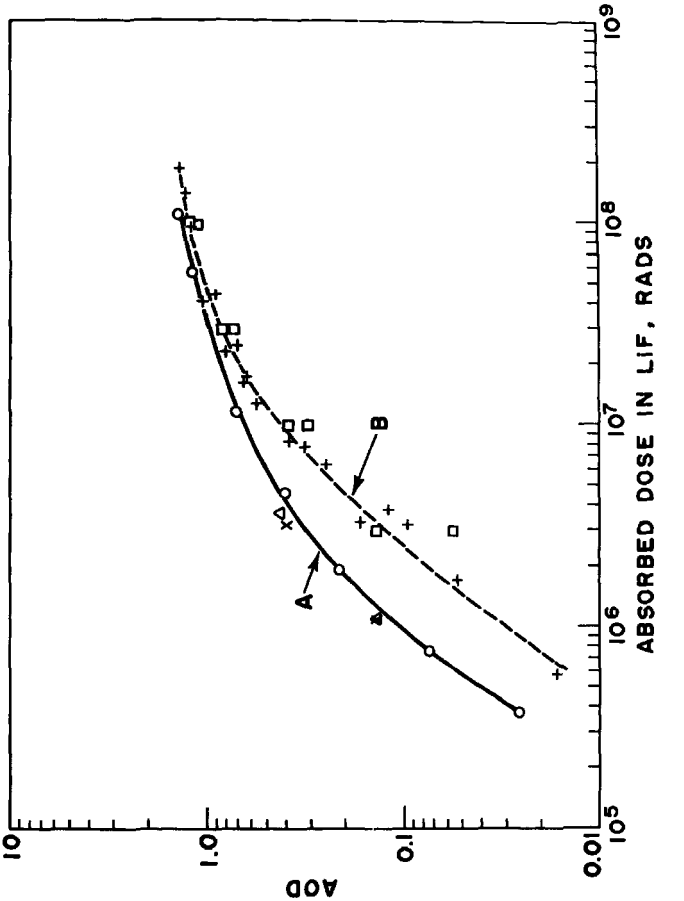

Fig. 3. M-Band absorption in Leitz LiF. Monochromator: 450 nm; PM-tube filter: 3 mm Corning #5562.
Curve A, O : ^{60}Co γ rays at ≈ 10^3 rad/sec
△ : 43 kV X rays at ≈ 10^2 rad/sec
X : 25 kV X rays at ≈ 10^2 rad/sec
Curve B, + : 2 MeV pulsed electrons at ≈ 10^{14}-10^{15} rad/sec
□ : 2 MeV-Van de Graaff-electrons at ≈ 10^4 rad/sec

	origin of CaF_2	gamma dose in Mrad	optical absorption (nm)									
				V^{**}				V^{**}	F	V^{**}		V^{**}
O'Connor and Chen (1963)	Harshaw with 5×10^{-4}% Y	5		580				400		335		225
present work	Vinor (Y free)	5.7							377			
	M R C	5.7		580				406		328		228
	Semi-Elements (0.1 % Mn)	5.7	700	580			420					
	M R C (2%Mn)	0.1			557	435				320		
		5			563		420				304	

Table 1 Color centers in CaF_2 crystals.

	Philips	MRC	Semi-El.	Harshaw
Y	0.03	7.6	8.3	0.17
Lu	≤0.006	0.07	0.08	0.006
Yb	≤0.02	0.3	0.4	0.02
Tm	≤0.2	≤0.2	≤0.2	≤0.2
Ho	≤0.3	0.4	0.3	≤0.3
Tb	≤0.002	0.04	0.04	0.002
Eu	0.009	0.2	0.04	0.006
Sm	≤0.2	0.2	0.2	≤0.2
La	0.03	0.1	0.1	0.1
Nd	≤0.1	≤0.1	≤0.1	≤0.1
Ce	≤0.1	≤0.1	≤0.1	≤0.1
Au	0.002	0.002	0.002	0.005
Cd	≤1	1.5	1	≤1
Sr	200	70	70	250
Sb	0.3	0.05	0.15	0.04

Table 2 Impurities (ppm) in CaF_2 samples.

sample \ center	D_s krad		F						(Y_{Mn}		Y**				
			e⁻	h⁺	e⁻			e⁻	h⁺(e⁻)		e⁻				
MRC	6	TSEE	99		161	174	213				390	340	363	381	398
7.6 ppm Y	6	TL	108	133	161						309				370
Semi-Elements	6	TSEE	108		153	169	206		263*	294*	312	328	355		395
0.1% Mn 8.3 ppm Y	6	TL	90	124		170	213		259		298				
MRC	6	TSEE									311				
~2% Mn	6	TL							267						
Philips	6	TSEE								292					
~3% Mn 0.03 ppm Y	6	TL							260						
idem, with post-irr. annealing to 270°C	6	TSEE								303					
	6	TL								294					
Vinor	5000	TSEE				175		263		309		343		379	390
no Y	5000	TL	104		148			250				323		340	
Harshaw	5000	TSEE			152	168				304				371	
0.17 ppm Y	5000	TL				180				279				333	

* D_s=5000 krad

heating rate 24 °C/min

Table 3 TSEE and TL peak temperatures of CaF_2 samples, using a linear heating rate of 24°C/min. An optical filter with a band pass of 485-515 nm was mounted under the photomultiplier. The main peaks are underlined.

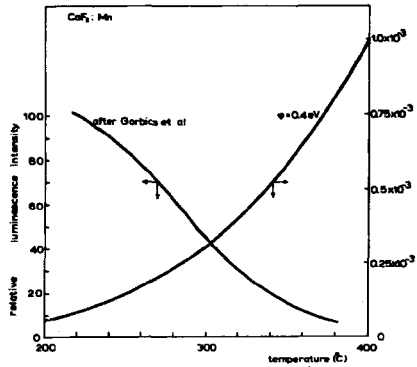

Fig. 3 Effects influencing the positions of the TL and TSEE peaks of CaF_2:Mn. Both the relative radioluminescence intensity as measured by Gorbics et al.[4] in CaF_2:Mn and the influence of the work function are shown as a function of the phosphor temperature.

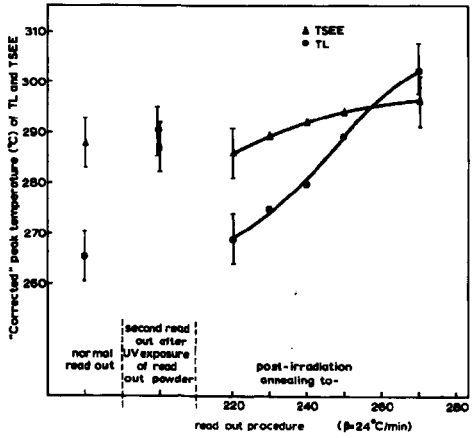

Fig. 4 'Corrected' TL and TSEE peak temperatures of CaF_2: 3 mole % Mn (Philips) using different read out procedures.

Moreno

I should like to mention the convenience of using a multichannel analyzer operated in the pulse height analysis and multiscaler modes for TSEE measurements.

Formation Kinetics of Color Centers in RPL Glass Dosimeters

A. M. Chapuis, M. Chartier, and H. Francois
Département de Protection
Section Dosimétrie, CEA
France

Theoretical investigations on radiophotoluminescent (RPL) glass dosimeters betray quite a number of gaps. They are frequently carried out in different experimental conditions and are difficult to be compared. The authors performed new investigations with French made metaphosphate (C.E.C.) glass dosimeters. Fluorescence, optical absorption and paramagnetic electronic resonance spectra have been studied. The results show several color centers, and the kinetics of their formation has been studied.

By modifying the glass compositions and the experimental irradiation conditions, it is possible to explain the nature of these centers. The authors have compared their relative stability with regard to heat annealing processes and to U.V. irradiation.

A RPL Dosimetry System

with fully automated Data Evaluation

by

M. Dade *)
A. Hoegl *)
R. Maushart **)

*) Frieseke & Hoepfner GmbH, Erlangen-Bruck
**) BF - Vertriebsgesellschaft mbH, Karlsruhe

Abstract

A RPL dosimetry system is described consisting of a dosimeter and the fully automatic reading device. They have been designed as corresponding units that together enable the useful energy range of the system to be extended down to 15 keV.

The dose value is displayed by Nixie tubes in steps of 50 mR up to 100 R, and in steps of 500 mR up to 1000 R. Data printout, including the coded dosimeter number, is done by means of either a typewriter or a tape puncher so that further processing of the measured values by a computer will be possible. The use of a gas-tight sealing protects the glass from dirt and dust so that the cleaning procedure becomes unnecessary.

The light output of the UV lamp is stabilized by a compensation circuit. After each measuring cycle the photomultiplier sensitivity is corrected automatically by means of a calibration glass. Thus any long time drift effects are eliminated.

The system will evaluate 200 dosimeters per hour with an error of less than 5% + 50 mR.

1. Present Stand

1.1 Application of RPL-Dosimetry

Phosphate glasses useful in routine personnel dosimetry are available since nearly 10 years by nov. The properties of the glasses and their behaviour under various conditions have been thoroughly studied during this period [1,2,3]. Nowadays glass dosimeters rank among the most accurate and reliable personnel dosimeters.

Nevertheless they have met with relatively little favourable reception in routine dosimetry. Only in Japan, France and particularly in Germany where the energy compensation filter, that is essential for energy independent and direction independent dose measurement, had also been developed, the first endeavours were to be noticed in the early sixties to replace the film dosimeter method which is likely to give erroneous results by a glass dosimeter system, especially in the field of nuclear research and engineering. Here the spherical casing according to PIESCH has been greatly successful, which in the meantime has even been improved by the Japanese[5]. Nearly 15000 pieces of this kind of dosimeters have hitherto been manufactured. Even for the international comparison measurements of the IAEA[6], this system is being used.

In other countries, on the other hand, more attention was paid to the development of thermoluminescense, particularly as this promised a higher measuring sensitivity and better properties for the detection of low-energy quantum radiation.

The commercial availability of thermoluminescent dosimeters and related evaluation equipment is accordingly remarkably broader and more sophisticated than what is the case in glass dosimetry. This can certainly be reasoned by the fact that the principal field of application of thermoluminescent dosimetry does not lie so much in personnel dosimetry, but in the region of medical and biological dosimetry for research purposes.

1.2 Evaluation Equipment

While there are equally a good number of diverse dosimeters and evaluation equipment available with phosphate glasses for accident dosimetry, namely for the dose range above approx. 0,5 R, which will not be discussed here in detail, in actual practice there is only a single manufacturer for evaluation equipment in the lower dose range above approx. 50 mR, as they are required in routine dosimetry. In any case, however, the glasses can be measured only one by one and manually. The resulting cumbersomeness in evaluation with these instruments might as well be one reason why glass dosimeters are not particularly favoured in the routine dosimetry, for here it resolves itself into a question of time and work saving processing of a few thousands of dosimeters without causing

any reading and transmitting errors by it. The development of an automatic evaluation equipment could therefore significantly contribute in creating the essential technical conditions for the application of phosphate glasses in routine personnel dosimetry and ensuring a widespread use that they should receive by virtue of their other favourable properties.

1.3 Energy Range

But even with this, the facility to detect such low energy radiation as they are encountered in personnel monitoring in the field of radiology is yet missing. This is peculiarly important for the particular reason that a majority of people who fall under official personnel monitoring are employed in this field.

Due to the inherent high energy dependence of the useful phosphate glasses this problem could not so far be overcome through energy filtering in a single glass. Lithium-boron-glasses offer rather better properties, but are mechanically too delicate and moreover hydroscopic to play any role in practical application. The assessment of depth dose distribution in glass[7] is still too complicated for routine operation.

In the nuclear research centre at Karlsruhe already in 1964 a system was developed which is based on the difference measurement with two glasses with different filters. In the meantime such dosimeters seem to be supplied commercially from Japan[8]. As in all multifilter systems (also for film dosimeter) the direction dependence plays a dominant role relating to the measuring accuracy. However, there is good chance for practical application if it becomes possible to automate evaluation process and likewise the computation connected with difference formation.

A newly developed dosimeter system which takes account of these considerations will be described in the following.

2. The new Dosimeter System with Automatic Evaluation

2.1 Object

The following were the objectives set in the development of the evaluation equipment.

1) The evaluation is done automatically. It means that it should be possible to insert a definite number of dosimeters into the instrument in a single operation and to obtain as result, independent of the sequence of insertation, a printed or stored pair of figures for each dosimeter which contains the dose value and the dosimeter marking.

2) The measured dosimeters must leave the instrument in working or dispatchable condition.

3) The dosimeter must be sealed dust-tight so that the washing can be omitted.

4) The measuring instrument must permit a routine long-time operation reliably, without any need for recalibration. Facility for calibrations or stabilizations that may eventually become necessary, must be provided for in the control system.

5) The measuring range must cover the entire dose range required by the dosimeter without any change-over operation.

6) Feasibility to extend the useful energy range as far down as possible that the system can also find application in personnel dosimetry in the field of radiology.

It was quite evident right at the beginning of the development that all these requirements could only then be fulfilled if the evaluation equipment and the dosimeter are considered as an integral, mutually balanced system. The evaluation equipment in its present form cannot therefore measure any desired glasses, but form an integral functional unit with the related dosimeters.

2.2 Description of the System

2.2.1 Dosimeter (Fig. 1)

The dosimeter has the designation FH 38 B. In its mechanical construction it resembles somewhat the film badge quite customarily used in the Federal Republic of Germany. It has, however, only half the size. A glass base with a phosphate glass having the dimensions 14 mm dia x 1,5 mm, hermetically sealed in a plastic bag by welding forms the unit which corresponds to the film. The glass base has bore-holes for coding the 7-digit dosimeter reference number. The plastic bag lies in a dosimeter casing equipped with energy dependent correction filters. The outer dimensions of the dosimeter are 46 mm x 32 mm x 6 mm and its weight is 15 gms. The glass base is an aluminium plate 22 mm x 32 mm large and 2 mm thick with a 14 mm dia cavity for receiving the phosphate glass and a 10 mm wide illumination window. The boreholes on the glass base permit the marking of the dosimeter with a 7-digit number. This number is moreover decoded and engraved on the glass base. The glass base is beveled on one side in order to avoid wrong arrangement in the magazine.

The metaphosphate glass of Messrs. Schott & Gen. is 14 mm dia x 15 mm large, has polished edges and a polished phase. It is firmly fixed to the glass base so that an unequivocal allocation of glass and coding warranted.

The glass base together with the phosphate glass is sealed in a plastic bag by welding. The actual dosimeter casing has

a suitable opening for receiving the plastic bag which ensures a proper adjustment of the phosphate glass with respect to the correction filter incorporated in the casing.

The filters are 0,65 mm thick lead discs with 4 mm dia holes. The dosimeter casing is closed with a self-locking slide which has likewise a correction filter of the same size. Moreover an observation window in the slide permits to check the dosimeter reference number. The dosimeter casing is also marked with the name and dosimeter reference number of the user.

2.2.2 Automatic Measuring Equipment

The measuring equipment has the designation FHT 380 B (Fig. 2). It comprises an inserting device, a tempering furnace, an evaluation apparatus with decoder measuring chamber and data output as well as the packaging device for the measured dosimeters.

The block diagram (Fig. 3) shows the functional relationship between the various units as well as their fundamental functions.

The insertion of the dosimeter is done from the magazine which is sent into the instrument by means of the insertion device. The magazine has a holding capacity of 150 dosimeters. The dosimeter is conveyed from the magazine to the measuring chamber (Fig. 4) for evaluation. There it is placed between two photomultipliers (EMI 9524) and is stimulated by ultra-violet light from one side. One of the photomultipliers measures the luminescence radiation of the entire glass, namely the filtered and unfiltered components. Solely with this measured value the dose in the energy range above 40 keV can be assessed. For extending the measuring range down to 15 keV the second photomultiplier is additionally used, which measures only the luminescence component of the unfiltered glass volume and its output current is combined in a suitable way with that of the first photomultiplier.

The respective doses will be displayed in luminous digits and simultaneously printed on the IBM-typewriter together with the dosimeter reference number. The measuring range reaches from 0 - 100 R in steps of 50 mR and from 100-1000 R in steps of 500 mR. Dose values higher than a preselected value will be printed in red.

2.2.3 Stabilization

The instrument is automatically stabilized in two ways. In one, a photoelectric cell which is installed in the incident radiation path of the ultra-violet light regulates a control system which fully compensates by itself UV-light fluctuations of $\pm$ 30%. Besides the photomultiplier gain will be

$U_{RÖ}$	Combination filter			E_{eff}	
kV	mm Pb	mm Cu	mm Al	keV	
29	0	0	0,3	13	
43	0	0	0,6	18	Dermopan
50	0	0	1,0	22	
50	0	0	0	25	
50	0	0	5,0	33	
60	0	0,2	2,0	38	
70	0	0,4	2,0	46	
80	0	0,7	2,0	55	+ 2,0 mm inherent filteration of Al
100	0	2,0	2,0	72	
150	0	7,0	2,0	113	
220	1,2	5,0	2,0	170	
300	3,5	5,0	2,0	245	

Figure 5, curve b, shows the result of the measurement of the entire glass volume with the first photomultiplier. An energy dependence of ± 20% between 35 keV and 2 MeV is achieved.

For the measurement with the second photomultiplier which "sees" only the glass volume that has received the unfiltered radiation (4 mm dia hole), the energy dependence shown in the curve a is obtained.

By combining both measured values using the equation

$$\left[10_a - 20\ (a-b)\right] + b = c \qquad \text{(positive bracket values only)}$$

an energy dependence within ± 20% in the measuring range up to 15 keV (cirve c) is achieved.

Because of the unsymmetrical construction of the dosimeters, its dose sensitivity is direction dependent. The direction dependence is also energy dependent due to the different filteration in diverse directions of incident radiation (Fig. 6).

The control circuit, in combination with the repeated recalibration by means of the built-in reference-glass, renders it possible to evaluate the dosimeter with an instrument error which is less than ± 5% + 50 mR up to 100 R and ± 5% + 500 mR up to 1000 R, as long as only the energy range above 35 keV is evaluated.

In lower energy range the measuring accuracy is slightly worse due to the difference formation of two measured values, of which one in addition to that has to be provided with a large factor. Under extreme conditions the error may go up to ± 10% + 1 R.

automatically controlled after each measurement with the aid of a calibration glass and readjusted whenever necessary.

2.3 Evaluation Process

The dosimeters are inserted into the instrument one by one. The inserting device opens the plastic bag, draws out the dosimeter and stacks it in a magazine with a holding capacity of 150 dosimeters.

Now it must be decided whether the magazine should first be sent to the tempering furnace or directly to the evaluation chamber.

The tempering including heating and cooling takes an hour (20 min at 115°C). If the doses are below 100 R tempering of the dosimeters is essential only if the period between exposure and evaluation is less than a few hours. For higher doses tempering must always be carried out. In actual practice the dosimeters which show higher doses will therefore be sorted out after the first evaluation, tempered, and then evaluated again.

After the magazine is inserted into the evaluation apparatus, the dosimeters will be drawn out from the magazine automatically one by one, the code number decoded and printed, the dose evaluated and printed, and finally the dosimeters are sealed again in plastic bags by welding. After this the dosimeters of a magazine will leave the instrument as a continuous band.

The various devices for the evaluation of the dosimeters are arranged in the instrument in such a way that they can be operated by an operator in sitting position. The evaluation instrument has the height of a typewriter table (68 cm) in order to permit comfortable working as far as possible. The operator has enough space for his legs so that he can sit right in front of the instrument. Altogether the equipment is 91 cms wide and 70 cms deep.

3. Energy Dependence and Measuring Accuracy

The energy dependence of the dosimeter has been studied with hard filtered X-rays of various energies in the energy range of 15 keV to 1,2 MeV. The Stabilipan- and Dermopan-instruments of Messrs. Siemens have been used for this purpose with the following combination filters.

4. Working Procedure in Routine Dosimetry

The Central Evaluation Laboratory receives the glass bases sealed in plastic bags (without dosimeter casing) from the dosimeter user. These are arranged in containers, separate for each sender, for ready evaluation. The evaluation can be done by a skilled worker.

The dosimeters of a particular sender are arranged in the respective magazine and his address is marked with the corresponding magazine number. Moreover the address of the sender is written at the top of the report sheet which receives all the evaluation results of the dosimeters arranged in a magazine, with an IBM-typewriter before the evaluation.

When all the dosimeters have been evaluated the sealed dosimeters will be cut off from the band foil and packed together with the evaluation report.

The working time including all extra work for the evaluation of 200 dosimeters is approx. 1 hour. In detail the working time will be as shown below. Here an unfavourable case has been selected where 20 magazines each with 10 dosimeters come for evaluation.

Extra work		Automatic evaluation	
Unpacking	10 min	Evaluation	60 min
Arranging	20 min		
Change of magazine	2 min		
Writing address	10 min		
Cutting off dosimeters	10 min		
Packing	10 min		
	62 min		60 min

When tempering is required, an additional time of 1 hour per magazine will be needed. Complete evaluation time for one single dosimeter is about one minute.

This work has been supported by the Bayerisches Staatsministerium für Wirtschaft und Verkehr. The Authors wish to acknowledge this gratefully.

Bibliography

1 R. Maushart, E. Piesch, RPL Glass Dosimeters, in IAEA Technical Report Series No. 109, Wien 1970

2 E. Piesch, Developments in RPL Dosimetry, in Progress in Radiation Dosimetry, Pergamon Press New York, in print

3 J.F. Fowler, F.H. Attix, Solid State Integrating Dosimeters in Radiation Dosimetry Vol. II, New-York 1966

4 R. Maushart, E. Piesch, Phosphate Glass Dosimetry in Nuclear Installations, Prov. Int. Symp. Luminescence Dosimetry, Stanford 1965

5 R. Yokota, Y. Muto, J. Maoi, S. Nishijima (1969): Some improvements on spherical capsule type glass dosimeter. J. nucl. Sci. Technol. 6,46

6 G.A. Dorofeev, S. Somasundaram (1971): IAEA International Glass Dosimetry Intercomparison Experiment. 1970, Proc. Symp. on new development in Physics and Biological Radiation Detectors, IAEA Vienna

7 H. Kiefer, E. Piesch, 2nd Int. Congress of IRPA, Brighton 1970

8 Toshiba Catalogue

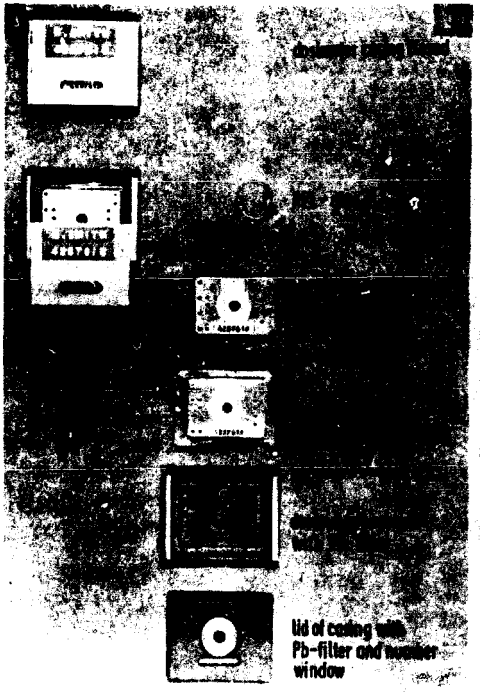

Fig. 1 The Dosimeter Arrangement

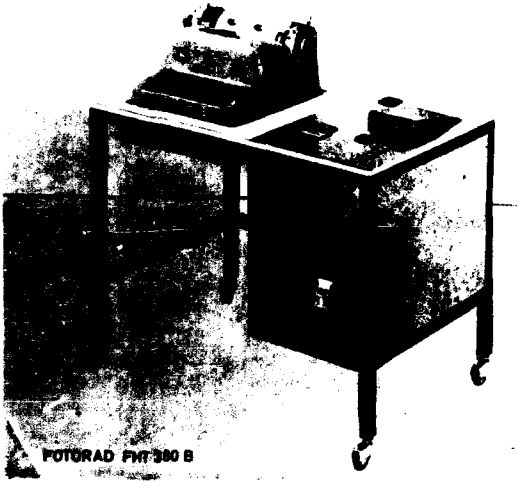

Fig. 2 The Dosimeter Reading Device

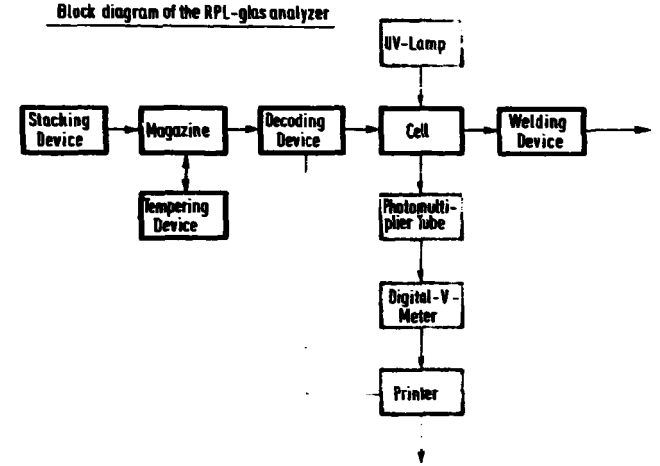

Fig. 3 Block Diagram of Evaluation System

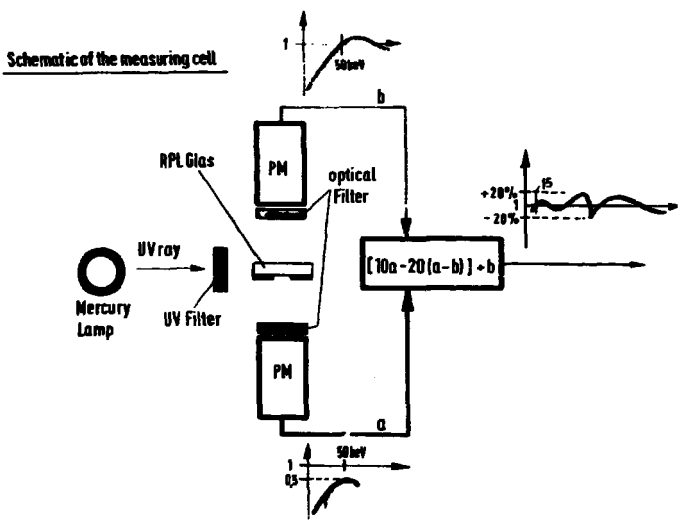

Fig. 4 Block Diagram of Measuring Arrangement

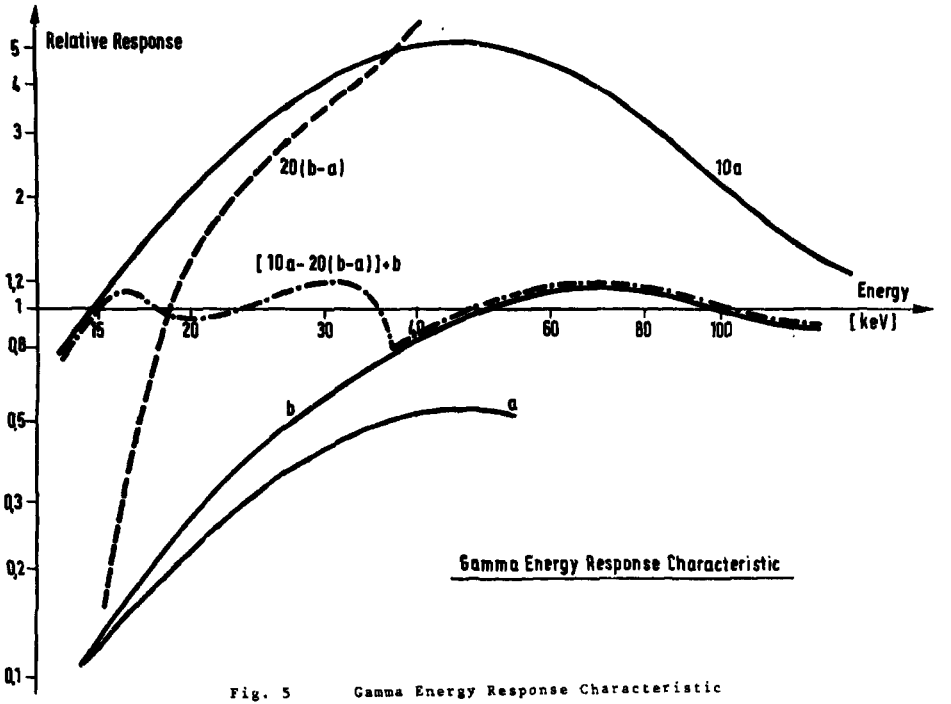

Fig. 5 Gamma Energy Response Characteristic

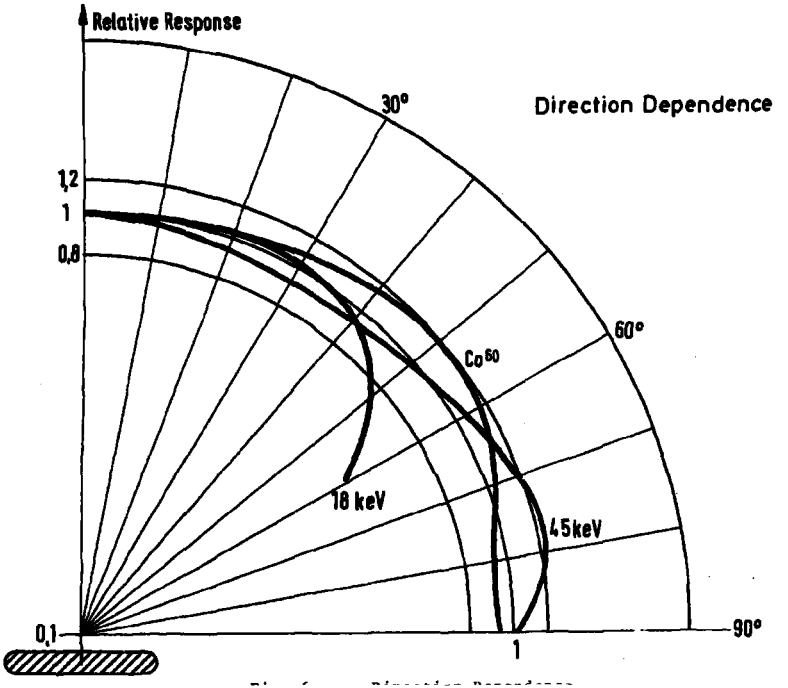
Relative Response
30°
Direction Dependence
1,2
1
0,8
60°
Co 60
18 keV
45keV
0,1
1
90°

Attix

What type of glass do you use? Is it Toshiba, or if not, is it similar to one of the Toshiba glasses in characteristics?

Becker

The glass is produced by Jenaer Glaswerke Schott, Mainz Germany. It is similar, but not identical in composition and properties to the FD-3 glass. For the exact composition, which I do not recall right now, please contact Dr. Jahn at Schott/Mainz.

Regulla

Can you tell me in what energy range your impressive lower limit of detection (50 mR) is valid?

Dade

Above 45 keV.

Naba

For personnel dosimetry beta measurement is necessary. What do you think of beta measurement by fluoroglass in this automatic system?

Maushart

Beta radiation will not be measured in this system.

Naba

Concerning fluoroglass dosimetry, the most important problem for the accuracy is washing for the purpose of elimination of extra luminescence caused by dust, touch of fingers, etc. How can you wash the glasses after irradiation with the automatic system?

Maushart

By automatic opening and sealing again of the plastic foil wrapper the glass is fully protected against dust and dirt so washing will become unnecessary.

New Type of High-Sensitive and Soil-Insensitive RPL Glass Dosimetry

by

R. Yokota, Y. Muto, Y. Koshiro and H. Sugawara

Toshiba Research and Development Center
Tokyo Shibaura Electric Co., Ltd.
Komukai, Kawasaki, Japan

Abstract

The 'predose' of RPL glass dosimetry limits the sensitivity, and the soil on glass surface must be cleaned thoroughly.

The decay time for the visible luminescence, which is a measure of the absorbed dose, is ten times longer than the decay times of both the unexposed low-Z silver-activated phosphate glass and the organic contamination.

By using low cost ultra-violet N_2 gas laser, this principle was materialized experimentally and the exposure dose of 1 mR can be measured by the new pulse technique, where the fluctuation of the output of the laser is cancelled.

Introduction

The low-Z silver-activated phosphate glass dosimeter[1] has the basic advantage — the permanence of the radiation effect which permits an unlimited remeasurement and intermittent measurement during long time dose integration and has the uniform sensitivity and the capability of the incident energy and direction with the scanning method.[2][3]

The predose of RPL glass dosimeter limits the sensitivity and the soil on glass surface must be cleaned thoroughly in order to measure the low dose accurately.

Kastner et al[4] discovered the phenomenon that the decay time for RPL is 3.0 μsec which is ten times longer than the decay times of the unexposed dosimeter glass. He used the 3472 Å UV pulse derived from a ruby laser by frequency doubling. This was a proof-of-principle experiment. Later, Kastner et al[5] proposed several measuring methods based on this phenomenon for obtaining the practical measuring systems, but no methods have been succeeded to measure as low as 1 mR.

UV pulse by N_2 gas laser is noticed by us and the measurement of 1 mR of ^{60}Co γ-rays has been succeeded with FD-3 ($8 \times 8 \times 4.7 mm^3$) dosimeter glass.

Experimental Procedure

After trying several methods including KDP electro-optical shutter, finally we succeeded with the use of 3371 Å UV pulse generated by N_2 gas laser. The pulse duration is 15 nsec, and peak power is about 5 kW. N_2 gas pressure is 6 Torr. Both ends of laser tube have silica glass window with Brewster angle.

The power source is relatively simple and cheap. By triggering spark gap which is sealed in glass bulb filled with one atmosphere of N_2 gas, the stored energy in coaxial cable excites N_2 gas and the UV laser pulse is generated.

One part (about 7 %) of the UV pulse is reflected by silica glass plate and goes to the monitoring photomultiplier, and the remaining part of UV pulse passes the silica glass and excites the RPL dosimeter glass.

Nd doped glass plate and orange glass filter are located in front of the monitoring photomultiplier, and UV cut-off filter and orange filter are located in front of the measuring photomultiplier. Both photo multipliers have multi-alkali photo-cathode. In this case, the luminescence decay time constant of Nd glass is about 20 μsec. The output by the monitoring photomultiplier after passing the preamplifier operates the Schmitt circuit and generates the electric pulse which acts as the time standard.

Then, by the circuit determining the delay time and sampling gate time, the sampling gate circuit is opened and the sampled part of the luminescence of Nd glass is stored in the integrator. For the measuring photomultiplier, after passing the different delay time and the same sampling gate time circuit, the one part of RPL luminescence by opening the sample gate circuit is stored in another integrator.

The voltage ratio of dosimeter glass to monitor is indicated by the meter, by which the fluctuation of the output of UV pulse is cancelled. The block diagram of the measuring system is shown in Figure 1.

The luminescence decay curve of FD-3 glass obtained by memory synchroscope is shown in Figure 2. The reference glass is used as the calibration of the reader.

Thus, we have been able to measure 1 mR of ^{60}Co γ-rays. When the measuring photomultiplier is cooled down to -20°C by the electrical means, we have been able to detect 0.2 mR. The input pulse and sampling relation is shown in Figure 3, where T_d and T_s are the time of delay and sampling, respectively, and m and g represent 'monitoring' and 'dosimeter glass', respectively. In this experiment, we adopt the following values:

$T_{d,m} = 0.4$ μsec, $T_{s,m} = 1.5$ μsec; $T_{d,g} = 5$ μsec, $T_{s,g} = 1.5$ μsec.

The photographs of the electric part, the outer appearance of the optical part, and the N_2 gas laser and the power source are shown in Figures 4, 5 and 6, respectively.

The sensitivity of the reader is changed by tne gain of the linear amplifier and the optical filter insertion in front of the dosimeter glass.

The dosimeter glasses are FD-3 and FD-7 ($8 \times 8 \times 4.7$ mm^3) where FD-7 glass has 1.62 times higher sensitivity and one-third lower energy dependence than FD-3 glass which has been used now. Both FD-3 and FD-7 glasses have the same luminescence decay curves and therefore have the same decay time constant of 3.2 μsec.

The predose luminescence decay time constant is one-tenth of RPL's. The decay time constants of oil and soil by the finger touching are less than that of the predose.

Consequently, this new measuring method has the characteristics of soil insensitivity as far as the attenuation of UV pulse by the soil is negligibly small. This means that the careful washing of glass is unnecessarily.

The composition of the dosimeter glass and the energy response are given[6] in Table 1 and Figure 7, respectively.

Table I

Glass No.	Composition (wt %)					
	Na	Li	P	O	Al	Ag
FD-7	11.0	—	31.55	51.16	6.12	0.17
FD-3	—	3.58	34.53	53.51	5.11	3.27

Discussions and Conclusions

The present success has been achieved only experimentally. In order to be used widely, the following two problems must be achieved.
— The miniaturization of N_2 gas laser and its power source.
— The refinement and simplification of the electric part.

These problems are being achieved steadily, and we have the conviction that they will be solved within two years.

The wavelength of N_2 gas laser, that is, 3371 Å is especially suitable to excite the RPL dosimeter glass, because the absorption of RPL centers at 3371 Å is very high.[7]

The electronic disturbance due to the laser excitation does not affect the measurement, because in our measuring system the sampling measurement of luminescence for both Nd glass and dosimeter glass is performed after decay of disturbance with very short duration period.

In conclusion, the N_2 gas laser excitation is very suitable for our measuring system, and 1 mR can be measured, being separated from the predose and soil contamination effect, experimentally. This measuring system is considered to be less expensive than those of Kastner et al.

References

1) R. Yokota, S. Nakajima, E. Sakai, Health Phys. 5, 219 (1961).

2) H. Kiefer und E. Piesch, Direct Information 10/67, in: Atompraxis, Heft 11/12, (1967).

3) H. Kiefer und E. Piesch, Atompraxis, Heft 2, (1969).

4) J. Kastner, D. Eggeberger, A. Longnecker, D. King and D. Scott, Proc. IAEA Symp. Solid-State and Chemical Dosimetry, Vienna, 115 (1967)

5) J. Kastner, R. K. Langs, B. A. Cameron, M. Paesler and G. Anderson, Proc. 2nd Int. Conf. Lum. Dosimetry, Gatlinburg, 670 (1968).

6) R. Yokota, Y. Muto, J. Naoi and I. Yamaji, Health Phys. 20, 662 (1971).

7) R. Yokota and H. Imagawa, J. Phys. Soc. Japan 23, 1038-1048 (1967).

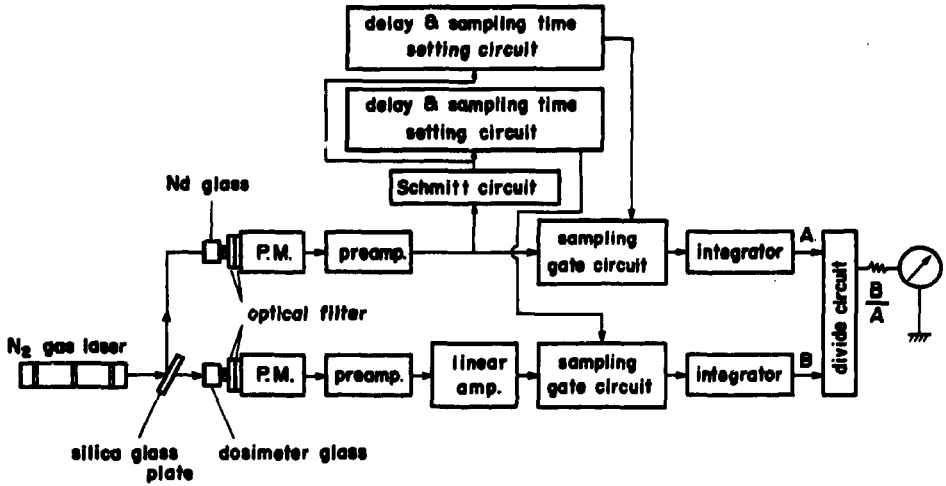

Figure 1. Block diagram of the present measuring system.

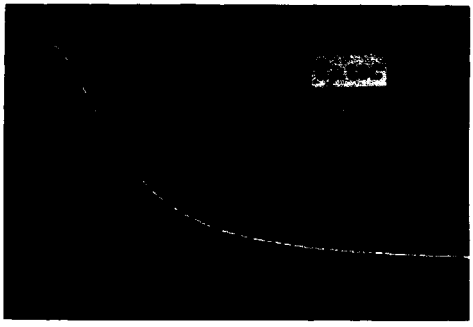

Figure 2. Luminescence decay curve of FD-3 glass.

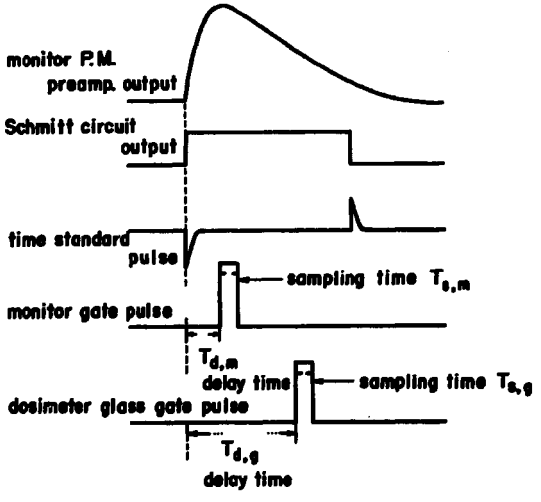

Figure 3. Time relation between input pulse and sampling pulse.

Figure 4. Photograph of the electric part.

Figure 5. Photograph of the outer appearance of the optical part.

Figure 6. Photograph of N_2 gas laser and its power source.

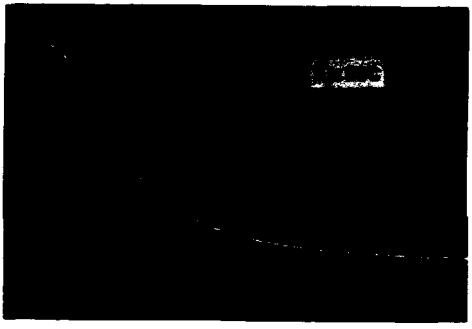

Figure 2. Luminescence decay curve of FD-3 glass.

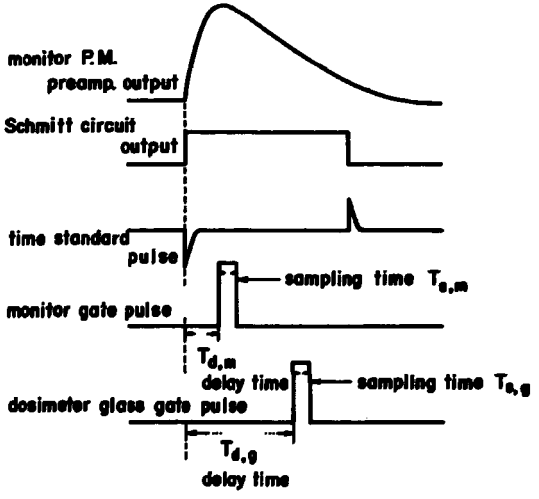

Figure 3. Time relation between input pulse and sampling pulse.

Figure 4. Photograph of the electric part.

Figure 5. Photograph of the outer appearance of the optical part.

Figure 6. Photograph of N_2 gas laser and its power source.

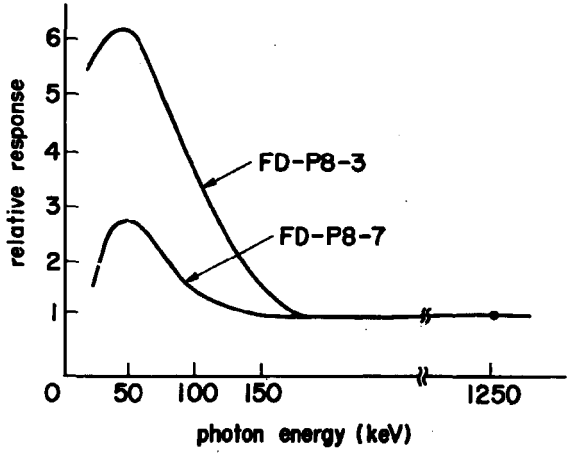

Figure 7. Energy response of FD-3 and FD-7 ($8 \times 8 \times 4.7 mm^3$) glasses.

Table I Glass compositions of FD-3 and FD-7 used in this experiment.

glass No.	composition (wt%)					
	Na	Li	P	O	Al	Ag
FD-3	11.00	—	31.55	51.16	6.12	3.27
FD-7	—	3.58	34.53	53.51	5.11	0.17

Herrmann

What magnitude of dirt effect is it possible to discriminate against by this method? Can you detect mR doses with glasses which would give above 1 R dirt effect on conventional readers?

Becker

According to Dr. Yokota's paper, surface contamination only interferes if it results in a significant absorption of either the existing UV or the emitted RPL light.

Laser Pulse Excitation of Radiation Induced Photoluminescence in Silver-Activated Phosphate Glasses

F. Hillenkamp and D. F. Regulla

Abteilung für Kohärente Optik and

Institut für Strahlenschutz

Gesellschaft für Strahlen- und Umweltforschung mbH. München,
D-8042 Neuherberg, W. Germany

Abstract

The detection of small doses of ionizing radiation with phosphate glass detectors is limited by the "predose fluorescence" exhibited by the non-exposed glasses under DC UV-excitation. Several authors have recently reported on the possibility of discriminating the pre-irradiation from the post-irradiation fluorescence through their different time decay constants after pulse excitation. This has stimulated interest in the laser excitation of the glass dosimeters.

Glass cubes of four different manufacturers (Toshiba, Schott, Leitz, CEC) have been excited with frequency doubled, Q-switched ruby-laser pulses (λ = 347 mm, texc=2. 10^{-8} s). A specially designed sample holder and detection head and the use of highly discriminating UV filters completely eliminated laser and other background light. This, along with a very careful cleaning procedure of the glasses allowed the observation of the complete fluorescence pulse including the first few hundred nanoseconds as distinguished from the results reported by others.

The measurement of doses as small as 10 mR is demonstrated and a dose-effect curve for the range of 50 mR - 2R is shown. As compared to the DC evaluation of glass dosimeters the laser pulse evaluation leads to a much less detrimental effect of the regeneration cycles on the non-radiation induced predose. The time decay of the fluorescence of the various glasses is discussed and it is concluded, that an approximation of the decay curve by two or more exponential functions does not as yet render any better insight into the processes involved.

Introduction

The detection of small doses of ionizing radiation with phosphate glass detectors is limited by the "predose fluorescence" exhibited by the non-exposed glasses under DC UV-excitation. Several authors (J. KASTNER et al.[1,2], J. P. BACIOTTI et al.[3] and J. BARTHE et al.[4]) have recently reported on the possibility of discriminating the pre-irradiation from the post-irradiation fluorescence through their different time decay constants after pulse excitation. This has stimulated interest in the laser excitation of the glass dosimeters.

Experimental Setup

We have conducted experiments of this type with the experimental set-up shown in Fig. 1. The light of a ruby laser, Q-switched with a Pockels cell (PC), is frequency doubled by a nonlinear KDP crystal (FD). The resulting light pulses have a wavelenght of 347 nm and a width of about 20 ns. Because of the extremely hight intensity available, these pulses produce a strong fluorescence in the glasses visible even with the naked eye, despite of the fact, that the wavelenght is rather in the wing of the excitation. The filter F_1 suppresses the remaining red light by app. 150 db relative to the transmitted UV light. Through the stop FS a 2 x 6 mm field of the front surface of the 8 x 8 x 4.7 mm glasses is illuminated. The laser light transmitted through the glass P is diffusely reflected by a MgO block onto a fast ITT F-4000 vacuum photodiode (PD). The fluorescing field of the glass P is imaged by the lens L onto the photocathode of a EMI 9558 type photomultiplier (PM).

With the extremely short, very high intensity excitation light pulses used, the stray and scattered light is a major problem; moreover, the fluorescence produced by this scattered light in usual UV absorption filters and the optics severely interferes with the radiation induced fluorescence from the phosphate glass. With the specially designed filter F_2 we were able to reduce these signals to a level small compared even to the RPL of only a few mR's. Along with this, a very careful cleaning procedure of the glasses allowed us to register the total fluorescence signal including the first few hundred nanoseconds following the laser pulse without saturating the multiplier

or the electronics. The Filter F_3 has a sharp edge at 570 nm, transmitting only the red part of the RPL.

The electrical signal from the laser detector PD is integrated by the electronic circuit J with a time constant of 75 ns, and then applied to a single trace fast oscilloscope (O). The fluorescence from the multiplier is electronically delayed (D) by 150 ns and then added to the laser signal.

Results and Discussion

Fig. 2 shows oscilloscope traces for three glasses: a nonexposed one, one exposed to 200 mR and one to 2R. The height of the first peak is a measure of the incident laser pulse energy and is used to normalize the fluorescence signal. This laser signal has almost decayed to zero, before the fluorescence signal sets in 150 ns later. The second sharp peak originates from glass fluorescence and corresponds to the "predose" measured with the usual DC excitation, though no quantitative relationship of this value to the predose measured with a Toshiba Fluoro-Glass Dosimeter FGD-6 could be found. The time dependence of this fast fluorescence was not resolved by our multiplier with a bandwidth of about 0 - 10 MHz, but we intend to use a faster detector in future experiments. Despite of the fact, that even with a larger number of cleaning cycles and/or a more elaborated cleaning procedure this peak could not be made smaller than shown it is quite likely that this fluorescence is due entirely to surface contaminations. In virgin glasses and ones which have gone through as many as 10 irradiation-regeneration cycles no "predose fluorescence" with a decay constant comparable to that of RPL was found. For the exposed glasses, the signal 1 μs after the onset of the fluorescence was taken as measure of the applied dose.

Fig. 3 shows a dose-effect curve for Toshiba and Schott glasses. Each value is the average of nine measurements (3 shots for 3 individual glasses of each manufacturer). The glasses were regenerated after each exposure and then exposed to the next higher dose. These regenerations did not affect the fluorescence at 1 μs. When evaluated with DC excitation on the contrary, the "predose" to be subtracted from the dose reading increased significantly with increasing

number of irradiation-regeneration cycles. This observation must be attributed to the sharp excitation wavelenght of the laser at 347 nm as compared to a rather broad excitation band around 365 nm in the FGD-6 reader; the wavelength band selected in the emission path was very nearly identical for both methods.

This seems to make the laser pulse excitation quite superior to the DC excitation method particularly for the repeated measurements of small doses. The reproducibility of the values is relatively poor so far. Even for a single glass and equal laser energy the observed fluctuation of the fluorescence signal was up to $\pm$ 15 %. Most likely these fluctuations originate from the varying energy distribution over the laserbeam cross section from shot to shot together with the rather severe optical inhomogeneities of the glasses. This, however, must be verified by future experiments.

Fig. 4 shows time decay curves for glasses of the manufacturers Toshiba, Schott, Leitz and CEC normalized to the same value at 0.5 μsec. Whereas the Toshiba, Schott and Leitz glasses show identical behaviour within the measurement accuracy, the CEC glass differs markedly from these, exhibiting a much slower decay. For the Toshiba and Schott glasses we did not observe any significant influence of the applied dose or the number of preceding irradiation - regeneration cycles on the time decay behaviour. The Leitz and CEC glasses were not virgin and as yet we have no data on their behaviour in this respect. In the semi-log diagram the decay curves show a rather continuous bending toward longer time - constants with increasing time. We hope, that the analysis of these curves will eventually help to better understand the processes involved. However, we do not feel that the approximation of these curves by two or more straight lines, as attempted by other authors helps very much, because these different components cannot as yet be correlated to specific fluorescence centers.

Fig. 5 is a demonstration for the capability of the method for the measurement of doses as small as 10 mR. Because of the increased laser intensity applied at this experiment, a somewhat higher background signal even at

times beyond 0.5 μsec is apparent for the unexposed glass, but the increase in fluorescence after irradiation remains striking. It seems then, that the lower limit of doses detectable with glass dosimeters is not set by the sensitivity of the measurement procedure, but is rather a function of the stability of the individual glass cubes and the reproducibility from sample to sample. Large scale experiments over an extended period of time are necessary to further clarify this point. The full details of our experiments will be published elsewhere.

References

1. J. KASTNER, G. EGGENBERGER and A. LONGECKER, Proc. IAEA Symp. on Solid State and Chemical Radiation Dosimetry in Medicine and Biology, Vienna, October 3 - 7, 1966

2. J. KASTNER, M. PAELSLER and R. K. LANGS, Proc. Symp. Micro-dosimetry, Euratom, ISPRA, November 1967

3. J. P. BACIOTTI, D. BLANC, J. L. TEYSSIER, H. FRANCOIS and G. SOUDAIN, Nucl. Instr. Meth. 50, 93 (1967)

4. J. BARTHE, D. BLANC, L. COMMANAY, J. L. TEYSSIER, Hlth. Phys. 18, 573 (1970)

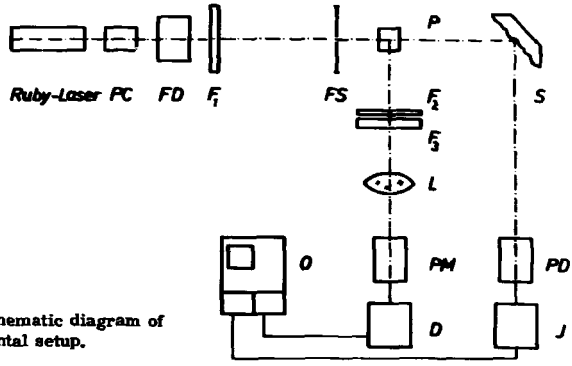

Fig. 1: Schematic diagram of experimental setup.

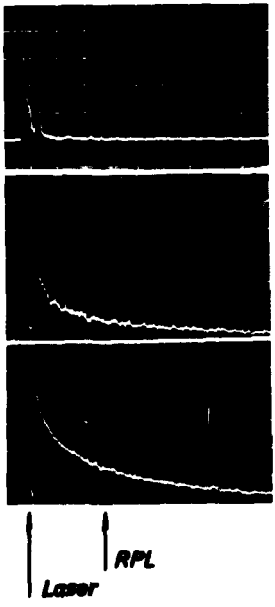

Fig. 2: Time decay of RPL (Toshiba Glass).

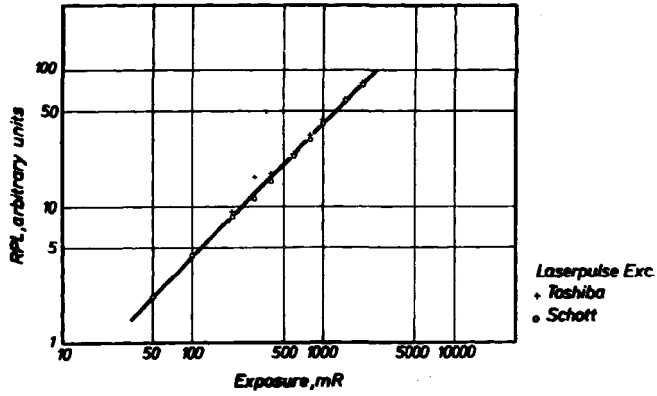

Fig. 3: Dose-effect curve for glasses regenerated after each exposure.

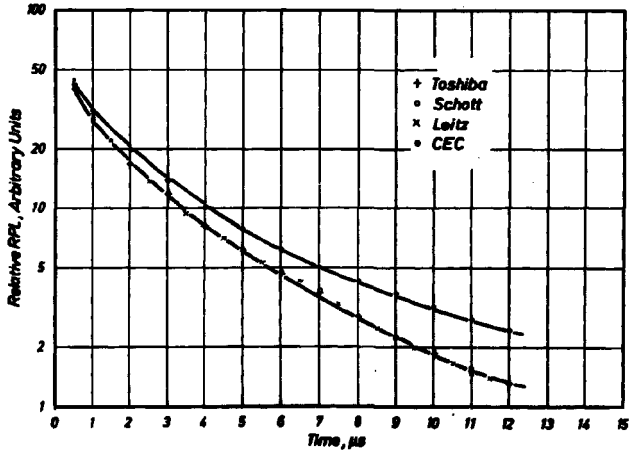

Fig. 4: Semi-log representation of time decay curves of RPL (Exposure: 2R).

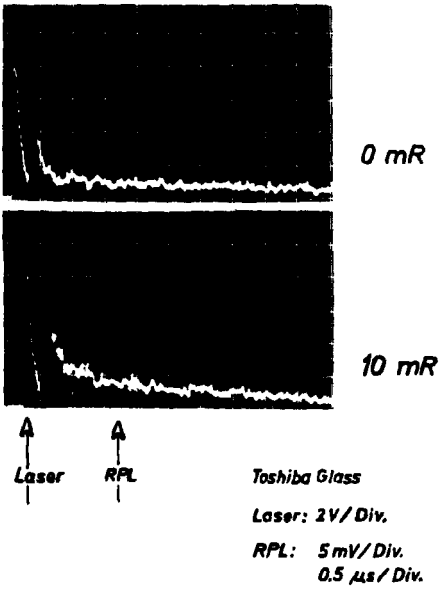

Fig. 5: Luminescence decay curve before and after a 10 mR exposure.

Becker

There have been claims by Yokota et al. that with a conventional reader doses as low as 10 mR can be measured. Do you feel that the relatively small gain which appears to be possible by pulsed excitation justifies substantial efforts in this area from the practical point of view?

Hillenkamp

Yes, we do if one sets out to measure doses below about 1 R. It has been shown by other authors, and it is our experience also with the FGD-6, that the standard error of single measurements below 1 R increases rapidly to at least a value of about 10% at a 100 mR reading. Because this is essentially a random error, we do not believe that measured doses of 10 mR obtained as the difference between two readings around 100 mR have any reliability. We are sure that the range of the laser evaluation methods can be extended to at least 1 mR if the random errors caused by the glasses themselves can be made sufficiently small.

Moran

In studying the decay curve of the fluorescence, have you found any dependence upon the laser pulse intensity?

Hillenkamp.

No. We have varied the incident laser energy within a range of 1-100 without observing changes in the normalized fluorescence and without the decay variation exceeding the fluctuation within the accuracy of measurement.

The Response of Radiophotoluminescent Glass to ^{60}Co γ- and 10-30 MeV Electron Radiation

by

L. Westerholm and G. Hettinger,

Radiation Physics Department

University of Umeå

S-901 85 Umeå, Sweden.

ABSTRACT

Toshiba RPL-dosimeters (FD-R1-1) and a Toshiba reader (FGD-6) were used in this investigation. A washing procedure was developed which reduces the fluorescence of deliberately soiled glass to values characteristic for unsoiled glass. Stabilization can be performed as long as 2 h after irradiation without altering the fluorescence yield. The dependence of the fluorescence yield on temperature during irradiation was found to be less than ± 0.1 %/°C. A special initial pretreatment (irradiation, repeated heat-treatment with subsequent cooling) was found necessary in order to assure that the sensitivity

of the dosimeters would be independent of the number of regenerations. Such pretreated dosimeters have a precision which is approximately a factor of 2 better than those not pretreated. No correlation between sensitivity and the mass of the glass rod was observed. - The relationship between fluorescence and absorbed dose in the range of 30 to 800 rads could be approximated by a straight line.

Glass dosimeters were absorbed dose-calibrated at different depths in a water phantom which was irradiated with electrons, the incident energy of which was 14, 24 or 31 MeV, or with ^{60}Co γ-radiation. The calibration values were found to be independent of the type of radiation and depth in the phantom.

INTRODUCTION

In the clinical dosimetry of 10-30 MeV electron radiation there is a need for small, energy-independent dosimeters for the study of for example the effect of inhomogeneities on the absorbed dose distribution. The aim of the present study was to investigate the possibility of using glass dosimeters for clinical measurement of absorbed dose in the region of approximately 30 to 1000 rads. The response of the dosimeter has therefore been tested with respect to its regeneration, linearity, dependence on radiation quality, and precision.

APPARATUS

Toshiba RPL dosimeters (FD-R1-1) and a Toshiba reader (FDG-6) were used. The reading instrument was modified by replacing its high-voltage supply with an external high-voltage aggregate and replacing its manual compensation for the current from the photomultiplier by a servosystem with a digital display. Measuring precision was thereby improved by approximately a factor of 2

over the original instrument.

In such investigations in which the radiation quality was expected to be of secondary importance (for example, in the study of stabilization and regeneration), the ^{60}Co-radiation source was used.

WASHING PROCEDURE

The precision of the fluorescence measurements depends strongly upon the cleanliness of the glass surface. With the washing procedure which was devised (Table 1), the fluorescence of delibe: ately soiled glass was reduced to values characteristic of unsoiled glass rods. During the ultrasonic washing, the dosimeters were placed in plexiglass cassettes. No mechanical damage to the dosimeters was observed.

STABILIZATION

After irradiation, the fluorescence increases with time at room temperature, reaches a saturation value after 3 days, and remains within $\pm$ 1 % (S.D.) of that level for at least 80 days (Fig. 1). It is possible to increase the rapidity of fluorescence build-up by warming the dosimeter [1,2]. This stabilization was carried out by immersing the dosimeters in boiling water for ten minutes. The stabilization may be carried out any time during at least the first 2 hours after irradiation and will result in the same fluorescence yield within $\pm$ 1.7 % (S.D.). After stabilization, the fluorescence is approximately 11 % higher than the saturation value for non-stabilized dosimeters. The increase in fluorescence after stabilization was found to be dependent on temperature (+ 0.3 %/°C at 100°). A change in the air pressure of $\pm$ 30 mb gives a change in the boiling point of the water of less than 1°C and therefore alters the

fluorescence yield after stabilization by less than $\pm$ 0.3 %. The temperature during storage before and after stabilization has been maintained at 23 $\pm$ 2°C.

TEMPERATURE DURING IRRADIATION

The dependence of fluorescence yield on temperature during irradiation has been studied in the range of + 25 to + 40°C. The dosimeters were placed in a temperature stabilized bath ($\pm$ 1°C). The dependence was found to be less than $\pm$ 0.1 %/°C. This value is less than those published earlier for dosimeters with the same chemical composition [3,4,5]. The difference might possibly be explained by the fact that, in this study, we used only pretreated dosimeters (see section Regeneration).

REGENERATION

Introduction: Both sensitivity and precision are changed after regeneration [6]. This is due to several factors, among them the regeneration temperature and time and the pretreatment. These factors have received much attention in this investigation.

Time and temperature of regeneration: Dosimeters were irradiated with an exposure of 300 R after which they were heat-treated at 350, 400, 450 or 500°C for 0.2, 0.5, 1, 2 or 3 h. The residual fluorescence is graphically presented in Fig. 2. At 500°C the dosimeters were damaged. At shorter times of regeneration than 1 h, the fluorescence values obtained were not reproducable. Therefore, in all further studies, 450°C and 1 h were the temperature and time of regeneration of choice. Using these parameters, the residual fluorescence is approximately equal to that from non-irradiated dosimeters.

Sensitivity and precision versus number of regenerations: The effect of up to 10 regenerations has been studied for exposures of 150 and 600 R (Fig. 3). The sensitivity, which is defined as the quotient between net fluorescence and exposure decreases after the first few regenerations and thereafter increases to a value which exceeds by approximately 7 % that for unregenerated dosimeters. The difference between extreme values is approximately 12 %. The precision decreases with the number of regenerations.

Initial pretreatment: The variations in sensitivity tend to be stabilized after 7 to 8 regenerations (Fig. 3). The possibility of reducing the variation during the first 6 regenerations by an initial pretreatment has been studied. As a first attempt to such pretreatment, the dosimeters were irradiated with an exposure of 13 kR (^{60}Co-γ), followed by heat-treatment at 450°C for 6 h. Subsequently, the sensitivity was again studied in relation to the number of regenerations. The results showed that the decrease in sensitivity through the 3rd regeneration was eliminated but that the increase in sensitivity through the 6th or 7th regeneration remained. It was therefore determined that pretreatment should also consist of 5 repeated heat-treatments at 450°C for 1 h. After such pretreatment described variations in sensitivity are eliminated (Fig. 4). The precision of the dosimeters was improved by about a factor of 2 by this pretreatment, despite the fact that these dosimeters were exposed to more extensive handling than those which were not pretreated.

As is seen in Fig. 4, the sensitivity values for 150 R and 600 R differ from each other. The proportionality between the net fluorescence and exposure has thus been lost through the pretreatment. If not a proportional but a linear relationship is applied the results in Fig. 5 are obtained. The distance between the extreme values during the first 10 regenerations has now been reduced to 2.5 %.

The effect of the initial pretreatment lasts for at least 6 months. The results for different levels of exposure were the same as

those in Fig. 5 for as many as 20 regenerations.

THE EFFECT OF MASS

The dosimeters used differed in mass by ± 3 % (S.D.). 50 dosimeters which were initially pretreated were divided with respect to mass into 5 groups with 10 dosimeters in each. The average sensitivity for each group during the first two regenerations is presented in Table 2. There is clearly no correlation between sensitivity and mass.

LINEARITY

A comparison of Fig. 3 and Fig. 4 reveals a change in the relationship between net fluorescence and exposure caused by the initial pretreatment. A separate study of linearity was therefore indicated. The results, presented in Fig. 6, show that the relationship between net fluorescence and absorbed dose in water can be approximated by a straight line within the range of 30-800 rads with a precision of ± 1.5 % (S.D.). The established range of linearity is less than that reported by Freytag [7] who worked with dosimeters and reader of the same manufacturer.

Spot checks with glass dosimeters which have been regenerated more than three times show the same region of linearity. The linearity of the reader has continuously been checked by making measurements of quinine-sulphate solutions of different dilution.

DEPENDENCE ON RADIATION QUALITY

Dosimeters were attached to a thin bar of polystyrene to a maximum depth of 16 cm in a water phantom (30 x 30 x 30 cm)

along the central axis of the radiation beam. The phantom was irradiated with ^{60}Co γ-radiation or electrons. The energy of the incident electrons was 14, 24 or 31 MeV. The average electron energy at different depths in the water phantom was estimated by the method given by Harder[8].

The individual glass dosimeters were calibrated against the absorbed dose distribution in the water phantom which was determined using an ionization chamber [9,10,11]. The results of the calibration are given in Table 3. Given limits of error correspond to the expected standard deviation for a single glass dosimeter. The same calibration factor within ± 1.2 % (S.D.) was obtained independent of the type of radiation and depth in the water phantom.

CONCLUSIONS

Initially pretreated dosimeters can for as long as 6 months be irradiated and regenerated up to about 20 times with the same sensitivity. The relationship between net fluorescence and absorbed dose is linear from approximately 30 rads up to 800 rads. Furthermore, the calibration value of the dosimeters is independent of the type of radiation and depth in the water phantom in which they are irradiated.

In the estimation of the precision of a single measurement of absorbed dose, the following sources of uncertainties must be accounted for, stabilization, fluorometer reading, radiation quality, regeneration and linearity. The root mean square uncertainty based on the in Table 4 presented standard deviations was found to be about 3.5 %.

With pretreated dosimeters and a modified reader, sufficiently good precision has been achieved for glass dosimeters to be used in clinical dosimetry.

ACKNOWLEDGEMENTS

This work was supported by grants from the Swedish Cancer Society.

REFERENCES

1. K. Becker, Solid State and Chemical Radiation Dosimetry in Medicine and Biology, IAEA 1967.

2. R. Yokota and H. Imagawa, Journal of the Physical Society of Japan 5, 1038-1048 (1967)

3. H. Kiefer, R. Maushart und E. Piesch, Atompraxis 11, 88-93 (1965).

4. K. Becker, Nukleonik 5, 154-159 (1963).

5. I. Miyanaga and H. Yamamoto, Health Physics 9, 965-972 (1963).

6. D. Regulla, H. Pychlau and F. Wachsmann, Solid State and Chemical Radiation Dosimetry in Medicine and Biology, IAEA 1967.

7. E. Freytag, Health Physics 20, 93-94 (1970).

8. D. Harder, in Symposium on high energy electrons, p. 26. Edited by A. Zuppinger and G. Poretti, Springer Verlag, Berlin 1965.

9. G. Wickman, A digitized unit for precision charge measurements on ionization chambers. To be published.

10. C. Pettersson and G. Hettinger, Acta Radiol. Ther. Phys. Biol. 6, 160-176 (1966).

11. H. Svensson and C. Pettersson, Arkiv för Fysik 14, 377-384 (1967).

TABLE 1 - Washing programme

1. Ultrasonic washing, 5 min
2. Rinsing in tap water
3. Washing in a 50 % neutral detergent (RBS), 15 min
4. Rinsing in tap water
5. -"- in distilled water
6. -"- in special grade alcohol
7. Drying

TABLE 2 - Sensitivity versus mass, Co-60 radiation

Average mass (relative units)	1.000	1.020	1.044	1.060	1.081
Average sensitivity (relative units)	1.000	1.000	0.992	1.006	0.996

TABLE 3 - Absorbed dose calibration factors of Toshiba RPL-glass (FD-R1-1) at different mean electron energies, E_M, and Co-60 γ-radiation. E_M is the mean energy of primary electrons at different phantom depths estimated according to Harder.

	Photons	Electrons				Average value
Energy interval (MeV)	Co-60	$E_M \leq 5$	$5 < E_M \leq 10$	$10 < E_M \leq 20$	$20 < E_M \leq 30$	
Calibration factor (rad x scale div^{-1})	23.2±0.3	23.5±0.3	23.4±0.7	23.6±0.6	23.8±0.4	23.5±0.3

TABLE 4 - Estimated uncertainties in the measurement of absorbed dose with an individual glass rod.

Source of uncertainty	Relative S.D./%
1. Stabilization	1.7
2. Fluorometer reading	1.6
3. Radiation quality	1.2
4. Regeneration	1.9
5. Linearity	1.5
	Rms 3.5

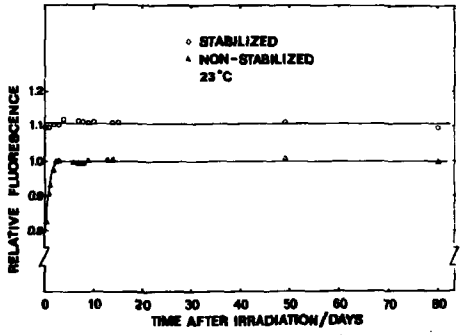

Fig. 1 Relative fluorescence versus time after irradiation for both stabilized and non-stabilized glass dosimeters.

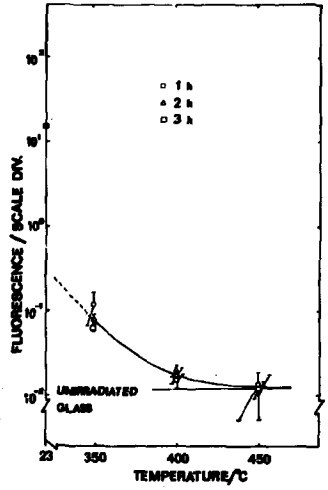

Fig. 2 Residual fluorescence versus temperature after heat-treatment 1, 2 or 3 hours.

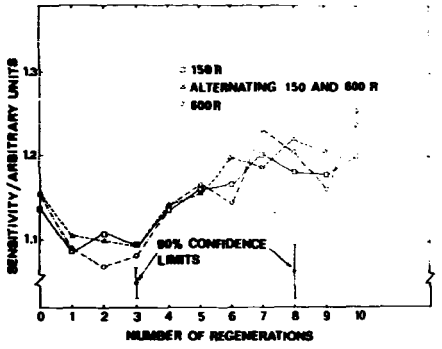

Fig. 3 Sensitivity versus the number of regenerations. Dosimeters were exposed with 150 or 600 R.

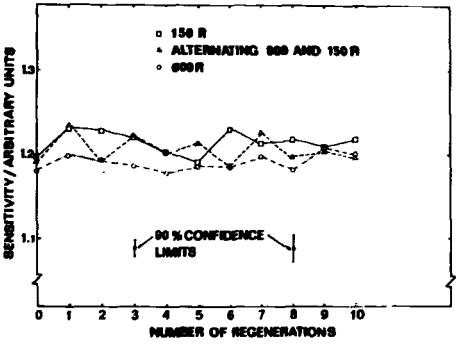

Fig. 4 Sensitivity versus the number of regenerations after an initial pretreatment of the dosimeters. Dosimeters were exposed with 150 or 600 R.

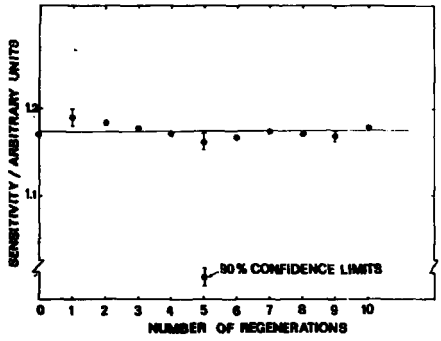

Fig. 5 Sensitivity versus the number of regenerations. Linear relationship between fluorescence and exposure applied.

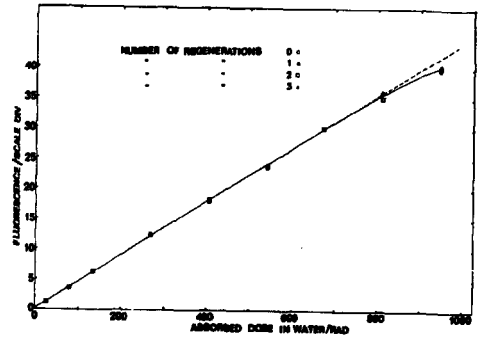

Fig. 6 Fluorescence versus absorbed dose in water after 0, 1, 2 and 3 *regenerations*.

Regulla

Can you tell us something about the level and the fluctuation of the predose of the glasses in the course of the multiple regeneration processes involved in your investigation?

Westerholm

The magnitude of the predose corresponds to an absorbed dose in water of about 0.5 rads and there was no significant change in this value as a result of repeated regenerations.

Some Ways of Applying the Capabilities of Various Luminescence Methods in Personnel Monitoring

by

M. Toivonen
Institute of Radiation Physics
Helsinki, Finland

Abstract

The principal advantage of RPLD, namely, the possibility of reading its indication repeatedly, at arbitrary intervals, throughout a period of long-term dose integration, proved to be of no value when used as a measuring technique in a personnel monitoring service. TLD proved more practical in routine measurements, even when powdered luminophors and simple read-out arrangements without automation were used. RPLD seems to be more versatile than TLD if information concerning the type of radiation and its incidence is needed in interpreting whole-body or organ doses involving high, abnormal exposures.

A development of dosemeter badges is discussed, details of the RPL and TL techniques used are described, and the usefulness of a new general purpose dosemeter approach is assessed in the light of experience gained in film dosimetry practice. Studies of the technique of scanning the RPL distribution in glass blocks are presented and typical results are stated.

Introduction

The Government institute for radiation protection in Finland has maintained a personnel monitoring service since 1963. Phosphate glasses were introduced as additional badges carried simultaneously with film dosemeters, with the aim of eliminating systematic errors due to inadequate filtering in connection with the film badges with regard to exposures involving mixed γ radiation and X-rays. In order to avoid the necessity of simultaneously wearing two separate badge cases we designed multi-glass badges having special characteristics for a range of different working conditions. This glass method was in routine use for four years, a maximum 700 persons, out of those 1500 - 2500 who used our facilities during the time in question, being monitored with glasses. In the cource of last two years the glasses were partly replaced with TL dosemeters. The original glass badges and the associated methods of evaluation have been described elsewhere[1]. However, the results of the study are included here, in order to provide a basis for discussion of our recent activities.

The difficulty of separating low-energy X-rays and β radiation from the more penetrating photon radiation have been considered to constitute a principal disadvantage of the RPLD system. Even so development of the RPL reading technique has enabled information to be obtained concerning the type of radiation and its spectrum, as well as the direction of radiation incidence, from a single glass body if this body has been irradiated with sufficient exposure in a non-isotropic radiation field. A method for scanning the fluorescence in the three dimensions of a glass block, or circumferentially and axially in the case of a cylindrical glass, has been described by Kiefer and Piesch[2,3]. Yokota et.al[4] improved the response of glasses to β radiation by stimulating the RPL with a narrow UV light beam passing through the effective glass layer with total reflection from the inner glass surface. We have made experiments to find the optimum means of applying standard 8 x 8 x 4.7 mm^3 glass blocks, instead of special glasses with trapezoidal form, for the same purpose.

Experiences with the Previous Badges

The badge cases and accompanying dosemeters are illustrated by Fig.1. Metal filters, 1.6 mm of Sn or Cd and 0.1 mm of Cu + 0.9 mm of Al, could be selected to obtain specialized dosemeter badges meeting the requirements of measuring accuracy in different working environments. The most complex badges, mainly intended for mixed X-ray and γ and neutron radiation fields, proved impractical and they were withdrawn soon after the requisite competence could be more conveniently attained with the aid of TL dosemeters. The original bi-glass holder with an energy compensation filter, 1.6 mm of Sn or Cd, and supplemented with a TL dosemeter as shown in Fig.1 was subsequently the most practical badge. In special X-ray dosemeters the advantages of RPLD compared with film dosimetry seemed to be questionable. The sharp fall in sensitivity of the glass at photon energies below 40 keV, wich is due to the inhomogeneous absorbtion of energy, was found to introduce a significant uncertainty in measurements. As regards directional dependency, however, it was possible to improve the accuracy of measurement compared to the film dosemeter.

From the point of view of the accuracy of measurement the experience with RPLD was fairly promising, when the badge change interval was three months. For instance, comparisons in practice with $Li_2B_4O_7$:Mn Tl dosemeters enclosed in the badges between the glasses have shown agreement within ± 15 per cent in medical Ra therapy environments. In the smaller number of equivalent comparisons which we were able to institute with dosemeters exposed to X-rays in actual industrial or medical working conditions, the results were in almost equally good agreement.

The greatest difficulties were encountered in the practical arrangements. The main principle of the project, that is to accomplish the monitoring economically over short intervals, and with quite high accuracy over long periods, was based on the special feature inherent in RPL glasses, i.e. the possibility of repeated readings without changing the dose memory. It was expedient to provide the badges with individual identification numbers. Since their dispatching was by mail,

two dosemeters were needed for each person, of which one was in use and the other was being measured. These practical arrangements proved to involve much more work than the film dosimetry system. There were two main reasons for these difficulties:

First, for administrative reasons, and sometimes also as a radiation protection policy, a periodical rotation of duties or of personnel in certain working environments is often practiced. This, together with spontaneous personnel replacements, reduce the need for highly accurate individual dose measurements over several years. It also introduced the risk of mix-ups of the specialized dosemeters, and the recording of predose values was difficult.

Secondly the risk of false evaluations increased more powerfully than was expected with increasing dose memory from previous periods of use. The potential influence of damaged glass surfaces could only be controlled with sufficient dependability for low dose measurements by withdrawing any glasses displaying increased predose level after extinquishing of the dose storage luminescence. This reduced the practical value of the dose storage over consecutive control cycles, because time cycles shorter than three months for change of badges could not be applied.

RPL Reading Technique

The experiments aiming at improving performance of the glass were performed by making the necessary modifications in a self-built reader[5]. The principal set-up used is shown in Fig.2. The manner of focusing the light beam was simplified from the original system by removing the first lens. This system provided an almost parallel beam without harmful reflections from the holder surfaces if a sufficiently narrow stop was placed before the lens. The risk of error due to wrong positioning of the light source or lens is also greatly reduced. Owing to the favourable focus geometry of the DC-supplied UV lamp, Osram 200W/2, the minor movements of the discharge have no influence on the sensitivity, even though a quite narrow

aperture, 0.5 mm, is used before the glass. The glass holder and the driving unit with synchronous motor for scanning the fluorescence are illustrated in Fig.3. The figure also shows the different ways of placing the glass for photon and β radiation measurements, respectively.

In order to demonstrate the response of glassess with different types and energies of radiation, glasses were irradiated as is shown in Table I. The ^{60}Co and X-ray irradiations could be directly measured with secondary standard instruments whereby the accuracy was within ± 3 per cent. Because of the low activity of the sources in other instances, these irradiations were made with a distance of 30 cm in the case of γ irradiation and 10 cm in that of β irradiation. The accuracy is thus not equally good, but is within ± 10 per cent for γ irradiations. The β irradiations were measured by means of LiF TLD-100 powder in plastic sachets, with a 14 mg/cm^2 PVC window and also as a thin uncovered layer on paper. The response calibrations of Peabody and Preston[6] were utilized. The dose values stated represent the dose in soft tissue at a depth of 7 mg/cm^2. The calculated dose rates from the $^{90}Sr/Y$ and ^{204}Tl sources were in fair agreement with the measurements.

Table I. Types and qualities of radiations used in irradiations

Source and equipment	Added filtration	Radiation type and quality			
			keV_{max}	keV_{eff}	kV_p
^{60}Co		γ		1250	
^{99}Tc		γ		140	
^{241}Am		γ		60	
Diagnostic X-ray unit	3 mm Al	X			100
Therapy X-ray unit	3.8 mm Al	X		20	29
- " -	-	X			10
$^{90}Sr/^{90}Y$	>100mg/cm^2	β	2250		
^{204}Tl		β	770		
^{147}Pm		β	220		

An investigation as to the optimum manner of focusing the stimulating UV light was made, and the results are given in Table II. As can be seen, the most favourable sensitivity and background values were achieved with the old glass holder. However, the most sensitive glass positioning for differential evaluation gives equally low predoses, and the higher PMT dark current is not harmful, especially if the output is read by means of a recorder. An investigation as to the optimum method for measuring β radiation was made, using glasses irradiated with a ^{204}Tl source. The results are given in Fig.4. The sensitivity depends only slightly on the glass positioning. The main reason for which the angle of 6^{o} between the UV light beam and the reflecting glass surface was chosen consisted thus of the imperfect ability of the recorder to register the narrow peak at 0^{o} angle.

Fig.5 illustrates the scanning results for photons and Fig.6 those for β radiation. Fig.7 shows some typical background curves and the lowest predose values that were obtained. Besides the typical curve measured with the glass in positioning II, an example has also been shown of the disturbing effect of surface faults in low dose measurements. The results were obtained with Toshiba FD-1 glasses[7], which had been in practical use for several years and which had thus been heated several times.

Table II. Results of investigation on optimum method for stimulating RPL.

Glass positioning and opening in the front of lens (1)	Relat. sensit.	Background (2) predose	without glass (3)	PMT dark current
		equivalent to Co exposure (R)		
I Ø 20 mm	4.4	0.350	0.008	0.045
25 mm	7.3	0.360	0.012	0.027
30 mm	11.1	0.360	0.065	0.018
II 25 x 5 mm^2	1.0	0.620	<0.300	0.200
III - " -	1.9	0.350	<0.170	0.110
IV - " -	1.2	0.500	<0.250	0.160

(1) The adjustable light stop is illustrated in Fig.2
(2) PMT dark current subtracted
(3) The glass quenches the influence of light reflections. Therefore, the values cannot be considered to represent the "pseudo-predose" from the glass holder.

The energy response measured at various depths below the glass surface, seen in Fig.8, agrees well with the results of Kiefer and Piesch[3]. The energy response for β radiation seems to agree well, with ^{204}Tl and at higher β energies, with the nearly flat response curve obtained by Yokota et.al[4], but with ^{147}Pm β energy our arrangement displayed a significantly lower sensitivity.

TLD Practice

The TL dosemeters have been read using a self-built reader[5], which initially had certain electronic units in common with the RPL reader. Some significant changes were made after the RPL measuring head was detached. The heating element, originally consisting of constantan, was replaced with a Kanthal strip of 0.1 mm thickness. The greater mass of the new heating tray made it unnecessary to use a Teflon ring as a heat absorber around the powder sample, but this ring also confines the volume of the measuring chamber and improves the purity of the nitrogen. However, the ring was taken off in order to guarantee reproducibility of the heating procedure over prolonged periods. The A/D converter, which provides a wide linear range in the measurement of PMT output charge, was replaced with a new adjustable unit, Fig.9. Furthermore, the reading programme was curtailed to have a duration of 30 seconds only. Compared to the commonest type of TL reader, the sole difference is our heating programme, with a very rapid rise of the heater temperature up to desired level.

The PM tube EMI 9558B with S20 photocathode, together with optical filter Schott BG38, has proved to be suitable for most TL phosphors. Results of an investigation concerning low dose performance with the light-sum integration method, with the original reading programme, have been stated earlier[5]. Fig.9 shows the corresponding results when the modified reading programme and heater were used. Two $Li_2B_4O_7$:Mn materials with

different origins [8,9] displayed nearly the same sensitivities, but a phosphor prepared by BDH Chemicals Ltd had a lower relative value, 0.8. The corresponding values for LIF:Cu,Ag and LiF:Mg,Ti [10,11] were 15 and 1.5 compared to 1 for $Li_2B_4O_7$:Mn. The relative sensitivity of LiF TLD-100 was 1.5-2.5, depending on the pre-annealing procedure.

Powder bags and capsules, and finger dosemeter sachets with 14 mg/cm^2 windows, were used in practical monitoring applications. Samples of 20 mg were dosed prior to reading, by using a simple volumetric measuring device, which is rapidly cleanable in an air flow.

Modified Dosemeter Badges

Fig.1 shows the modified badge cases, the identification strip and the dosemeters normally used. The glass positioning is standardized, the rough 8 x 4.7 mm^2 surface facing backwards. Further significant departures of the new general purpose badge from the preceding type consist of the two open windows and of the number aperture. Several types of solid TL dosemeters or powder bags can be inserted under the upper open window. Furthermore, two additional TL dosemeters can be placed in the centre of the plastic case if a pair of dosemeters in identical conditions is required for neutron indication.

Since the individual doses are low in most working conditions, it is mostly of no interest to distinguish the low energy photon and β radiations from more penetrating radiations, and mere evaluation of the TL dosemeter under the open window is sufficient. If necessary, further investigations are possible by using the RPL glass. At high dose levels a single glass is equally competent as a relatively complex TL dosemeter system in supplying information wich may be useful in interpreting abnormal measurements. Phosphate glass is also useful as a neutron dosemeter because the ^{31}Si β activity induced by fast neutrons can be used for dose evaluation several hours after the exposure, as Piesch [12] has reported.

Conclusions

As a result of developments, the competence of the badges has substantially improved. The risk of false information on safety due to inadequate understanding of the response limitations has thus been reduced. A critical examination of data obtained with film dosemeters from the field shows, however, that the information on exposure conditions has quite often been useful when direct radiation protection measures have been necessary on the basis of individual dose measurements. A summary of the reports that have been sent to radiation users shows that the lucid information furnished by the radiographic pattern on the film has revealed 10-20 cases of bad practice every year, while the corresponding number of yearly or quarterly over-exposures has been less than five. Furthermore, about 10 per cent of the films used in isotope laboratories have shown contamination. The best substitute for radiographic pattern is to organize a short-term control with sensitive dosemeters, but difficulties will be encountered when dosemeters have to be issued by mail to a great number of radiation users.

References

1. M. Toivonen, SFL-A7, Helsinki 1967
2. H. Kiefer, E. Piesch, Direct Information 10/67, Atompraxis 13 (1967)
3. H. Kiefer, E. Piesch, IRPA/2/53, Abstracts Health. Phys. (1970)
4. R. Yokota, Y. Muto, and T. Miyake, Proc. Sec. Int. Conf: Luminescence Dosimetry, p.773-782, USAEC CONF-680920
5. M. Toivonen, SFL-A13, Helsinki 1969
6. C.O. Peabody, H.E. Preston, AEEW-R 497, Winfrith 1967
7. R. Yokota, and S. Nakajima, Health. Phys. 11 241-253 (1965)
8. R.T. Brunskill, IRPA/2/62, Abstracts, Health. Phys. (1970)
9. P. Christensen, Proc. Sec. Int. Conf. Luminescence Dosimetry, p.90-117, USAEC CONF-680920
10. T. Niewiadomski, Nukleonika 12 281-301 (1967)
11. M. Jasinska, T. Niewiadomski, E. Rybs, Nukleonika 14 995-1009 (1969)
12. E. Piesch, Neutron Monitoring, Proc. Symp., Vienna 1966, p.471-493, IAEA, Vienna 1967

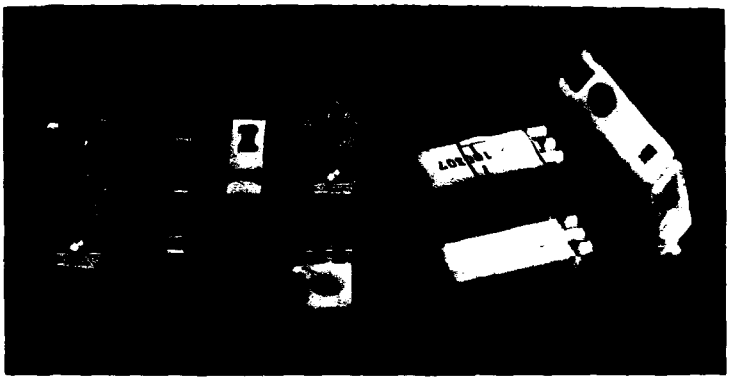

Figure 1. The previous (left) and new (right) dosemeter badges and associated dosemeters.

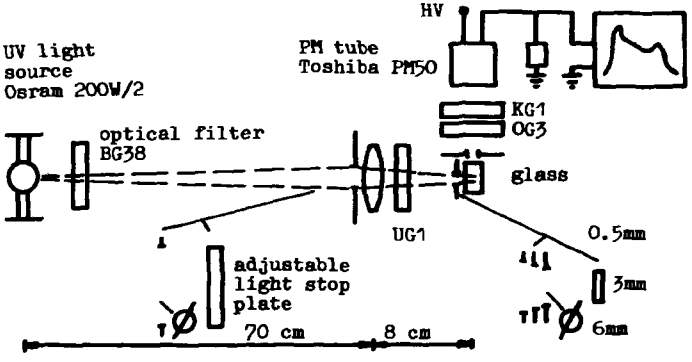

Figure 2. Principle of the RPL reading arrangement.

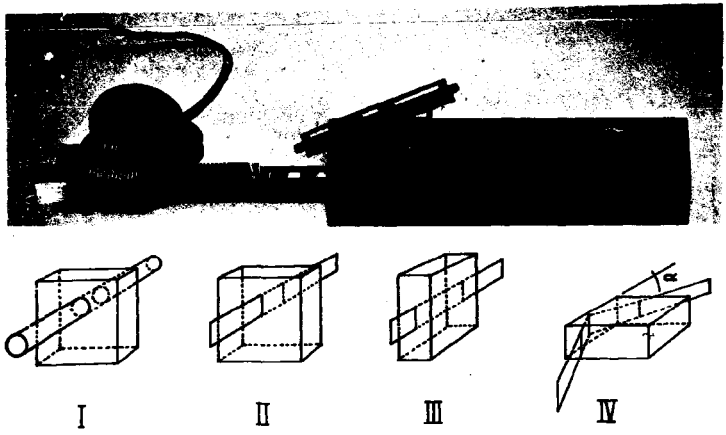

Figure 3. The new glass holder of the RPL reader, the driving unit for differential evaluation and the different glass positions in relation to the UV beam.

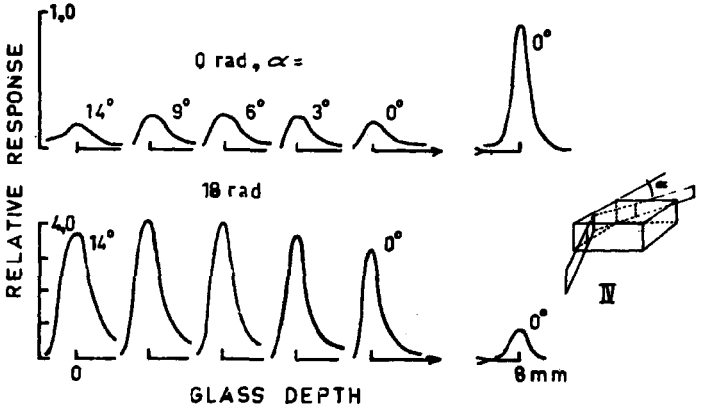

Figure 4. Relative response to ^{204}Tl β radiation for different angles between glass face and UV beam.

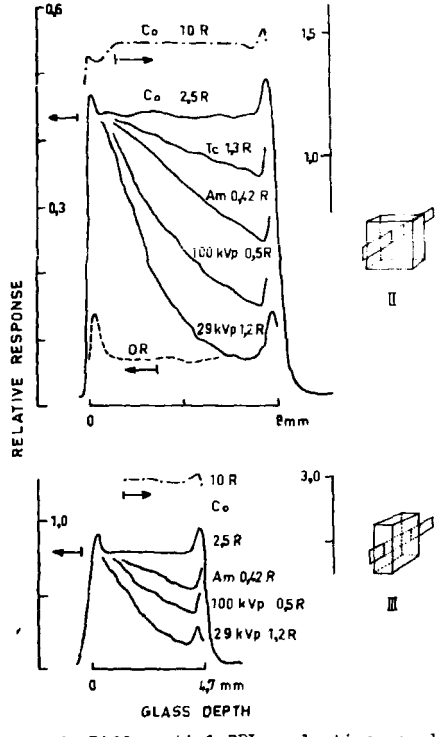

Figure 5. Differential RPL evaluation results.

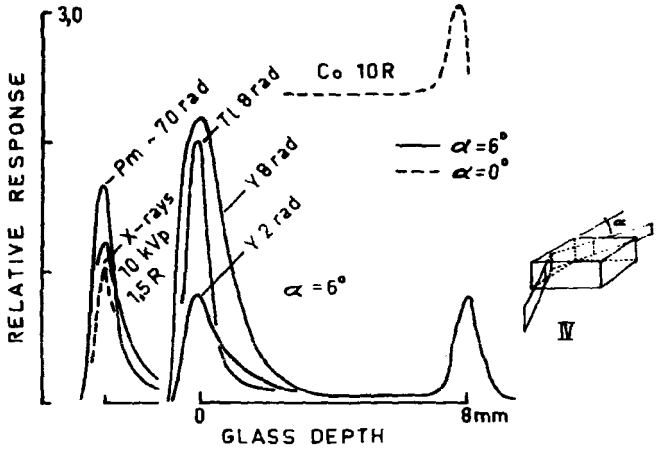

Figure 6. Differential RPL evaluation results for β radiations and comparison of β radiation, soft X-ray and γ radiation sensitivities.

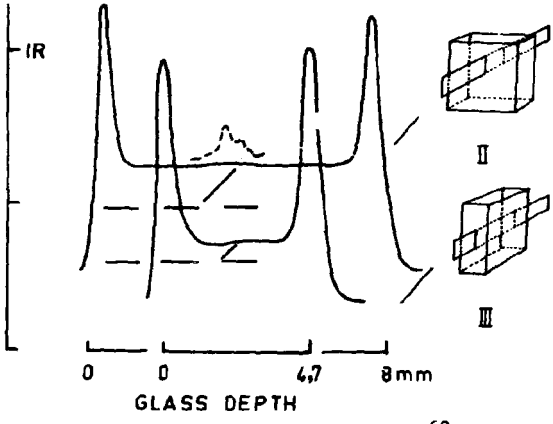

Figure 7. Equivalence between predose and ^{60}Co exposure. Typical curves, the lowest values obtained and typical effect of surface damage.

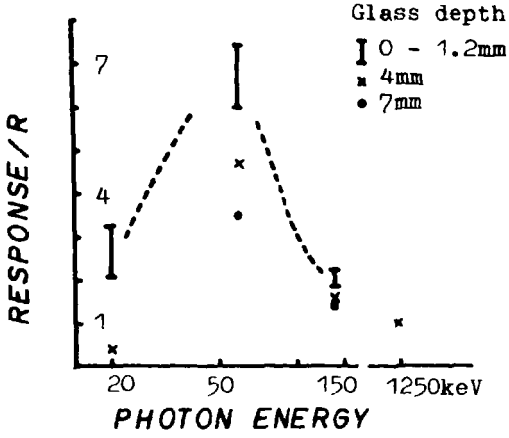

Figure 8. Energy dependence of response of phosphate glass measured at different glass depths.

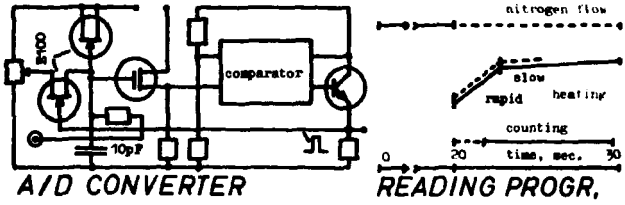

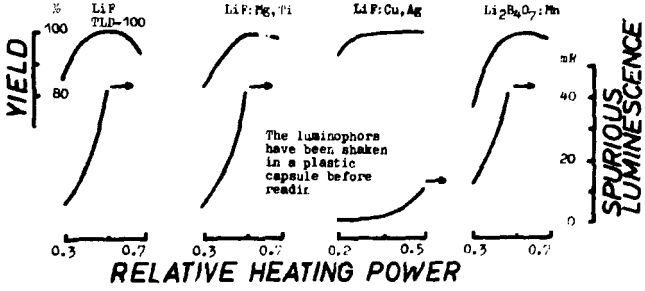

Figure 9. Top: Technical details of the TL reader. Bottom: Luminescence yield and equivalence between spurious luminescence and ^{60}Co exposure versus heating power.

Radiation-Induced Optical Absorption and Photoluminescence of LiF Powder for High-Level Dosimetry*

by

Esther W. Claffy, Steven G. Gorbics, and Frank H. Attix

U. S. Naval Research Laboratory, Washington, D. C. 20390

Abstract

Undoped LiF powder and the diffuse-reflectance apparatus described form the basis of a nondestructive technique for dosimetry in the 10^5-10^8 rad region. The properties determined are optical absorption in the M and R_2 bands and radiophotoluminescence (RPL) of the M centers. From 10^5 to 10^7 rad, M-center RPL is useful; from 10^6 to 10^7 rad, absorption in the M band is applicable; and absorption in the R_2 band from 10^7 to 10^8 rad. The stability of both absorption bands and the M-center RPL as a function of time at room temperature after irradiation is adequate for most practical applications. The lack of linearity in absorption or in the RPL vs. dose necessitates the use of a suitable calibration curve. Absence of measurable dose-rate dependence is indicated by essentially the same response per rad in the LiF for 2-MeV electrons, whether in a Van de Graaff beam depositing 10^4 rad/sec or in a high-intensity 30-ns pulsed beam giving 10^{14}-10^{15} rad/sec. However, ^{60}Co γ rays and low-energy x rays ($\approx$ 15 keV) yield 2- or 3-fold greater absorption and RPL than do electrons. This can be characterized either as a difference between the effects of electrons and photons or as an energy dependence, negligible between 15 keV x rays and ^{60}Co γ rays (which produce an equilibrium secondary-electron spectrum of $\approx$ 0.3-MeV average energy) but important between 0.3 MeV and 2 MeV. Use of a powder allows the homogenization of large quantities of material for uniform performance, and at reasonable cost for only 15-30 mg is needed per dosimeter. Since readout does not disturb stored signals, thermoluminescence can be subsequently measured to verify dose information on a single dosimeter.

Introduction

It was suggested by Nakajima[1] that density changes in the optical absorption bands of LiF crystals might be useful in the dosimetry of ionizing radiations. Vaughan and Miller[2] investigated this possibility with cleaved crystals of Isomet UV-window-grade LiF, and found that the R band (370 nm), M band (450 nm), and N_2 band (550 nm) all increased in optical density (OD) more or less linearly within the γ-ray exposure region 10^6-10^8 R. Moreover, they reported that little or no change in the measured optical densities was observed after 24 hours following irradiation.

* This work was supported by Defense Atomic Support Agency (now the Defense Nuclear Agency) contract NWET/TID Subtask 11XASX502.

Goldstein et al.[3] have made use of the same type of LiF, but ground and sieved to a 100-200 mesh powder, for thermoluminescence (TL) dosimetry at high exposures. The height of the glow peak occurring in the 400-475°C region was the measured parameter, increasing with exposure over the range 10^5-10^8 R, with some variations from sample to sample.

It seemed to us worthwhile to investigate the possibility of employing optical absorption measurements with powdered samples of LiF as a dosimetry method, for the following reasons:

(a) Optical absorption measurements can be practically non-destructive of the stored signal. They could therefore be performed on a sample before it was heated to obtain the TL reading, thus achieving desirable replication of dose information especially in cases where repetition of the exposure would not be feasible.

(b) The use of single crystals for dosimetry applications generally has not been found practical because of high cost and large variability in radiation sensitivity from crystal to crystal. Thus the future application of the LiF optical absorption method in dosimetry probably depends on whether it can be shown to work with powdered samples.

(c) In radiation exposures accompanied by severe mechanical shock, single crystals are not likely to survive without fracture.

In addition to the foregoing, we wanted to examine the possibility that the radiophotoluminescence (RPL) of the M center in LiF, as first reported by Molnar[4] and later by Klick[5], might also have dosimetric possibilities. We were unaware until later that Regulla[6] was also investigating this problem, but little duplication was involved since he studied single crystals of Harshaw LiF (TLD-100), while our work was based on powdered samples of relatively pure LiF. We extended our study to include TLD-100 powder so that a comparison could be made with Regulla's results.

There was the further possibility that the RPL of R_2 and N_2 centers, which develops under higher radiation exposures, might serve to extend the dose range to correspondingly higher levels. Okuda[7] reported luminescence from R_2 centers at low temperature and Görlich et al.[8] confirmed this for room temperature measurements. Luminescence from true N_2 centers has been less clearly established, although excitation in the general region of 550 nm was reported to produce luminescence[8].

Materials

The LiF employed in the present study was obtained through the courtesy of E. Tochilin*, and was a sample of a large boule (No. 246B) of Leitz UV-grade LiF which had been ground and thoroughly mixed for homogeneity, then sieved to 100-200 mesh. This material was selected partly because of its known ability to perform as a TL dosimeter in the 10^6-10^7 R range of γ-ray

* Radiation Detection Company, 385 Logue Avenue, Mountain View, California 94042.

exposures, since one of our secondary objectives (see paragraph (a) above) was to verify that the readout of dose information through the measurement of O.D. was possible without disturbing the stored TL signal. The availability of a kilogram of homogeneous LiF powder from a single source for possible later applications was also viewed as a considerable advantage, should the method prove to be useful.

Irradiation Techniques

^{60}Co γ Rays. LiF powder samples of 30 mg each were placed in gelatine capsules, several of which were enclosed in a graphite pillbox with walls 6.3 mm thick for electronic equilibrium. This was positioned in the NRL ^{60}Co facility, at a location having a calibrated exposure rate of 4×10^4 R/min, and removed after various total exposure times to extract one or more of the samples. The absorbed dose in the LiF was computed from the relation:

$$D_{LiF} = k(1-a) \frac{(\mu_{en}/\rho)_{LiF}}{(\mu_{en}/\rho)_{air}} X$$

$$= 0.869\ (1 - 0.028) \frac{0.0247}{0.0265} X$$

$$= 0.784\, X$$

where k is the absorbed dose in rad to air exposed to 1 roentgen of γ rays under electronic equilibrium conditions;

a is the fractional reduction in γ-ray exposure due to broad-beam attenuation in the 6.3 mm graphite wall;

$(\mu_{en}/\rho)_{LiF,\ air}$ is the mass energy-absorption coefficient for LiF and air, respectively; and

X is the γ-ray exposure at the sample location, in the absence of the graphite pillbox.

X-Rays. A beryllium-window x-ray tube was operated at constant potentials of 25 kV and 43 kV, with an added filtration of 0.25 mm of Al and 0.25 mm of Teflon. LiF powder samples were evenly distributed in a monogranular layer (6 mg/cm^2) in a shallow Teflon cup, 3 cm from the x-ray window. This close spacing was required in order to achieve the necessarily large doses within reasonable exposure periods of a few hours. The exposure rate (1×10^6 R/hr.) was calibrated by placing a 25-R Victoreen ion chamber with its active volume bisected by the plane of the phosphor layer. This ion chamber was in turn calibrated against the NRL standard free-air ionization chamber at 50 cm from the x-ray tube, employing the same voltages and filtration. The x-ray spectra were determined by means of a lithium-drifted silicon detector, reducing the beam intensity by passing it through a

microdiaphragm. The ratio of $(\mu_{en}/\rho)_{LiF}/(\mu_{en}/\rho)_{air}$, averaged over the x-ray spectra, was found to be 1.19 for both 25 kV and 43 kV, indicating an effective average x-ray energy of about 15 keV in both cases. Thus the absorbed dose (rads) in the LiF is given by

$$D_{LiF} = (0.869)(1.19)X = 1.03X$$

where X is the exposure in roentgens.

Pulsed Electron Beam. Samples of 30 mg of LiF were enclosed between the two halves of No. 3 gelatine capsules, with the small end of each capsule inserted backwards into the larger end, thus compressing the phosphor into a thin lenticular layer ≈ 0.6 mm in thickness. These samples were exposed in vacuum to the pulsed electron beam at the HIFX generator at the Harry Diamond Laboratory, Washington, D. C. The phosphor layers were located between a thick supporting slab of aluminum and a thinner plate 1.3 mm in thickness, upon which the ≈ 2.4 MeV electrons were incident. The average electron energy in the samples was therefore reduced to about 2 MeV, and the samples were located at the maximum of the depth-dose curve in aluminum. The dose in the plane of the LiF samples was measured simultaneously for each pulse by a calorimeter consisting of a copper-constantan thermocouple spot-welded to a 6-mm diameter disc of copper foil 0.1 mm thick. The dose in the LiF was deduced from that in the copper by applying a factor of 1.13 to account for the stopping-power difference at 2 MeV. Doses per pulse (≈ 30 nsec in duration) were 10^6-10^7 rad; 1 to 16 pulses were delivered to each sample at roughly 1-minute intervals to obtain a variety of doses. The aluminum pieces were water cooled to avoid cumulative heating. As a check on the dose as well as the beam uniformity, 2-cm squares of "dye-cyanide" colorimetric dosimetry film* were exposed simultaneously, positioned in the same gap between the aluminum plates as the LiF samples and the calorimeter. This film showed no significant difference in response per rad for the pulsed electrons, ^{60}Co γ rays, and low-energy x rays, as will be discussed in a separate paper by Attix, Gorbics, and Claffy. Further details about these irradiation techniques will be included there as well.

Van de Graaff Electron Beam. The electron beam from a 2-MeV Van de Graaff generator was used to determine the response of LiF to relatively low rates of electron irradiation (2×10^6 r/min). A small sample of powder (≈ 50 mg) was spread over an area of about 3 mm in diameter on the surface of a 1-mil aluminized mylar film mounted on a 6" diameter metal ring. The resulting thin layer of phosphor (≈ 5 mg/cm^2) is placed in the electron beam for irradiation.

Calibration of the beam intensity is accomplished by replacing the sample with a Faraday cup at the same position in the beam. The current from the Faraday cup is converted to the number of electrons/cm^2/sec. The energy deposited by each 2-MeV

* Obtained from Kent Humpherys, EG&G Inc., Goleta, California.

electron is then determined from the stopping power of LiF, as given in published tables[9].

Apparatus

The diffuse reflectance apparatus used for measuring the optical absorption and RPL of powdered LiF samples has been described in detail elsewhere[10] and will be considered only briefly here. Figure 1 is a schematic diagram showing its essential features.

A light beam of appropriate wavelength is passed horizontally from a monochromator and collimator into a box having a diffusely reflecting inner surface. The beam is reflected downward by a front-surface mirror onto the sample, typically 30 mg of LiF powder evenly distributed over a circular depression in an aluminum planchet positioned in the plane of the bottom surface of the box. The depression in the planchet is 0.10 mm deep by 6 mm in diameter. As little as 15 mg of sample gives satisfactory results. Light is diffusely reflected from the sample and the aluminum surface beneath it. At some exciting wavelengths RPL light is emitted by the sample. The light is diffusely reflected by the walls of the box and enters the photomultiplier (PM) tube window. A two-position optical filter drawer and shutter allows discrimination against either the incident wavelength or the RPL, or the complete exclusion of light from the PM cathode-face (S-20, tri-alkali type; quartz window; spectral sensitivity range 165-850 nm). Current from the PM tube is measured by means of a Keithley guarded differential voltmeter, Model 660A.

Optical Absorption Measurements

The concept of optical density as a measure of absorption is itself less well defined for the case of diffuse reflectance from a powder than for direct transmission of a flat-surfaced single crystal. In our apparatus one is measuring the total effect of many individual rays which have passed through a distribution of distances in the LiF material. Nevertheless, one can treat the resulting signal as though it were some measure of "apparent optical density" (AOD) for convenience in plotting dose-response curves for dosimetry purposes.

In terms of measured light signals, the AOD due to dose is given by

$$\mathrm{AOD} = \log_{10}\left[\frac{I_U - I_B}{I_D - I_B}\right]$$

where I_U = intensity of diffusely reflected light (PM-tube current) from an undosed virgin sample,

I_D = intensity of light from a dosed sample, and

I_B = intensity of background scattered light from an absorbing black velvet disc in place of the sample.

The term AOD is meaningful only as an empirical parameter under fixed conditions of sample mass, configuration and particle size.

Fig. 2A shows the absorption spectra of two LiF samples which

received exposures of 6.38 X 10^6 and 6.67 X 10^7 rad of ^{60}Co-γ radiation, respectively. The values plotted are AOD, in terms of measured PM-tube current, as a function of wavelength for 30-mg powder samples. The Corning No. 9788 filter excluded the sample's RPL signal (predominantly a 670 nm band) from the PM tube.

By comparison with Fig. 2B, which reproduces Vaughan and Miller's plot of OD as a function of wavelength for 1.5-mm thick single crystals of γ-irradiated LiF (1some1, 2 X 10^7 R), it is evident that the present apparatus does detect absorption bands in the same regions - the M band, 450 nm; R_2 band, 380 nm; N_2 band, 550 nm. The diffuse-reflectance apparatus gives somewhat poorer wavelength resolution, however, partly because of the replacement of the monochromator exit slit by a circular diaphragm 6 mm in diameter used to illuminate the entire sample surface with a uniform spot of light. Some variation in relative peak positions and heights also results because the spectra are uncorrected for the wavelength sensitivity of the PM tube.

In Fig. 3 are shown the changes in optical absorption (AOD) of the M band in Leitz LiF with increasing dose. The samples were illuminated with 450-nm light and the reflected light was viewed by the PM tube through a Corning No. 5562 filter to remove RPL arising from excited M centers - a predominant emission band at 670 nm and a lesser band at 520 nm[8]. Curve A delineates the trend in samples irradiated with ^{60}Co γ rays (O points). The absorption of samples irradiated with 2-MeV pulsed electrons was sufficiently different so that a separate curve (B) is drawn through those points (+). Other samples were irradiated in the electron beam of the 2-MeV Van de Graaff accelerator, and these points (□) are indicated for comparison; they tend to follow Curve B. Samples irradiated with x rays at 25 and 43 kV gave data points (X,Δ) lying close to Curve A. The significance of the difference between Curves A and B will be discussed later. The ^{60}Co points represent average values for several measurements, which accounts for the evidently smoother fit with Curve A. Doses ranged from 2 X 10^4 to 2 X 10^8 rad, but below ≈ 5 X 10^5 rad the resulting absorption could not be clearly determined.

Vaughan and Miller[2] found linear response for the growth of the M band, based on transmission measurements of single crystals in the dose range 10^6 - 2 X 10^7 R. The M-band curves in Fig. 3, based on reflectance from powders, only roughly approach linearity of response in this dose range. A pronounced saturation effect flattens out the curves at higher doses, unlike the results of Vaughan and Miller. This apparent saturation probably results from the multiplicity of path lengths followed by individual light rays in penetrating the powdered sample, giving rise to a distribution of absorption thicknesses rather than the single well-defined thickness traversed in a flat crystal. At large enough doses the diffusely reflected light signal consists predominantly of rays which have passed through little or none of the darkened LiF material, but have been merely reflected from the crystal surfaces or aluminum tray. This accounts for the apparent convergence of Curves A and B.

Fig. 4 shows a similar plot of the data for the R_2 absorption

band with 377-nm incident light, viewed through a Corning No. 5330 filter to remove the RPL of excited R_2 centers (predominant 530 nm band; lesser 670 nm band)[8]. Again the data fall along two curves: A for ^{60}Co γ irradiation, with a few points representing x-ray dosed samples; Curve B for 2-MeV pulsed-electron and Van de Graaff-electron irradiations. There appear to be several significant differences from the M-band results shown in Fig. 3: (a) The R_2 band is weaker and the AOD values tend to be generally lower by about a factor of 8 in the 10^6-10^7 rad dose region; (b) Better linearity, and less saturation at the higher doses, is evident with the R_2 band; (c) The points on Curve B show even greater scatter in Fig. 4, partly because of (a); and (d) One of the 25-kV x-ray points, indicated by X, falls more closely on the B than the A curve, but the AOD value is so small this is probably not significant. On the other hand, the response to the pulsed electrons and the Van de Graaff-electrons again tends to be lower than that for γ rays and x rays to a degree comparable with that for M-center coloration, persisting over the full dose range studied.

Absorption changes in the N_2 band as a function of dose are similarly displayed in Fig. 5. Here the sample is illuminated with 550 nm light, and viewed through Corning No. 9780 glass to filter out possible RPL from excited N_2 centers (largely a 670 nm band)[8]. The N_2-absorption first becomes detectable at still higher irradiation levels than does R_2 absorption, and the AOD values are roughly 30-fold less than for the M band in the lower part of the dose range, leading to excessive scattering of points. The x ray data tend to agree more closely with the γ-ray curve than the electron curve, but the agreement is very poor at 10^6 rad. The electron response again appears to be markedly less than the γ-ray response, and again, the points for Van de Graaff-electron irradiation fall more in line with the pulsed-electron curve than with that for γ rays. The latter is distinctly steeper than linear for the low-dose end, as was the case for the M band also.

Stability of Optical Absorption. Kaufman and Clark[11] noted, among other optical changes, that in Harshaw LiF crystals the 450 nm band increased and then stabilized during the first 30 hrs. post-irradiation, during dark storage at room temperature. Vaughan and Miller[2] reported that no measurable change in optical density was observed in any of the three absorption bands between 24 hrs. and two months after irradiation of the Isomet crystals. It was deemed desirable therefore to determine what changes in absorption, if any, took place in the irradiated Leitz LiF powder used in the current investigation.

Figs. 6 and 7 summarize our findings. Identical samples were dosed to $\approx 6 \times 10^6$ rad with ^{60}Co γ rays and 2-MeV Van de Graaff electrons. Initial measurement of AOD at the peak of each band was made within one hour, after which samples were stored in the dark at $\approx 25^{\circ}C$ (ambient temperature) until subsequent measurements. Results were the same for both the γ and electron-dosed samples, and these are reproduced in Fig. 6. The curves in Fig. 7 are based on a similar sequence of measurements made on samples dosed to $\approx 1.6 \times 10^7$ rad with 2-MeV electrons from the Van de Graaff generator. Those samples were stored at a controlled

temperature of 20°C, but the air-conditioning system failed after one week and thereafter the ambient temperature was ≈ 25°C. It will be seen in both figures that the M band increases slowly but continuously with time to at least one month. In Fig. 6 the R_2 absorption fades during the first 5 hrs. and then rises again, whereas for the larger dose (Fig. 7) a steady rise is observed. (This difference in behavior may be due to the influence of the overlapping short-wavelength tail of the M band.) The N_2 absorption fades during the first week, more or less, and then flattens out or rises slightly. In no case was the coloration completely stable with time, as has been reported for single crystals of (Isomet) LiF after 24-30 hrs delay following irradiation.

We have also observed visual changes in body color of irradiated LiF powders stored in the dark at ambient temperature, ≈ 25°C. Immediately after γ-ray or electron irradiation (e.g. ≈ 10^7 rad) samples are green in color, changing to yellowish green during several hours, and to yellow within about 24 hours. The yellow color, perhaps resulting from predominant M-center absorption at 450 nm, seems permanent. Okuda[7] has reported that optical energy from intense light sources such as a 500-watt xenon lamp or high-pressure mercury lamp produces fading of the R_2 band and an increase of the M band, and under certain conditions the reverse effects are produced. It was desirable, therefore, to assess the behavior of the three absorption bands under the working conditions of our apparatus for dosimetry applications. Exposure of irradiated samples of Leitz LiF powder for as long as one hour to the light from the tungsten-filament quartz-iodine lamp as set up in the reflectance apparatus did not produce detectable changes in either the M, R_2 or N_2 bands. This was determined by measuring the samples immediately after irradiation and again after 15, 30 and 60 minutes total exposure to 450, 377 and 550 nm light. Furthermore, there was no detectable difference in TL output as measured in the 400-475°C region, with or without a prior 60-minute exposure to light in the apparatus. Dose determination by AOD measurement can, therefore, safely precede standard TL readout procedures as described by Goldstein et al.[3].

Radiophotoluminescence Measurements

When M centers in LiF single crystals are excited with approximately 450 nm light the RPL which is produced consists of an emission band at 670 nm and a less intense band at 530 nm[8], or at 520 nm[6]. Regulla[6] has noted that in single crystals of TLD-100 LiF (Mg-doped), the relative intensity of these bands is 4:1. To measure the RPL in LiF powders with our apparatus, optimum excitation was found to be at 455 nm, and the emission was viewed through three different PM-tube filters: Corning No. 2424 for the 670 nm band, No. 9830 for the 520 nm band, and No. 3384 for both bands combined. The amount of RPL was determined by subtracting the PM-tube reading obtained for an undosed sample from that of the dosed sample. The net difference in PM-tube current is the RPL value plotted as the ordinate in Figs. 8 - 10. Fig. 8 represents the RPL from Leitz LiF powder, and Fig. 9 that from Harshaw TLD-100 LiF powder, exposed to ^{60}Co γ rays and read out one day later. Fig. 10 compares the RPL (combined bands only, from Leitz powder) produced by irradiation sources of differing energy and dose rates.

Regulla[6] reported linear response with dose from 10^2 R up to 10^6 R for the M-center luminescence in single crystals, but illustrates the dose-dependence of the weaker 520 nm emission band only. Our data for TLD-100 powder, as plotted in Fig. 9, show response approaching linearity in the approximate working range 4×10^4 - 3×10^6 rad for the total RPL, but distinctly steeper variation vs. dose for the individually measured 670 and 520 nm bands. The RPL response of Leitz LiF powder to dose, as plotted in Fig. 8, is approximately linear over part of its range (2×10^5 - 2×10^6 rad) for the 520 nm band, but the 670 nm band and the combined output for both bands are linear only in the immediate vicinity of 10^6 rad, being steeper below that dose and saturating at higher doses. The steeper-than-linear behavior of the RPL output at the lower doses appears to be related to an optical absorption effect, inasmuch as a slightly irradiated LiF ($<10^5$ rad) produces a smaller PM-tube current than does an unirradiated sample. Subtracting the latter from the former results in a negative net RPL signal. Maximum RPL for the combined emission bands in Leitz LiF, Fig. 8, occurs at 1.1×10^7 rad, whereas the 670 nm band continues to rise until 5.6×10^7 rad. The 520 nm-band component is saturating at the faster rate. Difference in behavior of the component emission bands is likewise suggested by Regulla's observation that the color of the RPL from TLD-100 is green, yellow or red, depending on dose.

If the RPL curves for LiF shown in Fig. 10 are compared with the M-band absorption curves in Fig. 3, it will be noted that there is reasonably good correspondence. There is approximately threefold greater response from ^{60}Co γ-irradiated LiF as compared with electron-irradiated samples, at 10^6 rad for example, whether RPL or absorption is measured. In Fig. 10 the curve, B, for electron-irradiated samples is based largely on a series of Van-de-Graaff exposures. This is in contrast to Fig. 3, where pulsed-electron-dosed samples predominate in Curve B. However, 2-MeV electron exposures regardless of dose-rate give much the same response. In Fig. 10, the pulsed-electron points represent measurements on samples dosed one year before, rather than the usual 24 hours, and are meaningful in a qualitative rather than quantitative sense.

Stability of Radiophotoluminescence. Our measurements of RPL in both Leitz LiF and Harshaw TLD-100 LiF after one month of storage show an increase roughly approximating that observed in the AOD of the M absorption band, shown in Fig. 7. Furthermore, in one experiment RPL measurements were initially determined on samples irradiated at least one month before, and presumably "stabilized" in the Vaughan-Miller sense. These samples also showed a rise in RPL output after an additional month's storage. Regulla[6] reports a much greater increase in RPL of TLD-100 crystals during the first week of storage. Whether this seemingly anomalous behavior is attributable to the different trace-element composition of the materials is not clear. In view of the discrepancy, it is desirable to check out the time-stability of any batch of LiF to be used for this type of measurement.

RPL from R_2 and N_2 Bands. The R_2 and N_2 absorption bands are very small (Fig. 2). Using our most heavily dosed sample (4×10^8 rad), we could detect no RPL when exciting into the peak of the

N_2 band and only a very weak signal from peak R_2-excitation. In the dose-range of interest, therefore, RPL from the R_2 and N_2 bands is not useful for dosimetry application by our technique.

Discussion and Conclusions

Optical Absorption. In some respects, LiF powder as an optical absorption dosimeter does not fulfill expectations based on the earlier single-crystal work of Vaughan and Miller[2]. The linearity of OD vs. dose observed by them is only crudely approximated in the present results, and the complete time stability of the coloration (after the first 24 hrs following irradiation) which those authors reported has not been achieved with the Leitz LiF powder. Nevertheless, the present results indicate that

(a) The M-band coloration provides a useful measure of the X- or γ-ray dose over the range $4 \times 10^5 - 1 \times 10^7$ rad, above which the AOD saturates excessively.

(b) The R_2-band coloration is useful for X- or γ-ray dose measurements over the range $2 \times 10^6 - 1 \times 10^8$ rad, and perhaps even somewhat higher.

(c) The N_2-band is too weak to be of much practical value as a dose parameter.

(d) There seems to be no significant dependence of the M- or R_2-band absorption response per rad in LiF upon quantum energy in comparing ^{60}Co γ rays with 25 and 43-kV x rays. Thus a LiF-dosimeter calibration with ^{60}Co γ rays is applicable for measuring soft x rays as well. It is likely that this energy independence applies as well to the intervening quantum energies, but additional measurements should be made to verify this.

(e) The optical absorption is significantly less for 2-MeV electrons at both the exceedingly high rates of 10^{14}-10^{15} rad/sec, and the relatively low rates of 10^4 rad/sec employed in the present work. The similarity of results at the high and low electron-dose rates makes it unlikely that the still lower dose rates of the x and γ irradiations can account for the difference between Curves A and B in Figs. 3-5. Ruling out a dose-rate effect, one is left with either a difference in damage mechanisms between electrons and photons, or a dependence on the energy of the radiation. Since x and γ rays deposit nearly all of their dose via secondary electrons, it is difficult to attribute special damage mechanisms to the photons. Rather, it seems reasonable to focus attention on the differences in electron kinetic energy involved. The equilibrium spectrum of the secondary electrons from ^{60}Co γ rays has an average energy of about 0.3 MeV and for the x rays it is about 0.01 MeV, as compared with the 2-MeV electron beams. It thus appears that between electron energies of 0.3 and 2 MeV a decrease in effectiveness of producing color centers occurs in the LiF employed in this study. Ritz[12] has reported a decreasing trend of F-center production efficiency with increasing radiation energy in LiF, which is qualitatively consistent with the present findings, although Ritz's irradiations were done at low temperatures.

(f) Combining the conclusions in (d) and (e), it should be possible to calibrate LiF optical-absorption dosimeters with ^{60}Co γ rays at relatively low dose rates, and then employ that calibration in interpreting the coloration produced by high-

intensity pulses of x rays. This involves the assumption that the lack of dose-rate dependence observed with electron beams will apply as well to x rays, which is not unreasonable.

(g) The increase with time in the AOD for the M band, as shown in Figs. 6 and 7, is practically the same for the two dose levels, 6×10^6 and 1.6×10^7 rad. Relative to the reading 24 hrs after irradiation, the AOD has increased by 5% at one week after irradiation, and by about 8% at 1 month. This degree of instability is comparable with that of some other practical dosimeters (e.g., the CaF_2:Mn TL dosimeter), and can easily be corrected for. The R_2 band shows approximately similar instability at the higher dose level, but considerably greater time variations at 6×10^6 rad, suggesting that where time stability is important, the R_2 band will be most useful for dosimetry above 10^7 rad, employing the M band for lower doses.

(h) The reflectance apparatus used as a reader for the present study produces no bleaching or other effect on the coloration of samples, nor on TL readings which may be made later on the same samples to further verify dose determination.

Radiophotoluminescence. In the 10^5-10^7 rad range, the RPL signal from the M center in LiF powder can provide a useful measurement of the dose, effectively extending the dose range of the M-band absorption technique one decade lower. The R_2 and N_2 RPL signals are too weak for dosimetry applications. The M-center RPL response and its build-up with time are similar to those of the AOD of the M band. Conclusions (d), (e) and (f) for optical absorption apply likewise to the M-center RPL.

In comparing the RPL data for the Leitz LiF (Fig. 8) with that for Harshaw TLD-100 LiF (which is doped primarily with 100-200 ppm of Mg) in Fig. 9, we see that the latter is roughly a factor of two brighter under similar dose and illumination conditions. Moreover, the combined-band curve for TLD-100 tends to be more nearly linear than is the corresponding curve for Leitz LiF. Regulla's[6] data for single crystals of LiF (TLD-100) showed linear RPL response over the dose range from 10^2 to 10^6 rad for the 520-nm band. He did not publish the corresponding results for the 670-nm or combined bands. Obviously the use of large (8 x 8 x 4.7 mm) crystals weighing some 780 mg provides much greater RPL sensitivity, and allows the measurement of much smaller doses, than does the small powdered LiF samples employed in the present experiment. Regulla's results, furthermore, give no indication of optical-absorption effects distorting the linearity of the RPL signal vs. dose, as seems to be the case in the present work.

Summary

LiF powder and the diffuse-reflectance apparatus offer a means for high-range dosimetry which allows the dose to be read out in several nondestructive ways: the optical absorption of the M band for 10^6-10^7 rad, the R_2 band for 10^6-10^8 rad, and the M-center RPL for 10^5-10^7 rad. None of these measuring operations disturbs the stored signals, nor the TL signal which may be measured subsequently by separate means described by Goldstein

et al.[3]. Thus, verification of dose information is obtainable, which is especially valuable for measurement of nonrepeatable exposures.

The stability of the M-band coloration and RPL as a function of time at room temperature after irradiation is adequate for most practical applications. The R_2-band-coloration stability is also satisfactory in the dose range above 10^7 rad where it is most likely to be useful.

The powder form allows the homogenization of large quantities of material for uniform performance from sample to sample, at reasonable cost, since only 15-30 mg is needed per dosimeter.

The lack of linearity of the AOD or the RPL vs. dose of course necessitates the use of a suitable calibration curve extending over the entire range of doses to be measured. A ^{60}Co γ-ray calibration will suffice for use with x rays, at least in the region of $\approx$ 15 keV.

Indications are that the absorption bands and the RPL as measured by this technique are independent of dose-rate, but are somewhat dependent on energy in the range between ^{60}Co γ rays and 2-MeV electrons.

References

1. T. Nakajima, Japan J. Appl. Phys. 7, 1418 (1968).

2. W.J. Vaughan and L.O. Miller, Health Phys. 18, 578 (1970).

3. N. Goldstein, E. Tochilin, and W.G. Miller, Health Phys. 14, 159 (1968).

4. J.P. Molnar, Absorption Spectra of Trapped Electrons in Alkali Halides; Thesis, MIT, 1940.

5. C.C. Klick, Phys. Rev. 79, 894 (1950).

6. D.F. Regulla, Health Phys. 19, 93 (1970) (Abstract).

7. A. Okuda, J. Phys. Soc. Japan 16, 1746 (1961).

8. P. Görlich, H. Karras and G. Kötitz, Phys. stat. sol. 3, 1803 (1963).

9. M.J. Berger and S.M. Seltzer, NASA SP-3036 (1966).

10. S.G. Gorbics, E.W. Claffy, and F.H. Attix, Diffuse Reflectance and Fluorescence Measuring Apparatus; in press, Rev. Sci. Instr.

11. J.V.R. Kaufman and C.D. Clark, J. Chem. Phys. 38, 1388 (1963).

12. V. Ritz, Phys. Rev. 133, A 1452 (1964).

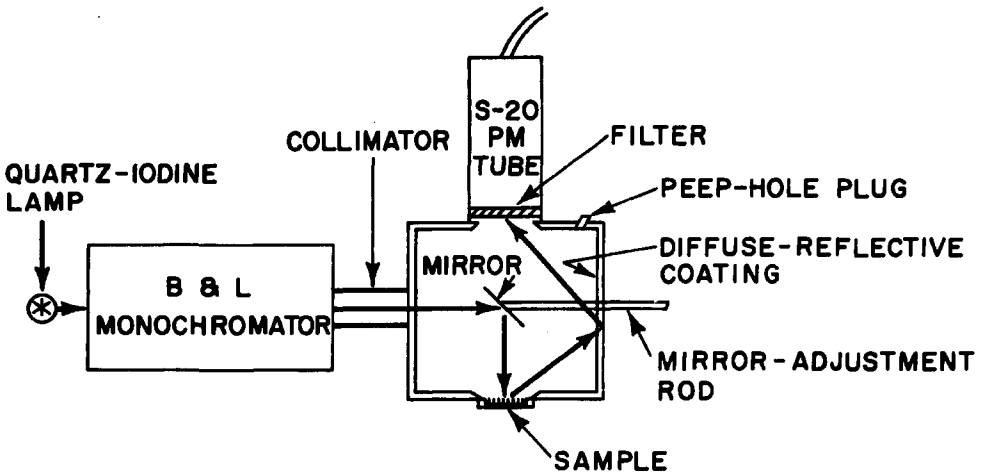

Fig. 1. Schematic diagram of apparatus for diffuse reflectance and fluorescence measurements.

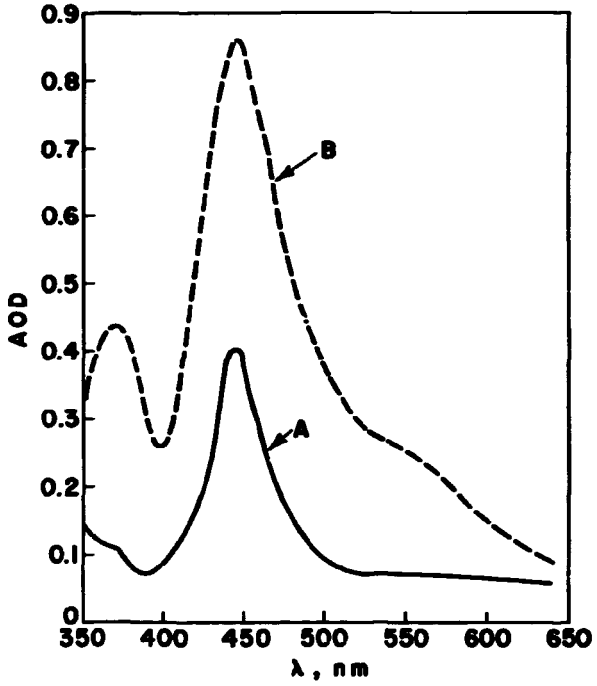

Fig. 2. A)Absorption spectra of Leitz LiF powder, in terms of apparent optical density. Curve A, 6.38 X 10^6 rad; Curve B, 6.67 X 10^7 rad; ^{60}Co γ rays. PM-tube filter: 3 mm Corning #9788.

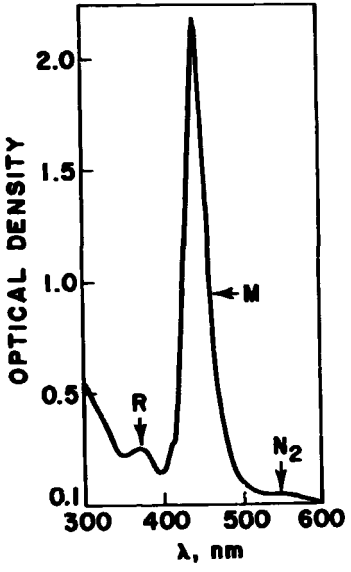

B) Absorption spectrum of Isomet LiF single crystal, 1.5 mm thick; 2 X 10^7 R (≈ 1.6 X 10^7 rad), ^{60}Co γ rays. (Reproduced from Vaughan and Miller, ref. 2, fig. 1, permission Health Phys. Soc.).

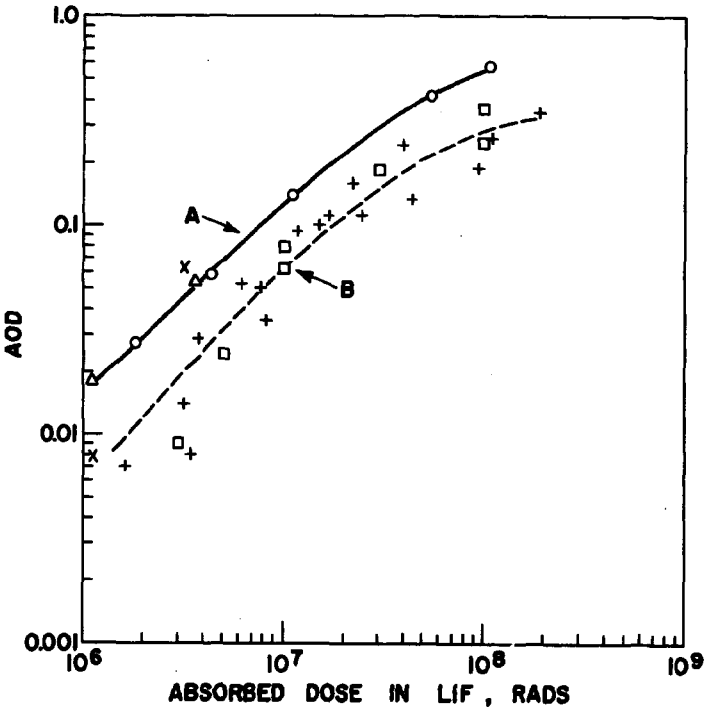

Fig. 4. R_2-Band absorption in Leitz LiF. Monochromator: 377 nm; PM-tube filter: 3 mm Corning #5330. Curves and points as designated in Fig. 3.

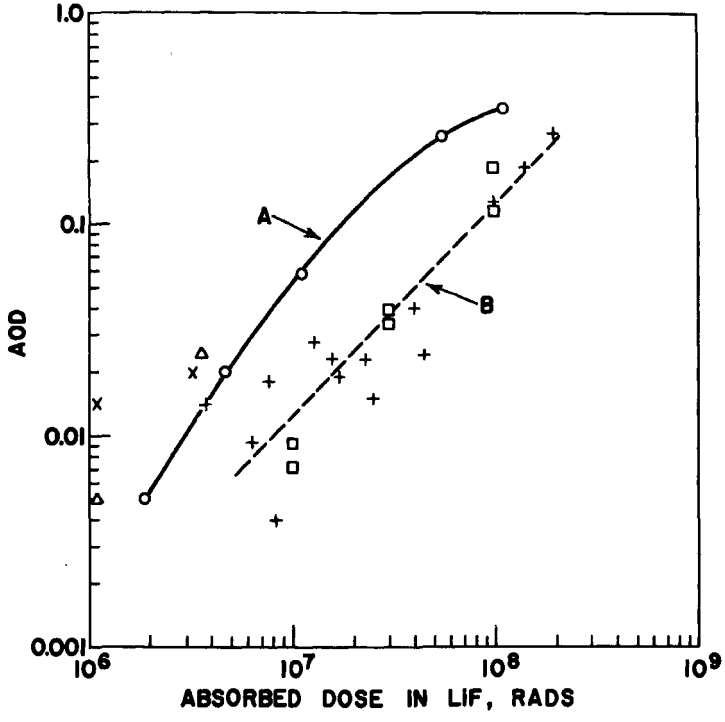

Fig. 5. N_2-Band absorption in Leitz LiF. Monochromator: 550 nm; PM-tube filter: 3 mm Corning #9780. Curves and points as in Fig. 3.

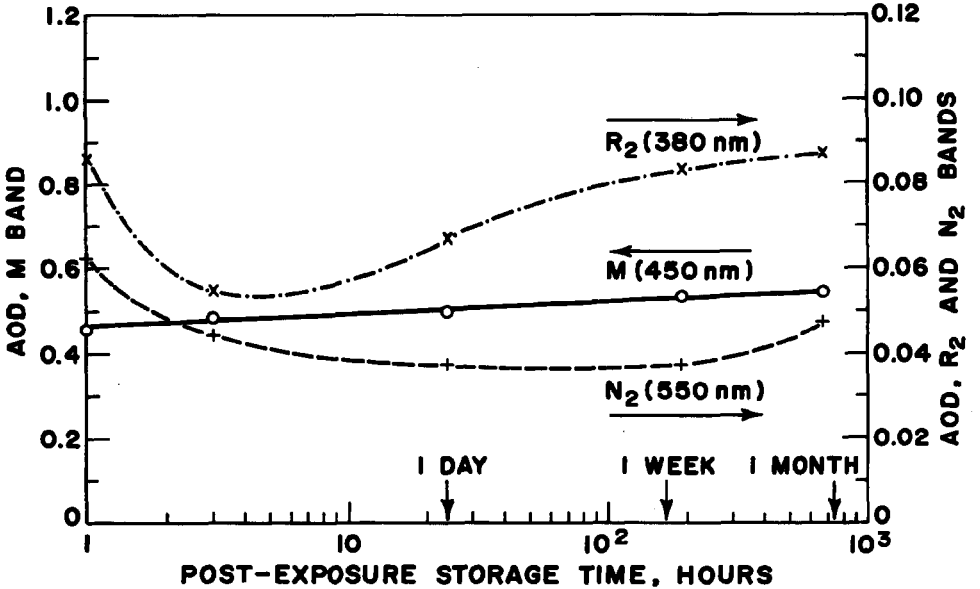

Fig. 6. Time-stability of absorption bands in Leitz LiF. $\approx 6 \times 10^6$ rad, ^{60}Co γ rays at $\approx 10^3$ rad/sec or 2 MeV Van de Graaff electrons at $\approx 10^4$ rad/sec. Ambient temp. ($\approx 25^\circ C$). PM-tube filters: M - #5562, R_2 - #5330, N_2 - #9780.

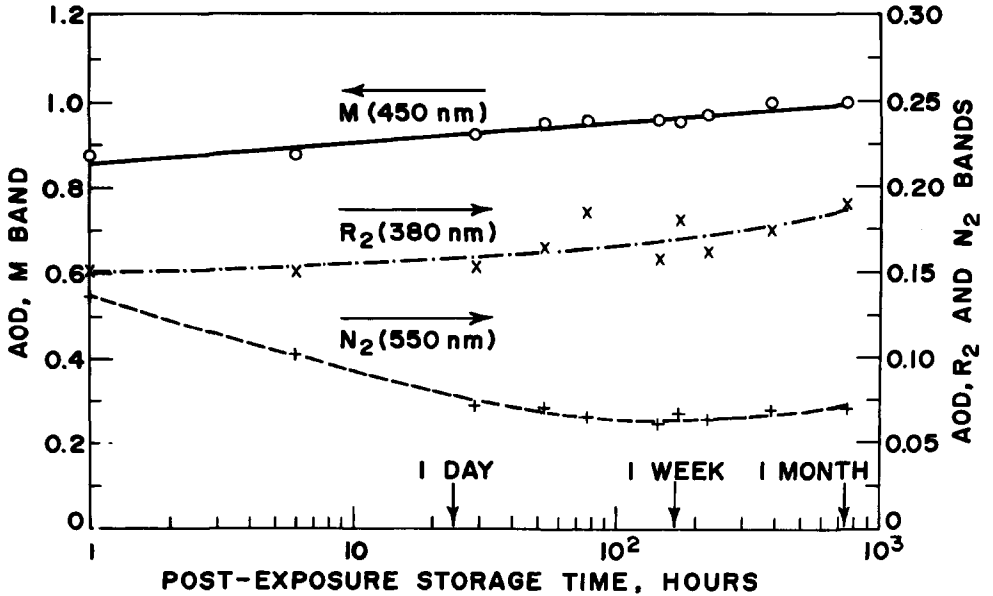

Fig. 7. Time-stability of absorption bands in Leitz LiF. 1.6×10^7 rad, 2 MeV-Van de Graaff-electrons at $\approx 10^4$ rad/sec. 20°C to 1 wk, ambient temp. ($\approx$ 25°C) thereafter. Filters as in Fig. 6.

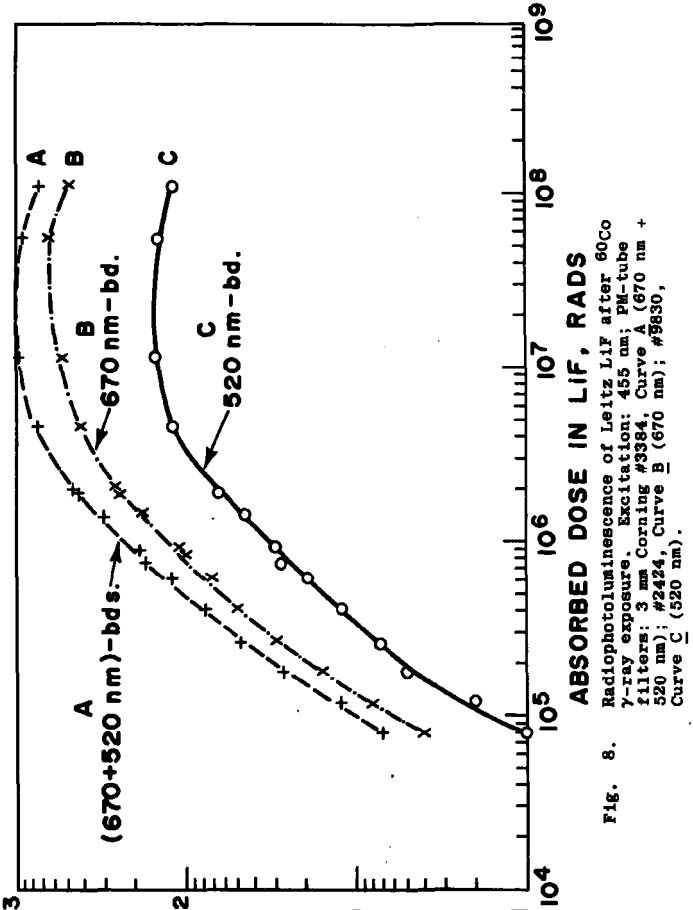

Fig. 8. Radiophotoluminescence of Leitz LiF after ^{60}Co γ-ray exposure. Excitation: 455 nm; PM-tube filters: 3 mm Corning #3384, Curve A (670 nm + 520 nm); #2424, Curve B (670 nm); #9830, Curve C (520 nm).

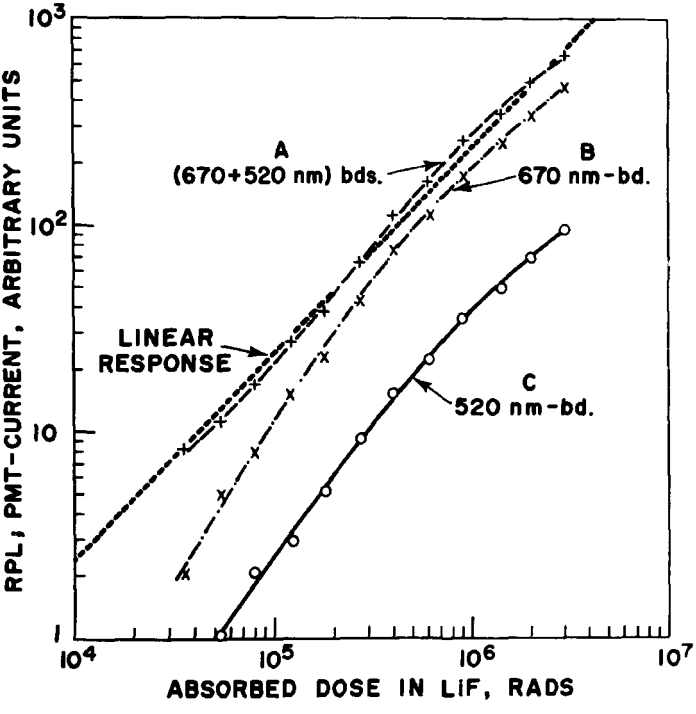

Fig. 9. Radiophotoluminescence of TLD-100 LiF after ^{60}Co γ-ray exposure. Excitation: 455 nm; Curves and filters as in Fig. 8.

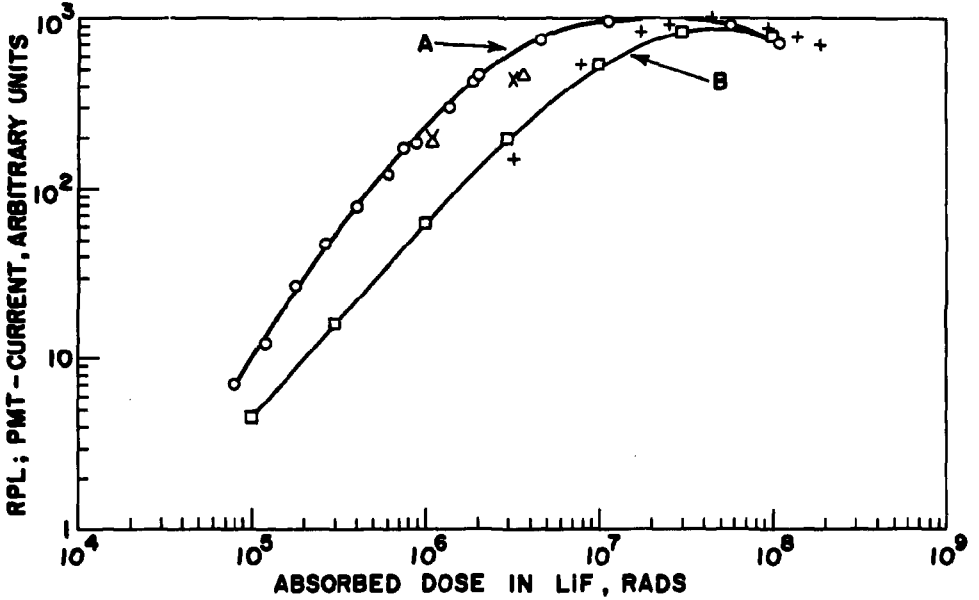

Fig. 10. Radiophotoluminescence of Leitz LiF after differing dose-rate-and-energy exposures. Combined 670 + 520 nm bands (Corning #3384 filter); 455 nm excitation. Curve A (same as A in Fig. 8), ^{60}Co γ rays; Curve B, 2 MeV electrons. All points as designated in Fig. 3.

Hillenkamp

If, as mentioned in your paper, the value measured for the optical density in reflection depends on grain size, geometrical conditions, etc., would it not be advisable to use an integration sphere arrangement to eliminate these effects?

Claffy

A Beckman "DK" reflectance spectrophotometer with integrating sphere was used in our preliminary survey. Use of an integrating sphere was sacrificed in the later experimental set-up in order to have a simple, inexpensive apparatus that would readily accomodate very small amounts of coarse-grained dosimetry powder as samples so long as it still gave some experimental measure of optical density.

Regulla

Did you investigate the emission spectrum of the pure LiF studied by you which might be different from that of LiF TLD-100 used by us?

Claffy

No, we did not. It is reported in the literature by Garlich and others that M-centre and R-centre luminescence in pure (undoped) LiF consists of 670 nm and 520 nm emission bands in differing proportions.

Regulla

Just as a comment I want to add that our RPL measurements with single crystals of LiF TLD-100 showed that there is a linear dose-effect relation between at least 10 R and more than 10^6 R, and it seems possible to extend the range further (details will be published in Health Physics).

Carlsson, C.

The large difference in apparent optical densities when the same absorbed dose in LiF is given by Co-60 gamma rays and 2 MeV electrons is remarkable,

especially as there is no difference between the response to 25 kV X-rays and Co-60 gamma rays. If this effect is true, it seems to be an excellent method of showing differences in LET-distributions in the region of very low LET-irradiation. It seems unlikely that such a small change in LET-distribution can give rise to such a large effect, so I just wonder whether the dosimetry is correct.

Claffy

We believe the dosimetry to be correct. However, the observed differences between the 2 MeV electron results and those for lower-energy photon irradiations are probably not related to LET differences, but rather to some unidentified energy-threshold effect.

Two Years Experience of Clinical Thermoluminescence Dosimetry at the Radiumhemmet, Stockholm

by

Bengt-Inge Rudén
National Institute of Radiation Protection
S-104 01 Stockholm 60, Sweden

Abstract

Thermoluminescent dosimeters (TLD) have been used extensively for patient dose measurements at the Radiumhemmet during recent years. About 17 000 clinical measurements were performed during 1970 and two thirds of these were made with TLD. The majority of the dose measurements were performed with dosimeters containing LiF, but $Li_2B_4O_7$:Mn and $CaSO_4$:Mn were also employed.

The precision of the dosimeters is within ± 2% provided an individual calibration schedule is used. Calibrations have been performed to ascertain the differences in sensitivity for various radiation energies. The conversion of dosimeter reading to absorbed dose in tissue is included in these calibrations. The clinical TLD applications that are discussed include routine measurements for ^{60}Co γ-rays 6 - 42 MV x-rays and 5 - 39 MeV electrons; verification through intracavitary and intravenous measurements of the dose distributions obtained in patients; determination of absorbed dose from beta emitters; and investigation of neutron contamination in the use of high radiation energies.

Introduction

R. Sievert began experiments with a new method of radiation measurements in 1926. This lead to the design of an ionization chamber which was entirely separated from the measuring instrument. Later on another ionization chamber was developed by Sievert [1], which was usable for larger exposures. The latter chamber become a routine tool in measurements at the Radiumhemmet. The total number of annual measurements using this so called condenser chamber was about 10 000 in 1940 and the number has since increased.

Difficulties in the use of these ionization chambers became evident in conjunction with the commencement of high energy x-ray and electron irradiation around 1968. Thermoluminescent dosimeters were therefore introduced in the determinations of doses in routine therapy. During 1970 the number of clinical measurements amounted to 17 000 of which two thirds were made with TLD. During 1971 the number of TLD measurements has further increased. Both disc and rod-shaped dosimeters have been used. The majority of the dosimeters used contains LiF but dosimeters holding $Li_2B_4O_2$:Mn and $CaSO_4$:Mn have also been employed.

Read-out apparatus and thermal treatment of the dosimeters.

In clinical routine the thermoluminescence of the dosimeters was measured with a Harshaw apparatus (Model 2000). For research purposes a modified Con-Rad read out unit (Model 5100 A) was used. The modification of the latter implied that a feed-back operational amplifier (Keithley 301) was substituted for the original electrometer amplifier. A digital voltmeter has been connected to this amplifier. The advantages are that the drift and noise is considerably reduced. The photomultiplier has also been replaced by the more sensitive EMI 9514SA.

Thermal treatment of the LiF-dosimeters before they have been exposed to ionising radiation (pre-annealing) depends on the type of application of the dosimeters. In some measurements fading influences the accuracy appreciably. This is, for instance, the case in situations where difficulties are encoun-

tered in keeping the time between exposure and read out constant and when continuous exposure during prolonged periods is used. This occurs for patient dose measurements as well as for radiation protection measurements. We have then used the following thermal treatment; for teflon dosimeters 30 min at 300°C and for Harshaw ribbons and rods 60 min at 400°C and 24 hours at 80°C pre-annealing and 15 min at 80°C before read-out. Separate ovens have been used for the various thermal treatments. In measurements where we were able to cancel the effect of fading the heating during the read-out procedure was used as the only method for pre-annealing [2]. In such measurements the time interval between the irradiation and the read-out of a dosimeter was kept the same in both calibration and experiment. In order to allow identical coding-cycles for all the dosimeters they have been retained in the read-out apparatus 1 min after the integration was completed.

The energy response to high energy electron and photon radiation of thin LiF-teflon dosimeters

The dosimeters used in this investigation were 0.1 mm thick LiF-teflon dosimeters Li7, Li6 and LiN (Isotopes Inc). The thermoluminescence of the LiF was measured in the modified Con-Rad read-out unit. The dosimeters were irradiated with ^{60}Co γ-rays, high energy electrons and x-rays in a polystyrene phantom. When ^{60}Co and 6 MV x-rays were employed the dosimeters were placed at a depth of 5 cm. When 42 MV x-rays were used the depth was 10 cm and when the electron energies at the surface were 5, 7.5 and 10 to 39 MeV, the depth were 1.0, 1.5 and 2.4 cm respectively.

The absorbed dose in water was obtained from ionization chamber measurements (Siemens Sondfingerrmtkammer) in the polystyrene phantom by a true two step process. First the ionisation measurement was converted to absorbed dose in polystyrene and secondly the absorbed dose in polystyrene was converted to absorbed dose in water. In the latter case we use the appropriate dose conversion factor for polystyrene for photons recommended by the American Association of Physicists in Medicine [3] and the dose conversion factor for electrons experimentally verified by Almond [4].

The calibration of the electron beam was performed with a Siemens Sondfingerrmtkammer according to the method described by Svensson and Pettersson [5]. The LiF-dosimeters were in all cases given a dose between 180 and 200 rad. The relative sensitivity was defined as the thermoluminescent response per rad in water for various radiations of different energies divided by the thermoluminescent response per rad in water for ^{60}Co γ-rays. The results of the experimental measurements are listed in Table 1.

Table 1. Measured response of thin LiF-teflon dosimeters Types 7, 6 and N to various radiations relative to ^{60}Co γ-rays

Electron radiation						Photon radiation			
Energy at surface MeV	Ref. depth cm	Av. energy at ref. depth MeV	7	6	N	Rad. quality	7	6	N
4.3	1.0	2.2	0.94	0.94	0.93	^{60}Co	1.00	1.00	1.00
7.4	1.5	4.1	0.93	0.92	0.92	6 MV	1.00	1.00	1.00
9.8	2.4	4.9	0.93	0.94	0.92	42 MV	0.99	1.09	1.01
11.6	2.4	6.7	0.93	0.95	0.93				
14.3	2.4	9.6	0.95	0.95	0.94				
19.4	2.4	14.7	0.95	0.95	0.95				
28.2	2.4	23.5	0.97	0.96	0.97				
39.2	2.4	34.5	0.98	0.98	0.98				

The observation was made that there is no difference (within the experimental error of ± 2 %) between the response of the different dosimeters for various electron energies. The dosimeters had a 7 - 5 % decrease in sensitivity between 2 and 15 MeV electron energy and about 3 % decrease in sensitivity for higher electron energies. For the studies will be made to investigate the possibility of explaining these results using cavity theory. The trend in the experiment is that the change in sensitivity of the dosimeters between 2 and 35 MeV is the same as the change with energy of the mass stopping power ratio, $S^{LiF}_{H_2O}$.

Our results show a decrease in sensitivity of less magnitude than that reported by Binks [6] and Almond [7], the difference probably being due to differences in the thickness of the dosimeters. These authors have used loose powder in a polystyrene tube. The sensitivity of the dosimeters used did not differ when 6 MV x-rays was employed. Furthermore the sensitivity for 6 MV x-rays was the same as for ^{60}Co γ-rays [8]. LiF has the same sensitivity for 42 MV x-rays as for ^{60}Co γ-rays, LiN shows a slight increase and Li6 about 10 % increase in sensitivity. The large increase of the sensitivity for Li6 and the slight increase for LiN for 42 MV x-rays depend on the large cross section of ^{6}Li for thermal neutrons. With high energy roentgen rays, neutron radiation is produced through nuclear reactions in materials with high Z in the betatron. This is further discussed in a later section.

Patient dose measurements

The verification of doses aimed at in the routine external beam therapy has been achieved, on the one hand by entrance and exit dose determinations and, on the other hand by measurements of doses in accessable body cavities. LiF-teflon discs (ϕ 8 mm, thickness 0.5 mm) have been employed for the entrance and exit dose measurements while extruded LiF rods, inserted in presterilized teflon catheters have been introduced for instance in the esophagus or in veins. High sensitivity ribbons have been utilized for the determination of doses, which represent only minor fractions of the therapeutic dose. Such measurements are of importance for instance for the estimation of dose contribution to organs, in which relatively small radiation doses might be particularly undesirable, e.g. the eyes and the gonads.

The dosimeters have been divided into separate groups, each containing 25. Calibration constants in rad/digit have been assigned to the individual dosimeters after calibration procedures. In addition, five dosimeters have been used for calibration purposes in connection with every measurement occasion. The change in the calibration constant for these five dosimeters which thereby was obtained was applied to all the other dosimeters included in the same group. Such a procedure was made possible by running all dosimeters within the group through exactly the same thermal treatment and cooling procedure [9]. It was observed that when a new dosimeter was employed its sensitivity increased markedly during the first applications. Comparing the quotients between the individual calibration constants and the preceding constants for the same dosimeters showed, however, that the variation between the dosimeters of the changes was always less than ± 2 %. At intervals all the dosimeters have been recalibrated in order to check their individual calibration constants. The dosimeters in a few groups have now been utilized more than 150 times but still the accuracy of dose determination remained at the same level as initially.

When in connection with external γ and x-ray therapy the reference dose is to be determined, two LiF-teflon discs are placed in a specially designed build-up cap (Fig. 1). This is attached to the body surface in the center of the beam. The thickness of the build-up layer has been 4 mm in a ^{60}Co beam and 15 mm in a 6 and 42 MV x-ray beam. The thickness of 15 mm is too small, however, when the reference dose from 42 MV x-rays is determined. Therefore a correction factor derived from depth-dose curves must be applied. These correction factors have been determined through measurements. They are

dependent upon the focus-skin distance and upon the size of the field and amounts to maximum 1.25.

When the reference dose is determined in connection with electron therapy a build-up cap is not used routinely. The relation between the surface dose thereby determined and the dose at the maximum build-up level varies, however, with the energy of the electrons. In order to arrive at information about the dose at the maximum build-up level, correction factors, maximum 1.30, must be applied. The magnitude of these factors is dependent on both the energy and on the size of the tube, and they have been determined through measurements.

Determination of dose distribution in the pelvis in gynaecologic, intracavitary radiation therapy

The availability during recent years of lithium fluoride thermoluminescent dosimeters in solid forms in a variety of shapes has led to their use for the determination of dose in narrow body cavities, such as blood vessels, preferably on the venous side. LiF rods have been used, for example, for the characterization of pelvic dose distribution at intracavitary treatment of carcinoma of the uterine cervix [10, 11]. The dosimeters in the latter investigations at Radiumhemmet were introduced in presterilized teflon catheters, inserted in the external iliac and common iliac veins from transcutaneous punctures in the inguinal regions (Fig. 2). The catheters remained in the vessels for treatment periods of up to 30 hours without any untoward reactions. In addition, LiF dosimeters were used close to the irradiators, e.g. in the urinary bladder and in the rectum. The use of lead spacers in between the LiF rods made it possible to determine the correlation between measurement locations and actual pelvic anatomy from ordinary orthogonal radiographs. In an investigation performed as a cooperative project of the departments of Gynaecology and Clinical Radiation Physics at the Radiumhemmet and the Unité de Radiophysique, Institut Gustave Roussy in Paris the correspondance was tested between computer calculated doses in various portions of the pelvis and the doses in the same sites measured with the LiF dosimeters. A marked discrepancy was observed at several cm distance from the irradiators, which necessitated detailed and precise experimental tests using a polystyrene phantom, (Fig. 3). Even though the phantom was constructed with the aim of arriving at a constant interrelationship between radiation sources and dosimeters it was observed that in the phantom the average difference between repeated dose determinations in the same locations was 6 %. The average variability of the calibration constants for the dosimeters used, however, was 1.0 %, maximum 2.0 %. The difference in precision may be explained by the difficulty, even in phantom experiments, of obtaining a constant interrelationship between the irradiators and dosimeters.

It was concluded as a result of the study that the movement in the caudal and in the dorsal direction of the irradiators during prolonged treatment periods accounted for the major part of the difference between the actual dose level in a certain specified point, measured with LiF, and the calculated dose in the same position. The calculation by computer is namely based upon cartesian coordinates in space of the radium needles as determined from localization roentgenograms exposed once only during the whole course of continuous irradiation. The solution might be the retrieval of information from respect localization roentgenograms or - better - the use of light weight radiation sources, fixed to the patient by use of individual moulds.

Calibration of LiF teflon rods to internal LiF beta-ray dosimetry

In vivo measurements of the radiation dose from pure beta-emitters is sometimes of interest, e.g. in the estimation of the dose to the epithelial lining of the gastrointestinal tract from non-absorbable radioactive compounds, administered orally.

LiF teflon rod dosimeters are convenient for such dose measurements. They need, however, calibration since the dose absorbed in them and probably also the relative light output from them will depend on the spectrum of beta particles that has impinged on them. Furthermore a rod dosimeter which has been immersed in a beta-radioactive solution will be exposed to a lower dose-rate than the solution itself due to the replacement of activity with the volume of the rod. Aqueous solutions of various beta-emitting nuclides were used as radiation sources. Neglecting second order effects due to the shape of the beta spectrum, the mean beta-energy should be a good measure of the range of the electrons.

The radionuclides used were (mean energy in MeV given within parentheses): ^{35}S (0.049), ^{99}Tc (0.094), ^{204}Tl (0.24), ^{32}P (0,69) and ^{90}Y (0.90).

The LiF rods were calibrated individually using ^{60}Co-radiation from a therapy unit. The beta dose from the different radionuclides was calculated from the exposure time and dose-rate formula $dD/dt = 51.2 \times 10^4 \times \bar{E} \times C$ rad/day wher C is the radionuclide concentration in Ci/kg and $\bar{E}$ is the mean energy in MeV.

The results are given in Fig. 4 as the quotient between the dose related to ^{60}Co-calibration factor (measured dose) and the beta-dose in the surrounding medium obtained from the dose-rate formula (calculated dose). The term "dose related to the ^{60}Co-calibration" refers to the relative light output normalized in such a way that 1 unit corresponds approximately to 1 rad in the dosimeter from ^{60}Co gamma radiation. The dosimeters act as solid state cavities and the dose was calculated using the general cavity theory derived by Burlin [12]. The approximation involved in the calculations gives an error of less than 3 per cent. The precision of the dosimeters is found to be within $\pm$ 3 per cent and the maximum error in the quotient is indicated in the figure.

A comparison between the experimental results of Kastner et al. [13] who used powder and single crystals of LiF (ø 0.1 and 0.2 mm), and the results obtained in this study when the LiF rods were completely surrounded by radioactive liquid show that the self-shielding effect plays an important role over the entire electron range studied. The results of theoretical calculations of Lindgren et al. [14] of the integral dose to infinitely long teflon cylinders (ø 1 mm) immersed in homogeneous solutions of ^{90}Sr and ^{90}Y seem to indicate that a possible dead surface layer does not yield a substantial effect since theory and experiment are in good agreement (within the limits of experimental error). This would also be consistent with a negligible dependence of light output per rad in the dosimeter material on the incident electron energy. LiF rods should be useful as dosimeters for pure beta emitters after calibration on theoretical calculations have been made to account for self-shielding.

In figure 4, curve b gives the quotient between the dose related to the calibration factor and the calculated dose at a point on the interior wall of the cylinder containing the beta sources (the latter dose is twice that in the liquid). At mean beta-energies lower than about 0.20 MeV the dose related to the ^{60}Co calibration factor is approximately the same for both these geometries which means that it does not matter if the dosimeters are pressed against the interior wall or completely surrounded by radioactive solution.

Measurements of dose contribution from neutrons with thin LiF teflon discs

During radiotherapeutic treatment with high-energy roentgen and electron-rays, neutron and proton radiation with high relative biological efficiency is produced through nuclear reactions in the patient, the collimators, the beam flattering filter and in those parts of t betatron which are made of materials with high Z. The neutrons are very penetrating and they contribute irradiation to the whole patient and even cause radiation protection problems for the staff.

With our measurements of the neutron radiation produced in the treatment room of the betatron, using 42 MV x-rays we have employed 0.1 mm thick LiF teflon discs of Li6 and Li7 (Isotopes inc.).

Li6 and Li7 teflon discs have been calibrated for fast and thermal neutrons. Fast monoenergetic neutrons with energies of 0.13, 1.0 and 2.0 MeV have been generated using a Van de Graaf apparatus. Thermal neutrons were obtained from two Po- Be-sources with activities of 2 Ci each. Polyethene, water and graphite were used as moderators. The dosimeters were surrounded by a 1 mm layer of tin with the aim of shielding them from the influence of protons. It was shown that Li6 and Li7 had a very low sensitivity for fast neutrons. The sensitivity found for fast neutrons was 5×10^{-10} rad/n x cm^{-2} which corresponds to the data published by Schietser and Gibson [15]. The unit of light output is defined as that obtained after placing the dosimeter in water and the absorbed dose in water using 1 rad. Using thermal neutrons, Li6 was observed to be more sensitive than Li7 with a factor of 160. In addition, the sensitivity of Li6 was 550 times higher for thermal neutrons than for photons (^{60}Co γ rays) per rad in water.

Preliminary experiments have been carried out in order to determine the thermal neutron dose using Li6 and Li7. As a consequence of the low sensitivity of the dosimeters for fast neutrons the contribution to the total dose from the fast neutron fluence generated in the betatron is less than the least detectable dose for these dosimeters. The photon dose at 42 MV x-rays was measured with Li7 in a water phantom in which dosimeters were placed both inside and outside the beam. This latter dose value was subtracted from the total dose measured with Li6. The results are listed in Table 2.

Table 2. Results of measurements in a water phantom. Absorbed dose from thermal neutrons (mrad/rad[m] in water).

Depth cm	Inside beam	Outside beam
5	0.086 ± 0.004	0.063 ± 0.014
15	0.050 ± 0.005	0.028 ± 0.008
40	0.027 ± 0.008	0.006 ± 0.001

[m]Photon-dose measured in water at the maximum point of the depth-dose curve

The values measured in the centre of the beam are uncertain because the difference between total dose and thermal neutron dose is only 10 %. In comparison, the quotient Li6/Li7 dose determination outside the beam amounts to 3 to 5.

Measurements of the neutron dose were also performed in the treatment room of the 42 MeV betatron with the Li6 and Li7 dosimeters surrounded by paraffin in a 8 cm thick layer. With such an arrangement the dose contribution from fast neutrons was determined. It was observed that the total neutron dose was in good agreement with the dose obtained by using a rem counter.

In order to measure the neutron dose affecting various organs in connection with abdominal irradiation a Temex-phantom was used in a 42 MV x-ray beam. If a dose of 5000 rad was given the neutron dose the the eyes amounted to 1.2 rem (QF = 20). The photon dose due to secondary irradiation was observed to be 3 rem.

From the results of the study it has been verified that Li6 and Li7 dosimeters can be used for the determination of the thermal neutron dose when irradiation is administered with 42 MV x-rays. The contribution from fast neutrons can be assessed by using $CaSO_4$:Mn teflon dosimeters.

Conclusion

It is apparent from the examples above that TLD can be widely applied in

the medical physics and that many difficult problems in dosimetry can now be solved by the use of thermoluminescent dosimeters.

Acknowledgement

This studies supported by grants from the Cancer Society of Stockholm and the King Gustaf V Jubilee Fund.

References

1. R. Sievert, Acta Radiol. Suppl. XIV (1932).

2. C.A. Carlsson, B. Mårtensson, and G.A. Carlsson, Second Int. Conf. Luminescence Dosimetry, Gathlingburg, 936-939 (1968).

3. The American Association of Physicists in Medicine, Phys. Med. Biol. 16, 379-396 (1971).

4. P.R. Almond, Int. J. of Appl. Rad. and Isotop. 21, 1-3 (1970).

5. H. Svensson and C. Pettersson, Arkiv för fysik 34, 377-384 (1957).

6. C. Binks, Phys. Med. Biol. 14, 327-328 (1969).

7. P.R. Almond, and K. Mc Ray, Phys. Med. Biol. 15, 335-342 (1970).

8. C.J. Karzmark and J. Geisselsoder, Second Int. Conf. Luminescence Dosimetry, Gathlingburg, 400-409 (1968).

9. B. Mårtensson, Phys. Med. Biol. 14, 119-130 (1969).

10. J.M. Johansson, B.Å.A. Lindskoug, and C.E. Nyström, Acta Radiol. 8, 360-372 (1969).

11. I. Joelsson, A. Bäckström, J. Diehl and C. Lagergren, Acta Radiol. 9, 33-54 (1970).

12. T.E. Burlin, Br. J. Radiol. 39, 727-734 (1966).

13. J. Kastner, R. Hukkoo, B.C. Oltman and Y. Dayal, Radiat. Res. 32, 625-640 (1967).

14. D. Lindgren, G. Eriksson and L. Ehrenberg, Mutation Res. 10, 335-351 (1970).

15. M. Schietzer and N.N. Gibson, NDL-TM-52, USAMDL (1968).

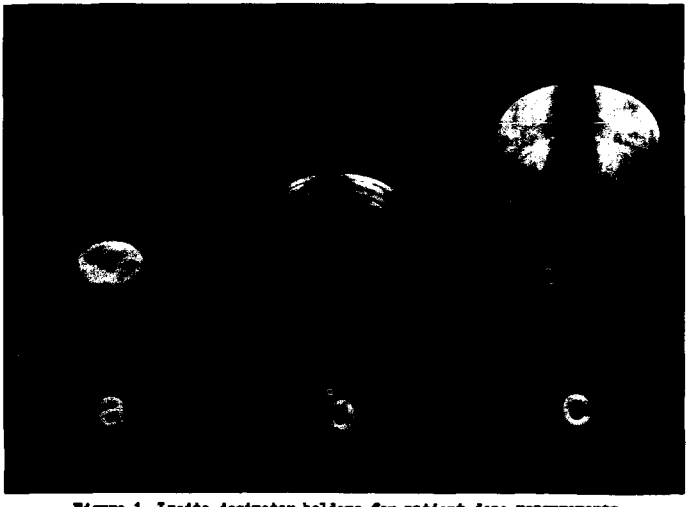

Figure 1. Lucite dosimeter holders for patient dose measurements.

a. The bottom of a holder containing two dosimeters.
b. The holder used for ^{60}Co γ rays.
c. The holder used for 6 and 42 MV x-rays.

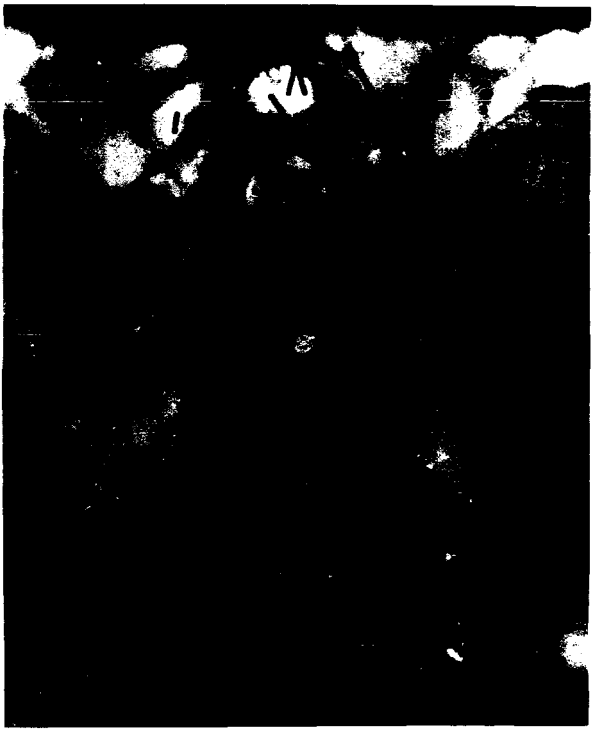

Figure 2. Roentgenogram in ap projection of one of the patients during the course of treatment. The intrauterine radium cylinder and the intravaginal box are held in place by means of gauze tampoon, packed into the vagina. LiF dosimeters, interspaced with lead rods, inserted in tephlon catheters, are introduced in the external and common iliac veins. LiF dosimeters are also placed in the urinary bladder and in the rectum.

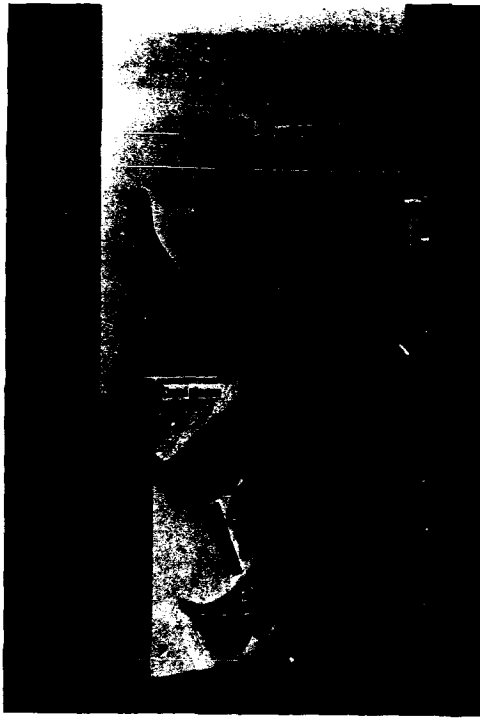

Figure 3. The phantom used for the investigation of the correspondance between calculated and measured doses about the combination of a cylinder and a box loaded with radium consisted of three parts. In the central phantom locations equivalent to bladder and rectum, and in the first wing phantom location mimicking the external pelvic veins, were arranged. The second wing phantom was used to represent the conditions prevailing in the region of the common iliac veins.

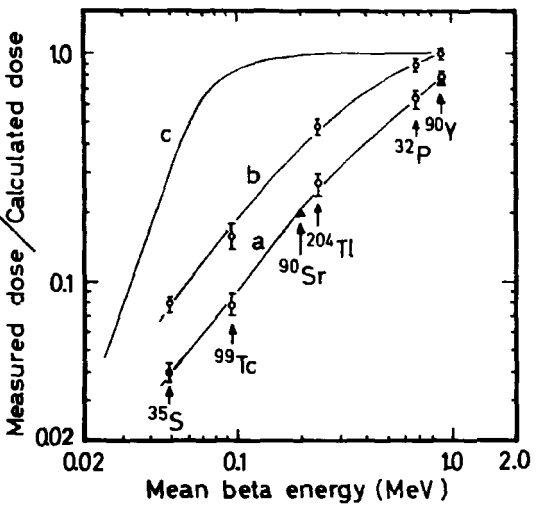

Figure 4. The ratio between the dose related to the ^{60}Co calibration factor (measured dose) and calculated dose for LiF powder and LiF teflon rods (ø 1 mm and length 6 mm) as a function of the mean beta energy. Curve a gives the ratio for dosimeters completely surrounded by radioactive liquid and curve b the ratio for dosimeters pressed against the wall of the exposure vessel. Curve c is reproduced from Kastner et al. who used LiF powder. The ratios for ^{90}Sr and ^{90}Y calculated from data given by Lindgren et al. are marked with ▲.

Suntharalingam

Your energy response data for both high-energy photons and high-energy electrons are different from previously published data. I tend to agree with your photon data, but could you explain why you see a 6% drop in sensitivity for 2 and 4 MeV electrons compared to the 6 MV photon beam?

Ruden

My energy response data for electron energies between 2 and 15 MeV are not different from previously published data. I cannot at this moment explain why there is a 6% decrease in sensitivity for 2 and 4 MeV electrons as compared to 6 MV X-rays, but I hope the results can be explained by cavity theory.

Thermoluminescence Dosimetry for Clinical Use in Radiation Therapy

by

David S. Gooden, Ph.D.* and T. J. Brickner, Jr., M.D.

St. Francis Hospital
and
The William K. Warren Medical Research Center
Tulsa, Oklahoma 74135, U.S.A.

Abstract

A complete thermoluminescence dosimetry system for use in radiation therapy is presented with a description of new techniques for dosimeter pairing, grouping, calibration and annealing. TLD-100 High Sensitivity Ribbons are proposed as the dosimeter of choice for routine dosimetry within a radiation therapy facility. The importance of a TL reader with a "two cycle" readout in which the luminescence associated with low temperature peaks is ignored is discussed. This TLD system lends itself well to routine dosimetry of a multitude of treatment techniques in a busy clinical practice. The entire system can be operated by a trained radiation therapy technician. The system is used within our department for external beam dosimetry, intracavitary dosimetry, calibration of treatment cones, experimental set-ups and others. It has shown an accuracy of better

---

* Consultant to the Eberline Instrument Corporation.

than ±2% under experimental conditions, and an estimated clinical accuracy of better than ±4%.

Introduction

It appears that a relation between thermoluminescence and ionizing radiation may have been observed as early as 1904[1]; however, it was not suggested as a dosimetry technique until much later. We are all familiar with the work of Farrington Daniel at the University of Wisconsin in the late 1940's and early 1950's and his unsuccessful attempts to interest people in the use of thermoluminescence techniques for radiation dosimetry. In the 1960's Dr. John Cameron revitalized the work which had been begun by Daniels and gave thermoluminescence techniques the impetus they needed to become a recognized dosimetry method.

Even now we feel that thermoluminescence dosimetry (TLD) has still not obtained the acceptance it deserves. This is especially true in the area of medical radiation therapy. The capabilities of good TLD are needed everywhere radiation therapy is practiced. Such capabilities can help assure good patient care and a more uniform delivery and reporting of radiation doses between existing radiation therapy facilities. It would be foolish to say that good radiation therapy cannot be practiced without the capabilities of good TLD; however, we certainly feel that these capabilities compliment a total program.

Unfortunately, we who would most like to see the techniques of thermoluminescence dosimetry widely accepted are largely to blame for the lack of acceptance. Even the most thorough reading of the literature available on the subject would leave many confused and reluctant to engage in the setting up of a TLD program for routine use. We feel that individuals who are knowledgeable in thermoluminescence techniques have an obligation to put the "dosimetry" back in TLD.

In light of what luminescence dosimetry has come to mean in the last half decade, neither of us can hold ourselves to be experts in this extensive field. However, we do feel qualified to discuss the thermoluminescence dosimetry of X- and gamma radiation within a radiation therapy facility.

Choice of Dosimeters for Routine Dosimetry

Although the TL reader is the heart of any T_D system we choose to discuss it last since the other considerations often influence the choice of readers. One of the most important decisions the TLD user must make is the choice of dosimeter material and its physical form. The user is faced with a wide selection of thermoluminescence dosimeters which include not only different compounds, such as lithium fluoride, calcium fluoride, and others, but also many different physical forms and shapes. Physical forms include powder, impregnated teflon dosimeters, glass encapsulated dosimeters and relatively new extruded solid dosimeters[2]. Harshaw Chemical Company* now supplies three different solid dosimeters as lithium fluoride (TLD-100, TLD-600, and TLD-700). Extruded dosimeters in other compounds are also available.

One of the most recently developed solid lithium fluoride dosimeters is the "High Sensitivity Ribbon"[2]. The standard geometry for this material is 1/8" x 1/8" x 0.035" and the mass of the dosimeters is approximately 25 milligrams (see Figure 1). The dosimeter consists of lithium fluoride without dilutant binder and is made of standardized lithium fluoride TLD powder using controlled temperature and pressure**.

We feel that presently lithium fluoride TLD-100 High Sensitivity Ribbon is unequivocally the best dosimeter for routine dosimetry in radiation therapy. Some of the advantages of the High Sensitivity Ribbon include optical transparency, mechanical ruggedness, capability of individualized calibration, small size, extended use and handling convenience[2].

The characteristics of TLD-100 have been well documented and are essentially "made to order" for radiation therapy applications. These characteristics include wide exposure ranges,[3,4,5] high exposure rate independence,[6,7] low energy dependence,[8,9] approximate tissue equivalence[2] and long term response retention.[10,11] The superlinearity with increasing exposure for TLD-100 has been discussed by several investigators[1,2,12].

---

* 6801 Cochran Road, Solon, Ohio 44139.

** U.S. Patent No. 3320180.

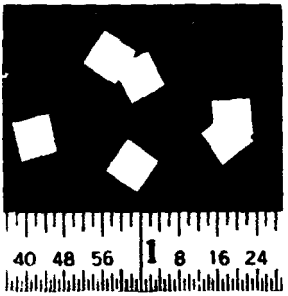

FIGURE 1: HARSHAW'S HIGH SENSITIVITY RIBBONS (1/8" x 1/8" x 0.035")

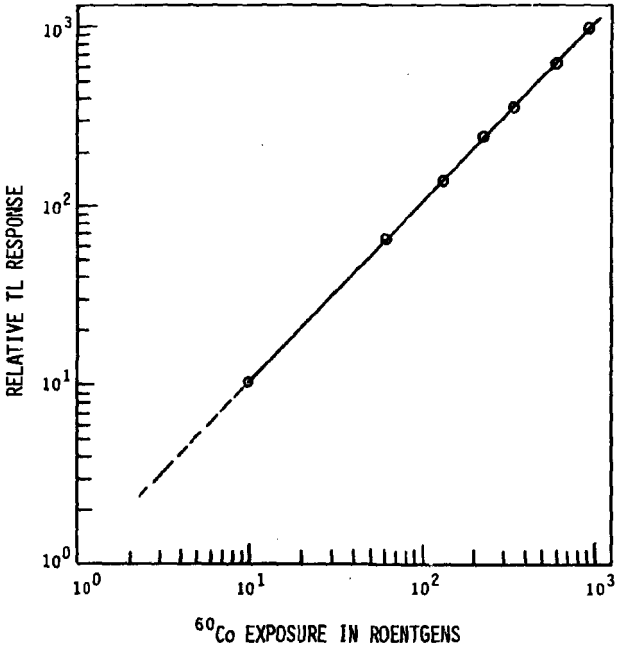

FIGURE 2: TL RESPONSE VS. ^{60}Co EXPOSURE

There is general agreement that superlinearity occurs above 1,000 R. However, in the exposure range of interest in radiation therapy (10-1,000 R), we have found the response of TLD-100 High Sensitivity Ribbons to be strictly linear (see Figure 2). The TL response versus photon energy for TLD-100 is also a parameter which has been investigated and reported.[1,2] Again, it is generally agreed that lithium fluoride exhibits the best linearity of response for photons with energies from 10 keV to many meV available today. However, for high accuracy dosimetry in radiation therapy sections the TL response per/R must be checked for each modality used to deliver radiation.

Readout Mechanism for Routine Dosimetry

The type of instrument readout is very important for routine dosimetry. A recording of the glow curve carries the most information; however, it is awkward and time consuming for routine dosimetry uses. The total integrated "counts" under the glow curve can also be used as the readout mechanism. This is convenient for routine applications; however, it has the disadvantage of including information from low temperature peaks which are rather unsuitable for dosimetry purposes. The "peak count rate" readout eliminates the problem for low temperature peaks but necessitates a highly reproducible temperature cycle and does not include all usable information associated with the high temperature peaks.

We feel that for dosimetry purposes the best readout mechanism is a "two cycle" one. During the first part of the cycle, the pan temperature is elevated and the unstable low temperature peaks are dumped with no counts recorded. During the second cycle, the pan temperature rises rapidly and the total counts are integrated for the luminescence associated with the high temperature peaks.

Figure 3 shows the two cycle readout sequence used in our TLD program. During the first part of the cycle (10 seconds), the pan temperature rises to 150° C. The low temperature peaks are dumped during this cycle with no counts recorded. During the second portion of the cycle (10 seconds), the pan temperature rises to 250° C. All luminescence associated with the

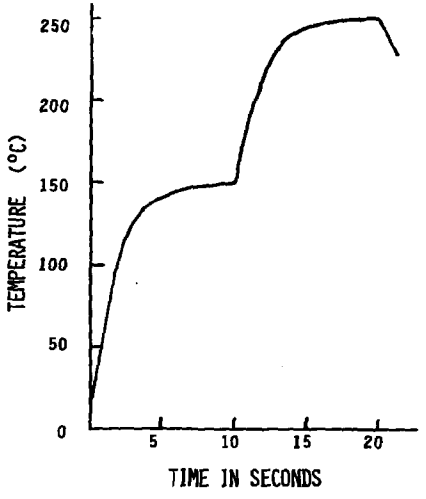

FIGURE 3: TWO CYCLE HEATING SEQUENCE FOR DOSIMETRY APPLICATIONS

FIGURE 4: SLOTTED STAINLESS STEEL PLATE USED TO HOLD RIBBONS DURING ANNEALING

second portion of the cycle is integrated and displayed as a 5 digit number on Nixie tubes.

A New Annealing Procedure for Use with the Two Cycle Readout

There are many annealing procedures (both pre- and post-irradiation) which have been reported in the literature for TLD-100.[1,13,14] Most of these procedures have been designed to minimize the influence of low temperature peaks which are unsuitable for dosimetry purposes. The use of a two cycle readout in which the low temperature peaks are dumped has allowed us to use a very simple pre-irradiation annealing procedure. This technique consists of placing exposed dosimeters in an oven pre-heated to 400° C. The pre-heat of 400° C should take approximately 8 hours to insure that equilibrium conditions are present. After placing dosimeters in the oven, the oven is left in the "On" position for 15 minutes and then is turned to the "Off" position. The dosimeters are allowed to gradually cool down within the oven. The cooling process takes approximately 10 hours to obtain equilibrium with room temperature. A slotted plate of stainless steel is used to hold the dosimeters during the annealing process (see Figure 4).

This annealing procedure is quite attractive for routine clinical dosimetry purposes. With this technique the oven can be turned to the "On" position at early morning and allowed to remain on throughout the day. At the end of the day any dosimeters which have been irradiated can be placed in the oven and the oven turned to the "Off" position after 15 minutes. The annealed dosimeters will be ready for use the next morning

As can be seen from Figure 5, this annealing procedure causes rather prominent low temperature peaks. However, since these are dumped during the first portion of the readout cycle, they do not effect high accuracy dosimetry. Our annealing procedure seems to enhance sensitivity of TLD-100 relative to the "standard annealing procedure". We have noticed increases in sensitivity of up to approximately 30% during the first several annealings; however, this seems to level out and variations in sensitivity between annealings become only a few percent. It

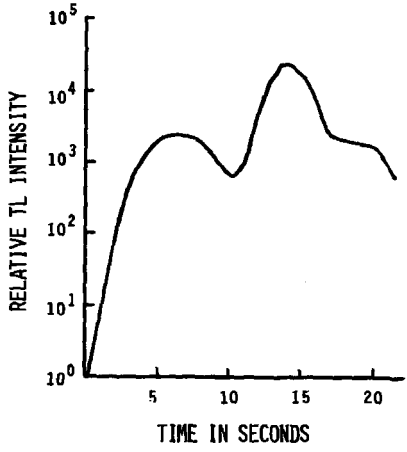

FIGURE 5: TYPICAL TL RESPONSE CURVE (300 R) USING TWO CYCLE HEATING SEQUENCE AND 400° C PRE-IRRADIATION ANNEALING WITH GRADUAL COOLING.

FIGURE 6: DOSIMETERS BEING PREPARED FOR IRRADIATION. THE DOSIMETERS ARE ARRANGED IN ROWS AND COLUMNS SO THAT THE POSITION OF EACH DOSIMETER IS KNOWN.

should be pointed out, however, that for high accuracy dosimetry calibrations it must be performed after each annealing.

Dosimeter Calibration and "Grouping"

The most important part of any TLD program is calibration. Dr. Cameron said it quite well, "TL dosimeters are not absolute radiation detectors; there is no direct way to relate the TL release from an irradiated sample to the amount of radiation exposure or to the rad dose received by the dosimeter material. Consequently, all TLD systems must be calibrated...and the accuracy of the overall result can be no greater than the accuracy of the calibration."[1] These words should be carved in rock and stand as the cornerstone for every institution using TLD. Unfortunately, calibration for high accuracy dosimetry is a personal thing. It cannot be done at the factory; it must be accomplished at the facility using the system. It is also a continuing thing; the TLD user must know at all times how his system (reader + dosimeters) is responding.

For routine dosimetry it is also important to establish large sets of dosimeters with the same sensitivity. The extruding process presently used by Harshaw produces large batches of TLD-100 High Sensitivity Ribbons of amazingly similar sensitivities. Batches of 50,000 dosimeters have been produced in which the luminescence associated with an exposure of 1 R of Cobalt 60 radiation exhibited a standard deviation of only 2% and extremes of only ±6%.[15] Although the technological ability to produce these larger batches with such narrow sensitivity limits is indeed admirable, the limits are still too large for high accuracy dosimetry in radiation therapy.

To establish large sets of dosimeters with narrow sensitivity limits, we recommend a procedure of pairing dosimeters. This procedure provides an increase in sensitivity of approximately 2, since the High Sensitivity Ribbons are used as pairs. We have found that we can routinely establish large groups (50-100 dosimeter pairs) with extreme readings within ±2% of the mean. Our procedures for "pairing" and calibrating are discussed below.

1) A reasonably large set of TLD-100 High Sensitivity

Ribbons (1/8" x 1/8" x 0.035") with a quality control of ±4% is ordered from a commercial vendor. The vendor should be requested to establish the ±4% deviation based on an exposure of approximately 100 R.

2) After receipt the dosimeters are annealed prior to any irradiation.

3) The dosimeters are then arranged in a specific order such that each individual dosimeter can be followed throughout the pairing procedure.

4) The dosimeters are given a dose of approximately 300 rads, using the modality which is most often used within the particular center. This modality is a Cobalt 60 unit in our case. The dose rate for the machine must be determined using a secondary standard and appropriate factors. Figure 6 shows a typical set-up. One hundred dosimeters have been arranged so that the position of each dosimeter is known. The dosimeters are placed on a lucite sheet with several thicknesses of pressed wood located beneath the dosimeters to provide a backscattering media. A 5 mm. thickness of paraffin or similar material is placed on top of the dosimeters to provide electron equilibrium. A thin sheet of plastic or paper should be placed over the dosimeters in such a manner that the dosimeters cannot be contaminated with the paraffin material. This is necessary since paraffin contamination will oxidize during the heating readout cycle and give an increased reading.

5) After irradiation, the dosimeters are read individually and the counts recorded. It is compulsory that the order of the dosimeters be maintained such that any specific dosimeter can be identified.

6) The entire group of dosimeters is now annealed and the above described procedure carried out two additional times.

7) The counts for the three runs are totaled for each dosimeter. From the information obtained from these runs the dosimeters are paired to provide increased sensitivity and enhanced accuracy for dosimetry measurement. The pairing is accomplished by choosing individual dosimeters from the group which have combined total counts which are within the accuracy

desired. Usually arranging the dosimeters in descending order (by total counts for the three runs) and pairing from either extreme towards the center will provide a set of dosimeters whose sensitivity limits exhibit extremes within approximately ±2% of the mean. Once this has been accomplished, the dosimeters are used only in pairs.

8) The paired dosimeters are now irradiated and counted several times to determine their characteristics and reproducibility as pairs. Any pair not reproducible within the required range is set aside and not used with the set. Gelatin capsules are used to house the dosimeter pairs when not in use.

9) After the dosimeters have been grouped in pairs and their reproducibility characteristics determined, they can then be calibrated for routine clinical use. The calibration entails placing four dosimeter pairs within a beam of known characteristics. A known dose is then given to the dosimeters and the calibration in counts per rad determined. This calibration is then used for the remainder of the dosimeters within that group of pairs. It is important to note that dosimeters should be annealed only in groups of pairs. For example, suppose that a group of 50 pairs has been determined to read within a specified sensitivity range. This being the case, the entire group should be annealed each time any dosimeter from that group is annealed. In other words, if only 10 pairs out of the 50 were irradiated during the day, then either those dosimeters should be placed aside until more dosimeters have been used, or the entire group should be annealed.

For high accuracy dosimetry it is compulsory that a group of dosimeters be recalibrated to determine the number of counts per rad after each annealing. Again this is done by placing four pairs of dosimeters at a reference point within a radiation field of known characteristics. We have found that the TLD-100 High Sensitivity Ribbons have a very long life. Even after many annealings the dosimeters give high accuracy results; however, periodic re-groupings are necessary.

Thermoluminescence Readers

There are several commercial TL readers available today. In general, all of the readers are excellent; however, they vary considerably in price, design and ease of use for routine dosimetry. Prices for commercially available readers range from under $2,000 to well over $5,000. In many instances the higher priced instruments reflect the specifications which are useful for carrying out basic research in thermoluminescence, but which are not necessary for routine dosimetry applications. The instrument chosen for our TLD program is the Eberline Instrument Corporation's* Model TLR-5. This instrument was chosen for the following reasons: simplicity and accuracy of operation, a two cycle readout with low temperature peak dump, and economical price.

Clinical Techniques

For any paper discussing the clinical use of thermoluminescence dosimetry in radiation therapy it is important to discuss the techniques employed. We certainly do not wish to imply that we are the first to use or report these techniques, or to suggest that the items discussed are all inclusive. Our intent is rather to describe our method of approach to what we consider some important routine clinical applications. Many of these applications are discussed in a report[16] published in the medical journal, *Radiology*.

Entrance Dose Determinations

For entrance dose determinations dosimeter pairs are individually packaged in small plastic envelopes so that the dosimeters will not be contaminated by the oils in the patient's skin. A 5 mm. thickness of paraffin or similar material is used for electron build-up when used for Cobalt 60 radiation. The dosimeter packets are placed on the patient's skin within the irradiated field during the course of a normal treatment. This

---

* P. O. Box 2108, Santa Fe, New Mexico 87501.

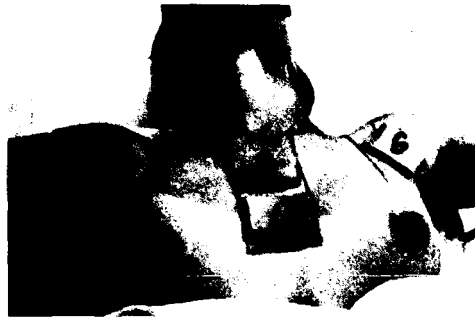

FIGURE 7: A clinical set-up designed to determine entrance doses for a mantle field treatment of a patient with Hodgkin's disease. The calculated given dose (Cobalt irradiation) using machine output and appropriate air effective factor and backscatter factor was 225 rads. Experimentally determined doses were as follows: Position 1 - 235 rads; 2 - 240 rads; 3 - 204 rads; 4 - 214 rads; 5 - 293 rads; 6 - 203 rads.

FIGURE 8: A clinical set-up designed to determine the entrance doses for a shaped post-op breast field. The calculated given dose (Cobalt irradiation) using machine output and appropriate air effective factor and backscatter factor was 238 rads. Experimentally determined entrance doses were as follows: Position 1 - 210 rads; 2 - 222 rads; 3 - 240 rads; 4 - 225 rads.

technique has provided interesting and useful information on large shaped fields such as mantle fields or shaped post-op breast fields where there is a wide variation in the shape of the field and in the SSD of the various anatomical points within the field (see Figures 7 and 8).

Tangential Breast Fields

The dosimetry for tangential breast fields is in general difficult to obtain; however, TLD lends itself nicely to this application. For this application, dosimeter pairs are placed at multiple points over the chest wall (see Figure 9). If orthovoltage or supervoltage with bolus is used, then the paraffin build-up blocks are not necessary.

Rectal Dosimetry

Rectal dosimetry is routinely performed in this department on all patients receiving intracavitary radioactive materials for carcinoma of the cervix. Five pairs of dosimeters are placed in a flexible plastic tube and separated by 2 cm. lengths of solder. The solder allows visualization of the dosimeter positions on post application positioning films (see Figure 10). In our department applications are routinely done in the early afternoon. The rectal dosimeters are put in place at the time of the application. They are left overnight and removed the next morning for counting and dose determinations. The fact that the flexible plastic tubing is left in place for an extended period of time under actual treatment conditions allows a very accurate determination of the rectal dose. We feel that this technique is superior to rigid probe rate meter determinations in which the bowel can be moved to an entirely unphysiologic relationship to the radioactive sources.

The rectal tube dosimeters are also used with multiple external field set-ups to the pelvis. This is especially useful in three field pelvic techniques and gives an accurate statement of the dose to the rectum during actual treatment.

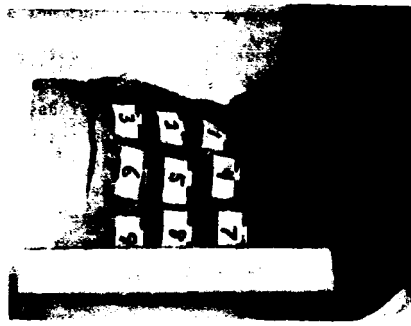

FIGURE 9: A clinical set-up designed to determine the skin doses for a chest wall radiation using tangentially opposed fields of Cobalt irradiation. An exposure was made with the unit in the position shown in the film and also with the machine rotated 180°. Bags filled with rice were used to provide a bolus material. Experimentally determined doses were as follows: Position 1 - 178 rads; 2 - 186 rads; 3 - 186 rads; 4 - 183 rads; 5 - 171 rads; 6 - 174 rads; 7 - 177 rads; 8 - 173 rads; 9 - 167 rads.

FIGURE 10: Radiograph showing intracavitary application consisting of uterine tandem and vaginal ovoids. The positions of dosimeters located in the rectum are marked by the solder spacers.

Vaginal Dosimetry

Vaginal dosimetry can be performed for both external beam and vaginal bomb therapy. For external beam therapy a plastic vaginal bomb is used with one or two pairs of dosimeters placed within the bomb. The bomb is inserted into the vagina and placed with its apex against the cervix and left there during routine external beam therapy. If multiple fields are used, the dosimeters may remain in the bomb for use on one or more treatment days to obtain a total dose from a combination of fields. With the use of the vaginal applicators for intracavitary therapy, the dosimeters may be attached to the surface of the applicator prior to its insertion. This technique gives an accurate measurement of the dose to the vaginal wall.

Special Dosimetry

It is possible to obtain accurate bladder dosimetry by placing a pair of sterilized dosimeters within the tip of a Foley catheter which is put in place within the course of the treatment. In addition, esophageal dosimetry may be determined by arranging dosimeters in a nasogastric tube similar to the technique described for the rectal tube. These techniques are not used routinely within this department but are available for special problems.

Phantom dosimetry is easily accomplished in water, pressed wood, paraffin and other phantoms with the LiF dosimeters. This has been found to be of great use in the calibration of special techniques such as moving strip therapy in which water and pressed wood phantoms have been used with as many as 100 pairs of dosimeters. This technique has also been used to advantage on individualized paraffin phantoms in which plaster of paris molds of the chest wall, larynx and facial structures have been cast in paraffin. These paraffin phantoms are cut and dosimeters placed at points of interest. The phantoms are exposed under clinical conditions.

Calibration of Treatment Cones

TLD provides real utility in rapid, simple and accurate calibration of output at the end of treatment cones. With

orthovoltage and superficial voltage radiation, the dosimeters are placed on a pressed wood phantom and the cone positioned under treatment conditions. If cutout lead shields are to be used, these are included in the set-up. This technique has been especially useful in malleable lead cones used for intraoral therapy. When these cones are bent and shaped, it is difficult to accurately determine the dose by conventional means.

Clinical Accuracy

It is one thing to talk about accuracy and reproducibility in controlled experimental conditions, but quite another to talk about the accuracy of TLD under routine, clinical use. In the clinical environment, small standard deviations in the readings of large sets of dosimeters are of little value. The important thing is that the TLD user be confident any dosimeter used for a dose determination will be accurate within a small specified range. We have checked this in our own program by studying patients who are receiving radiation through standard square fields (6 x 6 cm. to 18 x 18 cm.) or only slightly irregular rectangular fields (5 x 6 cm. to 15 x 18 cm.). Only patients who presented a relatively flat skin surface (small variations in SSD over the field) were studied. For these fields the calculated entrance dose using the machine output and appropriate air effective factor and backscatter factor[17] were considered to be accurate. We have studied over 50 such fields using TLD-100 High Sensitivity Ribbons; only three have given readings outside ±2% accuracy. The readings outside the ±2% accuracy range were -2.3% for a 5 x 6 cm. field, +2.6% for a 10 x 12 cm. field, and a -2.6% for an 18 x 18 cm. field. The dosimeter pairs used for these determinations were chosen at random from calibrated sets.

The thermoluminescence dosimetry program within our department has shown a reproducibility in variation within a paired set of dosimeters of better than ±2% at the extremes under experimental conditions. Under controlled clinical conditions (selected fields) the accuracy approaches ±2% at the extremes. The accuracy of our system for any clinical dosimetry is estimated to be better than ±4% at the extremes.

Summary

A complete thermoluminescence dosimetry system for use in radiation therapy is presented with a description of new techniques for dosimeter pairing, grouping, calibration and annealing. TLD-100 High Sensitivity Ribbons are proposed as the dosimeter of choice for routine dosimetry within a radiation therapy facility. The importance of a TL reader with a two cycle readout in which the luminescence associated with low temperature peaks is ignored is discussed. This TLD system lends itself well to routine dosimetry of a multitude of treatment techniques in a busy clinical practice. The entire system can be operated by a trained radiation therapy technician. The system is used within our department for external beam dosimetry, intracavitary dosimetry, calibration of treatment cones, experimental set-ups and others. It has shown an accuracy of better than ±2% under experimental conditions, and an estimated clinical accuracy of better than ±4%.

References

1. J.R. Cameron, N. Suntharalingam, and G.N. Kenney, *Thermoluminescent Dosimetry*, University of Wisconsin Press, 1968.
2. F.M. Cox, "New Solid Lithium Fluoride Thermoluminescent Dosimeters", *Proceedings of the Second International Conference on Luminescence Dosimetry*, 61-77, September 1968.
3. K.C. Palmer, *Int. J. Appl. Radiat. Isotopes*, *17*:413, 1966.
4. N. Suntharalingam, D.J. Zimmerman, and G.N. Kenney, "Personnel Dosimetry with Single Crystals of Lithium Fluoride", *Proceedings of the First International Conference on Luminescence Dosimetry*, 217-226, April 1967.
5. R.M. Hall, "Development and Applications of Thermoluminescent Dosimeters", DPMS-66-29, June 1966.
6. C.J. Karzmark, J. White, and J.F. Fowler, "Lithium Fluoride Thermoluminescent Dosimeter Powder", *Physics in Med. and Biol.*, *9*, No. 3, 273, July 1964.
7. E. Tochilin and N. Goldstein, "Dose Rate and Spectral Measurements from Pulsed X-Ray Generators", DASA 1703 USNRDL-TR-939, December 1965.
8. J.R. Cameron, *et al.*, *Science*, *134*:333-334, August 1961.
9. D.E. Jones, K. Petrock, and D. Denham, "Thermoluminescent Materials for Personnel Monitoring in Gloved Box Operations", TID-4500, US-41:33-35, 1966.
10. N. Suntharalingam, *et al.*, *Physics in Med. and Biol.*, *13*:97, 1968.
11. J.R. Cameron, *et al.*, "Thermoluminescent Radiation Dosimetry Utilizing Lithium Fluoride", *Health Physics*, *10*:25-29, 1964.
12. P.D. LaRiviere, "A Unique Throwaway LiF Dosimeter", *Proceedings of the Second International Conference on Luminescence Dosimetry*, 78-81, September 1968.

13. D.W. Zimmerman, C.R. Rhyner, and J.R. Cameron, "Thermal Annealing Effects on the Thermoluminescence of Lithium Fluoride", *Proceedings of the First International Conference on Luminescence Dosimetry*, 1965.

14. D.W. Zimmerman, C.R. Rhyner, and J.R. Cameron, "Thermal Annealing Effects on the Thermoluminescence of LiF", *Health Physics, 12*:525, 1966.

15. M. Cox (Harshaw Chemical Company), personal communication, 1971.

16. D.S. Gooden and T.J. Brickner, "The Routine Use of Thermoluminescence Dosimetry for Radiation Therapy", *Radiology*, March 1972.

17. *British Journal of Radiology, Supplement No. 10*, "Depth Dose Tables for Use in Radiotherapy", British Institute of Radiology, London, 1961.

Mason

With reference to your annealing procedure: The large doses of radiation used in radiotherapy will quickly give rise to changes in sensitivity which will vary from disc to disc depending on the individual accumulated dose. The necessity for efficient annealing is therefore obvious. Your discs will not spend more than 10-12 minutes at 400°C before the oven is switched off. Have you observed any effects of disc sensitisation over a number of re-use cycles as the accumulated dose increased?

Gooden

First let me emphasize that we use the high-sensitivity ribbons and not the teflon discs. Actually my annealing procedure is quite stringent, since the dosimeters are allowed to cool down in an oven which was previously at an equilibrium temperature of 400°C. I have found essentially no change of sensitivity within a group over a number of re-use cycles. However, as stated in the paper, periodic regrouping is necessary if high-accuracy dosimetry is desired.

Schlesinger

Our experience with LiF TLD-100 ribbons also shows that the best procedure for cooling the dosimeters is to leave them in the oven for some hours. This is in contradiction to the method suggested by the Harshaw Company, namely a further annealing for 24 hours at 80°C after the annealing at 400°C for 1 hour.

TLD - Calcium-Fluoride in Neutron Dosimetry; TLD - Calcium-Sulphate in Health Protection Service

D. K. Bewley and E. Blum
Hammersmith Hospital
London, England

Calcium-Fluoride (Mn)- Teflon TLD has been used for studies of the fast neutron beam from the MRC cyclotron. The very small intrinsic response of this phosphor to fast neutrons makes it suitable for investigating the γ contribution in the field. Aluminum, Tantalum, Nickel and Lead have been examined as shielding materials and all the latter three metals have been found suitable. Aluminum however, due to its activation by fast neutrons, is less reliable. The TLD of Calcium-fluoride agreed fairly well with data obtained by film measurements giving a γ contamination in the neutron beam of about 5%. The response to fast neutrons can be enhanced by surrounding the dosimeters with a hydrogenous material such as polythene. Exposure in pairs, one in polythene and one in lead, makes it possible to measure both γ and neutron components of the radiation field. This method has been applied to depth dose studies in tissue equivalent phantoms.

Accuracy is limited by the energy and angular response of the dosimeters which were discs of 0.13 x 6.0 mm supplied by TELEDYNE and read on CONRAD reader S100. Reproducibility of 3% has been obtained, using a controlled calibration and annealing technique. Dosimeter discs have not suffered significant sensitivity change after repeated irradiation cycles.

CALCIUM-SULPHATE (Dy)-TEFLON dosimeters in the form of 4 mm x 12 mm discs have been calibrated in the dose range of a few hundred rads, and linear response has been obtained over 5 decades of dose. The high sensitivity and high temperature peak make these dosimeters suitable for personal monitoring.

Lithium Fluoride Dosimeters in Clinical Radiation Dose Measurements

by

N. Suntharalingam, Ph.D.

and

Carl M. Mansfield, M.D.

Thomas Jefferson University Hospital
Philadelphia, Penna. U.S.A.

Abstract

Several types of LiF dosimeters have been used in a wide range of clinical dosimetry applications. The use of loose powder, wherever feasible, gives the highest precision and accuracy (±2%). When using the solid forms of dosimeters, special calibration procedures have to be accommodated in order to achieve a precision of ±3%. In-vivo measurements on patients receiving Cobalt-60 radiation therapy by tangential breast fields, Hodgkins-mantle fields, and for tumors in the head and neck area, bladder and esophagus, are reported. Patient measurements have been supplemented by measurements with tissue equivalent phantoms. The measured doses have been compared with calculated doses and shown to be in good agreement.

Introduction

In clinical radiation therapy several situations present themselves where it would be advantageous to know the radiation dose received by the patient. A knowledge of the dose delivered at the site of the tumor and also at critical anatomical sites, both within and outside the treatment volume, would be of value to the clinician in the planning of the treatment. In the past the problem of measuring the radiation dose, in-vivo, presented many difficulties because of inherent limitations of the then available radiation detector systems. The availability of thermoluminescent dosimeters in various physical forms and different geometric shapes and sizes has made possible their use in a wide range of clinical radiation dose measurements[1-3]. Even though many thermoluminescent phosphors have been investigated, Lithium Fluoride has many characteristics most applicable for clinical dosimetry[4]. However, the choice of the most appropriate LiF dosimeter for a particular clinical study has presented some difficulty because of the general confusion of the pre-use annealing requirements. In this paper, the performance characteristics of suitable LiF dosimeters with examples of their use in radiation therapy clinical studies, both in-vivo and phantom, are presented.

TL Dosimeters

Lithium Fluoride was the only TL phosphor material used. LiF(TLD-100) loose powder, extruded rods and extruded high sensitivity ribbons[5] and LiF(TLD-700) impregnated Teflon discs[6] were the different forms of dosimeters investigated. For different applications, each of these forms have certain advantages.

Whenever a large number of dosimeters were required for an investigation of the spatial distribution of radiation dose, LiF(TLD-100) loose powder has been used because of its versatility and good reproducibility. Also, for phantom studies, loose powder, encapsulated in either gelatin capsules (#5) or small thin plastic packets were found to be the most convenient.

The LiF(TLD-100) extruded rods, 1 mm diameter and 6 mm length, were used for in-vivo dose measurements by inserting them in special catheters. The extruded rods were placed one alongside another, totalling usually four or five dosimeters, inside either a small piece of Teflon tubing with metal markers at the ends or inside a small section of radio-opaque angiographic catheter and heat sealed at both ends. These small sections of tubing were then placed at the tip end of the standard nasogastric tube for esophageal measurements and at the end of a Foley catheter for bladder dose measurements.

The LiF impregnated Teflon discs, 13 mm diameter and 0.13 mm thickness, were used for surface and skin dose measurements. These dosimeters were also used to investigate the build-up of dose as a function of depth and the relative electron contamination of the photon beam due to the presence of scattering material within the beam. In some instances, entrance and exit doses at different sites of an irregular blocked field were measured with either the LiF-Teflon discs or LiF(TLD-100) extruded ribbons. On the entrance side, to ensure adequate electron dose build-up appropriate thickness of lucite (tissue equivalent) was placed over the dosimeters.

All solid forms of dosimeters show about ±10% non-uniformity of response from one dosimeter to another even though they are from the same batch of purchased dosimeters. For use in clinical studies, dosimeters having a uniformity of response within ±2% were pre-selected, by comparing the response of the individual dosimeters to 50 rads of Cobalt-60 gamma radiation.

TLD-Readers

All the dosimeters were usually read on the Harshaw-2000 TL Analyzer. This reader measures the total light emitted and displays the integrated light output in digital form.

Whenever it was necessary to investigate the nature of the emitted TL glow curves, the dosimeters were read on a "research reader" where the PMT current is measured using a high impedance electrometer (Keithley Model 610B) which in turn drives a X-Y recorder. With this reader simultaneous integration of the current is also possible.

Irradiation

All irradiations, both phantom and patient, were done on the AECL Theratron-80 and the Picker-C3000 Cobalt teletherapy machines.

The phantom used in the study was the chest and upper abdomen portions of the Alderson-Rando phantom(7).

Dosimeter Annealing

The glow curve from a single crystal of LiF(TLD-100) annealed for 1 hour at 400°C and irradiated to 10 rads of Cobalt-60 gamma radiation is shown in Figure (1). Repeated irradiation and read-out gave identical glow curves (shown by dotted lines in the figure) with or without the 1 hour at 400°C annealing, indicating no changes in sensitivity. The 400°C annealing was found to be necessary only to restore the crystal to its original sensitivity after any radiation induced increase in sensitivity. LiF(TLD-100) loose powder gave similar glow curves with the relative heights of the different peaks being the same as for the single crystal, except for differences in overall sensitivity. The annealing of 24 hours at 80°C was necessary only to remove the low temperature peaks and this annealing did not show any measurable change in the main high temperature dosimetry peak height. Figures 2 and 3 show the glow curves from LiF(TLD-100) extruded rods and high sensitivity ribbons respectively, for a dose of 100 rads of Cobalt-60 gamma radiation after annealing the dosimeters for 1 hour at 400°C. Curve "a" is when the dosimeters were read promptly, within 15 minutes, after irradiation, curve "b" is for a read-out 24 hours after irradiation and curve "c" is for a dosimeter that also received a pre-irradiation annealing of 24 hours at 80°C. Note that while the extruded ribbons gave a glow curve similar in structure to that of the single crystal or loose powder, the glow curves from the extruded rods showed the low temperature peaks to be dominant. The differences in the magnitude of the low temperature peaks in the glow curves of these dosimeters appear to indicate differences in techniques used in their fabrication. It was necessary to remove the low temperature peaks by the 80°C annealing, to achieve a precision of ±3% in the measurements. Repeated use after standard annealing gave glow curves identical to curve "c", implying no changes in sensitivity.

For use in clinical studies the LiF(TLD-100) loose powder, extruded rods and ribbons always received before each use the standard annealing(8) (1 hour at 400°C, cool to room temperature in 15 minutes followed by 24 hours at 80°C). The LiF(TLD-700)-Teflon discs were annealed for 5 hours at 300°C, allowed to cool to room temperature in 15 minutes, and then annealed for 24 hours at 80°C before each re-use. After irradiation, all dosimeters were stored for 24 hours at room temperature before read-out.

These annealing procedures, though they may appear to be inconvenient and cumbersome, have been strictly followed in all measurements. It was felt that the effort required in annealing and preparing the dosimeters was a small fraction of the total effort required for high precision measurements of clinical doses.

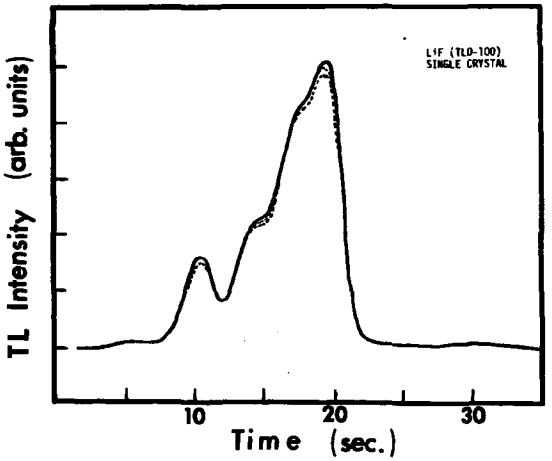

Figure 1. Typical glow curve from a single crystal of LiF(TLD-100) irradiated to 10 rads Cobalt-60 gamma radiation after annealing for 1 hour at 400°C. Heating rate used was approximately 600°C/min.

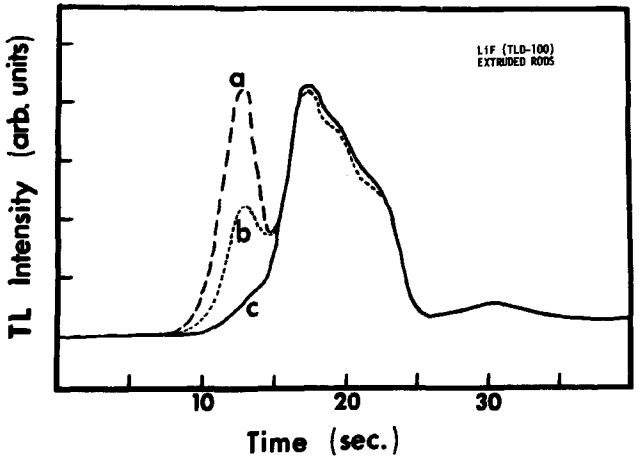

Figure 2. Typical glow curves from LiF(TLD-100) extruded rods, irradiated to 100 rads Cobalt-60 gamma radiation after annealing for 1 hour at 400°C. The heating rate used was approximately 600°C/min.
a. prompt(within 15 minutes) read-out.
b. 24 hours at room temperature before read-out.
c. standard annealed dosimeter.

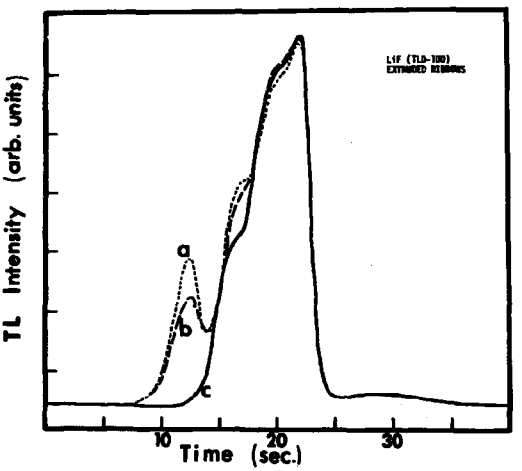

Figure 3. Typical glow curves from LiF(TLD-100) extruded high sensitivity ribbons, irradiated to 100 rads Cobalt-60 gamma radiation after annealing for 1 hour at 400°C. The heating rate used was approximately 600°C/min.
a. prompt(within 15 minutes) read-out.
b. 24 hours at room temperature before read-out.
c. standard annealed dosimeter.

Clinical Applications

In certain clinical areas that presented interesting and difficult problems in dosimetry and treatment planning the measurement of radiation dose with TL dosimeters has been implemented. Some of these applications where both phantom and in-vivo measurements have been undertaken are discussed below.

a) Breast:- Clinical evidence of skin reactions following Cobalt-60 treatments of the breast and chest wall areas suggested the desirability of measuring the skin doses received during treatment. Also, it was necessary to determine how the surface curvature of the skin, the angle of incidence of the beam, the electron contamination of the photon beam and the presence or absence of bolus affected the dose at the superficial layers of the skin.

The measured surface doses and doses at depth as a function of the angle of incidence of the beam are given in Figure 4. These measurements were made using LiF-Teflon discs on a breast phantom and with a 15x15 cm^2 radiation beam and a source phantom distance of 80 cm. The data points are a mean of five separate irradiations with a standard deviation of ±3%. Note that the surface dose for normal incidence(90^o) is about 40% of dose maximum and is as high as 65% when the beam is tangential(0^o). Also the depth at which the dose reaches a maximum is dependent on the angle of incidence.

While variations in the angle of incidence can affect the surface dose, the presence or the breast applicator results in electron contamination of the photon beam and further increases the surface dose. Table I summarizes the measurements of surface doses on the breast and chest wall of an Alderson phantom. The indicated doses are expressed as a percentage of the tumor dose and are the mean of several readings, with a standard deviation of ±3%.

TABLE I

TANGENTIAL BREAST TREATMENT
MEASUREMENTS ON ALDERSON PHANTOM
USING LiF-TEFLON DISC DOSIMETERS

COBALT-60 80 cm SSD	SURFACE DOSE (% of Tumor dose)	
	Breast	Chest Wall
Opposed fields with breast applicator and with bolus (20x20 cm blocked to 20x10 cm)	100	100
Opposed fields with breast applicator but without bolus (20x20 cm blocked to 20x10 cm)	78-86	80-85
Opposed fields without breast applicator and without bolus (20x10 cm)	55-60	58-62

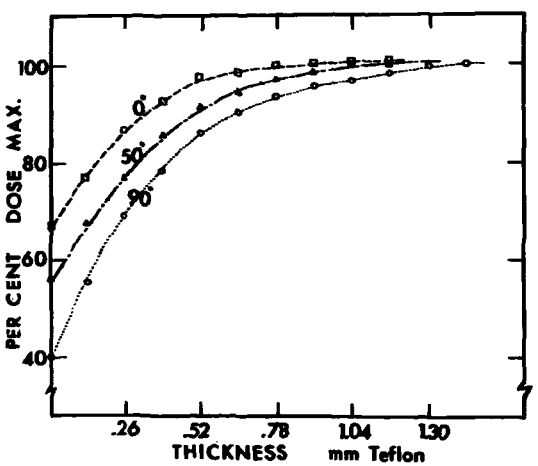

Figure 4. Build-up of dose for Cobalt-60 gamma radiation as a function of depth and angle of incidence, measured using LiF-Teflon discs.

The surface doses and the doses at points within the irradiated volume were measured for a tangential chest wall treatment, using the Alderson phantom to simulate the patient. The measured doses without bolus in the mid-plane section of the phantom are shown in Figure 5. The surface doses were measured using LiF-Teflon discs and these are indicated by numbers within brackets. The doses at depth within the irradiated volume were measured using LiF(TLD-100) powder contained within gelatin capsules. The measured doses at any one level agree to within ±2% and are in close agreement with the doses calculated using standard isodose data. The dashed lines are the calculated isodose lines.

Using LiF-Teflon discs the measured skin doses on a patient treated with tangential opposed fields without bolus are shown in Figure 6. The calculated tumor dose was 180 rads to point P delivered by both fields. The surface doses are again seen to be about 70-80% of the tumor dose and is in agreement with the phantom measurements. The measured skin doses on the same patient when treated with bolus and the same radiation fields are given in Figure 7. In this situation the skin doses measured about 10% higher than the calculated tumor dose of 180 rads (this higher dose was attributed to the insufficient bolus used to compensate for the lack of tissue).

b) Hodgkins Mantle field:- In the radiation treatment of Hodgkins disease the nodes in the neck, superclavicular, axillary and the mediastinal areas are treated simultaneously using a large beam appropriately shaped to shield the lungs. The dosimetry of the resulting radiation beam becomes increasingly difficult, due to the irregular shape of the large field, the presence of scattering medium in the beam and also the presence of tissue inhomogenities. Computer methods are available for the calculation of dose to arbitrary points within the irradiated volume and also to points within the shielded area. Because of possible inaccuracies in positioning the patient with respect to the shaped field, it was necessary to measure the dose and compare them with the calculated dose.

Doses at points within the irradiated volume of the chest portion of the Alderson phantom were measured using LiF(TLD-100) powder. The measured values were found to be in close agreement to the computer calculated doses. A typical example of the doses at specific points within one slab of the phantom are shown in Figure 8. The measured doses are the numbers within the brackets. The agreement between calculated and measured doses in most instances was in the order of 2-3%. Note that the doses at points within the lung, that is in the blocked area, are almost independent of depth and are about 20% of the mid-line dose.

The doses at depth within a patient treated with a Mantle field are almost impossible to measure. However, both the entrance and exit doses could be measured. This has been done on several patients, using both LiF-Teflon discs and LiF(TLD-100) extruded ribbons, and two examples are given in Table 2. The measured values are in reasonable agreement with the calculated values, within ±5%, considering the uncertainties in the calculative method.

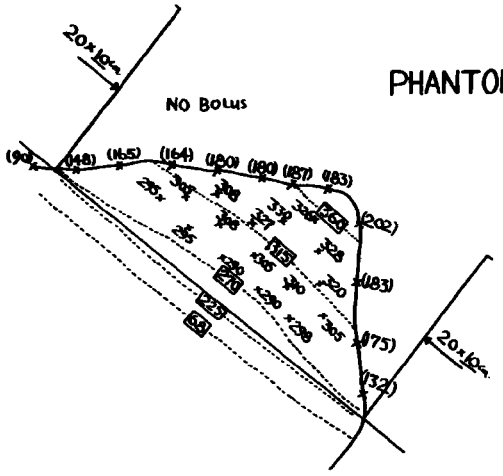

Figure 5. Measured doses in rads at the surface(numbers in brackets) and at depth for a phantom chest irradiation without bolus using tangential opposed fields. The calculated isodose lines are shown by dashed lines.

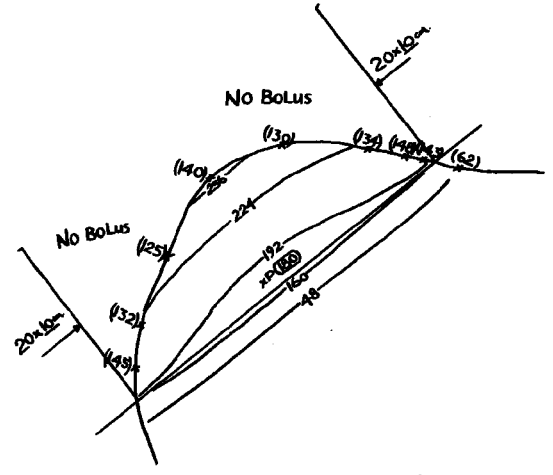

Figure 6. Measured doses in rads on the skin surface(numbers in brackets) of a patient during tangential opposed fields breast treatment without bolus. Also shown are the calculated isodose lines.

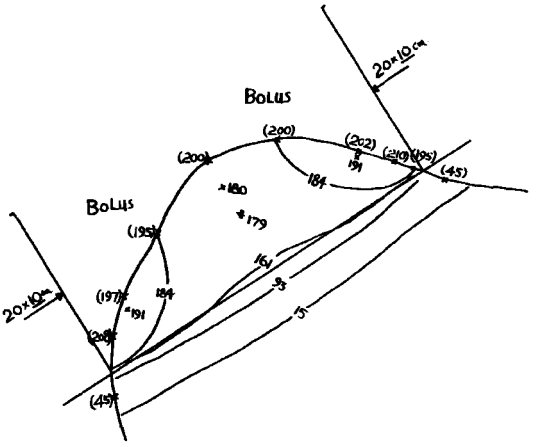

Figure 7. Measured skin doses in rads(numbers within brackets) on the same patient but treated with bolus. Also shown are the calculated isodose lines.

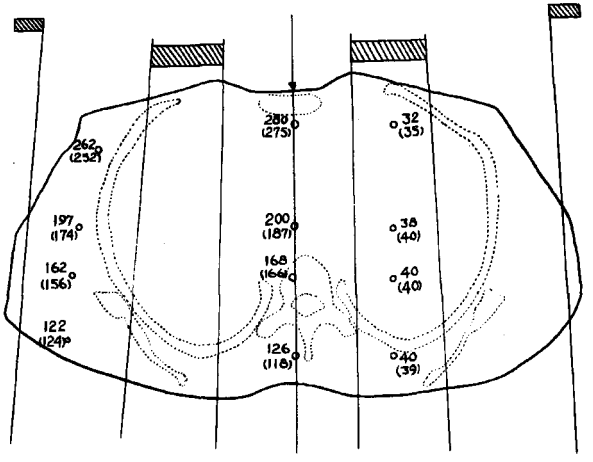

Figure 8. Comparison of calculated and measured(numbers within brackets) doses at depth within one slab of the chest phantom for a typical Hodgkins-Mantle field irradiation.

TABLE 2

IN-VIVO DOSE MEASUREMENTS ON PATIENTS
TREATED BY MANTLE FIELDS

		ABSORBED DOSE(rads)	
		COMPUTED	MEASURED
H.G.	*Mediastinum*		
(field shaped using 7 cm thick styrafoam cut out,filled with lead shots)	entrance	290	314
	exit	93	99
LiF-Teflon discs	Axilla		
	entrance	270	255
	exit	110	130
	Lung		
	entrance	32	41
	exit	40	40
R.C.	Mediastinum		
(field shaped using 2" thick lead blocks)	entrance	283	292
	exit	93	84
Extruded ribbons	Axilla		
	entrance	252	248
	exit	93	89
	Lung		
	entrance	30	25
	exit	35	32

In the mantle field technique,since a lucite stage to hold the lead blocks has to be positioned at a certain distance away from the patient,it was necessary to measure the increase in surface dose due to electron contamination of the photon beam. Table 3 shows the measurements on a Cobalt machine for typical treatment distances. LiF-Teflon discs were used in these measurements. The experimental data indicates that when large fields are used, the surface dose could be as high as 75% even at distances of 30 cm from the stage, thus decreasing the skin sparing effect of Cobalt radiation.

c) Head and Neck:- The treatment of certain head and neck tumors especially those located in the area of the mouth, for example the tongue or floor of the mouth, gingiva, antrum or mandible, require sophisticated irradiation techniques. Acceptable isodose distributions can be obtained by the combination of two fields directed almost at right angles. Also, in most cases it is necessary to make each field non-uniform across the beam by the use of wedge filters. Further, due to the pronounced surface curvature of the facial area, tissue compensators have to be custom designed for each patient. The dose delivered during this somewhat complicated

TABLE 3

COBALT-60 SURFACE DOSE MEASUREMENTS USING LiF-TEFLON DISCS
(influence of scattered electrons)

	Surface Dose (Percent of dose max.)	
Source surface distance	80 cm	100 cm
Stage surface distance	10 cm	30 cm
Field size (cm^2)		
10x10	58	35
20x20	76	51
33x33	94	77

treatment technique was measured using LiF(TLD-100) extruded rods placed within Teflon tubing and positioned inside the mouth. An example of the measured doses on a patient treated for a tumor in the gingival area is shown in Figure 9. The doses measured agree to within ±3% of the calculated doses. The calculated isodose distribution is also shown for comparison. Measurements were also made when this same patient was treated without tissue compensators and these data are shown in the same figure by the numbers within the brackets.

d) Other areas:- Tumors of the esophagus and bladder are usually treated by either moving field therapy or multiple field techniques. Using patient contour data and the radiation beam parameters, it is possible to calculate the dose to the tumor area. These computer calculated doses were verified by measurements with TL dosimeters. Typical examples of in-vivo measurements of the doses at the esophagus and the bladder, using LiF (TLD-100) extruded rods inside catheters, are given in Table 4.

TABLE 4

IN-VIVO PATIENT DOSE MEASUREMENTS
USING LiF(TLD-100)EXTRUDED ROD DOSIMETERS IN CATHETERS

		COMPUTED DOSE(rads)	MEASURED DOSE(rads)
ESOPHAGUS (Parallel opposed fields)	D.C.	230	235
	S.L.	210	230
BLADDER (2-140° Arc, skip rotation)	F.I.	220	230
	G.M.	233	237
	P.M.	200	160*

*Dosimeters contaminated with body fluids.

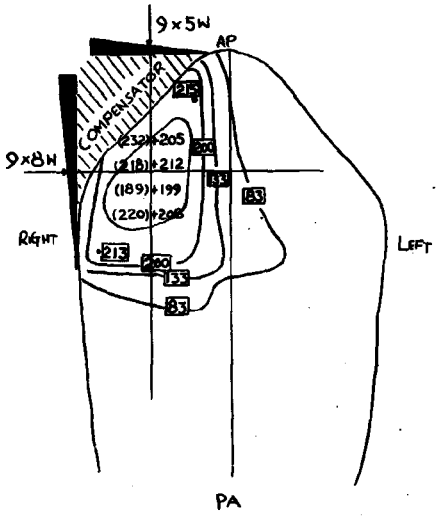

Figure 9. An example of doses measured inside the mouth using LiF(TLD-100) extruded rods on a patient treated for tumor in the gingiva area. The numbers within brackets are the measured doses in rads when tissue compensators were not used. The calculated isodose values are shown by the solid curves.

Acknowledgements

The authors would like to thank Michael Chow, John Henderson and Betty Stibitz for valued technical assistance during all phases of this study.

References

1. J.R. Cameron, F. Daniels, N. Johnson and G. Kenney: Science 134, 333 (1961).

2. H.J. Eichhorn: Radiology 88, 1154 (1967).

3. C.M. Mansfield, B.M. Galkin, N. Suntharalingam, M.C. Chow: Radiology 93, 401 (1969).

4. J.R. Cameron, N. Suntharalingam and G.N. Kenney, Thermoluminescent Dosimetry. Chapter 4, University of Wisconsin Press, 1968.

5. F.M. Cox: Proceedings of the Second International Conference on Luminescence Dosimetry, 60, 1968, CONF 680920.

6. B.E. Bjarngard and D. Jones: Proceedings of IAEA Symposium, Solid State and Chemical Radiation Dosimetry, 99, 1966.

7. S.W. Alderson, L.H. Lanzl, M. Rollins and J. Spira: American Journal of Roentgenology and Radiation Therapy, 87, 185 (1962).

8. N. Suntharalingam, J.R. Cameron, E. Shuttleworth, M. West and J.F.Fowler: Physics in Medicine and Biology 13, 97 (1968).

Watanabe

I would like to add a comment. We are doing some measurements of Co-60 gamma-ray doses inside the esophagus and stomach, introducing TL dosimeters through plastic tubes. The measurements were done during irradiation of the patient.

A Personal Dosimeter System Based on Lithium Fluoride Thermoluminescent Dosimeters (TLD)

by

A. R. Jones

Atomic Energy of Canada Limited
Chalk River Nuclear Laboratories
Chalk River, Ontario, Canada

Abstract

The system comprises:

- a personal dosimeter
- an automatic reader for it
- a semi-automatic reader for finger tip dosimeters

Two TLDs are mounted on a plaque bearing the identity of the wearer as a hole code. One TLD, 0.9 mm thick, registers the penetrating component of radiation and the other, 0.25 mm thick, the skin dose.

The reader automatically identifies 200 plaques and measures 400 dosimeters in one and a half hours. These identities and doses are printed and punched on paper tape by a teletype writer. The TLDs are read by heating them with a hot anvil until a thermocouple on the other side of the TLD reaches the temperature for complete readout.

The semi-automatic reader measures the dose registered by teflon disc lithium fluoride TLDs. The discs are placed by hand onto a planchet fitted with a ring whose diameter is just right to keep the TLD flat during heating.

Energy dependence results for the TLDs for gamma and beta rays are given. Data on linearity, reproducibility and the effect of cycling TLDs through the reader are also presented.

Introduction

Following measurements made with lithium fluoride TLDs, in ribbon form, it was concluded that photographic film dosimetry could and should be replaced by a TLD system [1, 2]. Furthermore, experience obtained while making these measurements showed a need for automatic reading if the benefits of TLD were to be realized economically for large groups ($\sim 10^3$) of workers [1].

This paper describes a TLD system designed to replace the photographic dosimetry system now in use at the Chalk River Nuclear Laboratories. The system comprises:

- the dosimeter plaque
- the automatic TLD reader for the plaque
- a semi-automatic reader for use with finger tip dosimeters.

Finally, the paper gives results obtained with the system and points to the direction of further work needed to improve it.

The Dosimeter Plaque

TLDs are mounted in a plaque, the same size and shape as the dosimetric film pack, because it

- obviates design and tooling for a new badge
- could be used in other film badge holders
- lends itself to automation.

Plate I shows the plaque inserted into the film badge. Two high sensitivity lithium fluoride TLDs [2] are mounted in the plaque by sticking them to adhesive "Kapton" tape. The top one is 3.2 x 3.2 x 0.9 mm and, when the badge is closed, is sandwiched between two aluminum slabs, 2 mm thick. This TLD registers the penetrating component of the radiation. The second (3.2 x 3.2 x 0.25 mm) has only a thin paper covering in the badge and registers the skin dose (β and γ).

The plaque is an aluminum stamping which carries the identity number of the wearer. Also, it carries a 5-digit, 8-hole, teletype code for identification in the automatic reader. All holes are stamped but over this a punched mylar tape is cemented. The tape can be punched by a teletypewriter which also types the legible number.

The missing corner in the plaque helps to ensure correct orientation of the plaque in the reader.

To permit a continuous personal monitoring program on a two-week basis, two plaques are needed for each worker. One is in use while the other is being read. To avoid confusion between the two they are colour coded blue and red with A or B before the number. Special plaques for issuing to visitors or other purposes can be printed, colour coded white, and the

identity code preceded by an S to prevent the dose from being added to the record of a worker with the same number. Standard dosimeter plaques carry, instead of identity numbers, "0 rad" and "1 rad".

The Automatic TLD Reader

Plates II and III are views of the complete prototype reader and of the automatic mechanism. Figure 1 shows the reader diagramatically.

Up to 200 plaques are stacked in the magazine which is inserted in the reader. The normal sequence of operations in the automatic mode follows:

The lowest plaque drops into a hole in the shuttle which transports the plaque to a position under the teletype hole code reader. This identifies the plaque and then transmits the information to the teletypewriter for printing and punching on paper tape.

The shuttle next moves the plaque so that the thick TLD is under the end of a light pipe (as shown in Figure 2), optically coupled to a cooled (at constant temperature) photomultiplier. At this point a hot anvil, whose tip is maintained at about 270°C, presses up against the bottom of the TLD. Between the TLD and the light pipe is a 0.25 mm diameter thermocouple which monitors the temperature on the cooler, top face of the TLD. When, and only if, this temperature rises sufficiently to release all thermoluminescence, a signal is applied to drop the anvil. If this process takes too long, because of improper heating, an alarm is sounded and the reader stops. If the process is too quick, the same thing happens. This serves to detect a missing TLD or the emptying of the magazine. These precautions ensure that incorrect processing of a TLD is noticed by the operator. Unlike systems which only control the heater temperature, it checks the heat transport to and through the entire TLDs.

Light is emitted as the temperature front moves through the TLD. During this time, about 8 seconds, the photomultiplier current-pulse drives the analog-to-digital converter (A.D.C.). This circuit produces a train of pulses whose total number equals the dose in mrads and it is fed to a zero subtraction circuit. This is adjusted to subtract any number of pulses, up to 100, from the pulse train and it is designed to automatically remove any contribution due to black body radiation, photomultiplier or spurious luminescence. It is set up by first passing an unexposed dosimeter through the reader. The reduced pulse train is then fed to a six decade scaler whose content, at the end of the heating period, is printed and punched by the teletypewriter. Shoud the A.D.C. give a million, or more, pulses ($\geq$ 1000 rads) an alarm sounds and an over-range indication is given. An alarm is also sounded if a dose of 800 mrad is exceeded. This dose is greater than that normally permitted for 2-week exposures. Following such a measurement, a standard dosimeter plaque exposed to 1000 mrad is inserted to test the reader.

Next, the thin dosimeter moves into the reading position. In this case the average reading time is reduced to 4 seconds because the tempera-

ture front penetrates the thin dosimeter more quickly. Each pulse from the A.D.C. corresponds to 10 mrads so that indicated doses of 10 mrads to 10,000 rads can be read.

The shuttle then moves to its most extreme position and drops the plaque into a reject magazine where it is placed in the same sequence as it went into the reader. The shuttle returns to pick up the next plaque and the complete cycle is restarted when a proximity switch detects that the shuttle, driven by toothed belt and stepping motor, has returned to its starting position. The average cycle time is 28 seconds so that 200 plaques (a full magazine) may be processed in 90 minutes. During this period the reader requires no attention if there is no alarm. The operator is free for other work for this time, provided the alarm can be heard or seen.

Calibration is done with dosimeters which have been exposed to 1 rad or 0 rad. In this connection, a "0 rad" dosimeter is one which has been stored shielded for two weeks during the working days. At night and weekends, it is unshielded since we do not wish to record the dose absorbed by dosimeters when their wearers are away from work [3]. If the reading is more than 10% in error for the 1 rad standard the photomultiplier voltage is adjusted before proceeding with the automatic reading. No light source is used because I feel that this only tests the optics and electronics which are probably the most reliable parts of the system. There is no real substitution for testing the system with exposed dosimeters.

Annealing

No annealing after reading and before exposure is needed. This is very fortunate since the labour of processing would be much increased by it.

The reader is of the integrating kind and it is important that the contribution from low temperature traps should be small to avoid dependence on time between exposure and reading. This is done by storing the dosimeters at 50°C from Friday evening when the badges are changed to Monday morning when the working week begins. If a dosimeter must be measured quickly, the same is achieved by storing it at 100°C for 10 minutes.

Semi-automatic Reader for Finger Tip TLDs

Lithium fluoride-teflon disc (13 mm dia. x 0.4 mm) TLDs are used at Chalk River Nuclear Laboratories for finger tip dosimetry because of their convenience for measuring β contact doses without interfering with work [4]. Since the scale of use is small, only a few hundred pairs per month, a completely automatic unit is not required. However, a semi-automatic one which transfers the results to a teletype page printer and tape is useful because it saves time and facilitates data processing. The reader used does this with the same type of circuits as those employed in the fully automatic reader.

Experience at Chalk River has revealed a serious problem in the heating of teflon discs, particularly when they are folded or bent. This results in heating of the teflon only at points of contact so that an incorrect

low reading results. We must keep the TLD flat without cutting down on the light output too much (which meshes do). By selecting the appropriate diameter for a thin, spring-loaded ring, the teflon disc can be held flat without the centre or perimeter rising. This is illustrated in plate IV.

Since speed is less important with smaller numbers of TLDs, a post-irradiation anneal is built into the reader. The dosimeter is rapidly raised to 150°C and held there for 10 seconds while the shallow traps are emptied. During this period, the gate to the counting circuits is closed. Then the dosimeter is taken rapidly to 240°C, when the counting gate is open. As with the high sensitivity ribbon, no other annealing process is used. Since the dosimeter retains about 0.2% of the light those that have been exposed to more than 10 rad are re-read before re-issue. The reader will also accept high sensitivity ribbon TLDs (not mounted in a plaque). By changing a switch, the appropriate sensitivity and zero correction can be selected for each type of dosimeter.

Performance

The semi-automatic finger tip reader has been in satisfactory operation for seven months with about 100 pairs of readings each month. 1000 dosimeters were all bought at one time to avoid buying other batches later which might not have the same sensitivity. 90% of the dosimeters had sensitivities within 12% of the mean value when exposed to 1 Roentgen. 90% of them had zero readings within 9 mR of the mean value.

The fully automatic reader has been tested for small scale user trials (eleven subjects) with small exposures (0-50 mR) over a period of ten months. It has also been tested for three months on a larger scale (160 subjects) at low and moderate exposures (0-1000 mR).

Prior to user tests, measurements were made on the system, dosimeters, holders and reader to examine the effect of the following factors:

- number of reading cycles
- reading precision
- linearity of the dosimeters and reader, taken together
- energy dependence of the dosimeter
- directional dependence of the dosimeter.

Sample dosimeters were exposed to 1 R and their readings compared with standards and were then processed through the reader 50 times. They were then again exposed to 1 R and the reading again compared with standards (which had not been cycled through the reader). This was repeated for another 50 cycles to process them 100 times which corresponds to over 8 years service at one reading each month. The results are shown in the following table.

Dependence of Relative Sensitivity
on Number of Reading Cycles

Cycle	Thick dosimeter	Thin dosimeter
1	1.00	1.00
50	1.01	0.96
100	1.01	0.98

During these 100 cycles the zero readings declined from 16 mrad to 14 mrad in the case of the thick dosimeter and from 30 to 20 mrad with the thin ones. These results show that the reading process would not affect the dosimeters during a useful working life.

Reading precision depends on the variance of the TLDs themselves and also on variations caused by their mounting in the plaques and non-uniformity in reading. The TLDs are purchased from the manufacturer with a ± 10% tolerance on the thick ones and ± 15% tolerance on the thin ones.

Measurements made on a batch of 35 plaques yielded standard deviations of 3.5% and 8.8% for the thick and thin TLDs. From a practical point of view it is more important to note that 32 of them had sensitivities lying within 7 and 15% of the mean values. This precision is sufficient for radiation protection.

For measurement of small exposures the uncertainty is set by the variations in black body radiation and spurious light signals. These variations again depend upon factors associated with the TLDs, their mounting and reading. The same batch referred to above were immediately re-read to obtain their zero readings and these yielded standard deviations of 2.8 and 6 mR for the thick and thin TLDs respectively. All 35 TLDs of each kind were within 10 mR of the average. This means that readings of 10 mR and 20 mR for the thick and thin TLDs respectively are probably significant.

Supralinearity in lithium fluoride TLDs has been well documented [5] but in a TLD system the observed linearity depends upon the reader also which must operate over about seven decades. Figure 3 shows the total effect which really has two components. The first depends upon the individual exposure and the second upon the whole history of exposure. The difference between the two is shown by the dosimeters which were given a final small exposure of 10 R after a series of much larger ones. It should be remembered that the only heating was that of reading and the low temperature anneal (10 minutes at 100°C). From a practical view-point the results suggest the need to check the calibration of results over 300 R and also to throw away the dosimeters. However, even accumulated exposures of 300 R to radiation workers are rare.

To measure the energy response of the plaque in the photobadge, it was mounted at waist height on a realistic phantom* and the dose was

*The phantom was made of tissue equivalent rubber containing a complete skeleton with the dimensions of the average man.

measured, with an ion chamber, at the testes site. This site was chosen since the testes are the most exposed critical organ [6, 7]. Thus, the energy dependence is referred to tissue dose and also the final calibration of the dosimeter.

Figure 4 shows the observed results over the energy range 0.03 - 1.25 MeV. The response depends upon the energy dependence of the lithium fluoride itself, the variation in scattering and absorption in the phantom at the two sites. At lower energies the 2 mm aluminum cover is also important. It should be noted that the average response to tissue rads while mounted on the phantom is significantly different from the response to γ-rays in free air and this must be accounted for if calibrations are done in free air since a personal dosimeter should give an estimate of dose.

Figure 5 shows the calculated response of the two thicknesses of lithium fluoride to β rays of different end point energies. The calculations were made assuming a source "distance" in air of 30 mg/cm^2 ($\sim$ 230 mm) [8]. They show a clear advantage for the thinner one for end point energies below 1 MeV. Since β-ray hazards figure prominently at most reactor research establishments (and, potentially, at nuclear power plants) the thinner TLD should be used. The table shows results obtained with the two thicknesses and β particles of various energies.

Response of TLDs to Beta Rays as a Percentage of their Response to Radium γ-Rays

End-point Energy(ies) MeV	Isotopes	Distance mm	0.9mm TLD	0.25mm TLD
2.3 and others	natural U	contact	62	92
3.0 and 0.32	Ce-Pr-144	300	49	56
2.3 and 0.54	Sr-Y-90	300	42	53
0.77	Tl-204	150	28	69
0.225	Pm-147	110	14	57

As predicted, the thick dosimeter is substantially lower in response for end point energies below 1 MeV.

The results shown in figure 4 for energy response to γ-rays refer to normal incidence. Although this is the most probable single direction, since workers normally face their work, other directions are possible.

To test this effect, two TLD badges were mounted at waist height with the reference ion chamber at the testes site. Figure 6 shows the results obtained for 660 keV γ-rays and 100 keV X-rays. For angles of incidence up to 60° no large effects are noticeable. However, when irradiated from the side, the dosimeters overestimate the dose because the ion chamber is shielded by a leg. From behind, the TLDs are shielded by the body, thus underestimating the dose. Changes in the design of the filter might reduce the effect at the side. In view of the variation in where and

how the badge is worn, the value of such a change is doubtful.

Conclusions

The reported results of measurements on this TLD system show that it could replace film dosimetry with advantage.

Two deficiencies remain to be corrected.

It would be useful to have one TLD which remains with the badge during the whole of the wearer's employment. It could act as a back-up for the main TLD system in case of failure or of a very large exposure. At the end of employment it could be stored as a "permanent record" or read out for comparison with the sum of all readings.

In the event of an exposure to thermal neutrons (improbable at Chalk River), serious overestimation of dose would occur. For this reason, a second dosimeter without high sensitivity to thermal neutrons would be desirable.

Both requirements could probably be met by a single TLD for which there is ample space in the existing badge.

Acknowledgements

Thanks are due to Messrs. W.F. Richter and J.H. Sneddon for their work in the design of the reader and dosimeter. Thanks are also due to the many who are helping to test the system in service.

References

1. A.R. Jones, "A Thermoluminescent Dosimetry System based on Extended Lithium Fluoride Dosimeters", Proc. 2nd International Conference on Luminescence Dosimetry, 757 (1968).

2. F.M. Cox, "New Solid Lithium Fluoride Thermoluminescent Dosimeters", Ibid. 60.

3. A.R. Jones, "Background Compensation of Personal Dosimeters", Health Physics 21, 323 (1971).

4. I.A. Berslerim, B.E. Bjarngard and D. Jones, "On the Use of Phosphor-teflon Thermoluminescent Dosimetry in Health Physics", Health Physics 14, 33 (1968).

5. J.R. Cameron, N. Suntharlingham, C.R. Wilson, S. Watanabe, "Supralinearity of Thermoluminescent Phosphors", Proc. 2nd International Conference on Luminescence Dosimetry, 322 (1968).

6. ICRP Publication 6, Pergamon Press, Oxford (1964).

7. A.R. Jones, "Proposed Calibration Factors for Various Dosimeters at Different Energies", Health Physics 12, 663 (1966).

8. W.G. Cross, "Tables of Beta Dose Distributions", AECL-2793 (1967).

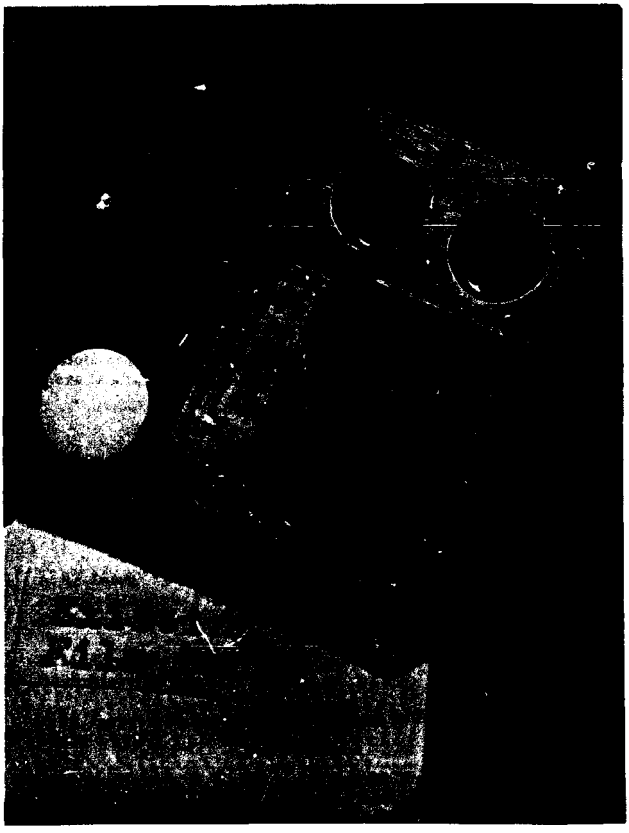

Plate I. **Dosimeter plaque inserted into the film badge**

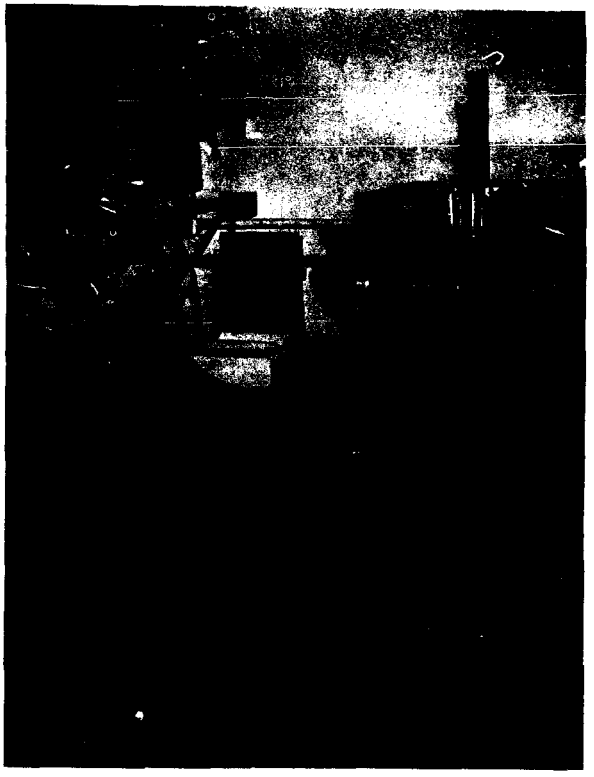

Plate II. Prototype automatic TLD reader and teletypewriter

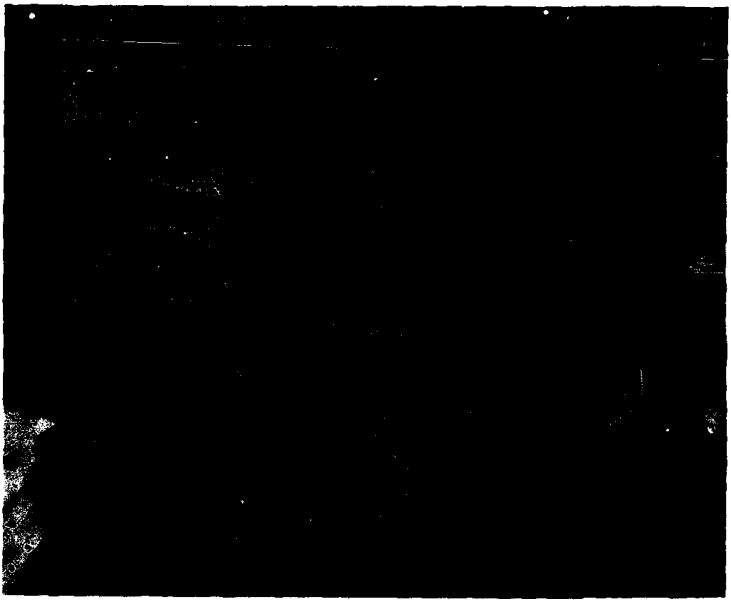

Plate III. Automatic mechanism of TLD reader

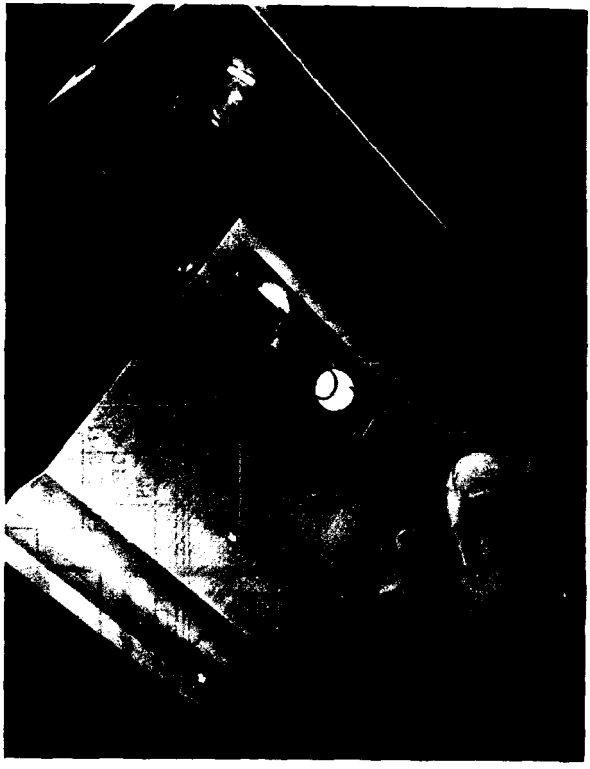

Plate IV. Insertion of Teflon disc into semi-automatic reader

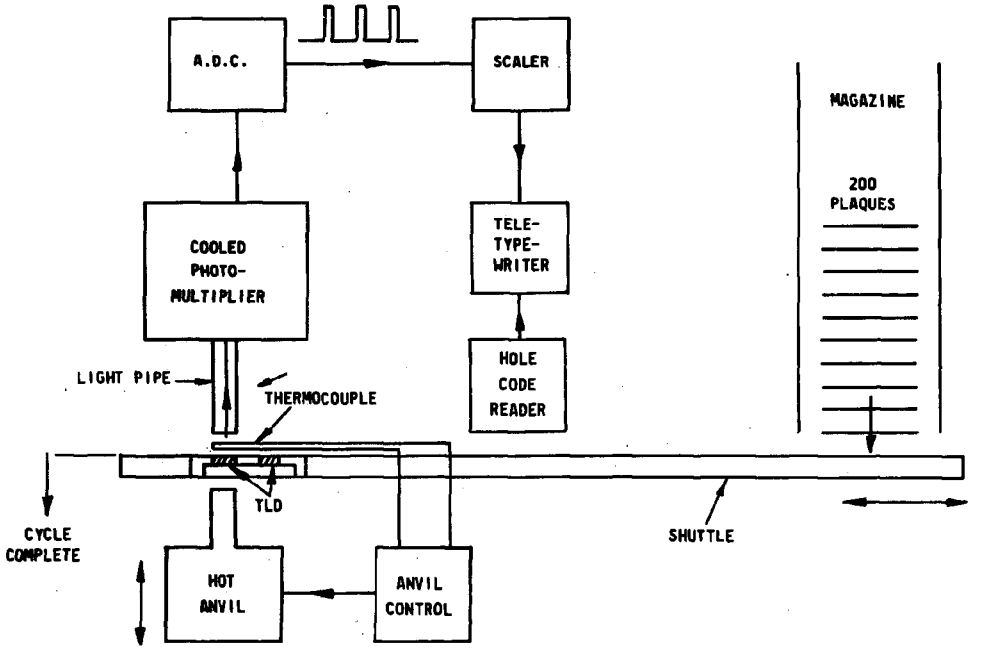

Figure 1. Diagram of automatic TLD reader

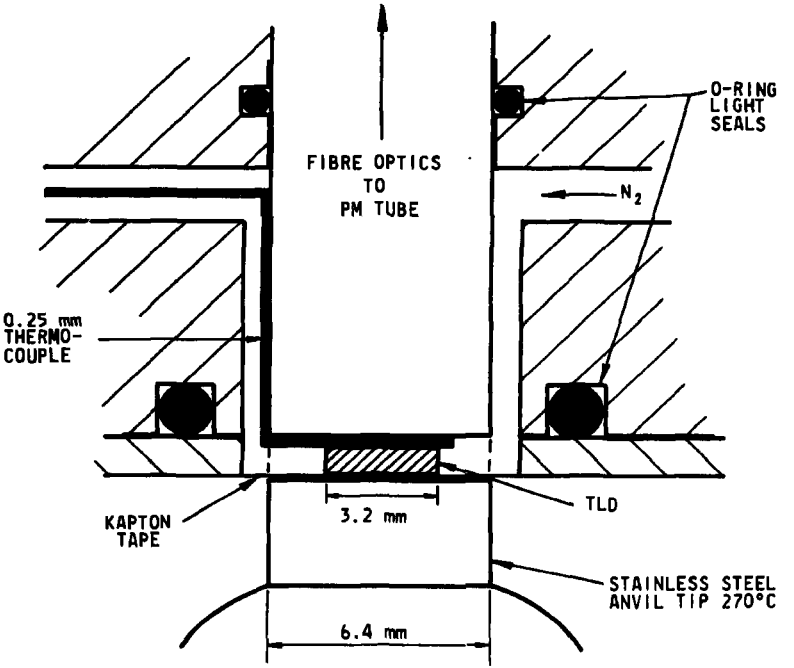

Figure 2. Detail of TLD heating and optics

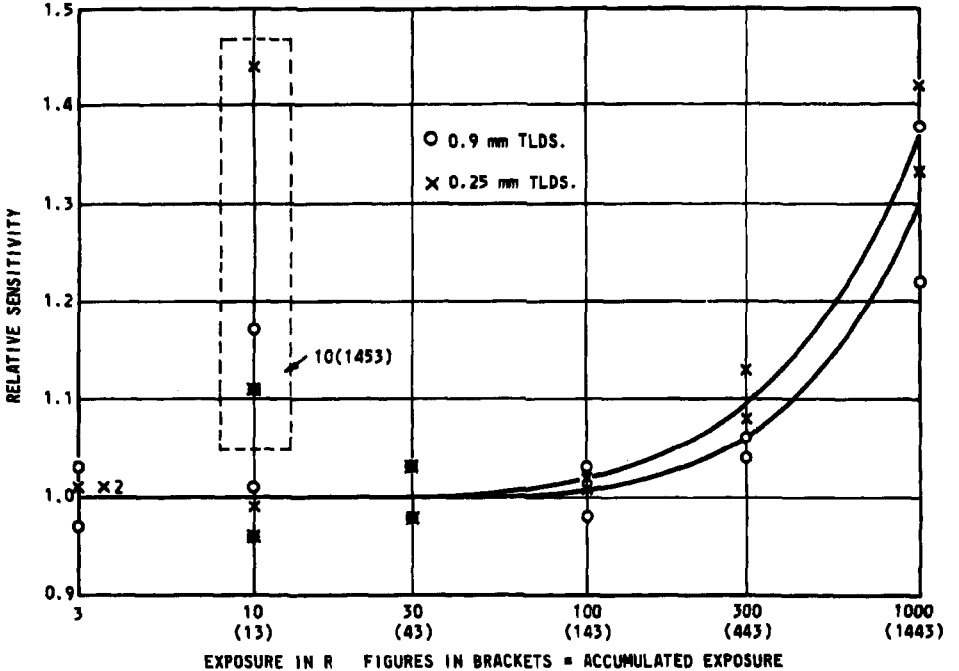

Figure 3. Linearity of TLDs

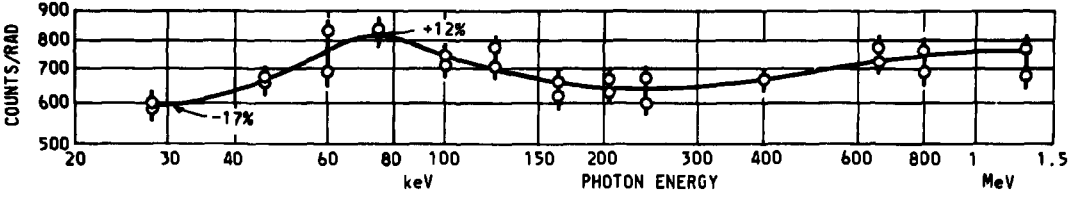

MEAN = 712 COUNTS/RAD AND 621 COUNTS/R IN FREE AIR

Figure 4. Energy dependence of TLD mounted on phantom

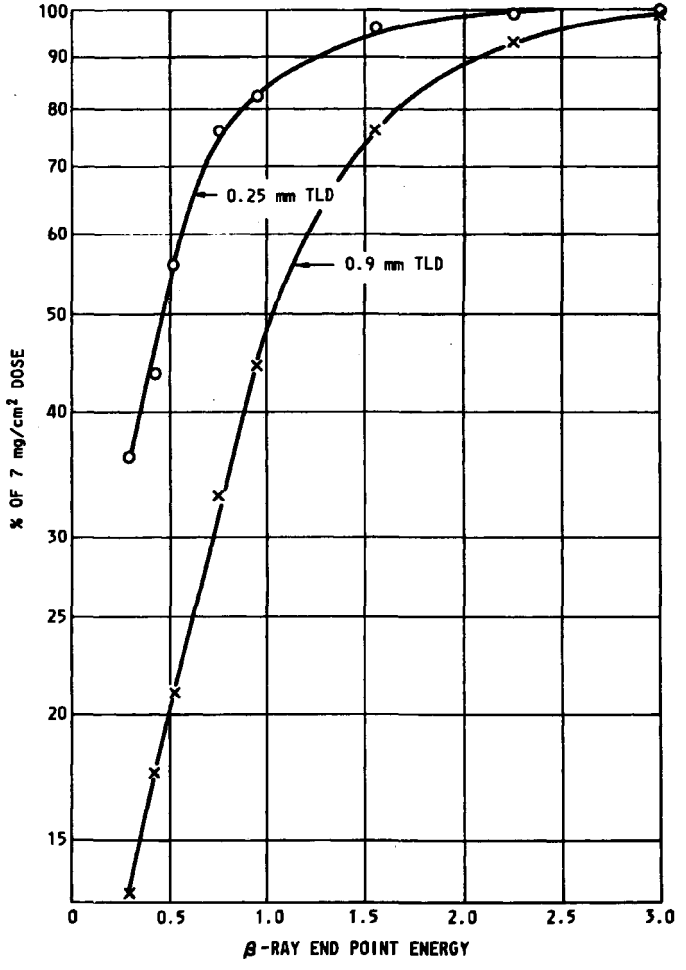

Figure 5. Calculated energy response to beta particles

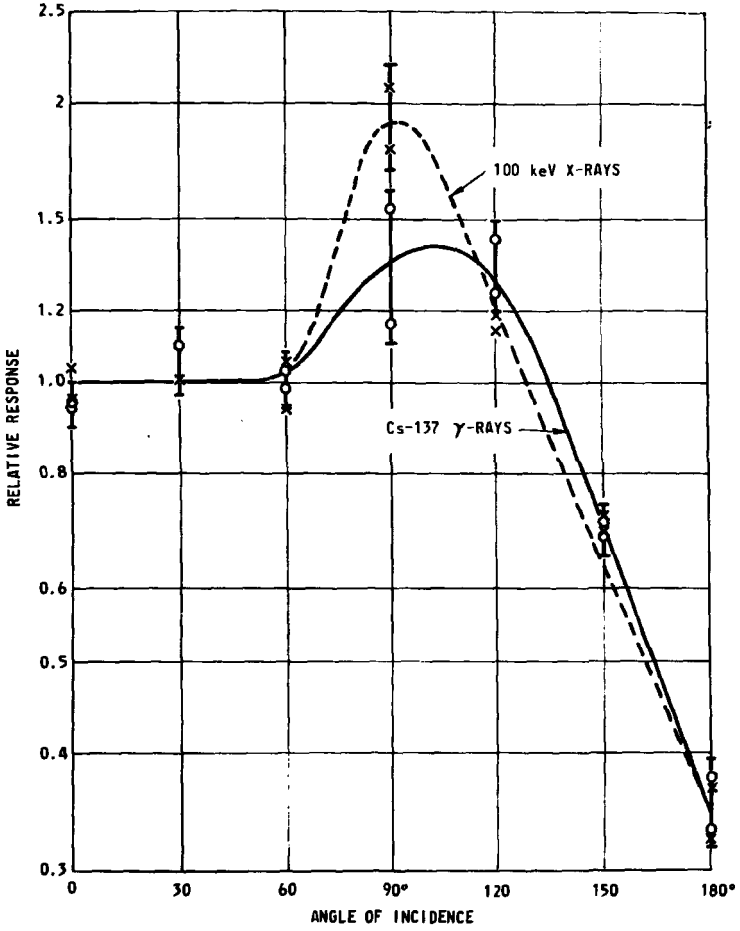

Figure 6. Angular dependence

Marshall, T.O.

When the dosimeters are passed through the reader, are the chips removed from the holder during the heating?

Jones, A.R.

No. The chips remain fixed to the plaque by means of the adhesive kapton tape. The identity is carried by the plaque.

Progress Towards Automatic TLD Processing for Large-Scale Routine Monitoring at Risø

by

Lars Bøtter-Jensen
and
Poul Christensen
Danish Atomic Energy Commission
Research Establishment Risø
Roskilde, Denmark

Abstract

A TL dosimeter unit (badge) was designed to facilitate automatic processing. The badge, which is made of heat-resistant plastic material and covered with 1 mm Al shielding, contains four dosimeters and a binary identification code. Three dosimeters are read in an automatic procedure and the fourth is retained for manual read-out in case of failure. The dosimeter badge is used as standard unit for several dosimetry purposes including personal and environmental monitoring.

A major component of the overall system is an automatic reader which accepts a stack of TLD badges, reads the identification number and lifts the TLD from the badges into a read-out chamber where they are heated by hot nitrogen gas.

The badge-unit was adapted for personal β-γ-monitoring by unshielding one of the four dosimeters. Results are presented from investigations of a personal monitoring system consisting of two Lithium borate dosimeters for routine β-γ-monitoring and one Lithium-7-fluoride dosimeter intended for long-term monitoring and back-up in the case of exposures to thermal neutrons. The investigations include dosimeter response to neutrons, beta- and gamma radiation of different energies.

Introduction

Recently several nuclear facilities have taken up TLD for routine monitoring, and many laboratories are investigating and designing dosimetry systems based on thermoluminescence with the purpose of using this technique in their routine monitoring program.

At Risø, TLD is now in routine use for several purposes involving personal monitoring, environmental monitoring and dating of ancient ceramics.

To facilitate automatic processing, a TLD unit (badge) containing four solid dosimeters was designed intended for the evaluation of personal doses and as a universal unit for other routine measurements.

The TLD unit was designed for the use of small solid dosimeters such as hot pressed 25 mg 3 x 3 x 0,8 mm LiF squares (Harshaw Chemical Company) and hot sintered 25 mg $4{,}5^{\phi}$ x 0,8 mm $Li_2B_4O_7$:Mn,Si tablets. The latter are produced at Risø from lithiumtetraborate powder containing 0,1 wt. % manganese and 0,25 wt. % silicon. The main advantages of $Li_2B_4O_7$:Mn, Si are the low cost, the re-useability after the read-out process without any annealing requirements and, in addition, an excellent energy response.

A major component of the overall system is an automatic reader which will accept a stack of dosimeter units to be read in sequence together with an identification code incorporated in the badge.

The badge design

Several criteria were considered on the design of the TLD badge; it should be small and light, it should be easy to adapt for automatic processing and it should be able to detect different radiation qualities for the evaluation of personal doses in order to replace film badges.

Fig. 1 shows the TLD unit schematically. The unit consists of an insert and a cover mainly made of heat resistant plastic material which allows annealing procedures up to 100°C. The insert contains the dosimeters in four depressions together with an identification number and a corresponding binary code consisting of a $1\ mm^{\phi}$ punched holes. The insert is placed into the cover which has a 1 mm aluminium shielding on both sides and a beta window thus situated that it corresponds to one of the dosimeter positions.

For personal monitoring the badge should contain two $Li_2B_4O_7$:Mn,Si dosimeters for routine γ- and β-recording and one ^7LiF dosimeter to enable slow neutrons to be detected and for use as long-term dosimeter. A fourth dosimeter is reserved for manual read-out in case of failure or accidents.

1 mm aluminium shielding of the dosimeters was chosen as a compromise between the absorption of soft γ-rays and the penetration of high energy β-rays.

The binary code is detected by light transmission through the punched holes when scanned by a pair of photo diodes. A special encoding punch was designed to 15 pairs of hole positions allowing for continuous numbering from 00000 to 32767. See fig. 2.

Apparatus

Fig. 4 shows a block diagram of the automatic TLD reader system. For evaluation of the results from the TLD units, three main operations are required: 1) The automatic loading and handling of the TLD , 2) The detection of the TL and decoding of the identification number and, 3) The transfer of the results via a Teletype printer to punched tape for further treatment in a computer.

A schematic diagram of the automatic reader is shown in fig. 3. A stack of TLD badges are loaded into a movable magazine. When a badge is in position, the insert is pulled out of the cover by a movable slide with a coupling device and led to the measuring position. During this transfer, the coding holes are scanned by a photo detection device consisting of two gallium arsenide light emitters and two photo diodes. The signal from the photo diodes are fed to a decoder and further to registration on the Teletype printer.

Three dosimeters are automatically lifted in sequence into a read-out chamber by means of a vacuum probe. A hot nitrogen gas stream of app. 250°C is used for heating the dosimeters thus avoiding mechanical heating elements.[1] After read-out the dosimeters are returned to the insert which is fed back to its cover.

The entire automatic procedure is controlled by a pneumatic system where the overall component is a special pneumatic programmer unit. The only non-pneumatic component that interrupts the automatic cycle is an adjustable electronic timer for preset of the time required for integration of the glow curves. A photograph of the entire set-up is shown in fig. 5.

Radiation Response

a) X- and γ-rays

The gamma-ray response (^{60}Co) of the ^{7}LiF- and $Li_2B_4O_7$:Mn,Si dosimeters is linear for exposures from a few mR and up to about 1000 R, where a small supralinearity is observed. Based on the glow curve area, the LiF squares are about two to three times as sensitive as the borate dosimeters. Both dosimeter types are suitable for measurements of person doses down to a few mrads. The standard deviation for a 10 mR measurement has been determined to 3.2 and 9.1% for the measurement made with the ^{7}LiF and $Li_2B_4O_7$:Mn,Si respectively[2]. The borate dosimeters do not require any annealing for doses below about 100 rads except if the reading is made within a few hours after the exposure when the low-temperature peak has to be removed by a short low-temperature annealing (e.g. 5 min at 100°C). A standard annealing procedure of 1 hour at 400°C followed by 2 hours at 100°C before the exposures and 20 min at 100°C after is at present applied to the ^{7}LiF-squares. The X-ray energy dependence of the three dosimeters contained in the batch is shown in fig. 6. The dose rates were determined by means of calibrated ionization chambers (Dr. Püchlau). The decreased response observed below 30 keV for the shielded dosimeters is analogous to the energy dependence curves showing the absorbed dose in the critical organs in the body[2]. The dependence of the response of the badge on the incident angle of the radiation is shown for 58 keV in fig. 8.

b) β-rays

Beta response data for the dosimeter unit were obtained by placing the unit on 1 cm thick gelatine moulds of the isotopes ^{14}C, ^{45}Ca, ^{204}TL and ^{90}Sr-^{90}Y. The response expressed as the equivalent of rad ^{60}Co γ-radiation pr. one rad beta radiation at the surface of the moulds is shown in table 1.

Table I

Beta-ray response of the dosimeter unit

Average beta energy MeV	Response eqiv. rad ^{60}Co γ-radiation pr one rad beta radiation		
	$Li_2B_4O_7$:Mn,Si open window	$Li_2B_4O_7$:Mn,Si behind Al.	^{7}LiF behind Al.
0.93	0.44	0.10	0.08
0.24	0.15	0.00	0.00
0.076	0.03	0.00	0.00

It appears that high energy β-rays, e.g. from ^{90}Y will to some degree penetrate the Al-shield and give rise to an overestimate of the gamma dose. The thickness of the two dosimeter types used does not make them ideal for β-monitoring; however the response is not very different from that of the film badge used at present. Some experiments have been carried out to produce a thin skin dosimeter by sintering a thin layer of fine grain phosphor onto a nonactivated (and hence radiation insensitive) lithium borate base. The phosphor was placed onto the borate tablet by sedimentation from a methanol suspension. By means of this technique dosimeters with thicknesses down to 1 mg/cm^2 were produced. Fig. 7 shows the difference in beta response for a normal lithium borate dosimeter and a thin $CaSO_4$:Dy dosimeter of thickness approx. 2 mg/cm^2. Both curves were obtained with the dosimeters placed in the open window position of the dosimeter unit. The dependence of the response of the batch on incident angle of beta rays is shown for ^{90}Y in Fig. 8.

c) Neutrons

Because of the great difference in response of $Li_2B_4O_7$:Mn,Si and ^7LiF to thermal neutrons, a combination of the two dosimeters can be used for evaluation of neutron doses from mixed radiation fields of gamma and thermal neutrons. If A is the response of $Li_2B_4O_7$:Mn,Si and B that of ^7LiF both expressed as γ-ray tissue rad and

$$m = \frac{\text{response of } Li_2B_4O_7\text{:Mn,Si per neutron tissue rad}}{\text{response of } Li_2B_4O_7\text{:Mn,Si per γ-ray tissue rad}}$$

then the neutron dose $D = \frac{A-B}{m}$ rads. The value m for thermal neutrons was determined by means of paraffin-moderated neutrons from a 5 Ci Pu-Be source calibrated by gold-foil activation technique. The γ-ray contribution measured with ^7LiF dosimeter was subtracted. Using a factor of $6{,}8 \times 10^{-11}$ rad-cm^2/n (excluding the n,γ contribution) for conversion of n_{th} fluence to tissue dose m was determined to have the value 390. If the body is exposed to fast neutrons, some of the neutrons will be moderated to thermal neutrons which will diffuse out to the dosimeter. In that case indirect detection of fast neutrons will occur and the evaluation of the neutron dose becomes complicated. Under specific conditions (3) the value of m can be determined and used for the dose evaluation. A value for m of 2.8 was found if the dosimeter was placed in front of a 30 cm thick water phantom and exposed to neutrons from a Pu-Be source 50 cm from the source. In this case a conversion factor of $4{,}9 \times 10^{-9}$ rad-cm^2/n valid for 4,0 MeV was used.

d) Field Experiments

Fig. 9 shows results from an earlier investigation of the behaviour of the two dosimeter types in practical use[2]. Plastic capsules each containing two shielded ^{7}LiF and $Li_2B_4O_7$:Mn,Si dosimeters for γ-monitoring and two unshielded dosimeters for (β+γ)-monitoring were worn as personnel dosimeters, together with film dosimeters, by people working in different radiation areas. The investigations covered monitoring periods of one to four weeks. The good agreement found between the two TL dosimeters in the measurement of gamma doses in neutron-free areas illustrates the accuracy of the system. The results of the gamma doses from reactor areas show a small overdose for the borate measurement, thus indicating the presence of small dose contributions from thermal neutrons. The beta-ray doses measured with the TL dosimeters, taken as the difference in the response of the unshielded and shielded dosimeters, were all in agreement to within 23 mrads. The correlation between the film and TL doses was poor for both γ and β-doses.

Conclusion

A TL dosimetry system intended for automatic processing for large scale routine monitoring has been described. The system includes the possibilities for accurate evaluation of personal doses received from mixed radiation fields.

Preliminary results of the system when applied to different radiation areas indicate that TLD is a very attractive alternative to film dosimetry systems for personal monitoring.

Acknowledgements

Thanks are due to Mr. P.O. Heidemann, Mr. F. Willumsen, Mrs L. Jørgensen, Mr. J. Lippert and Mr. H. Mundt for valuable assistance during the work.

References

1. Bøtter-Jensen, L., Read-out Instruments for Solid Thermoluminescence Dosimeters, Using Hot Nitrogen Gas as the Heating Medium. (IAEA-SM-143/20). In: Advances in Physical and Biological Radiation Detectors. Proceedings of a Symposium on New Developments in Physical and Biological Radiation Detectors held by the International Atomic Energy Agency in Vienna, 23-27 November 1970. (IAEA, Vienna, 1971) 113-124.

2. Christensen, P., A Combined Lithium Borate and Lithium Fluoride Thermoluminescence Dosimeter for Routine Personal Monitoring. (IAEA-SM-143/19). In: Advances in Physical and Biological Radiation Detectors. Proceedings

of a Symposium on New Developments in Physical and Biological Radiation Detectors held by the International Atomic Energy Agency i Vienna, [illegible] November 1970. (IAEA, Vienna, 1971) 101-112.

3. Nash, A.E. and Attix, F.H., Health Physics 21 1971 pp. 435-439

4. L.R.L. Hazards Control Progress Report No. 34 UCRL-50007-69-2.

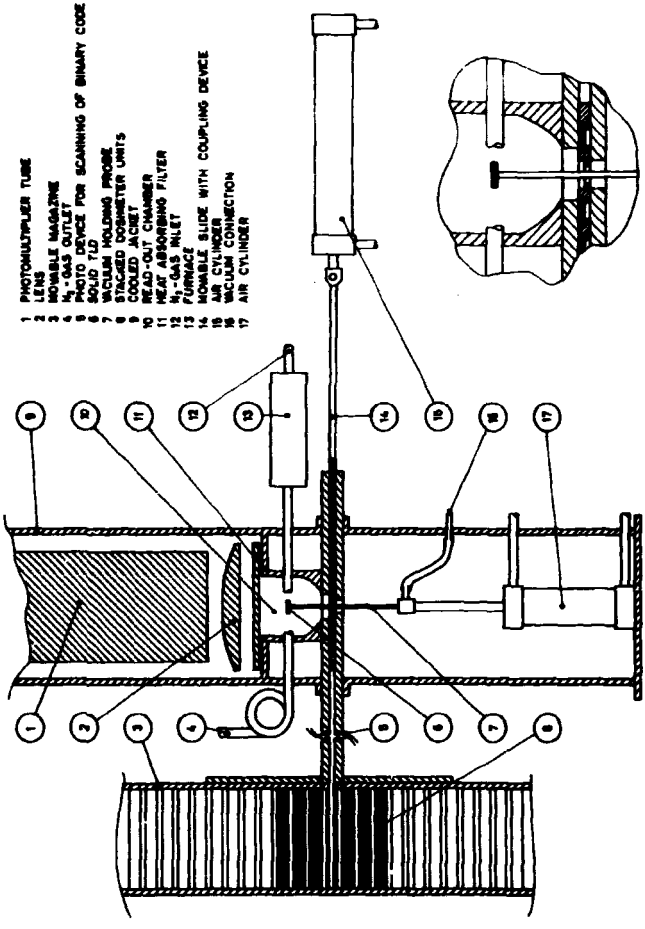

Fig. 3. Schematic diagram of the automatic TLD reader

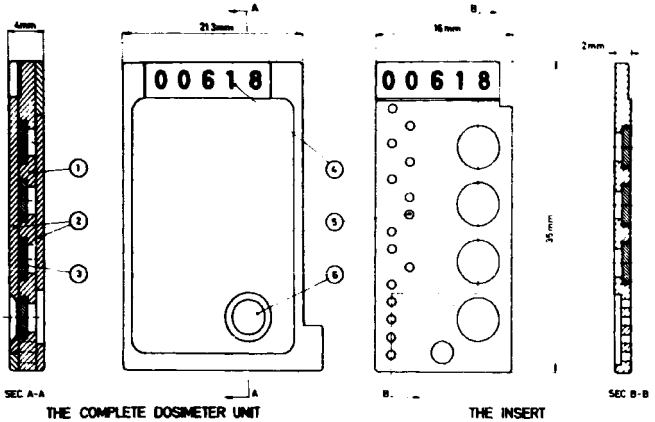

Fig. 1. Schematic diagram of the TLD unit.

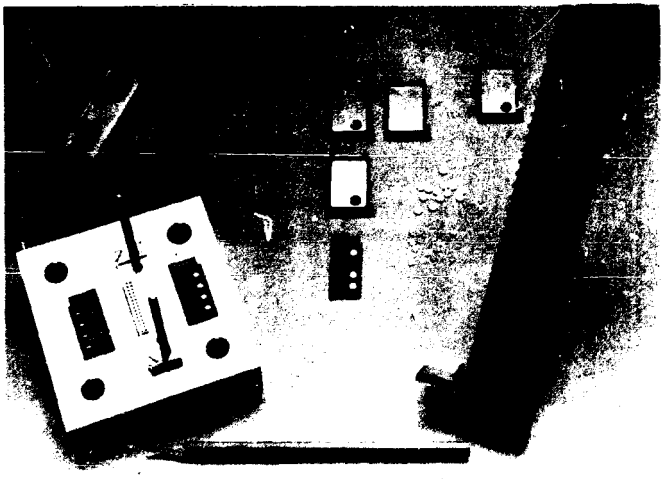

Fig. 2. Photograph showing the encoding punch, dosimeter units and magazine for automatic processing.

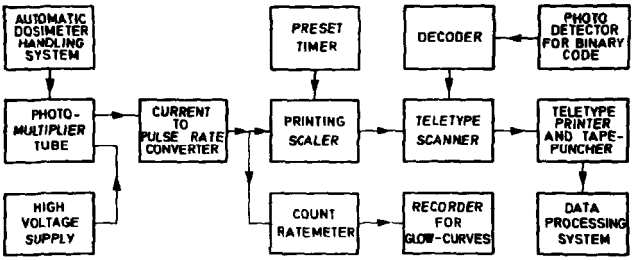

Fig. 4. Block diagram of the automatic TLD reading system.

Fig. 5. Photograph of the entire set-up.

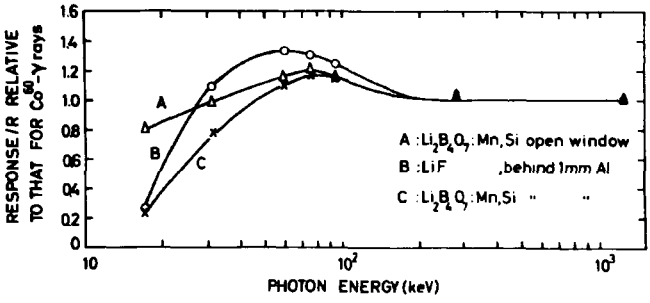

Fig. 6. Photon energy dependence curves of the dosimeter unit.

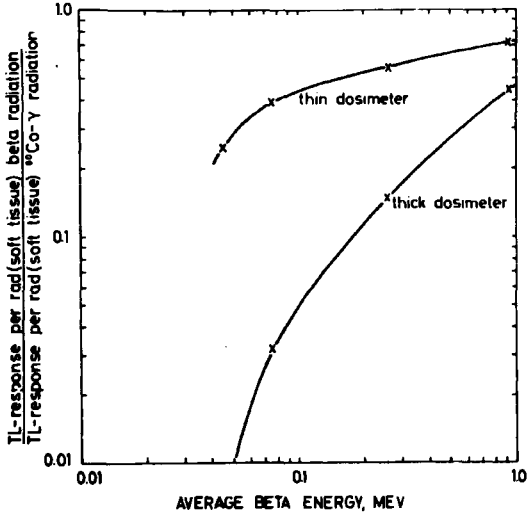

Fig. 7. Beta-ray response curves of normal $Li_2B_4O_7$:Mn,Si and thin $CaSO_4$:Dy dosimeters.

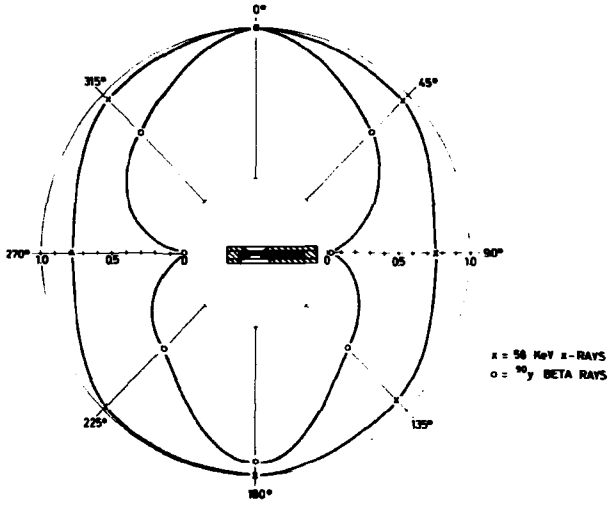

Fig. 8. Directional dependence curves for the dosimeter unit. Exposures: 58 KeV X-rays and Y-90 beta-rays.

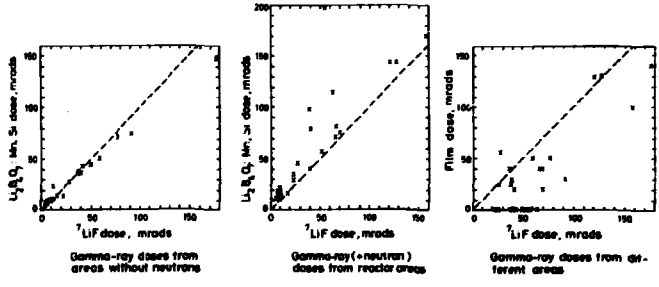

Fig. 9. Comparison between ^{7}LiF, $Li_2B_4O_7$:Mn,Si and film dosimeters when used for personal monitoring of γ-ray doses.

Becker

Why did you add silicon as an additional activator in your $Li_2B_4O_7$:Mn, and what is the exact composition and preparation procedure?

Bøtter-Jensen

Addition of 0.25% of silicon (by weight) has made the dosimeters more resistant to chemical attack from the atmosphere. The Si was added as SiO_2 together with $MnCO_3$ during the wet production of tetraborate. The dry material was then pressed into tablets and sintered at 900°C.

Suntharalingam

One of the difficulties with $Li_2B_4O_7$:Mn dosimeters reported in earlier works was the hygroscopic nature of this material. Does your dosimeter not have the same characteristic and if not how did you overcome this problem?

Bøtter-Jensen

We found earlier a slight brownishing of our lithium borate dosimeters during use which might be due to the hygroscopic nature of the material; however, for dosimeters doped with silicon we do not find this effect.

Schlesinger

Is there any atomic energy institutions where the film badges were entirely replaced by TLD badges?

Attix

Yes, there are five such institutions; perhaps we can discuss this point in the panel discussion.

UV INDUCED THERMOLUMINESCENCE IN NATURAL CALCIUM FLUORIDE*

Emico Okuno and Shigueo Watanabe
Instituto de Física - University of São Paulo
Instituto de Energia Atômica, São Paulo-Brasil

ABSTRACT

Samples of a green variety of fluorite found at Criciuma, Brasil, annealed at 580°C for 10 minutes and then at 400°C for two hours were exposed to 365 nm UV light. The transferred TL from deep trap to lower temperature trap gives rise to a glow curve containing peaks I, II, III', III and IV in a readout up to 400°C. This TL response was measured as a function of UV exposure time t and the result is not a saturation curve, but, TL tends to zero for large t indicating a simultaneous bleaching effect.

The curve of TL vs. the number n of identical cycles in a exposure readout cycle was obtained for different durations of exposure in each cycle, showing that for large n the rate of decrease of log (TL) is independent of the exposure duration. The effect of duration and temperature of pre-annealing on TL transfer under UV exposure as well as the dependence of transferred TL on previous gamma radiation were investigated. Finally a mathematical model is proposed.

* *Based in part upon portions of a thesis submitted by E.Okuno to the Institute of Physics, University of São Paulo, in partial fulfillment of the requirement for the Ph. D. degree.*

INTRODUCTION

Schayes et al[1] discussed some of the thermoluminescent properties of M.B.L.E. (Manufacture Belge de Lampes et de Materiel Electronique S.A., Bruxelles, Belgium) natural CaF_2 due to ultraviolet light. They observed that samples of natural CaF_2 submitted to a complete heat treatment at 600°C to empty all traps formerly filled through the action of natural radioactivity; subsequently irradiated to γ -($\alpha\beta$- $\alpha\alpha$) rays, annealed at 400°C (to empty all traps up to number IV) and exposed to light (300 to 500 nm) present TL reading for peaks I to IV, with the exception of peak III, which is displaced to a higher temperature peak referred to as peak III' (~275°C). This result was interpreted as a transfer of charge carriers from traps corresponding to peaks V and VI to lower temperature traps.

Wilson, Lin, and Cameron[2] and McCullough and Cameron[3] discussed additional properties, having in mind possible use as a UV dosimeter. The high sensitivity to UV light, the stability of peak III', and the relative mechanical simplicity are considered advantages of natural CaF_2 over other UV dosimeters. Light effects in $CaSO_4$: Mn have been studied for some time[4], and more recently CaF_2: Mn was also suggested as a UV dosimetry system[5].

We have extended the study of thermoluminescent properties of fluorite found at Criciuma, Santa Catarina State, Brazil. This work concerns the effect of UV light on the TL of "green" fluorite.

TL RESPONSE AS A FUNCTION OF UV EXPOSURE TIME

Samples of green coloured virgin fluorite were first annealed at ~580°C for 10 min and then at 400°C for 2 hours were used in this experiment. Then for illumination a small amount of the sample was spread out homogeneously in an aluminum pan and exposed to 365 nm UV light, which was obtained with Corning Glass filters 7-37 and 0-52 and Osram HWL-250w mercury Lamp. The light intensity at the samples was 12 $\mu w/cm^2$. The light and the aluminum pan were enclosed in a box to avoid room light. Since the temperature inside the box

reached about 60°C, peak I decayed quickly and we consequently ignore it. Such procedures were repeated for time of exposure varying from 1 min to 780 hours. The reading of TL response of peaks II and III was carried out in CON-RAD TL reader model 1500, keeping the PMT voltage at 860V. The right hand curve in Fig.1 is the glow curve of green fluorite irradiated to 100 R γ-rays from ^{137}Cs source, while on the left we have a glow curve of a sample exposed to 365 nm UV light for 6 min. In the last case III' was observed at about 242 ± 4°C with a height much smaller than that of peak III, which appears at ~290°C.

Figure 2 shows the TL response vs. exposure time. In contrast to the case of M.B.L.E. fluorite, we always found peak III to be much more prominent than peak III', therefore we considered only peaks II and III. Linear response is not observed unless as an approximation for very short time intervals (of the order of 5 min). The overall behaviour of this curve suggests that the filling of low temperature traps is accompanied by a simultaneous bleaching by UV light. Thus in the beginning, trap filling predominates and peaks II and III grow, but as the traps are filled, bleaching becomes large. Since the population of deep traps decreases as the filling of shallow traps proceeds, there is a time when the rate of both filling and bleaching becomes equal so that finally bleaching predominates, and peaks II and III start to diminish. In the last section a mathematical model is proposed to describe this result.

At this point we should recall that the samples used in this measurement were pre-annealed at 580°C for 10 min. This means that traps corresponding to peaks IV and V were emptied, hence any charge carriers that are transferred must come from peak VI or a deeper one.

Samples treated as described previously, were irradiated to UV light for 0.25 to 130 hours. The planchet current was kept at 1.25 amperes so that peaks IV and V could also be read. Figure 3 presents the heights of peaks II, III, IV, and V as functions of exposure time. While peaks II, III, and IV have the behaviour described above, peak V only decreases, indicating that it may be one of the deep traps from which transfer occurs.

Peak III' could be resolved for short exposure only. As the exposu

re times becomes longer peak III grows faster and masks peak III'. It was found, however, that peak III' can be better resolved if the fluorite is pre-annealed at a temperature higher than 550°C, because as we will see later high temperature annealing diminishes peak III while peak III' is less affected.

The question of why peak III' is induced by UV radiation but not by X or γ rays is unanswered yet. It is possible that UV light first creates a new kind of trapping center and then fills it by transferring charge carriers from deep traps.

EXPOSURE-READOUT CYCLES

Virgin samples of green fluorite annealed at 580°C for 10 minutes and then at 400°C for 2 hours were subsequently subjected to:

1. Exposure to 365 nm UV light for 15 min;
2. Readout (primary current I = 0.8 A)
3. 400°C anneal for 15 min.

Let us call these three operations one cycle. The first experiment included series of eighteen such cycles. The result is shown in Fig.4 where (x) indicates the height of peak III and (+) that of peak II. We see that after the fifth cycle log(TL) decreases by a constant amount for each cycle. The slope of this line reflects the rate at which deep traps are emptied by incident photons.

In a second experiment, the material used in the above experiment without further treatment was irradiated to ^{60}Co γ-rays with an exposure of 10^4 R. Next, fifteen new cycles were carried out and the result is also shown in Fig.4, where black circles stand for peak III and white ones for peak II. We see that a high γ-exposure tends to restore initial conditions, probably by refilling deep traps, and that decaying behaviour continues for each cycle.

In the next experiment the annealing at 400°C for 15 min in each

cycle was eliminated. We found that it made no difference because each readout emptied the low temperature traps.

Next, we investigated the effect of longer exposure times to UV light in each cycle. In Fig. 5 the results for 5 min, 15 min, 1 hr, 5 hr, and 17 hr exposure are represented for peak III. It is interesting to note that the slope of lines for large numbers of cycles is independent of the cycle's exposure time. The peak height depends, of course, upon the exposure time in each cycle. The peak II has the same behaviour as peak III.

EFFECT OF DURATION AND TEMPERATURE OF PRE-ANNEALING

It is well known that the TL sensitivity for X- or γ-rays of fluorite decreases as the isothermal pre-annealing temperature is kept above 450°C. For such a high temperature it decreases also with the duration of the heat treatment. Since usually a TL dosimeter is pre-annealed at some high temperature to be used or re-used, we have to investigate the dependence of TL sensitivity to UV light on these factors.

Virgin samples of green fluorite were pre-annealed at 400, 450, 500 and 550°C for 10 and 30 min. For comparison's sake each group of samples was divided into two. One was irradiated to 10 R X-rays and the other one was exposed to UV radiation for 15 min. The way the sensitivity decreases in illustrated in Fig. 6 and 7. The reading for the sample pre-annealed at 400°C was taken as 100%. We see that the sensitivity decreases very fast for temperatures above 450°C, and as expected, if the time of annealing is longer, there is a larger decrease of sensitivity. Furthermore, it can be seen that the UV sensitivity drops faster than that for X-rays.

Two causes can account for this drop in the UV sensitivity: (1) the higher the temperature of pre-annealing the smaller is the number of electrons left in the deep traps that contribute to transferred TL, (2) the annealing may thermally damage traps corresponding to peaks II and III. In fact, as we already mentioned, peak III' suffers less heat effect than peak III.

DEPENDENCE OF TRANSFERRED TL ON PREVIOUS γ - EXPOSURE

Samples of fluorite were exposed to cesium γ-rays from 35 R to 10^6 R. After usual readout they were annealed at 400°C for 15 min and then exposed to 365 nm UV light for 15 min. The transferred TL of peaks II and III was subsequently read.

Figure 8 shows that previous γ-exposure has no effect on peak II up to about 2×10^5 R while the peak III height increases steadily starting at $\sim 3 \times 10^3$ R. No saturation above 10 kR was observed.

In connection with this result it was found that the position (peak temperature) of peak II remains unchanged while that of peak III shifts to higher temperature starting at about 3×10^3 R.

One might think that the growth of deep traps account for the increase in the peak III height as the γ-exposure increases. On the other hand this assumption does not explain why peak II remains constant. It is more reasonable to assume that the sensitization effect on γ-induced TL holds also for transferred TL.

Mathematical model . We proposed the following model to describe the mechanism involving transferred TL. Let us denote by:

N_{od} = initial number of filled deep traps (one kind),

N_d = number of deep traps that remain filled after time t of illumination to UV light,

α_d = constant probability factor per unit time for liberation of charge carriers from a deep trap,

N_3 = number of filled traps corresponding to peak III after time t,

β_3 = probability per unit time for the filling of traps III,

N_{3f} = maximum number of available traps III that are filled or not,

α_3 = probability per unit time for emptying of traps III.

Now we assume that

$$\frac{dN_d}{dt} = -\alpha_d N_d \longrightarrow N_d(t) = N_{od}\exp(-\alpha_d t)$$

$$\frac{dN_3}{dt} = \beta_3(-dN_d/dt)(N_{3f}-N_3) - \alpha_3 N_3$$

The solution $N_3(t)$ has the following form

$$N_3(t)=\beta_3 N_{od}\alpha_d N_{3f}\exp(-\alpha_3 t + \beta_3 N_{od}\exp(-\alpha_d t))\int_o^t \exp((\alpha_3-\alpha_d)t'-\beta_3 N_{od}\exp(-\alpha_d t'))\ dt'$$

N_3 vanishes as t goes to zero or to infinity in agreement with the experimental data. For very small values of t

$$N_3 \simeq \beta_3 N_{od}\alpha_d N_{3f} t$$

The numerical calculation for determination of parameters is under way and the result will be reported elsewhere.

CONCLUDING REMARKS

In the present work we found peak III' at a temperature below that of peak III. Both peaks can be observed after short exposures to UV light. Peak III being always larger than peak III' its height should be used in UV dosimetry.

The decrease of the height of peaks II and III in each cycle, descri

bed in third Section is due to the reduction of the number of electrons captured in traps VI. Therefore the rate at which log (TL) decreases in each cycle measures the rate for emptying of traps VI.

No evidence for direct induction of thermoluminescence by ultraviolet light was found. However the appearance of peak III' for UV light but not for γ-rays can be interpreted as creation of traps III' by UV light and subsequent filling by charge carriers transferred from deep traps.

The linearity of transferred TL with UV light is not observed.

The fluorite has a high sensitivity to UV induced thermoluminescence.

Acknowledgements

Thanks are due to Dr.Michael R.Mayhugh for discussions. The ^{137}Cs γ-ray source used in this work belongs to the Instituto de Biociências of the University of São Paulo.

REFERENCES

1. R.Schayes, C. Brooke, I.Koslowitz, and M. Lheureux, Luminescence Dosimetry, USAEC-CONF-650637, Clearinghouse for Federal Scientific and Technical Information, 1967.

2. C. R. Wilson, F. M. Lin, and J. R. Cameron, Annual Progress Report on AEC Contract AT-(11-1)-1105, COO-1105-136, 1967.

3. E. C. Mccullough and J. R. Cameron, Annual Progress Report on AEC Contract AT-(11-1)-1105, COO-1105-160, 1968.

4. T. Lyman, Phys. Rev. 48, 149 (1935); K. Watanabe, Phys.Rev. 83, 785 (1951).

5. J. K. Puite, Intern. Jour. of Appl. Rad. and Isotopes 18, 397 (1968).

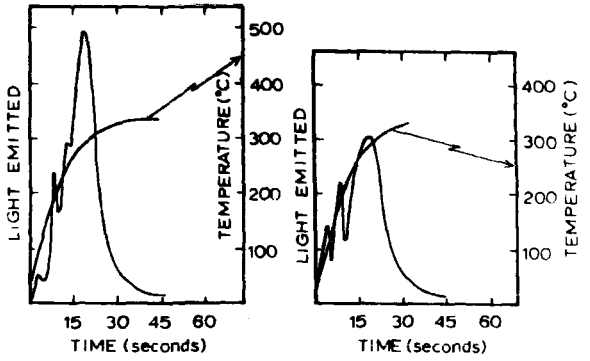

Fig.1. Right side. Glow curve of green fluorite irradiated to 100R γ-rays of ^{137}Cs. Virgin phosphor was preannealed at 580°C for 10 min then at 400°C for 2 hours. Left side - Glow curve of similary treated material exposed to 365 nm UV light for 6 minutes.

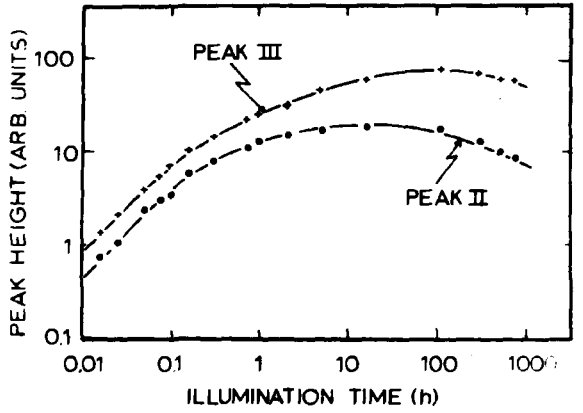

Fig.2. Peak height vs.time of exposure to 365 nm UV light. Primary current I= 0,8 A. Pre-annealing 580°C/10 min plus 400°C/2 hr.

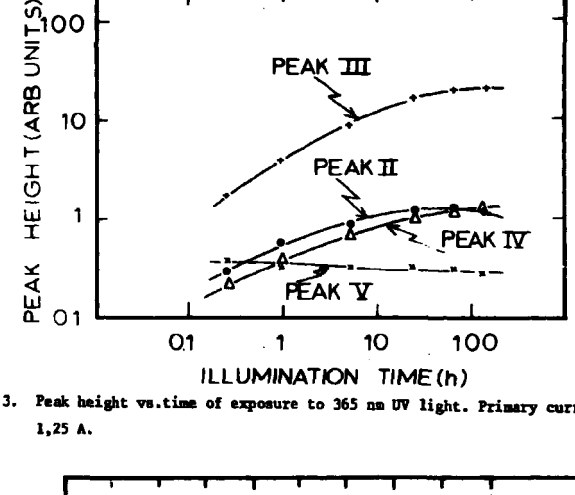

Fig.3. Peak height vs.time of exposure to 365 nm UV light. Primary current I= 1,25 A.

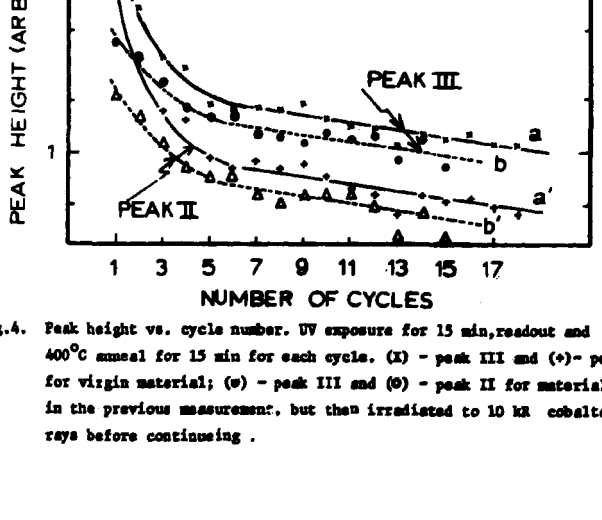

Fig.4. Peak height vs. cycle number. UV exposure for 15 min, readout and then 400°C anneal for 15 min for each cycle. (x) - peak III and (+)- peak II for virgin material; (o) - peak III and (o) - peak II for material used in the previous measurement, but then irradiated to 10 kR cobalto γ - rays before continueing .

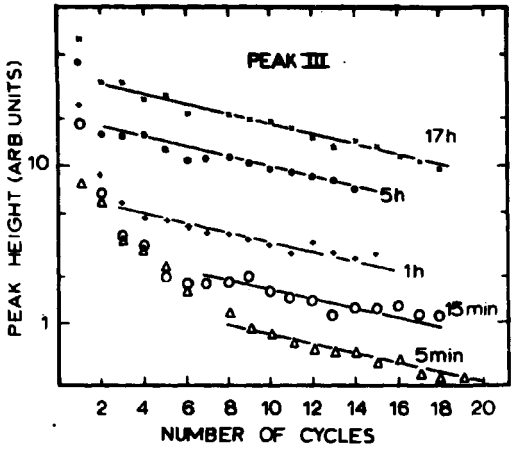

Fig.5. Peak height vs. cycle number for different exposure time intervals in each cycle.

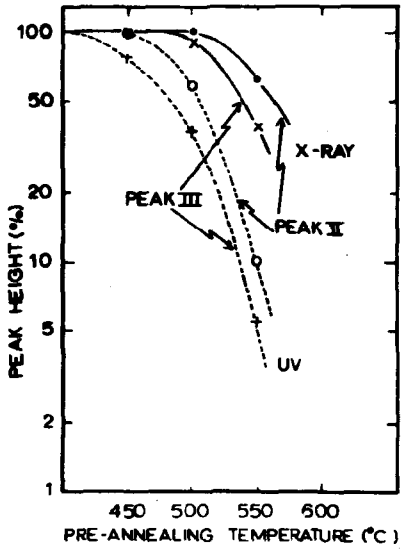

Fig.6. Sensitivity decrease with pre-annealing temperature for a 10 min annealing. Normalized to TL response for 400°C anneal.

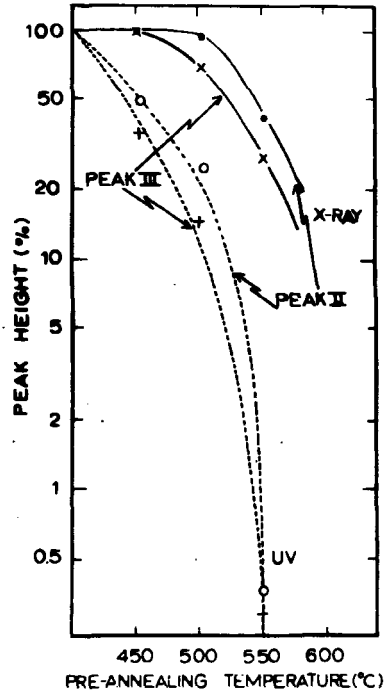

Fig.7. Sensitivity vs. pre-annealing temperature for a 30 min. annealing. Normalized to TL response for 400°C anneal.

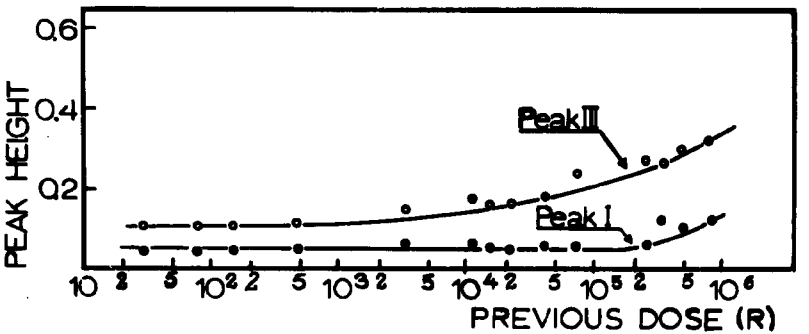

Fig.8. Transferred TL vs. previous γ-exposure.

A Current Look at TLD in Personnel Monitoring*

F. H. Attix
Nuclear Sciences Division
Naval Research Laboratory
Washington, D.C. 20390, USA

Thermoluminescent dosimeters have been studied vigorously for more than a decade now, and are gradually receiving acceptance in routine personnel monitoring. It has been difficult to assess just how much progress has been made in this latter direction, leading the author to seek more information through a questionnaire, sent to 140 establishments of various types in 26 countries. 105 completed forms were returned for evaluation, reporting on the monitoring of some 200,000 persons by badges of various kinds. Roughly one-third of the establishments now include TLD's as part of the badge, covering 65,000 employees. However only 14 institutions and 15,000 employees use TLD's for record keeping purposes in place of film. Within the next 3 years 25 more institutions (41,000 employees) plan to adopt TLD's and 18 establishments (50,000 employees) plan to use them in place of film for record keeping of $\beta\gamma$ radiation exposures. TLD with LiF chips or Teflon discs is now the method of choice for extremity monitoring, being so used by 57 establishments. 46 use TLD's for area monitoring and 19 for measuring patient exposure. Only 21 are not now using TLD at all in some radiation protection application.

In reply to a question on the importance of TLD's to the establishment's radiation protection operations at this time, 54 replied "important", 28 "somewhat useful", and 21 "insignificant". (2 did not respond to the question).

---

*This paper was prepared with partial support from the Division of Biology and Medicine of the U. S. AEC. It will be published in full in the Health Physics Journal.